EXPLORING THE IMPACT OF

OSTEOPOROSIS ON MYOGENESIS

A DISSERTATION IN
Nursing

Presented to the Faculty of the University
Of Missouri-Kansas City in partial fulfillment of
the requirements for the degree

DOCTOR OF PHILOSOPHY

by
Janalee Isaacson

B.S.N., University of Kansas, 1983
M.S.N., University of Kansas, 1998

Kansas City, Missouri
2015

EXPLORING THE IMPACT OF

OSTEOPOROSIS ON MYOGENESIS

Janalee Isaacson, Candidate for the Doctor of Philosophy Degree

University of Missouri-Kansas City, 2015

ABSTRACT

Aging is accompanied by a significant decline in bone mass and strength (osteoporosis) and in muscle mass and strength (sarcopenia). These conditions pose a tremendous threat as each year, one in three older adults living in the community falls. Muscle weakness is a primary risk factor for falls and the associated morbidity and mortality, especially among older adults with osteoporosis. Nurses are aware of the risks and are often in a position to effect a change. For this reason, nurses are positioned to be involved in and to direct research aimed at better understanding these conditions and to make discoveries with translational impact.

Until recently, bones and muscles were viewed to function in a mechanical partnership. Emerging research, however, demonstrates a much more complex relationship, resulting not only from mechanical forces, but also from an exchange of biochemical factors. The purpose of this *in vitro* controlled trial was to explore this biochemical exchange, and investigate the impact of bone factors on skeletal muscle cell differentiation (myogenesis) in the presence of osteoporosis. A series of studies have been completed in mouse models, and our concomitant goal was to expand these studies into humans. Serum used was collected from research subjects in an ongoing case-control study designed to characterize defects in bone quality that contribute to low trauma fractures in postmenopausal women. Using a

combination of biophysical, biochemical, and physiological approaches, the serum from subjects with (CASE) and without (CNTRL) osteoporosis was applied to human skeletal muscle cells. The extent of myogenesis in each group was assessed through immunostaining for visualization and calculation of fusion index (i.e., the myogenesis index), flow cytometry for cell cycle analysis, and intracellular calcium measurements for data related to cellular function.

Findings from this study will contribute to the growing body of knowledge related to the biochemical communication between bones and muscles, bone-muscle crosstalk. In addition, this study illustrates an excellent opportunity for basic scientists and clinicians to work together to decrease the devastating impact of sarcopenia and osteoporosis.

Keywords: aging, crosstalk, myogenesis, osteoporosis, sarcopenia

The faculty listed below, appointed by the Dean of the School of Nursing and Health Studies have examined a dissertation titled "Exploring the Impact of Osteoporosis on Sarcopenia," presented by Janalee Isaacson, candidate for the Doctor of Philosophy degree, and hereby certify that in their opinion it is worthy of acceptance.

<u>SUPERVISORY COMMITTEE</u>

Marco Brotto, BSN, MS, Ph.D., Committee Chair
Dale & Dorothy Thompson Missouri Professor of Nursing Research
UMKC School of Nursing & Health Studies and School of Medicine

Patricia Kelly, Ph.D., MPH, RN, FNP
Professor
UMKC School of Nursing & Health Studies

Eduardo Abreu, MD, DEng
Assistant Professor
UMKC School of Nursing & Health Studies

An-Lin Cheng, Ph.D.
Associate Professor
UMKC School of Nursing & Health Studies

Janet Pierce, Ph.D., APRN, CCRN, FAAN
Christine A. Hartley Centennial Professor
University of Kansas Medical Center School of Nursing

CONTENTS

Appendix

LIST OF TABLES

LIST OF ILLUSTRATIONS

LIST OF ABBREVIATIONS

ATP	Adenosine triphosphate
BMD	Bone mineral density
BQ	Bone quality
CA	Certificates of Analysis
DHPR	Dihydropirydine receptor
DKK1	Dickkopf-related protein 1
DMP1	Dentin matrix acidic phosphoprotein 1
DXA	Dual-energy X-ray absorptiometry
ECC	Excitation-contraction coupling
FBS	Fetal bovine serum
FGF23	Fibroblast growth factor 23
FC	Flow Cytometry
GA	Gentamicin/ amphotericin
GBD	Global burden of disease
GST	General Systems Theory
hEGF	Human epidermal growth factor
HSMM	Human Skeletal Muscle Myoblast
IGF	Insulin-like growth factor
IRB	Institutional Review Board
KLF6	Kruppel-like factor 6
LIF	Leukemia inhibiting factor
MEPE	Matrix extracellular phosphoglycoprotein
MNRS	Midwest Nursing Research Society
MRF4	Myogenic regulatory factor 4
mTOR	Mammalian target of rapamycin
MUBIG	Muscle Bone Biology Group
NBF	Neutral buffered formalin
NHANES	National Health and Nutrition Examination Survey
NVSS	National Vital Statistics System
OPG	Osteoprotegerin
PG	Prostaglandin
PHEX	Phosphate regulating endopeptidase homolog, X-linked
RANKL	Receptor activator of nuclear factor-kappa B ligand
ROS	Reactive oxidative species
RT PCR	Reverse transcriptase polymerase chain reaction
RyR	Ryanodine receptor
SR	Sarcoplasmic reticulum
UMKC	University of Missouri-Kansas City
USDHHS	US Department of Health and Human Services
WHO	World Health Organization
YLD	Years lived with disability

ACKNOWLEDGEMENTS

I would also like to express my sincere appreciation to each of the distinguished members of my dissertation committee: Dr. Marco Brotto, Dr. Janet Pierce, Dr. Patricia Kelly, Dr. Eduardo Abreu, and Dr. An Lin Cheng, for investing in my professional growth and development. The expertise, feedback, input, and inspiration you provided will continue to guide me in my personal and professional life, as I reflect on all that I learned from each of you. Most importantly, I want to thank the chairperson of my dissertation committee, and my mentor, Dr. Marco Brotto. The depth of your knowledge and experience is staggering, and your passion for research is quite contagious. Especially, thank you for teaching me to "enjoy the journey." I have and I will. *Thank you!*

CHAPTER 1

INTRODUCTION

The population worldwide is aging at an unprecedented rate and is, therefore,

receiving much attention. Every year since 1948, the World Health Organization and

partners convene to discuss and draw attention to a public health issue of global significance.

The theme of World Health Day 2012 was aging and health. In her 2012 address to delegates

of the gerontology congress, the Director-General of the World Health Organization, Dr.

Margaret Chan stated, "Within the next five years, for the first time in history, the number of

adults aged 65 and older will outnumber children under the age of five" (Chan, 2012). This

is considered the largest demographic shift in history. In the United States, the first of the

baby boomers, born between the years of 1946 and 1964, turned 65 years of age in 2011.

Predictions are that by the year 2030, one in every five Americans will be 65 years or older

(Olson, 2013).

Aging is accompanied by a decline in cognitive and physical functioning and is listed

as a risk factor for a myriad of chronic diseases, including diabetes, dementia, cancer,

musculoskeletal, and cardiovascular disorders (Niccoli & Partridge, 2012; Satariano et al.,

2012). Due to the fact that average lifespans are increasing, more people each year are

suffering from chronic diseases. Approximately half of the population worldwide lives with

at least one chronic disease (Clark, 2011; Yach, Hawkes, Gould, & Hofman, 2004); and the

burden is carried not only by the individual, their family, but society. The economic costs of

chronic diseases include the direct costs of prevention, diagnosis, and treatment; the indirect

costs of lost human resources and productivity; and intangible costs, including the

psychosocial aspects of pain, bereavement, and loss of independence.

The 2010 Global Burden of Disease Study reported that musculoskeletal diseases have become the second greatest cause of disability worldwide, affecting 1.7 billion people (Vos et al., 2012). Regardless the measures and tools used to diagnose, the incidence of musculoskeletal diseases such as sarcopenia and osteoporosis increases with increasing age (Cruz-Jentoft, 2013; Leboime et al., 2010). Muscle weakness is one of the primary contributing factors leading to falls among persons age 65 and older (Dutta, 1997; Yamashita, Haesang, Bailer, Nelson, & Mehdizadeh, 2011). The morbidity and mortality associated with falls in this age group is even greater in the presence of osteoporosis. The aging world population and the increasing incidence of osteoporosis and sarcopenia threatens to impact the productivity, independence, physical, and psychosocial health of individuals; not to mention the widespread economic ramifications. For these reasons, it is important to pursue research exploring new facets of the relationship between these two musculoskeletal diseases.

Background

Sarcopenia is the progressive loss of muscle mass and strength. The most literal definition of osteoporosis is "porous" bones and leads to bones that break easily. Sarcopenia and osteoporosis have long been considered expected consequences of aging and are leading contributors to morbidity and mortality among older adults (Arthur & Cooley, 2012; Dutta, 1997; Brotto & Abreu, 2012; Evans & Campbell, 1993; Fielding et al., 2011; Rubenstein & Josephson, 2006). Mechanisms identified as contributing to the development of sarcopenia and osteoporosis include physical inactivity, genetics, hormones, changes in body composition, chronic inflammation, and oxidative stress (Arthur & Cooley, 2012; Buford et al., 2010; Crepaldi & Maggi, 2005; Karasik & Kiel, 2010; Romano, Serviddio, de Matthaeis,

Bellanti, & Vendemiale, 2010). Research now supports what clinicians who work with the geriatric population have long suspected; there is a significant association between sarcopenia and osteoporosis, i.e. persons with one diagnosis often have the other (Di Monaco, Vallero, Di Monaco, & Tappero, 2011; Sirola & Kroger, 2011). Together, sarcopenia and osteoporosis pose significant risks to individual safety, independence, and the economic health of the nation (Crepaldi & Maggi, 2005; Janssen, 2006; Janssen, Heymsfield, & Ross, 2002). In the United States, the estimated direct cost of sarcopenia in 2000 was $18.5 billion (Janssen, Shepard, Katzmarzyk, & Roubenoff, 2004). Adjusted to the normal and not the health care inflation, the current costs would surpass $25 billion per year. Experts have estimated the annual health care costs related to osteoporosis to be $20 billion or more (Becker, Kilgore, & Morrisey, 2010; Blume & Curtis, 2011). As people are living longer, the need to better understand these conditions is critical to the advancement of therapeutic approaches to decrease associated morbidities and mortality. Therefore, any intervention that would for example reduce the burden of these twin diseases by as little as 10% would save at least $5 billion dollars, which could then be re-invested into research aimed at further reducing their burden.

One strategy to develop preventative and therapeutic interventions targeting sarcopenia and osteoporosis is to study how these conditions are linked together and how one might affect the other. The relationship between bones and muscles is emerging as more than simply a function of mechanical load, as recent findings have revealed an endocrine-like "crosstalk." Crosstalk is the response in cell morphology and function to factors from distant sites and systems. Crosstalk has been recognized as one of the primary means by which intracellular communication occurs in mammalian physiology (Gruning, Lehrach, & Ralser,

3

2010; Holz & Habener, 1992). Preliminary research performed by the Muscle Bone Biology Group (MUBIG) at the UMKC Schools of Dentistry, Medicine, Nursing and others has provided data supporting this biochemical relationship between bones and muscles (Abreu, Stern, & Brotto, 2012; Dallas, Prideaux, & Bonewald, 2013; Karasik & Kiel, 2010). Conditioned media from skeletal muscle cells preserves osteocytes from the damaging effects of dexamethasone (Jähn et al., 2012), and factors from osteocytes accelerate myogenesis of skeletal muscle myoblasts into muscle cells (Mo, Romero-Suarez, Bonewald, Johnson, & Brotto, 2012). This crosstalk relationship between bones and muscles opens an entirely new area of research and provides opportunities for developing interventions to delay the devastating effects of sarcopenia and osteoporosis. The experiments performed for this dissertation were designed to explore the factors produced by normal bone and osteoporotic bone and compare the impact they have on human skeletal muscle cell differentiation, also called myogenic differentiation, or simply myogenesis.

Study Purpose and Working Hypothesis

The *overall objective* of this study was to add to the body of knowledge related to bone-muscle communication in the context of osteoporosis. This *research applied* what has been learned about the biochemical relationship between bones and muscles from the murine mouse model and expanded the investigation to human skeletal muscle cells. The *working hypothesis* for this study was that human skeletal muscle myoblast (HSMM) cells treated with media containing serum from subjects with osteoporosis will experience decreased myogenesis compared to HSMM cells treated with media containing serum from subjects without osteoporosis as evidenced by fewer nuclei within myotubes, reduced fusion index, and decreased sarcoplasmic reticulum calcium release response to stimulation with caffeine.

This hypothesis was tested by investigating the effects of media containing serum from subjects with and without osteoporosis on HSMM cells through the utilization of optical and fluorescent microscopy, and flow cytometry (histomorphometric/ biochemical), MTT assay for evaluation of mitochondria function and cell proliferation (biochemical/ functional), and by measuring resting levels of intracellular calcium ($[Ca^{+2}]_i$) as well as upon stimulation with caffeine (biochemical/ functional), which induces robust release of Ca^{+2} from the sarcoplasmic reticulum.

Specific Aim (SA)

To investigate biochemical, histomorphometric, and functional differences in human skeletal muscle myoblast (HSMM) cells treated with conditioned media containing serum from patients with and without osteoporosis.

Research Question (RQ)

What is the extent of difference in biochemical, histomorphometric, and functional adaptations in HSMM cells treated with conditioned media containing serum from subjects with and without osteoporosis?

<center>**Significance**</center>

The significance of this research lies in its promise to provide a deeper understanding of factors released from bones and their effect on muscles; specifically investigating the impact these factors have on myogenesis in the presence and absence of osteoporosis. Differences discovered in the effect on myogenesis between factors from osteoporotic and normal bones would then lead to treatments or specific interventions (for example specific exercise modalities and intensities) to amplify those factors that promote myogenesis, and/or inhibit those factors that impede myogenesis. This work will further research that has been

done by the UMKC Muscle Bone Biology Group (MUBIG) and others related to bone-

muscle communication by investigating the impact that factors from osteoporotic bone *in*

vivo have on human skeletal muscle cell formation and function.

CHAPTER 2

REVIEW OF LITERATURE

This chapter provides a review of the literature related to bone muscle crosstalk. To offer meaningful context, this chapter first presents a review of literature concerning older adults and the aging of the musculoskeletal system. This section includes individual, national and global impact of musculoskeletal aging as well as significant and applicable theories of aging. In order to build toward bone muscle crosstalk, the section following then presents an overview of the current body of knowledge related to the development and function of the musculoskeletal system. Following that, a review of literature pertaining to the primary diseases of the musculoskeletal system; osteoporosis and sarcopenia, is presented. The final section in this review of literature focuses on the interaction between bones and muscles: mechanical communication and biochemical communication. This chapter includes a number of proteins and other factors secreted from bones, muscles and tissues throughout the body. For the purposes of clarity, Appendix A has been prepared with a list of factors, information related to the factors discussed, commonly used abbreviations, notes on their known or suspected functions and key references.

Aging of the Musculoskeletal System

Advances in the prevention and treatment of many diseases have resulted in people living longer than in centuries past. The life expectancy in 1900 was only 47 years; in 1930 it increased to 60 years; and by 2006 the life expectancy from birth had risen to more than 75 years. Looking at this from a slightly different perspective, the percentage of the population aged 65 and older was only 4% in 1900, but nearly tripled to 13% in 2008, and is projected to nearly double again to 22% by the year 2030 (Haber, 2010). This has been reported as the

largest demographic shift in history by experts in fields from finance to sociology (Bloom &

Canning, 2006; Hayutin, Beals, & Borges, 2013). Many factors have contributed to this

increased life expectancy including the development of vaccines and antibiotics, improved

nutrition and processes to better the accessibility of clean water to more of the world's

population. The most recent National Vital Statistics Report published by the National Vital

Statistics System (NVSS) of the US Department of Health and Human Services (USDHHS),

Center for Disease Control and Prevention (2013) listed the life expectancy in the US to be

78.7 years in 2010. At this time, the segment of the U S population experiencing the greatest

increase in numbers is the segment of those who are 65 years of age and older. There has

been a 15.1 percent increase in the number of individuals aged 65 years and older in the last

ten years, compared with a 9.7 percent increase in the total population (U S Department of

Commerce, 2011).

This increasing age and rising life expectancy are, unfortunately, accompanied by an

increase in disability as aging adults experience a decline in physical functioning. In his

article on the preoperative assessment of the older adult, Muravchick (2000) points out the

significant decline in functional reserve that occurs with aging. There are 291 diseases and

injuries on the Global Burden of Disease (GBD) list, and 289 of those are known to cause

disability. In an extensive study, a systematic analysis was undertaken of the prevalence,

incidence, remission, duration and excess mortality of the 1160 sequela of the 289 diseases

and injuries known to cause disability. In this 2010 Global Burden of Disease (GBD) study,

researchers reported that the years lived with disability (YLD) per 100,000 people has

remained relatively constant over the years, but with the increasing population of those who

are 65 years of age and older, the YLD numbers have dramatically increased (Vos et al.,

2012). The seemingly undeniable fact of mortality is that aging is associated with the decline

in function of nearly every biological system in the mammalian body along with the

development of chronic conditions. Recognizing the impact chronic diseases and disorders

have on individual health and healthcare expenditures, several have studied the prevalence of

chronic conditions. The reports align and find that as many as 82% of the older population in

the US has one or more chronic health conditions (McLaughlin, Connell, Heeringa, Li, &

Roberts, 2009; Wolff, Starfield, & Anderson, 2002; Wu & Green, 2000).

One of the systems that experiences significant anatomical and physiologic changes

with aging is the musculoskeletal system. According to the 2010 Global Burden of Disease

Study (GBD), musculoskeletal diseases are the second greatest cause of disability, affecting

billions of people worldwide (Vos et al., 2012). Rubenstein and Josephson (2006) reported

that one in three older adults living in the community falls each year. Among older adults,

fall-related injuries were responsible for more than two million Emergency Department visits

and nearly 600,000 hospitalizations in 2009 (Auron-Gomez & Michota, 2008; Bradley,

2011). Ninety percent of hip fractures are the result of a fall, and the mortality rate one-year

post hip fracture is an astounding 25%. Only one in two older adults that experience a hip

fracture, return to their baseline level of activity (Bradley, 2011). Muscle weakness is a

primary intrinsic risk factor for falls, and the associated morbidity and mortality, especially

hip fractures, is greatly increased among older adults, and is a significant health risk for those

with osteoporosis. In addition to other chronic diseases and medication use, the decline in

musculoskeletal health and function is a growing problem (DiMonaco, Vallero, DiMonaco,

& Tappero, 2011; Haber, 2010; Scott, Blizzard, Fell, & Jones, 2011; Walsh, Hunter, &

Livingstone, 2006). Loss of muscle mass and strength can not only increase the individual's

risk of falls, it impacts the quality of life of older adults. In a review of cross-sectional and longitudinal studies investigating factors contributing to successful aging, Depp and Jeste (2009) reported that in the majority of cases, even the definition of "successful aging" is predicated by the absence of disability.

In addition to the devastating effects sarcopenia and osteoporosis have on the aging individual, the decline in musculoskeletal function poses a significant economic burden. Using prevalence-based, cost of illness methods and data collected from national surveys, Janssen, Shepard, Katzmarzyk, and Roubenoff (2004) prepared an article focused on the economic costs of sarcopenia in the United States. In it, the authors reported that healthcare costs attributable to sarcopenia in the year 2000 were $18.5 billion, or 1.5% of the nation's total direct healthcare costs that year. To provide perspective, they drew from the 1995 Report of the National Osteoporosis Foundation (Ray, Chan, Thamer, & Melson, 1997), adjusted for inflation and other factors to make the dollar values consistent, and reported the costs associated with osteoporotic fractures in the year 2000 were $16.3 billion. These costs included inpatient care, nursing home care, outpatient care, emergency room visits, radiology services, orthopedic medical supplies, and outpatient medications. The percentage of 1.5% would currently translate into more than $40 billion. In spite of such comprehensive considerations, these costs may be conservative, considering that the United States Center for Disease Control and Prevention website, updated in September of 2013, reports the direct medical costs associated with fall-related injuries among the older adult population was $30 billion in 2010, and is projected to climb to nearly $55 billion by the year 2020 (USDHHS, 2013).

Theories of Aging

To develop preventive and therapeutic strategies targeting the devastating effects of a decline in musculoskeletal function, a reasonable starting point is to examine the normal process of aging and its effect on bones and muscles. As with so many aspects of biomedical research, aging presents a bit of a conundrum. A biological organism is, almost by definition, one that is able to repair itself. Aging appears to be the inability of the organism to continue to self-repair, whether the assault is due to trauma, infection, or injury associated with the physiology of living. Many theories of aging have been developed over the years as researchers and clinicians have attempted to explain this paradox. Although they take on varying foci and perspectives, the theories can generally be categorized into those that view aging as a consequence of damage to or an error in the functioning of cells within the body and those that view aging as a pre-programmed process, determined largely by the DNA profile at birth.

Under the broad category of damage theories of aging falls the theory of mitochondrial free radical theory of aging. In 1956, Harman was the first to propose that cellular damage from the presence of toxic free radicals might accumulate and eventually compromise function, to the point of death (Harman, 1956). Although the theory attracted some support early on, it was not until 1972, when Harman modified his proposed theory by adding the hypothesis that the mitochondria could be the source of the free radicals (Harman, 1972), that the theory gained more widespread attention and became known as the mitochondrial free radical theory of aging. The theory has experienced opposition and support from biomedical researchers, which has contributed to its evolution to its current version (Knight, 1998; Miguel, Economos, Fleming, & Johnson, 1980). Researchers who

subscribe to this theory have focused their investigations on the reduction in mitochondrial adenosine triphosphate (ATP) (Drew et al., 2003; Jackson, 2009; Jackson & McArdle, 2011). Oxygen plays a crucial role in the production of ATP by the mitochondria and is necessary for the continuation of life in aerobic organisms. The stress induced from decreased oxygen, cellular hypoxia, leads to the production of mitochondrial reactive oxidative species (mROS). The process by which this occurs is not completely understood at this time, but research has found these mROS to be signaling molecules that serve to decrease the oxygen consumption of the cell. While this function of the mROS appears to be cell-protective and an adaptive response to the stress imposed by hypoxia, these ROS have also been shown to damage macromolecules such as lipids, proteins, and nucleic acids (Drew et al., 2003; Hekimi, Lapoint, & Wen, 2011). Drew and colleagues (2003) also report their findings that aging is associated with a decline in mitochondrial ATP, a state of imposed cellular hypoxia. This supports the mitochondrial free radical theory of aging, which hypothesizes aging to be the result of a vicious cycle in which ROS damage leads to the production of more ROS with its accumulated toxic effects. More recently in the literature, researchers are beginning to report that the toxic effects of the ROS are not due to direct damage, but alterations in cell signaling (Liochev, 2013; Sena & Chandel, 2012). This continues to be an area of focused research, with a growing interest in the role of protein oxidation as a contributing factor in the process of aging (Levine, 2002; Stadtman, 2004). In his recent review article, Poljsak (2011) presents benefits at the cellular level of regular exercise, stress reduction, and nutritional choices.

Another closely related theory of aging that belongs to the damage category is that of immunologic theory of aging. Evidence exists that the effectiveness of the immune system

declines with age (Cefalu, 2011), making the individual more susceptible to infections and the aging process. Recent findings linking chronic diseases such as rheumatoid arthritis and diabetes to autoimmune disorders lend support to this theory of aging (Sener & Afsar, 2012). Diverse in many ways, the theories of aging that belong to the damage or error category share a common allegiance to the second law of thermodynamics: entropy. Entropy simply describes the tendency of everything in the universe to fall into disorder; or, as any parent who has just walked into the room of their teenager will testify; energy is required to maintain order.

One of the most prevalent theories of the pre-programmed category is the genetic theory of aging. This theory has many facets, including the postulation that an individuals' trajectory for aging is a reflection of their genetic blueprint. After birth, the longevity of an individual is either determined by pre-programmed polymorphisms, innate to their own genome; or, as Pucca et al. (2001) suggests, that a chromosome exists on a gene or genes that influences an individuals' longevity. A related theory of aging focuses on the telomere, which is a specific repeating sequence located at the end of a chromosome in the DNA chain. The hypothesis of the telomere theory of aging is that shortening of the telomeres, is associated with accelerated aging (Ceflau, 2011). Fortunately, recent advances in the technological approach to biomedical research are making possible further investigations into these theories of aging.

The process of aging continues to be a complex and multifactorial phenomenon, as evidenced by the nearly 300 theories of aging that have been developed (Medvedev, 2008). And, yet, not one of these theories is accepted by all who work in the field of gerontology. It is therefore important to view the myriad of theories of aging as complementary to one

another, with each possibly providing a portion of the answer to the question, 'how do we age?'

Even without the complete answer to that question, several aspects of aging are quite apparent. With regard to the musculoskeletal system, aging is accompanied by a significant decline both in bone mass and strength (osteoporosis) and in muscle mass and strength (sarcopenia). This combination of conditions poses a tremendous threat to individual safety and is the greatest contributor to disability among older men and women. To develop the most effective therapeutic approaches aimed at preventing falls due to musculoskeletal weakness, it is important to gain understanding of how muscles and bones develop and physiologically respond to aging.

Development and Function of the Musculoskeletal System

Bones

The skeletal system has four components: bones, cartilage, tendons and ligaments. They work together to provide important functions, including support, protection, movement and mineral storage. For the purposes of this literature review, the focus will be on one of the four components of the skeletal system, the bones. Belying its inert appearance, bone is actually a dynamic tissue, which is in a constant state of formation and destruction. Renewed throughout life, it has been estimated that the entire skeleton is replenished on an average of every ten years (Papapoulos & Schimmer, 2007). Bone consists of two parts: extracellular bone matrix and bone cells. Extracellular bone matrix is comprised of approximately 35% organic material, collagen and proteoglycans; and 65% inorganic materials, primarily calcium phosphate. The three types of bone cells are osteoblasts, osteoclasts, and osteocytes. Osteoclasts have a lifespan of about two weeks, during which time they function to

breakdown, or resorb bone. This function is essential for the mobilization of calcium and

phosphate ions needed for metabolic processes throughout the body.   Osteoblasts have a

longer lifespan of about three months and function to promote bone formation. The vast

majority of bone cells are the osteocytes. The functions of these bone cells have been vastly

underestimated in the past. Before the early 1900s, the prevailing view related to bone

physiology was that osteoblasts promoted bone formation and osteoclasts promoted bone

resorption, but that osteocytes were little more than part of the supporting matrix of bones.

At the time, it was widely believed that the functions of osteoblasts and osteoclasts were

primarily influenced by hormones, dietary calcium and other non-mechanical agents, all

aimed at maintaining bone homeostasis (Bonewald, 2011).

In the 1960s, that view was challenged as experts in the field of bone physiology

began to differentiate between bone mineral density and bone strength in their research

findings. Interdisciplinary work hosted by the University of Utah initiated the development

of an impressive body of evidence in support of the biomechanical relationship between

bones and muscles. A refinement of Wolff's Law from the 19th century, this new paradigm

included the mechanostat model, which purports that bone strength and density are largely a

function of imposed mechanical force (Frost, 1996). Even though that model continues to

greatly influence investigations into bone physiology, a small part of the mechanostat model,

has been lost. The promoter of the biomechanical model acknowledged the possible role of

local and systemic nonmechanical agents effecting skeletal architecture. The biochemical

aspect of the relationship between bones and muscles has not until more recently been

explored to any great extent. Perhaps this was due, in large part to the need for a number of

basic research advancements to first be developed, such as innovative techniques, cell lines, and equipment, as well as new knockout and transgenic animal models.

One of the first published evidences that bones could function in an endocrine fashion was the suggestion by Marotti et al. (1992) that osteocytes might play a role in osteoblast modulation by way of gap junction signaling. Additional evidence of this suggestion was provided by studies conducted by Tanaka et al. (1995) demonstrating the production of soluble factors by osteocytes augmented osteoclastic development (Tanaka et al., 1995). Around that same time, Klein-Nulend et al. (1995) conducted experiments that revealed the sustained release of prostaglandins from osteocytes following mechanical stimulation (Klein-Nulend et al., 1995). In addition, in an attempt to explain how bone mass and structure is altered in response to mechanical load, Burger and Klein-Nulend (1999) postulated the presence of cell signaling molecules as a key portion of the cellular mechanisms.

Winkler and associates provided evidence that osteocytes function as more than just a sensory cell, but also as a regulator of bone density through the secretion of sclerostin, a protein that inhibits bone formation (Winkler et al., 2003). They hypothesized that the dysregulation in bone formation resulted from the phenotypes observed in osteosclerosis patients and were further supported through genetic testing and the development of transgenic mice with increased sclerostin production and low bone mass. Since those early observations, continued research by a number of biomedical scientists have continued to provide evidence in support of osteoblast/osteocyte-secreted factors that impact bone homeostasis and also distant tissues such as kidney, prostate, and brain as detailed below (Bonewald & Wacker, 2012; Karsenty & Wagner, 2002; Mo, Romero-Suarez, Bonewald, Johnson, & Brotto, 2012).

In a study conducted by Shimada and colleagues (2004), evidence was reported of the physiological role of FGF23 in phosphate and vitamin D homeostasis as well as the pathophysiological role of FGF23 in osteomalacia (Shimada et al., 2004). In their 2012 review, Bonewald and Wacker discussed FGF23 expression in osteocytes and its role in cardiovascular health (Bonewald & Wacker, 2012). Although the exact pathways through which this occurs is not known at this time, evidence gained from transgenic mice phenotypes demonstrates that osteocyte expression of FGF23 is under the influence of molecules such as DMP1, PHEX and MEPE (Martin et al., 2011).

Osteocalcin is a noncollagenous protein found in bone and dentin. In addition to providing structure, osteocalcin has been shown to have many functions, including energy metabolism, calcium ion homeostasis and male fertility (Karsenty & Wagner, 2002). More than twenty years ago, bone cells were postulated to be the primary source of osteocalcin (Lajeunesse, Kiebzak, Frondoza, & Sacktor, 1991), however recent advances in genetic engineering have allowed deeper insight in support this idea (Ducy et al., 1996; Ducy, Zhang, Geoffroy, Ridall, & Karsenty, 1997; Karsenty, Gerard, & Wagner, 2002; Lee et al., 2007). In fact, osteocalcin along with other hormone-like substances secreted by bone cells are now thought to interact with substances from the liver and adipose tissue that may predispose individuals to obesity, diabetes, non-alcoholic fatty liver disease and osteoporosis. Prostaglandins are a class of naturally occurring lipid autacoids that are derived from arachidonic acid and are produced by most cells, including bone cells. They have a wide range of functions, taking part in inflammation, pain mediation, smooth muscle contraction, and platelet aggregation. Prostaglandins also have been demonstrated to play a significant

role in bone homeostasis, particularly the E and F series of prostaglandins (Agas, Marchetti, Hurley, & Sabbieti, 2013; Mo et al., 2012).

The list of bone cell secreted factors is truly impressive, continues to grow, and includes: ATP, calcium, DKK1, DMP1, FGF23, Mepe, nitric oxide, OPG, osteocalcin, prostaglandins (particularly PGE_2), RANKL, sclerostin, and Sost. These factors represent a myriad of biochemical structures ranging from simple organic molecules to complex proteins, which illustrates the plasticity of bone secretory capacity. Furthermore, the diversity of factors implies the role of bones in the modulation of the physiology of tissues throughout the body (Karsenty & Ferron, 2012). As the understanding of these new discoveries continues to develop and begins to be translated into meaningful and innovative therapeutic approaches, unprecedented advances will be achieved in the fight to constrain the epidemics of chronic diseases such as obesity, diabetes, osteoporosis and sarcopenia.

Muscles

Skeletal muscle is so named for its functional connection and vicinity to the skeletal system. It is responsible for voluntary movement, facial expressions, postural support, and respiratory expansion. It is functionally connected to the skeletal system and also works with the nervous system and blood supply. Skeletal muscle develops from myogenic precursor cells and myoblasts to myotubes through the process of myogenesis. This process provides a predictable sequence of events with a definable end product as well as clear morphologic and functional changes along the way (Burattini et al., 2004; LeGrand & Rudnicki, 2007; Wagers & Conboy, 2005). The precursor of the muscle cell is either the mesoderm-derived structure in embryonic development or the quiescent satellite cell awaiting activation as a myoblast. Myoblasts are small, mononucleated cells capable of either dividing by mitosis and

proliferating, or fusing with other myoblasts to form myotubes. As myoblasts fuse and begin to form myotubes, they enlarge and take on an elongated shape. Myogenesis occurs not only in the embryonic and early stages but also throughout the lifespan. Skeletal muscle is a dynamic tissue, whose cells undergo myogenic differentiation repeatedly as muscles regenerate in response to injury (Nag & Foster, 1981; Shefer, Van de Mark, Richardson, & Yablonka-Reuveni, 2006).

The process that leads to muscle contraction begins when acetylcholine (Ach) is released by a motor neuron across the synapse at the neuromuscular junction. Motor neurons originate in the central nervous system and the cell bodies of these neurons are located in the spinal cord. The neuronal fiber (axon) projects outside the spinal cord to directly or indirectly control muscles. At the muscle level, nerve ending terminals spread and innervate each muscle fiber within a given skeletal muscle. Each muscle fiber is covered by a membrane called the sarcolemma, and within each muscle fiber are thousands of sarcomeres, which are the functional units of contraction. The sarcomere is composed of thick myofilaments called myosin, and thin myofilaments called actin. The neuromuscular junction is a synapse with the terminal end of the motor neuron on one side and the motor end plate of a skeletal muscle fiber on the other. Release of Ach from the motor neuron causes stimulation of a muscle fiber through the exchange of sodium and potassium ions. This leads to the generation of an action potential that spreads along the sarcolemma and is transmitted into the interior of the muscle fiber by structures called transverse tubules, or T-tubules. T-tubules are juxtaposed to the calcium ion storage units, the sarcoplasmic reticulum (SR). As the action potential travels along the T-tubule, it causes the voltage-sensitive receptor named Dihydropirydine Receptor (DHPR) to change shape, and it is this

allosteric modification of the DHPR that allows it to physically interact with the largest

known mammalian channels, the Ryanodine Receptors (RyR) precisely located on the

surface of the membrane of the SR. This DHPR-RyR contact, leads to the opening of the

RyR, which brings about the release of calcium from the SR into the cytosol of the skeletal

muscle cell. This rise in cytosolic calcium causes the binding sites on the actin filament to be

exposed, allowing myofilaments heads to bind. The myosin filaments pull the actin

filaments in, resulting in a shortening of the sarcomere. It is the shortening of sarcomere

throughout the muscle fibers that causes muscle contraction. The process by which the

electrical stimulation, or excitation is transferred into a mechanical contraction is called the

excitation-contraction coupling (ECC). This process is fundamental to skeletal muscle

physiology (Hopkins, 2006; MacIntosh, Gardiner, & McComas, 2006) and is the cellular and

molecular reason that can be executed from very fine controlled movements to the lifting of

several hundred kilograms of weight.

Much has also been learned about the important relationship that exists between

skeletal muscles and nerves, since motor neurons and the muscle fibers they innervate first

came to be viewed as a single functional unit in the 1920s. After Henry Dale and Otto Loewi

were awarded the 1936 Nobel Prize for their discoveries relating to chemical transmission of

nerve impulses, the body of knowledge continued to grow leading to an enhanced

understanding of differing muscle fiber types. The idea of the motor unit continues to be

strengthened as instruments enabling molecular and genetic exploration to be undertaken.

Investigations into muscle-to-nerve trophism led to the discovery of factors such as brain-

derived neurotrophic factor (BDNF), NT-3 and NT-4/5 (Gomez-Pinilla, 2002; Hirokawa,

Niwa, & Tanaka, 2010). Discoveries in these areas continue to provide potential therapeutics

for patients suffering from neuromuscular disorders such as the muscular dystrophies.

In the late 1970s, evidence emerged that skeletal muscle, as well as most tissues in

the body, secret prostaglandins in response to injury, as Goldspink testified to the importance

of skeletal musculature in terms of its metabolic effect on the body (Goldspink & Goldspink,

1986). However, it was only during the last decade that skeletal muscles became recognized

more fully for their secretory capacity (Barton, 2006; Florini, Ewton, Magri, & Mangiacapra,

1993; Kurek et al., 1997). Pedersen and colleagues were the first to use the term,

'myokines,' after their discovery that contracting muscles not only secrete IL-6, but that it

leads to a significant increase in IL-6 plasma levels. Building on earlier evidence from

murine models that IL-6 is produced by myoblasts and myofibers in response to

inflammation and injury, the Pedersen group showed that working muscles led to a 19-fold

increase in arterial plasma IL-6 concentrations compared to resting muscle (Pedersen et al.,

2003; Steensberg et al., 2000). This provided valuable evidence of skeletal muscle producing

factors that impact not only tissues in close proximity, but also those at distant sites in the

body. To support this it was important to rule out that the IL-6 productions and secretion is

not coming from immune cells. A notable observation has been made that with sepsis, there

is an increase in TNFα, followed by an increase in IL-6. In sepsis, it appears that monocytes

are the primary source of the increased TNFα. This is in contrast to the increase in IL-6 that

accompanies exercise, as it is not preceded by TNFα (Andersen & Pedersen, 2008). Keller

and colleagues demonstrated that the nuclear transcription rate of IL-6 increased markedly

and rapidly with the onset of exercise (Keller, 2001). Further evidence indicated that the IL-

6 produced by exercising muscles impacted the output of hepatic glucose, thus adding

strength to the premise that skeletal muscles do, indeed, function as endocrine organs (Glund, et al., 2007; Kim, et al., 2004).

In 2007, Chan, et al., identified more than thirty proteins expressed during the highly organized and predictable process of muscle development. They performed quantitative proteomics to explore the activity of myoblasts and myotubes throughout myogenesis. The list of factors secreted from skeletal muscles continues to grow, and includes IL-8, which has been shown to increase angiogenesis (Nielsen & Pedersen, 2007); IL-5, which is an anabolic factor being investigated for its role in muscle-fat crosstalk; IL-7, which is being studied for its impact on satellite cells during myogenesis (Pedersen, Akerstrom, Nielsen, & Fischer, 2007), and brain-derived neurotrophic factor (BDNF) (Matthews et al., 2009). Exercise has been found to induce a six-fold increase in mRNA of Chemokine CXC motif ligand-1 (CXCL-1) aka KC (keratinocyte-derived chemokine) and a 2.4-fold increase in serum CXCL-1 (Pedersen, Olsen, Pedersen, & Hojman, 2012). Murine CXCL-1 is a functional homolog for IL-8, and belongs to a group that has gained attention for its role in inflammation, chemotaxis, angiogenesis, neuroprotective activity and tumor growth regulation and is also associated with a decrease in visceral fat (Acharyya, et al., 2012; Addison, et al., 2000; Hol, Wilhelmsen, & Haraldsen, 2009; Rubio & Sanz-Rodriguez, 2006; Wang, Hamza, Wu, & Dionne, 2009).

Most research associated with skeletal muscle secreted factors is in relation to factors produced in response to injury. IL-6 and LIF are produced and have been shown to enhance the myocyte differentiation after injury. Muscle regeneration is an ongoing phenomenon throughout the life span, and provides an excellent opportunity for investigation into the endocrine function of this organ, as well as hope for targeted interventions to slow the

process of muscle wasting. Two additional factors secreted by injured skeletal muscle are TGFα and TGFβ1 (Kurek, Bower, Romanella, Koentgen, Murphy,F & Austin, 1997; Li & Huard, 2002). These factors have an inhibitory effect on muscle cell proliferation and differentiation. It is believed that TGFβ1 triggers connective tissue proliferation and tissue fibrosis. The worldwide epidemics of obesity and diabetes type 2 continues to propel the concept that lack of exercise might favor an unbalance or reduced secretion of myokines, thereby contributing to these chronic diseases (Pedersen, Olsen, Pedersen, & Hojman, 2012). Last year, a new myokine brought hope for the development of molecules to target fat tissue accumulation, since irisin was shown to regulate the conversion of 'bad' (white) fat into 'good' (brown) fat that is essential for thermogenesis in mice (Seale et al., 2008). Since the original publication, 49 papers have been published on effects of irisin and a recent study by Park (2013) concluded that irisin might be directly associated with a higher risk of cardiovascular diseases and metabolic syndrome in humans, suggesting that augmented secretion of irisin by either adipocytes or muscle cells might occur to overcome an underlying irisin resistance (Park et al., 2013).

Diseases of the Musculoskeletal System

Osteoporosis

As stated earlier, bones are in a constant state of destruction and rebuilding. In young, healthy individuals, the balance between bone formation and resorption is maintained. The decrease in bone density that has come to be known as osteoporosis appears to be the result in a growing imbalance of these two processes. The body of knowledge surrounding osteoporosis continues to grow and develop as it is now recognized as the most common metabolic bone disease in the United States. Age related bone loss has afflicted mankind for

centuries (Zaki, Hussein, & Abd El-Shafy El Banna, 2009). However, the first

documentation of osteoporosis has been attributed to the English surgeon, Sir Astley Cooper,

who kept meticulous notes on his observations. Cooper observed significant changes in the

bones of older adults:

> "with respect to the neck at the thigh-bone, a very principal cause of con-
> consolidation by bone is the advanced age at which it becomes obnoxious to fracture
> through that peculiar change which the part undergoes at this period of life without
> any apparent cause, but which renders it incapable of sustaining the superincumbent
> weight, and even in the continuity insufficient to maintain its function; therefore it
> may be fairly supposed, when broken incompetent to set up a restorative action"
> (Cooper, 1844, p.136).

The actual term, *osteoporosis* is attributed to the French pathologist, Jean Lobstein,

although, in retrospect, it seems likely that he was actually using the term to describe

osteogenesis imperfecta rather than osteoporosis (Schapira & Schapira, 1992). In 1941, the

American endocrinologist, Fuller Albright described his observation of postmenopausal

osteoporosis and proposed the idea that the decreased bone density was due to an estrogen

deficiency (Albright, Smith, & Richardson, 1941).

A simple PubMed search with the single term, osteoporosis, yields a staggering

61,164 results. The first publication listed in this search is from 1967, during which year

PubMed reveals 246 publications related to osteoporosis. This annual number of

publications remained remarkably stable until a slow, but steady rise in began in 1982 with

340 published articles. Since the mid-1990s, the annual number of publications related to

osteoporosis has never been less than 1000, with a remarkable 3151 listed before the end of

2013. The spike in publications coincides with the time that the World Health Organization

(WHO) introduced the definition of osteoporosis. According to the WHO criteria,

osteoporosis is defined as a bone mineral density (BMD) that falls greater than or equal to

2.5 standard deviations (SD) below the average value for young healthy women (WHO, 1994).

The risk of osteoporosis is higher among women than among men. The literature has established several additional risk factors for osteoporosis including increased age, Caucasian or Asian ethnicity, postmenopausal status, late menarche or early menopause, low peak bone mass, a family history of osteoporosis or low trauma fracture, low dietary calcium, vitamin D and vitamin K, low levels of physical activity, smoking, excessive alcohol intake and the use of certain medications such as steroids, anticonvulsants, immunosuppressants, and heparin (Cummings et al., 1993; Schwartz, Nevitt, Brown, & Kelsey, 2005; Taylor et al., 2004; Vermeer, Knapen, & Schurgers, 1998; Versluis et al., 2001).

Treatment plans for patients diagnosed with osteoporosis are related to the identified risk factors. The initial approach begins with lifestyle modification such as increased physical activity if possible as well as smoking cessation, and decreasing alcohol intake, if needed (Body et al., 2011; Habib, Eshra, & Dawood, 2012). Beyond these lifestyle medications to reduce the risk of injury, treatment goals are aimed at slowing or stopping bone loss and/or facilitating bone formation. Supplementations often recommended include calcium, vitamin D, and, in some cases, hormone replacement therapy (Rizzoli et al., 2008). The primary pharmacologic intervention is the classification of bisphosphonates, which have revolutionized the treatment of osteoporosis. Interestingly, bisphosphonates have been known as chemical entities for the past 100 years, as they have been widely used as industrial water softeners. Their introduction into the clinical realm was due to work conducted by Fleisch in the late 1960s (Fleisch, Graham, Russell, & Francis, 1969). At that time, and for the decade following, their primary use in the clinical setting was to treat Paget's disease.

Bisphosphonates inhibit osteoclast activity. They do this by binding to surfaces that are experiencing active bone resorption, which thwarts the osteoclasts attempt to form a ruffled border and continue the bone resorptive activity. It was through the work of Bijvoet and, in another area, van Breukelen that eventually ushered the use of these pharmacologic agents into the management of osteoporosis (Valkema, Vismans, Papapoulos, Pauwels, & Bijvoet, 1989; Van Breukelen, Bijvoet, & Van Oosterom, 1979). Bisphosphonates have been shown to have a protective effect on bone density, with effects noted even within the first week of administration. Research has demonstrated a reduction in biomarkers of bone resorption by as much as 90% early on in the course of administration (Christiansen et al., 2003). In spite of the identification of many risk factors for osteoporosis, and the success of such interventions as the bisphosphonates, osteoporosis continues to pose a significant risk to older adults.

Sarcopenia

Skeletal muscle represents the largest organ in the human body, accounting for 38% and 31% of the total body weight in the men and women, respectively (Janssen & Ross, 2005). Therefore, the age-related anatomical and physiologic changes in skeletal muscle have a significant impact on the overall health of the individual. Irwin Rosenberg first proposed the term 'sarcopenia,' in 1988 to describe age related muscle wasting. The term derives from the two Greek words, *sarx* (flesh) and *penia*, (loss). All individuals experience muscle wasting with age, therefore the prevalence of sarcopenia with age is essentially 100%. However, Rosenberg and others recognized that in many, the muscle loss that accompanied aging happened at a seemingly accelerated rate and contributed significantly to disability (Rosenberg, 1989). In 1988, a group of researchers and clinicians convened for a

meeting in Albuquerque, New Mexico to discuss various measurements being used to assess the health and nutritional status of the elderly population. It was in a summary report following that historic meeting that Rosenberg first coined the term, 'sarcopenia.' Part of his rationale for coining the term was to draw attention to this all too common physiologic phenomenon, for as mentioned elsewhere in this review of literature; age-related changes in the musculoskeletal system are one of the most frequent causes of disability. Since the time that Rosenberg proposed the term, sarcopenia, much research has been conducted into the process and effects of age-related skeletal muscle wasting. A recent PubMed search with sarcopenia as the only term entered, yielded 2113 results, beginning in the year 1993. Interestingly, this does not include Rosenberg's 1989 summary comments. The number of published articles prior to the year 2000 was a mere 75, according to this PubMed search; 237 articles in the years 2000 through 2004; 535 articles in the years 2005 through 2009; and 1266 articles cited from 2010 through November of 2013. These numbers reflect both the growing acceptance of sarcopenia as a condition with specific and measureable signs and symptoms as well as the recognition of the significance this condition has in the lives of individuals, the nation and the world.

In the mid-1990s, the measurement used to identify the presence or absence of sarcopenia among older adults, whether in the community or institutional setting, was upper-arm circumference. Even with this crude method of identification, researchers recognized a correlation between the presence of sarcopenia and the older adults' mortality risk (Muhlethaler, Stuck, Minder, & Frey, 1995; Protho & Rosenbloom, 1995). In 1998, Baumgartner and his team suggested a modified approach to determining whether the muscle mass in an older adult was within normal limits, or whether it reflected a state of

compromised health, i.e. sarcopenia. From the research he and his colleagues were conducting on older adults, Baumgartner defined sarcopenia as a height adjusted to muscle mass of two standard deviations (SD) or more below the mean of a young reference population. With this as his measurement, he reported the prevalence of sarcopenia in the New Mexico Elder Health Survey to be 14% in those 65 to 69 years of age, compared with greater than 50% in those 80 years of age and older (Baumgartner et al., 1998). Other researchers in the field of gerontology adopted this measurement standard in their investigation of age-related loss of muscle mass. Nearly all of the studies conducted prior to 2005 were cross-sectional, and focused on a correlation between sarcopenia and not only decreased muscle mass, but also the associated functional impairment leading to physical disability (Janssen, Heymsfield, & Ross, 2002; Morley, Baumgartner, Roubenoff, Mayer, & Nair, 2001; Newman et al., 2003; Roubenoff & Castenada, 2001; Vandervoot & Symons, 2001). At least one study in the early 2000s looked at the impact of muscle size and strength over time. Following a sample of 120 adults aged 46 to 78 for a period of ten years; Hughes et al. (2001) reported a less than 5% change in strength that was attributable to a corresponding change in muscle size. In an eight-year follow up to the Cardiovascular Health Study, Janssen (2006) reported a 27% increased risk of developing disability with sarcopenia when compared with individuals with normal muscle mass. Interestingly, at the beginning of that same study, the reported likelihood of having disability was 79% greater in those with severe sarcopenia than in those with normal muscle mass. The longitudinal analysis was three times smaller than the cross-sectional analysis, reported at the baseline. This suggests that the sarcopenia-associated risk of functional impairment and physical

disability reported in cross-sectional studies of older adults in the early 2000s may have been overestimated.

The questions surrounding a universally accepted definition of sarcopenia continue even to today. Ultimately, clinicians and researchers are in search of specific age-related musculoskeletal changes that correlate most strongly with the risk of disability. Evidence is growing that the rate at which muscles become weaker is much faster than the rate at which they become smaller (Mitchell et al., 2012). Subsumed in the concept of muscle strength are important considerations such as fatigability, power and force of contraction, all of which confound the overall question. Researchers are finding that it is the loss of muscle strength, even more than the loss of muscle mass, that carries the greatest risk of disability in the aging adult (Goodpaster et. al, 2006; Manring, Abreu, Brotto, Weisleder, & Brotto, 2014; Mitchell et al., 2012).

Baumgartner reported in 2000 his observations that as many of 15% of individuals with sarcopenia are also obese. The sarcopenic-obese older adult drew his attention because in his cross-sectional study examining older adults in the New Mexico Aging Process Study, he found this subsector of the elderly population to be at especially high risk of physical disability (Baumgartner, 2000). Jensen and Friedmann (2002) reported similar findings of an increased risk among obese older adults. As researchers and clinicians even more fully appreciate the risk to independence and safety posed by the decline in both lean muscle mass and bone density with increasing age, the body of knowledge related to these phenomena continues to grow. Studies have shown an increase in catabolic cytokines such as interleukin-6 (IL-6), as well as inflammatory markers such as C-reactive protein and sedimentation rate (Roubenoff, 2007; Roubenoff & Hughes, 2000; Zoico & Roubenoff,

2002). These same factors are not only observed in the development of obesity; many are of secreted by adipocytes (Roubenoff, 2008; Schrager et al., 2007). Findings such as these motivate additional investigation into connections between sarcopenia and obesity. Some research findings supported an increase risk in disability when sarcopenia and obesity occur together (Baumgartner, 2000; Jensen & Friedman, 2002). However, research conducted by others at that time did not support the notion that sarcopenic-obese older adults are at greater risk for physical disability (Davison, Ford, Cogswell, & Dietz, 2002; Zoico et al., 2004). In 2004, a group of researchers set out to replicate as a longitudinal study, the findings of their 2000 cross-sectional study, based upon the same cohort of individuals in New Mexico (Baumgartner et al., 2004). They reported that looking at the problem over time, that neither sarcopenia alone nor obesity alone increased the older adult's risk of functional impairment when compared with those with a normal body composition. However, they found that those sarcopenic-obese individuals had a 2.5 times greater risk (Baumgartner et al., 2004). Perhaps related to these findings, Lammes and Akner (2006) also reported that, as expected with a reduced skeletal muscle mass, the presence of sarcopenia leads to a decrease in resting metabolic rate. Since the mid-2000s, several researchers have investigated the combination of sarcopenia and obesity, specifically concerned with the risk for physical disability. The findings of some support an increased risk of physical disability in sarcopenic-obese older adults (Bouchard & Janssen, 2009; Janssen, 2007; Rolland et al., 2009), while the findings of other researchers do not support this notion (Bouchard, Dionne, & Brochu, 2009; Choquette, et al., 2010).

Attempts to understand the cause of age related loss of muscle mass and strength have predominantly focused on the loss of skeletal muscle fibers, especially type II fibers. In an

exquisite review of the pathophysiological mechanisms of sarcopenia, however, Walrand, Guillet, Salles, Cano, and Boirie (2011) delve into a wide variety of mechanisms involved including nutritional factors, activity levels, alterations in protein metabolism, and the impact of changing levels of hormones. In that review the authors suggested that sarcopenia impacted the development of other chronic conditions such as cardiovascular and metabolic diseases. These researchers were observing that sarcopenia apparently leads to dyslipidemia, insulin resistance and hypertension as well as a decline in immunologic function (Cosqueric et al., 2006; Karakelides & Nair, 2005).

Another point of view that is gaining momentum is that age-related decreases in muscle strength result from a combination of loss of muscle mass (atrophy) and reduced muscle specific force (i.e., muscle force per unit of cross-sectional area), suggesting reduced muscle quality. However, accumulating data show that it is principally the weakness that accompanies sarcopenia, not the loss of muscle size *per se*, that contributes to disability (Clark & Manini, 2008; Goodpaster et al., 2006; Hughes et al., 2001; Visser et al., 2000). For example, in one four-week study of muscle unloading in young adults, researchers observed a greater loss in strength than loss in muscle mass (Clark, Fernhall, & Ploutz-Snyder, 2006). These scientists, along with others, suggest the un-matching in loss of mass that is significantly surpassed by the loss of force and power originates inside the muscle fibers themselves, due to defects on the ECC process that ultimately lead to reduced availability of calcium to be released during each cycle of contraction-relaxation (Clark et al., 2006; Manring et al., 2014).

Additional health risks that have been observed in sarcopenic older adults include insulin resistance and the development of type 2 diabetes mellitus. Srikanthan, Hevener, and

Karlamangla (2010) conducted a study to investigate the relationship between sarcopenia, obesity and age-related insulin resistance. In their cross-sectional analysis of the National Health and Nutrition Examination Survey III (NANES III), they concluded that sarcopenia, independent of obesity, is associated with compromised glucose metabolism. Another study conducted around the same time concurred that type 2 diabetes was associated with an increased risk of sarcopenia (Kim et al., 2010). This suggests a relationship between diabetes and sarcopenia that skeletal muscle represents the largest target tissue for insulin-mediated glucose uptake. A decline in muscle mass with aging is, therefore, associated with a decrease in sites for glucose uptake, which would be further exacerbated by a decline in physical activity. Along with this, data support an increase in triglycerides with aging, which have been indicted both in age-related mitochondrial damage and with blocking of ability of insulin to facilitate glucose entry into the muscle cell. All of these phenomena contribute to an increase in blood glucose. Insulin may play a significant role in all of this, as it is a potent anabolic hormone that impacts glucose, protein and lipid metabolism. It facilitates glucose uptake, inhibits hepatic glucose uptake and triglyceride production, inhibits skeletal muscle protein synthesis and inhibits adipose tissue lipolysis (Magkos, Wang, & Mittendorfer, 2010). Recognizing this relationship, a recent study by Lee et al. (2011) provides data supporting a direct relationship between insulin resistance, the loss of lean muscle mass and the gain of fat mass in men aged 65 and older. The chronic complications of diabetes mellitus impact systems throughout the body; including bones. Individuals with type 1 diabetes mellitus have lower bone mass density, with impaired bone formation believed to be the primary cause (Hofbauer, Brueck, Singh, & Dobnig, 2007). Patients with either type 1- or type 2-diabetic patients experience hypercalciuria during times of glycosuria. This

increased loss of calcium has been hypothesized to contribute to impaired bone quality

observed with diabetes, although the direct effects of this loss of calcium on skeletal muscle

function remains elusive. As more is understood about these chronic conditions, the

connections between them are becoming undeniable. Recognizing these connections and

conducting research from this multifactorial perspective will increase understanding and

further the development of interventions.

<center>**Communication of the Musculoskeletal System**</center>

Bone-Muscle Crosstalk

The mechanical relationship between bones and muscles has been extensively

studied, and it can be observed and understood in the context of the three major ontogenetic

periods in the bone-muscle relationship; embryonic patterning, postnatal allometric growth,

and the homeostatic relationship of adult life (Orestes-Cardoso et al., 2001). Bones and

muscle cells not only share a common mesenchymal precursor, but also experience

organogenesis through a tightly orchestrated network of genes during intrauterine

development. The commonalities between these two tissues are reinforced through the

mechanostat theory that postulates loads that create strains below a certain threshold

stimulate bone loss through the inhibition of growth, while strains above a certain threshold

stimulate growth and inhibit haversian remodeling (Pearson & Lieberman, 2004). Some

researchers refer to the 'bone-muscle unit' in deference to these observations that bones

respond to varying levels of mechanical strain imposed by muscle mass and strength. The

varying levels of mechanical strain appear to be modulated primarily by hormonal effects

systemically, citing gender differences over time as evidence (Lang, 2011). There is

<center>33</center>

undeniably much evidence in support of the strong correlation between bone and muscle strength (Wang et al., 2007; Zanchetta, Plotkin, & Filgueira, 1995).

A deeper understanding of the physiological relevance of these bone and muscle endocrine properties may serve to bridge the gap between the mechanical and biochemical theories of bone-muscle interaction. A feasible way of interpreting the role of these interactions is that they may serve to sense and transduce biomechanical signals such as unloading, loading, inactivity, or exercise, and even perhaps the translation of systemic hormonal stimulation into effective biochemical signals. Another way of interpreting and bridging these two theories is that one specific form of interaction could work as a priming for the other, in that, the physical effects of contraction on bone cells may prime these cells for the simultaneous, consecutive or ulterior effects of a secreted molecule. The growing evidence of a mismatch between changes in muscle mass and muscle strength that accompany muscle unloading also lends support to the biochemical communication between tissues (Clark et al., 2006). The suggestion that in addition to mechanical force, other factors contribute to increasing muscle strength came more than three decades ago. In their work with isometric training, McDonagh and colleagues (1983) made experimental observations that led them to postulate "that the increase in the force of maximal voluntary isometric contraction must be related to factors other than the force-generating capacity of the muscle fibres themselves." (McDonagh, Hayward, & Davies, 1983, p. 355).

The close anatomical proximity of skeletal muscle and bone lends itself to hypothesize a relationship of paracrine nature, especially at the muscle fiber insertion sites along the periosteal interface. For evidence of such a relationship, we turn our attention to pathology and reflect upon conditions such as some of the bone stress syndromes where

inflammation localized to the muscle area underneath the periosteal region spreads into the bone itself. These situations are consistent with the paracrine relationship hypothesis, suggesting inflammatory molecules from adjacent muscle fibers may penetrate into this region of the bone. Another powerful clinical example of this paracrine relationship is the application of muscle flaps around compounded bone fractures and their effects in promoting significantly faster healing for these fractured bones. Although the specific molecular mechanism of action is not completely understood, the introduction of muscle flaps has been used as a successful therapeutic approach to treat chronic osteomyelitis and to accelerate the healing of bone fractures (Chan, Harry, Williams, & Nanchahal, 2012). These mechanisms might display further and specific importance during bone and muscle healing after musculoskeletal injury. Studies performed by our group in osteocyte and muscle cell lines, have determined that PGE_2 secretion from osteocytes is more than 1000 times larger than PGE_2 secretion from muscle cells. This excess amount of PGE_2 from osteocytes could interplay with injured muscles, which would aid in muscle regeneration and repair. Recent *in vitro* studies from our lab have provided support for a role of osteocyte secreted PGE_2 in aiding with the process of myogenesis (Mo et al., 2012).

To gain further insight into bone-muscle crosstalk, it is helpful to examine the phenotypic presentations of recently developed transgenic animal models. Myostatin was discovered in the late 1990s to be a potent inhibitor of muscle growth. It is expressed during development and in adult skeletal muscle, serving as an important negative regulator of skeletal muscle growth (Jouliaekaza & Cabello, 2007; McPherron, Lawler, & Lee, 1997). Myostatin appears to decrease myoblast proliferation. The myostatin-deficient mouse model has increased muscle size and strength, with individual muscles weighing significantly more

than wild type mice (Zimmers, 2002). Hamrick and collaborators used this myostatin deficient mouse model to investigate the effects of increased muscle mass on bone mineral content and density. They found that although a consistent correlation was not found in all regions of the skeletal system, there was increased cortical bone mineral density in the distal femur and an increased periosteal circumference along the humerus (Hamrick, 2003; Hamrick, McPherron, & Lovejoy, 2002; Hamrick, Samaddar, Pennington, & McCormick, 2005). Another group used the same myostatin-deficient mouse model to look at the impact of the chronic loss of myostatin on multiple organ systems and found that it appeared to preserve bone density (Morissette et al., 2009). From a contrasting perspective, Zimmers investigated the effects of myostatin overexpression in an animal model and observed a profound loss of muscle and fat, mimicking the presentation seen in chronically ill patients and commonly referred to clinically as cachexia (Zimmers, 2002). The authors encourage further research into the disruption of myostatin in an effort to preserve muscle mass in patients with chronic diseases.

As mentioned earlier, osteocalcin serves as a splendid example of the endocrine function of bone cells (Karsenty & Ferron, 2012). This osteoblast-derived factor, circulating levels of which increase with exercise, is not only effectively secreted by osteoblasts, but also affects distant tissues through the activation of its receptor, GPRC6A, in cells such as adipocytes, pancreatic β cells and Leydig cells of the testis. Perhaps to balance the physiologic scales, osteoblasts also naturally express the osteotesicular phosphatase gene (*Esp*), which inhibits the function of osteocalcin (Coiro et al., 2012). With this information in mind, it is of specific interest to the discussion of bone-muscle crosstalk that *Gprc6a* knockout mice display the phenotype of decreased muscle mass, while *Esp* knockout mice

have increased muscle mass. Through these observations, it can be proposed that

osteocalcin, a known bone cell factor, may play a role in the regulation of muscle mass. This

new knowledge could contribute to a better understanding of sarcopenia, and this osteoblast-

derived factor could be a target for the development of therapies to prevent, delay or slow the

progression of this highly prevalent disorder associated with aging. If this is useful for

sarcopenia, it is possible that it will also be useful for its associated disorder, osteoporosis.

CHAPTER 3

THEORETICAL FRAMEWORK AND METHODOLOGY

This study is an *in vitro* case-control trial in which the myogenesis of human skeletal muscle cells bathed in media containing serum from patients with osteoporosis was compared with the myogenesis of human skeletal muscle cells bathed in media containing serum from patients without osteoporosis.

Theoretical Framework

The skeletal myogenesis model provides the conceptual framework for this study. Skeletal muscle develops from myogenic precursor cells. Myoblasts proliferate in response to factors; some of which have been identified and many of which continue to be discovered. Proliferation continues until the myoblast exits the cycle of proliferation and begins differentiation into myotubes. Different factors continue to be identified as facilitators of differentiation. This process provides a predictable sequence of events with a definable end product as well as clear morphologic and functional changes along the way (Burattini et al., 2004; Le Grand & Rudnicki, 2007; Wagers & Conboy, 2005). The precursor of the muscle cell is either the mesoderm-derived structure in embryonic development or the quiescent satellite cell awaiting activation as a myoblast. Myoblasts are small, mononucleated cells capable of either dividing by mitosis and proliferating, or fusing with other myoblasts to form myotubes (Figure 1). As myoblasts fuse and begin to form myotubes, they enlarge and take on an elongated shape. Myogenesis occurs not only in the embryonic and early stages but also throughout the lifespan.
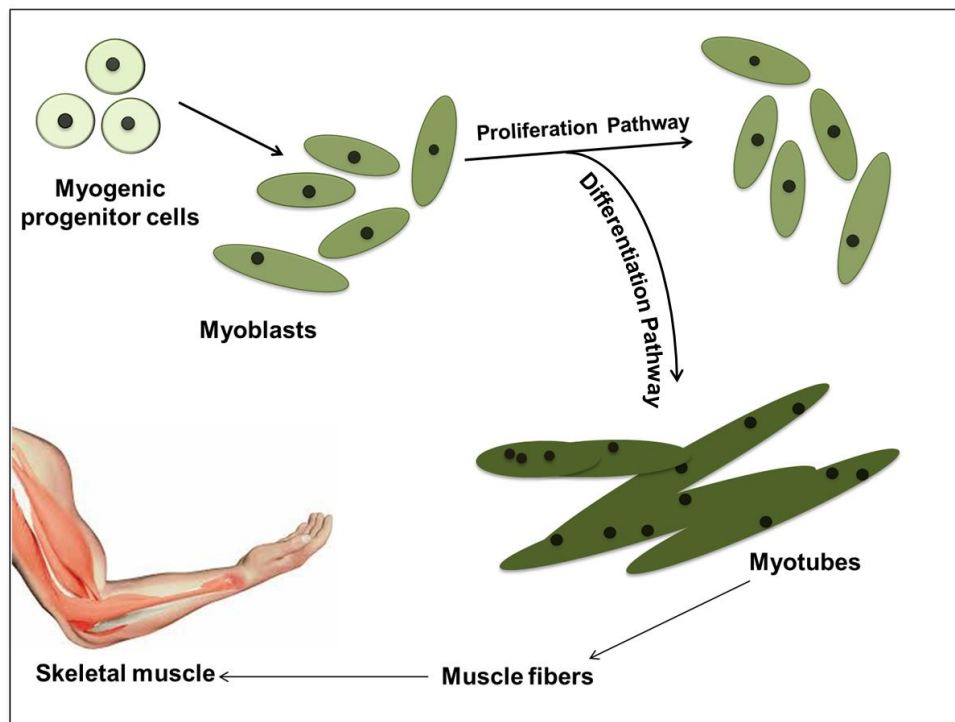
Figure 1. Skeletal Muscle Cell Myogenesis Model

Skeletal muscle is a dynamic tissue, whose cells undergo myogenic differentiation repeatedly as muscles regenerate in response to injury (Nag & Foster, 1981; Shefer, Van de Mark, Richardson, & Yablonka-Reuveni, 2006). Genes, proteins, ligands and other factors all play a role in determining the timing and route each myoblast will take along the path to differentiation (Burattini et al., 2004; MacIntosh, Gardiner, & McComas, 2006). Insight into just how these factors communicate with muscle cells and impact myogenesis is provided by an overview of cellular signaling pathways. A practical application of the Bertalanffy's (1969) General Systems Theory (GST), mammalian physiology demonstrates repeatedly how

systems are in constant communication with one another. According to the GST, a system is

a "complex of interacting maintaining entity or process." (Bertalanffy, 1969, p. 55). Russell

Ackoff (1981) identified three predominant propositions of this theory. He stated that within

a system: 1) each element has an effect on the functioning of the whole, 2) each element is

affected by at least one other element in the system, and 3) all possible subgroups of the

elements also have the first two properties.

These propositions provide an exquisite reflection of mammalian physiology, and in

this way pertain directly to this dissertation study, providing the framework that guides the

investigation into bone-muscle crosstalk, especially in the presence and absence of

osteoporosis. One of the primary ways the various elements, or systems within the body

affect one another is at the molecular level, through the signaling pathways that regulate

nearly all functions (Rappolee & Armant, 2009). Cells communicate in three ways: with

distant tissues via the circulatory system (endocrine); with one another, via cell-to-cell

communication (paracrine); and within the cell itself, intracellularly (autocrine) (Campbell &

Reece, 2004). The presence of factors produced by specific tissues, such as bones and

muscles, as well as these cell-signaling pathways offer further support for the framework for

this research. Bonewald (2011) and others who have recognized bone cells to be the source

of factors that regulate physiologic changes locally and in distant tissues (Bonewald, 2011;

Bonewald & Wacker, 2012; Mundy, 1993).

Aging brings about many physiologic changes in the body. Two well-defined

changes that occur with aging are a decrease in muscle size and strength (sarcopenia) and a

decrease in bone density and strength (osteoporosis) (Arnold, Egger, & Handschin, 2011;

Evans & Campbell, 1993). Literature supports the identification of factors produced by

muscle cells and by bone cells (Abreu et al., 2012; Arnold et al., 2011; Bonewald, 2011).

Additionally, evidence exists that factors secreted from bone cells change with aging

(Hamrick et al., 2006). As mentioned, research has already demonstrated that factors from

muscles impact bone cells (Jähn et al., 2012), and preliminary findings demonstrate that

factors from bones impact skeletal muscle cells (Mo et al., 2012). One-way to further

explore the presence of factors from bone impacting skeletal muscle cells is to compare

muscle formation in the presence of factors from healthy bones with muscle formation in the

presence of factors from osteoporotic bones. Thus, this dissertation study addressed the

myogenesis of human skeletal muscle cells under these two conditions.

Step 1: Each well/ dish was labeled and seeded with 35K HSMM cells bathed in 2 ml Growth Media, SkGM™-2.

After 24 hours acclimation, 1% serum sample was added to the corresponding well/ dish.

Media containing 1% serum sample was changed every 48 hours.

Step 1a: For those cells destined for Flow Cytometry, the media was changed to serum-free media for cell cycle synchronization for 24 hours.

Step 2: Once the cells were 60% confluent, the media was changed from Growth Media to Fusion Media, still with 1% serum sample.

This media containing 1% serum sample was changed every 48 hours until optimum myotube formation was achieved.

Step 3a: Immunostaining. Cells were fixed with 10% NBF and prepared for immunostaining followed by photographing.

Step 3b: Calcium Imaging. Cells were prepared for calcium imaging.

Step 3c: Cell cycle analysis with Flow Cytometry. Cells were fixed and prepared for Flow Cytometry using the MUSE™ Cell Analyzer.

Figure 2. Research Design. Flow of experiment from seeding of HSMM cells through myogenesis and fixation for data collection.

Methodology

Research Design

The design of this experimental study was an *in vitro* controlled trial (Figure 2). *In vitro* studies or those performed outside the living body are often performed in preclinical research to provide a stronger foundation for ongoing studies. They are the most reliable way of determining cellular and molecular insights that have led to important discoveries including a number of new drugs and molecules. *In vitro* studies offer several advantages

42

over *in vivo* studies including reduced cost, the ability to more directly assess the effects of the treatment and the ability to avoid many of the ethical considerations that must be weighed when human or animal participants are involved (Polli, 2008). While there was human involvement in the form of serum sample collection, this portion of the research had already occurred, with the due diligence that accompanies the successful IRB approval. All measures were taken to assure that the same diligence was applied to the IRB board approved addendum for "post collection" use of the serum collected (Appendix A). A commercially available cell line was used for this *in vitro* controlled trial. Commercially available cell lines provide the opportunity to work with cells of uniform morphology and functions, with predictable activity in predetermined environments. The cell line proposed contains normal human skeletal muscle myoblasts, usually from quadriceps or psoas tissue. Comparable groups of cells were optimized, with an increase in reliability, by using the same subculture passage. Passage refers to a cell culturing technique designed to maintain the life and health of the cell line. Additionally, optimization of comparable groups was enhanced by seeding each well with the same number of cells. The possibility of extraneous variables was reduced by holding constant as many of the influences as possible on the dependent variable of myotubes formation. The design of this study was for one group of cells to be treated with media containing serum from subjects with osteoporosis (CASE), and one group of cells to be treated with media containing serum from subjects without osteoporosis (CNTRL). (Appendices C, D, E, and F provide detailed study protocols). To maintain the fidelity of the procedures, the experiments were conducted with the investigator blinded to the patient information related to each serum sample. Also, this research was completed following only those protocols reviewed and approved by either the Director of the Muscle Bone Biology

43

Group (MUBIG) and/or the company from which the human skeletal muscle cell line was purchased.

Sample/ Subjects

Clonetics™ Skeletal Muscle Myoblast Cell System (HSMM) was the cell line used for this study. These cells are isolated from normal donor quadriceps or psosas tissue. According to the materials published by the manufacturer, Lonza (2012), Certificates of Analysis (CA) for the cells are shipped with each order, the cells are performance assayed and test negative for HIV-1, mycoplasma, Hepatitis-B, Hepatitis-C, bacteria, yeast and fungi. This information is important to ensure the safety of those working with the cells, to assure that the cells have not mutated, and to preserve the reliability of the data collected.

Serum samples used for this study were obtained from women enrolled in the ongoing Bone Quality Study at the Osteoporosis Research Center at Creighton University. Half of the patients have been diagnosed as having osteoporosis (CASE) and the other half have no evidence of osteoporosis (CNTRL). Those subjects in the CASE group are women who have experienced a fracture during the previous five years from little or no trauma. The serum samples were provided by the Creighton University Osteoporosis Research Center in Omaha, Nebraska, where IRB approval had already been obtained. For the purposes of their study, researchers at Creighton University defined low-trauma fracture as any fracture caused by trauma that is less than or equal to a fall to the floor from standing height (Recker & Barger-Lux, 2004). Fractures of digits, face or skull are not included. The serum samples used were from patients between the ages of 50 and 75, who were otherwise healthy and who were matched for age. Subjects excluded from the Bone Quality Study are those with history of cancer, except for superficial basal or squamous cell carcinoma of the skin, or another

malignancy that was treated curatively at least ten years prior to the study; serious effects from cerebral vascular disease; diabetes mellitus; kidney disease with a serum creatinine > 1.9 mg/dl; chronic liver disease or alcoholism; treatment with bisphosphonates or other bone active agents; treatment with calcitonin, estrogen or a selective estrogen-receptor modulator within the previous six months, any corticosteroid therapy within the previous six months; systemic corticosteroid therapy at pharmacologic levels for more than six months duration; treatment with anticonvulsants within the previous year; cardiovascular diseases including unstable angina, uncontrolled hypertension, or infarction within one year prior to the study; evidence of metabolic bone disease; active rheumatoid arthritis or collagen disease; major gastrointestinal disease within the previous year; or any disease or treatment judged to have a significant effect on the skeletal system. A minimum of ten patients is needed to detect a difference (median effect size 0.5; 0.05 significance level; power of 0.70).

Prior to initiating the experiments, a series of dose response experiments were first conducted to determine the optimum concentration of serum to use. Although the concentration of 10% serum appears to provide the greatest impact on proliferation and myogenesis, the concentrations of 3% and 1% appear to be very close in their impacts on the HSMM cells. For these reasons, the decision was made that the concentration of the serum samples provided to us by the Osteoporosis Research Center at Creighton University to use for the dissertation studies was 1.0%. (Appendix C provides protocols used for the HSMM cells).

Procedures for Data Collection

Using standard procedures and approved protocols, wells in six-well plates and optic dishes were seeded each with 35K HSMM cells. The cells were initially plated with Skeletal

Muscle Basal Medium-2 (SkBM™-2) as recommended by Lonza, and incubated at 37° C and 5% CO_2. This media contains Skeletal Muscle Basal Medium, 0.1% human epidermal growth factor (hEGF), 10% fetal bovine serum (FBS), 0.1% dexamethaxsone, 2% L-glutamine, and 0.1% gentamicin/ amphotericin-B (GA). The cells were observed daily and the media was changed every 48 hours according to established protocols. It was important not to allow the cells to become any more than 60% confluent to avoid spontaneous myotube formation prior to the application of fusion media. In the CNTRL group, cells were treated with fusion media containing 1% serum from patients without osteoporosis. In the CASE group, cells were treated with fusion media containing 1% serum from patients with osteoporosis. The decision to use a concentration of 1% serum was based upon results from the dose response experiments performed prior to the initiation of this study. The day that the fusion media was applied was considered DAY 0. Photographs were taken using the LEICA inverted light microscope every day beginning DAY 1, just hours after the initial application of the fusion media, through the time of optimal myotubes formation, usually DAY 7. At that time, the appropriate protocol was followed for either immunostaining for Fusion Index calculations, fixation in preparation for cell cycle analysis through Flow Cytometry using the MUSE™ Cell Analyzer by EMD Millipore. Cells cultivated in the optic dishes were prepared for Calcium Imaging, a technique for measuring intracellular function.

Measures

To evaluate the effect of media containing serum from patients with and without osteoporosis, several techniques were performed including Myogenic Differentiation, Calcium Imaging, and Cell Cycle Analysis using Flow Cytometry.

Myogenic Differentiation. Fusion indexing provides quantitative evaluation of the efficiency of myoblast fusion into myotubes by determining the fraction of total nuclei that are incorporated into myotubes. Fusion indexing is commonly used to quantify the extent of differentiation in skeletal muscle cells (Veliça & Bunce, 2011). This researcher selected fusion index as the primary biophysiologic instrument for measuring the dependent variable of myotube formation because it is an established method for quantifying myogenic differentiation, is one with which the researcher has experience, and is one to which the necessary equipment and solutions the researcher has access. At the peak of myotube formation, the media was removed and the cells were fixed for immunostaining, following the approved protocol (Appendix D). The fusion index was determined by randomly selecting five fields per well using the LEICA imaging system to assure a significant level of conclusion.

Intracellular Calcium Homeostasis, Calcium Imaging. Intracellular Ca^{2+} homeostasis is critical for myogenesis and for contractile function of muscles (Berchtold, Brinkmeier, & Müntener, 2000). The intracellular calcium was evaluated as recently described in the article by Mo (2012) by loading the cells from each group with Fura-2AM, a Ca^{2+} indicator. A PTI automatic spectrofluorometer (Photon Technology International, Birmingham, New Jersey), was used to determine the average resting ratio of bound- to unbound Ca^{2+}, the magnitude of changes in caffeine-induced intracellular Ca^{2+}, and the total amount of intracellular Ca^{2+}. For meaningful statistics, data from nine to fifteen myotubes from each serum sample were collected. (Appendix E).

Cell Cycle Analysis using Flow Cytometry (FC). Flow Cytometry provides the ability to measure several properties of individual cells as they are suspended in liquid and

passed through a laser light. The parameters of cell size, cell complexity and DNA content

are evaluated using this technique. This method of biophysiologic measure has been used to

identify morphologic, functional and apoptotic characterization of skeletal muscle cells

(Burattini et al., 2004; Salucci et al., 2010). To maintain the reliability of the data collected

from FC, a number of technologies were used in the MUSE™ Cell Analyzer and

accompanying software to maintain alignment and linearity, absolute cell counting beads,

compensation tools and cell sizing beads. Results obtained through FC have been deemed

comparable to results achieved with reverse transcription (RT)-PCR (Campana, 2003). For

use in cell cycle analysis, Heiden, Auer and Tribukait (2000) found FC to be analogous to

Image Cytometry, noting the importance of both adequate cell count in the samples tested

and the user's experience and judgment. (Appendix F).

Plan for Data Analysis

The data included immunostaining and resulting photographs of the cells from each

treatment condition; the total number of nuclei, the number of nuclei within myotubes, and

the calculated fusion index. This information was gathered from each well containing serum

sample treated cells. Using Origin Statistical Software, the data were tested for normality.

Independent t-tests were conducted to examine the differences in myogenesis between the

two groups, CASE and CNTRL.

The data collected from Calcium Imaging were used to evaluate the functional

differences in cells from both groups. Nine to 15 myotubes from each serum sample were

tested for calcium levels: resting, peak and area under the curve, which reflects the total

amount of calcium in response to stimulation. These data were also tested for normality

using the Origin Statistical Software before conducting independent t-tests to look at functional differences between the groups.

Flow Cytometry allows the data to be collected both in a linear run and, for DNA content, a logarithmic run. The software that is used with FC provides a full range of intrinsic methods for statistical analysis of the data collected. For the linear scale data, an arithmetic mean is used; and for the logarithmically displayed data, the geometric mean is chosen. In FC, the spread of a distribution, which is usually expressed in other settings as the Standard Deviation (SD), will be expressed as the coefficient of variation (CV). In the case of FC, it is the distribution, for example cell size and complexity that is being recorded. Therefore, the CV is preferred because it is dimensionless and, for the linear run, does not depend upon where on the histogram the data are recorded. Another feature of the FC data are that it provides the percentage of particular subset of cells, using an electronic sizing (Coulter) counter. This feature allowed for analysis of subsets within the cell population for both groups, since myogenesis leads to increasing cell size, complexity and DNA content. Values obtained, such as percentage of cellular subsets, were then entered into Origin to conduct independent t-tests for additional insight into differences between the two groups with regard to myogenesis.

CHAPTER 4

RESULTS

The Specific Aim (SA) of this study was to investigate biochemical,

histomorphometric and functional differences in human skeletal muscle (HSMM) cells

treated with conditioned media containing serum from patients with and without

osteoporosis. Serum samples were obtained from patients enrolled in the ongoing Bone

Quality (BQ) Study being conducted at the Osteoporosis Research Center at Creighton

University. Researchers involved in the BQ Study selected serum samples from sixteen

participants in the BQ study, eight who belong to the group with osteoporosis (CASE) and

eight who belong to the group without osteoporosis (CNTRL). The experiments were all

conducted with this researcher blinded to which of the groups each serum sample belonged.

The first section of this chapter presents a summary of the data collected for the HSMM cells

treated with each of the serum samples with regard to myogenic differentiation, intracellular

calcium homeostasis and cell cycle analysis. Data collected for each serum sample are

presented in Appendices G, H, and I.

The Research Question (RQ) that this dissertation study sought to answer was: **"What

is the extent of difference in biochemical, histomorphometric and functional adaptations in

HSMM cells treated with conditioned media containing serum from subjects with and

without osteoporosis?"** As presented in Chapter 3, this research question was explored by

evaluating the differences between the CNTRL and CASE groups in three ways: Myogenic

Differentiation, Intracellular Calcium Homeostasis, and Cell Cycle Analysis. According to

researchers at the Osteoporosis Research Center, patients who have experienced a fracture

from little or no trauma during the previous five years are considered to have osteoporosis,

and are entered into the CASE group of the BQ Study. Those who have not sustained a fracture within the previous five years are in the CNTRL group. Upon completion of all experiments, this researcher obtained from the Osteoporosis Research Center, patient information associated with each serum sample. Statistical analyses were performed to evaluate the differences between the CNTRL and CASE groups using the Origin Statistical Software, version 6.0. A significance level of 0.05 was set for the research question. The results of that statistical analysis are presented in section two of this chapter.

The patient information provided upon completion of the experiments provided insight into which of the serum samples belonged to patients who had sustained a non-traumatic fracture within the previous five years. It also provided the patients ages and results of dual energy x-ray absorptiometry (DXA) performed on each patient's lumbar spine (T-Spine), and hip (T-Hip). The National Osteoporosis Foundation (2010) defines osteoporosis as bone density of 2.5 standard deviations (SD) below the mean of a young adult, or a DXA score of less than or equal to -2.5. It is interesting to note that none of the T-Scores reported for any of the patients whose serum was used in this dissertation study had a T-Score of less than -2.5. It is undeniable that the patients in the CASE group had sustained non-traumatic fractures, and therefore suffered from decreased bone integrity. This researcher conducted a second data analysis; this time grouping the data based upon T-Scores. Data obtained from cells treated with serum from patients who had a T-Score less than -1.0 of either the lumbar spine or the hip were placed in the T-Score status, CASE group. In addition, data obtained from cells treated with serum from patients with T-Scores of both their lumbar spines and hip above -1.0 were placed in the T-Score status, CNTRL group. With these new groups defined, the data were once again analyzed using the Origin

Statistical Software. The results of that statistical analysis are presented in section three of this chapter.

Summary of Data Collected

This section presents a general summary of data collected in Phase I, Phase II, and Phase III of this dissertation study. During the time that the experiments were conducted, this researcher was blinded to the patient information associated with each serum sample.

Phase I: Immunostaining for Fusion Index Calculations, Data Gathered. According to the myogenesis model, myoblasts leave the cell cycle to enter into the differentiation pathway. It is along this pathway that myocytes fuse together to form myotubes. Fusion index provides a quantitative evaluation of the efficiency of this process by determining the fraction of total nuclei that are incorporated into myotubes. For this study, the fusion index was determined by randomly selecting five fields per well for each serum sample using the LEICA imaging system, and was calculated as the ratio of the number of nuclei inside myotubes to the number of total nuclei $\times 100$ at day 7 of myogenic differentiation. (Appendix G provides immunostaining images collected of HSMM cells for fusion index calculations for each of the serum samples and the control conditions).

Myogenic Differentiation
Data Collected: Immunostaining of HSMM cells
treated with media containing 1.0% serum sample
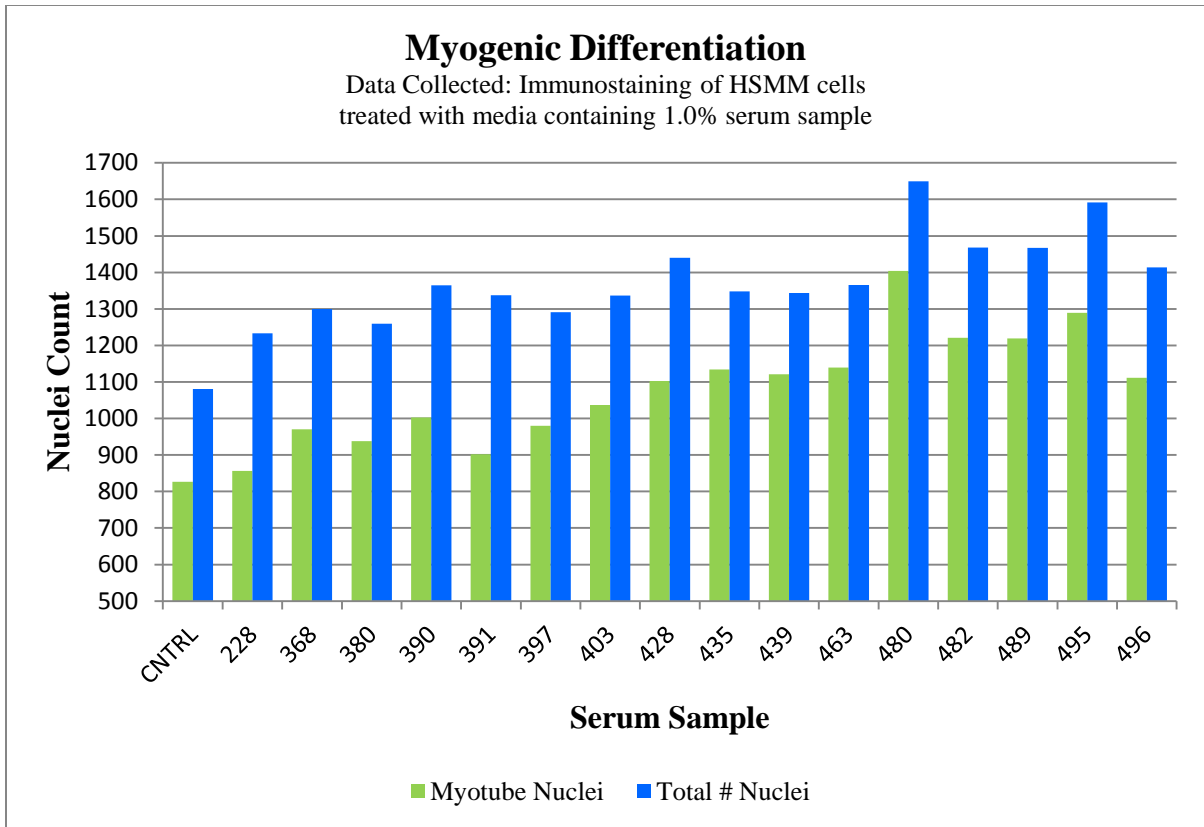
Figure 3. Myogenic Differentiation, Nuclei Counted. Myotube and total nuclei counted in HSMM cells treated with serum samples. The HSMM cells were fixed and stained on Day 7 after seeding.

Figure 3 provides a graphic representation of the number of nuclei counted for each of the experimental conditions, as well as a control well of HSMM cells. In this figure, the green bars present an average of the number of nuclei within myotubes and the blue bars represent an average of the total number of nuclei counted in a minimum of five fields for each experimental condition. The highest number of both myotube and total nuclei were counted in cells treated with media containing 1% serum sample number 480. The lowest

number of both myotube and total nuclei were counted in the control cells, which were

cultured in media with no human serum added.

Myogenic Differentiaion

Fusion Indexes calculated from averages of data
collected for cells treated with each serum sample.

Sample	Fusion Index
496	79
495	81
489	83
482	83
480	85
463	83
439	84
435	84
428	76
403	76
397	76
391	68
390	74
380	74
368	75
228	69
CNTRL	77

Fusion Index

Calculated as the ratio of nuclei within myotubes
to thetotal number of nuclei multiplied by 100.

Figure 4. Myogenic Differentiation, Fusion Index. Fusion Index of HSMM cells treated with serum samples. Fusion Indexes were calculated as the ratio of nuclei within the myotubes to the total number of nuclei, multiplied by 100.

Figure 4 provides a graphic representation of the fusion index calculated for each of the experimental conditions and the control cells. The fusion index is calculated as a ratio of nuclei within myotubes to the total number of nuclei, multiplied by 100 and presented as a percentage. The highest fusion index, 85%, was observed in those cells treated with 1% serum sample number 480. The control cells had a fusion index of 77%, and the lowest fusion index, 68%, was observed in cells treated with 1% serum sample number 391.

Phase II: Calcium Imaging, Data Gathered. Intracellular calcium (Ca^{2+}) plays an important role in skeletal muscle cell function, and its homeostasis is critical both for the process leading to myogenesis and for the contractile function of skeletal muscles. Using the fluorescent dye, Fura-2AM which binds to free intracellular calcium, the ratio of emissions at specific wavelengths is directly correlated to the amount of intracellular calcium. In the system used in our lab, the wavelength at which Fura-2AM is excitable when bound to intracellular calcium is 350 nanometers (nm). It is excitable at 375 nm when unbound. With the use of a PTI (Photon Technology International, Birmingham, New Jersey) spectrofluorometer the average resting ratio of bound- to unbound Ca^{2+}, the magnitude of changes in caffeine-induced intracellular Ca^{2+}, and the total amount of intracellular Ca^{2+} was determined. Please refer to Appendix H for images of calcium imaging tracings collected for each serum sample and control. An approximate average of ten tracings was obtained for each of the experimental conditions.

Intracellular Calcium Homeostasis
Data Collected: Calcium Imaging of HSMM cells
treated with media containing 1% serum sample.

	CTRL	228	368	380	390	391	397	403	428	435	439	463	480	482	489	495	496
Resting Level, Avg	0.66	0.71	0.66	0.71	0.68	0.67	0.66	0.69	0.63	0.67	0.71	0.68	0.71	0.66	0.72	0.69	0.66
Peak Level, Avg	0.77	0.80	0.76	0.79	0.78	0.78	0.75	0.81	0.75	0.78	0.78	0.80	0.78	0.80	0.82	0.80	0.74

■ Resting Level, Avg   ■ Peak Level, Avg
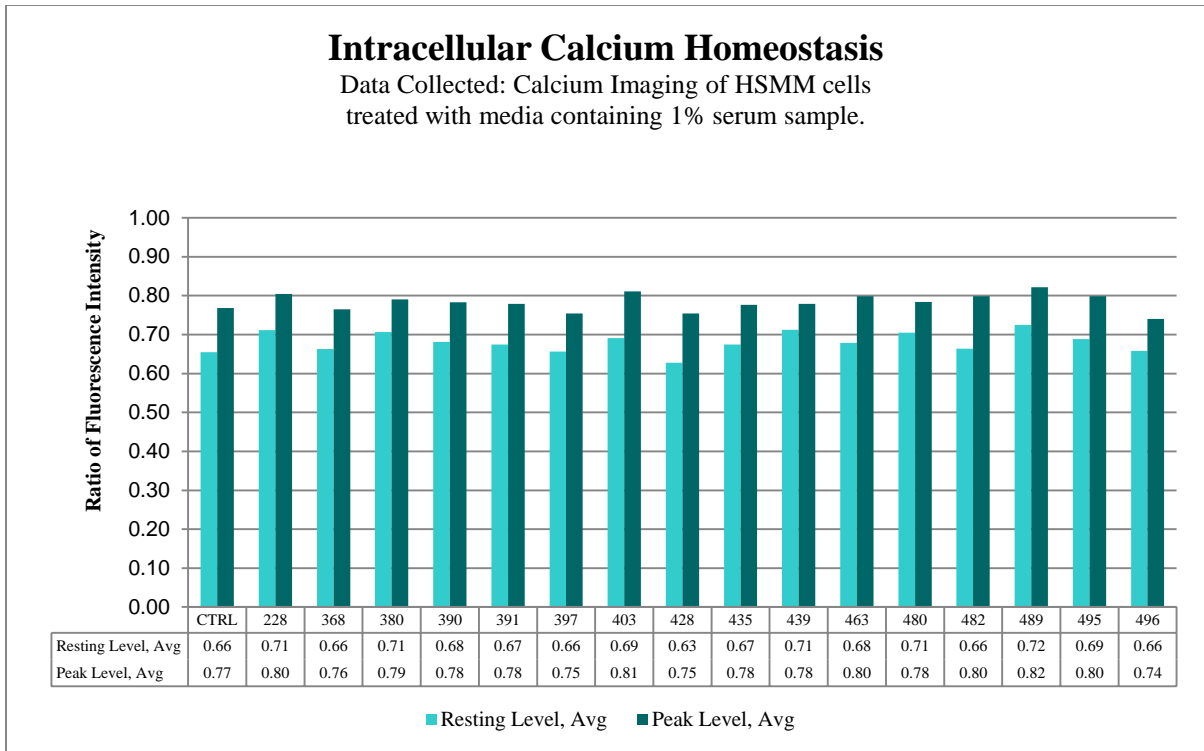
Figure 5. Calcium Imaging, Resting and Peak Levels. This graph presents a comparison of the fluorescence intensity of HSMM cells loaded with the calcium sensitive dye, Fura-2AM, before and following application of 20mM caffeine. The ~0.1 increase in the ratio while apparently small represents a substantial increase in the free levels of intracellular from ~100nM to 300nM.

Figure 5 provides a graphic representation of the both the resting and peaks levels of intracellular calcium; data collected from calcium imaging performed on cells treated with each of the serum samples. For the control cells, the resting and peak levels were observed to be 0.66 and 0.77, respectively. The highest resting level, 0.72, and the highest peak level, 0.82, were both observed in cells treated with media containing 1% serum sample number 489. The lowest resting level, 0.63, was observed in cells treated with media containing 1% serum sample number 428. But, the lowest peak level, 0.74, was observed in cells treated

with media containing 1% serum sample number 496. The resting level of cells treated in

media containing 1% serum sample number 496 was the same as the resting level of the

control cells.
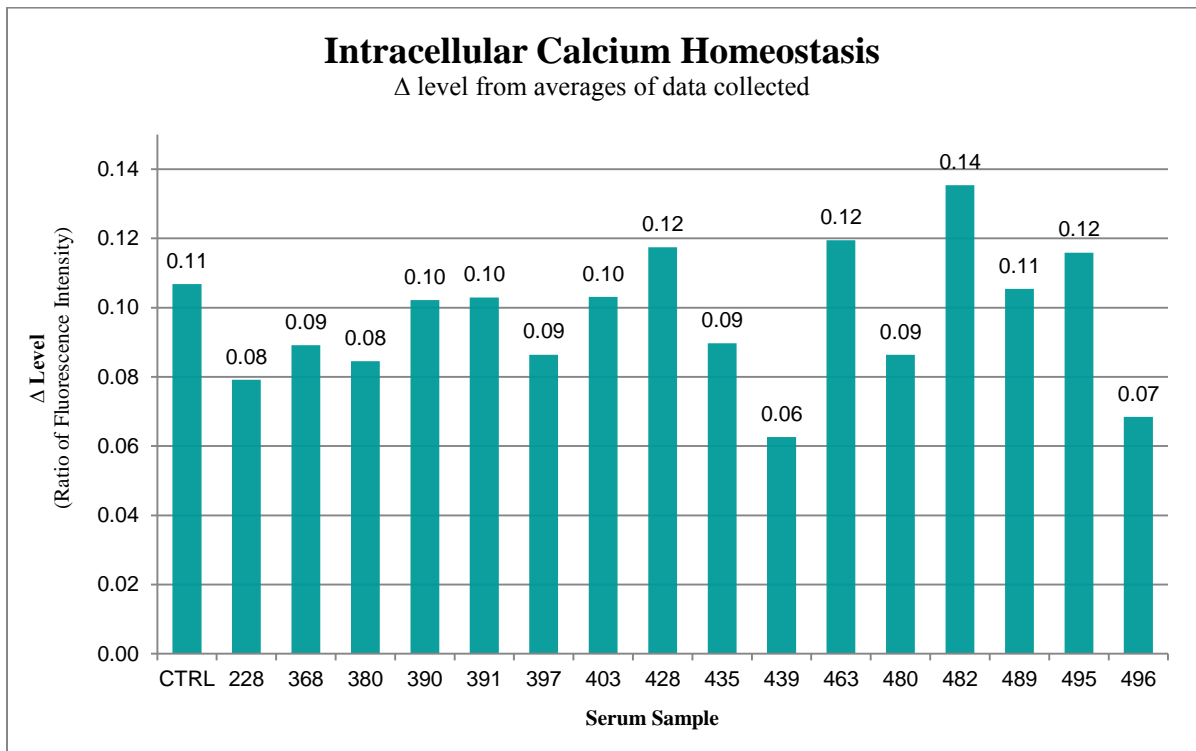
Figure 6. Calcium Imaging, Change in Level of Fluorescence Intensity. This graph presents a comparison of the change in fluorescence intensity of HSMM cells loaded with the calcium sensitive dye, Fura-2AM, following application of 20mM caffeine. The ~0.1 increase in the ratio while apparently small represents a substantial increase in the free levels of intracellular from ~100nM to 300nM.

Figure 6 provides a graphic representation of the change in fluorescence level with the introduction of 20mM caffeine for cells treated with 1% of each of the serum samples. The greatest change in level was observed in cells treated with media containing 1% serum sample number 482. Although the change in level for the control cells was 0.11, a lower level of change was observed in cells treated with all of the serum samples except 428, 463, 482, 489 and 495.
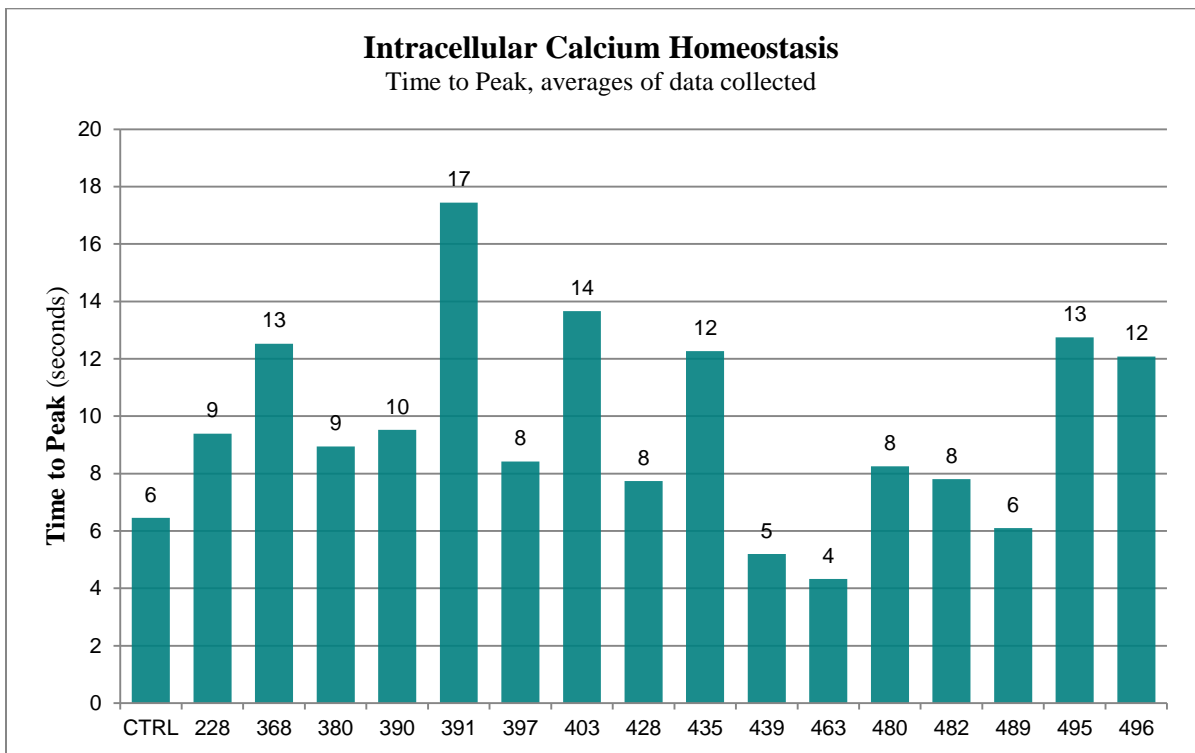
Figure 7. Calcium Imaging, Time to Peak. This graph presents a comparison of time to peak fluorescent intensity of HSMM cells loaded with the calcium sensitive dye, Fura-2AM, following application of 20mM caffeine.

Figure 7 provides a graphic representation of the time, in seconds, from resting to peak levels upon the introduction of 20mM caffeine. The time to peak observed in the control cells was 6 seconds. A quicker time to peak was observed in cells treated with media containing two of the serum samples, 439 and 463. The longest time to peak was observed in cells treated with media containing 1% serum sample number 391.

Intracellular Calcium Homeostasis
Calcium Imaging
Calcium Transients represented as Area Under the Curve

Serum Sample	Calcium Transients
496	275
495	287
489	297
482	282
480	288
463	287
439	
435	278
428	265
403	284
397	269
391	278
390	281
380	290
368	279
228	290
CT...	267

Calcium Transients
Measured by Fluorescence Intensity
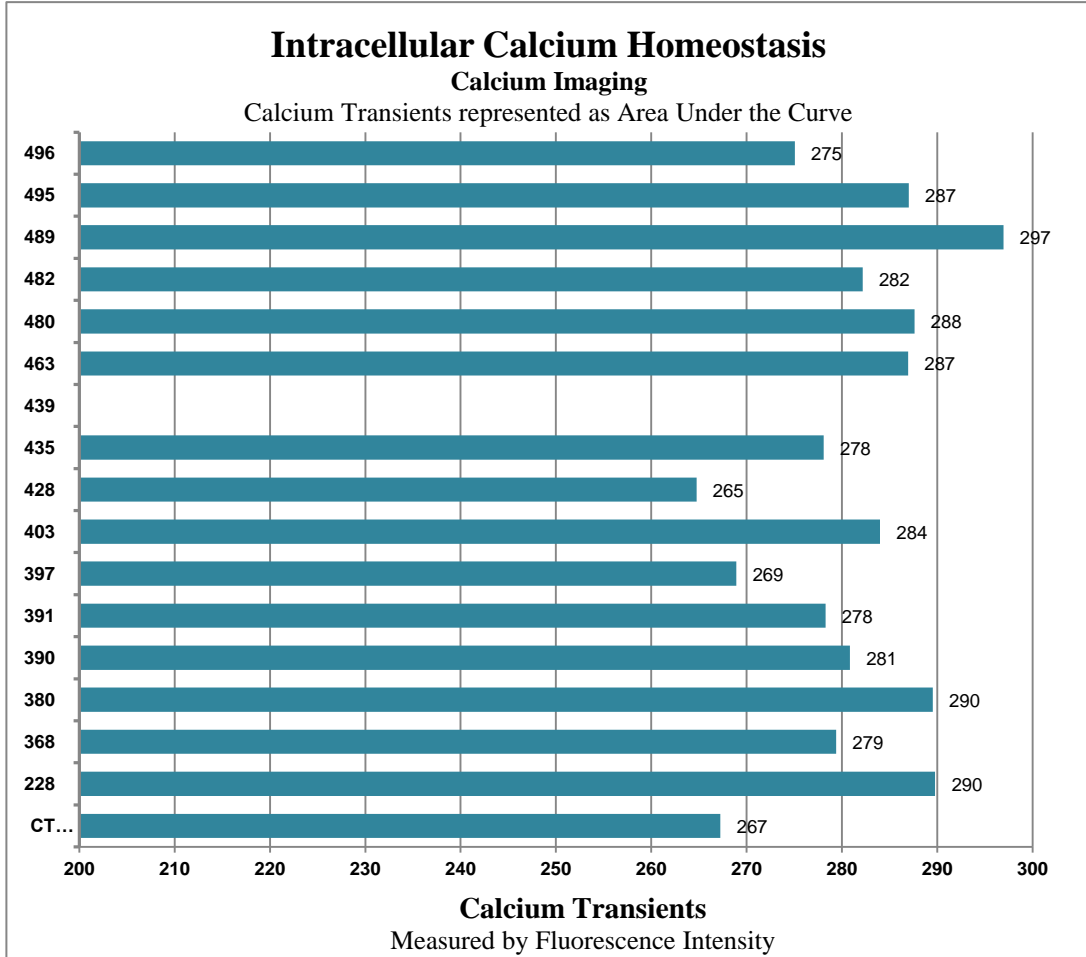
Figure 8. Calcium Imaging, Calcium Transients. This graph presents a comparison of the amount of calcium as determined by the area under the curve, which is the integral ($\int_{a}^{b} f(x)\,dx$) of the fluorescent intensity of HSMM cells loaded with the calcium sensitive dye, Fura-2AM, before and following application of 20mM caffeine. Each serum sample is listed along the y-axis, with the exception of 439. No data were collected for serum sample 439 due to data corruption or loss during experiment.

Figure 8 provides a graphic representation of the calcium transients, measured as the area under the curve following the introduction of 20mM caffeine for each of the experimental conditions. Data from cells treated with media containing 1% serum sample

number 439 were omitted due to logistical challenges in the collection of calcium imaging data for this dish. The calcium transients observed in the control cells was 267. The only experimental condition in which a lower level of calcium transients was observed was in the cells treated with media containing 1% serum sample number 428. All other experimental conditions yielded a higher level of calcium transients, with the highest level observed in cells treated with media containing 1% serum sample number 489.

Phase III: Flow Cytometry for Cell Cycle Analysis. As discussed, myogenesis leads to increasing cell size, complexity and, therefore, an increase in the DNA content, each of which can be evaluated using flow cytometry. Prior to differentiation, myoblasts progress through the four phases of the cell cycle: two gap phases, G1 and G2, a synthesis or S phase, as the 46 chromosomes are duplicated; and a mitosis, or M phase, as the genetic material and the cell divides. In order to enter into differentiation, the myocyte must exit the cell cycle. In this portion of the current project, data were gathered on cell cycle subsets and on DNA content for cells treated with each of the serum samples. Please refer to Appendix I for images of data collected from the MUSE™ Cell Analyzer.   One run was completed for each experimental condition, and two for the control.

Table 1. *Cell Cycle Analysis. This table compares HSMM cells treated with each serum sample and presents data on the number of events (cells) within each of the cell cycles listed: G0/G1, S, and G2/M collected from flow cytometry using the tabletop MUSE™ Cell Analyzer.*

Sample ID	Number of Events	G0/ G1	S	G2/M
CNTRL	11928	83.90	12.20	2.30
228	14097	84.35	11.55	2.36
368	8487	83.24	13.79	1.75
380	11887	79.83	15.45	2.82
390	11704	85.32	12.5	1.17
391	12326	85.52	11.7	0.98
397	21903	75.85	17.84	4.86
403	15948	79.59	15.34	3.04
428	17870	79.55	15.96	2.76
435	9287	79.4	15.93	3.14
439	9771	80.53	14.47	3.04
463	12360	85.95	10.6	1.87
480	17515	83.76	12.51	1.96
482	13213	79.82	15.58	2.34
489	15060	84.38	13.37	1.20
495	15752	80.95	13.29	3.80
496	14691	75.88	17.54	4.18

Table 1 provides the number of events recorded as well as the number of cells in each phase of the cell cycle for cells treated with media containing 1% of serum samples. The greatest number of events was observed in the cells treated with 1% of serum sample number 397. This was also the experimental condition in which the greatest number of cells was observed to be in the G2/M (mitosis) phase of the cell cycle. The greatest number of cells in the S phase was observed in those cells treated with media containing 1% serum sample number 397. The largest number of cells observed in the G0/G1 phase of the cell cycle was observed in cells treated with 1% serum sample number 463; although those treated with serum samples 391 and 390 were close behind.
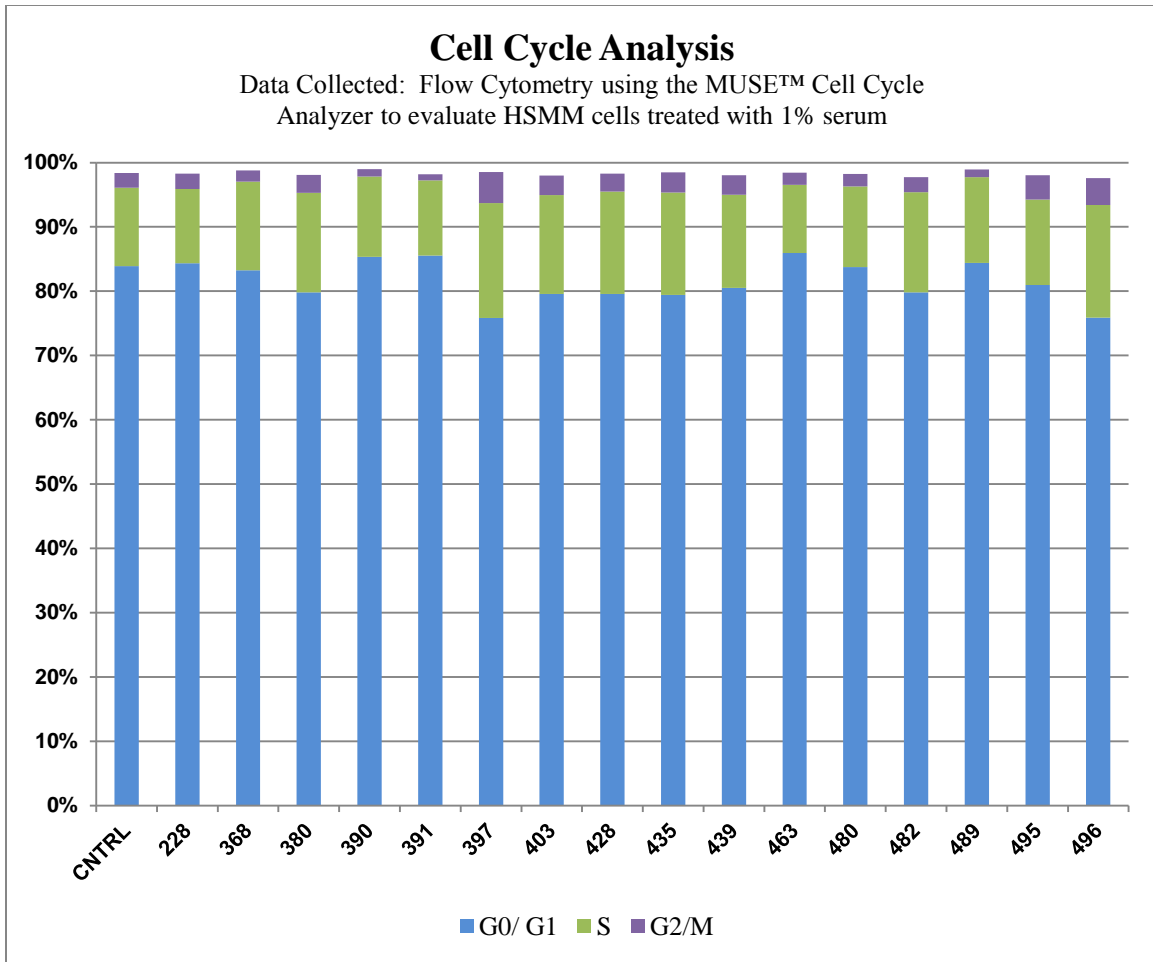
Figure 9. Cell Cycle Analysis. This figure provides a graphic representation of the cell cycle analysis performed comparing HSMM cells treated with each serum sample and presents data on the number of events (cells) within each of the cell cycles listed: G0/G1, S, and G2/M collected from flow cytometry using the tabletop MUSE™ Cell Analyzer.

Figure 9 provides a graphic representation of the distribution of cells throughout the phases of the cell cycle in each experimental condition. These are the same data presented in Table 2.

Data Analysis: Fracture Status Groups Compared

  Subjects with osteoporosis are identified in the Creighton University Osteoporosis Research Center Bone Quality Study as those who have experienced a fracture during the previous five years from little or no trauma. Therefore, when all the experiments were completed and the associated patient information was provided for serum samples used for this study, data were grouped according to the Bone Quality Study definition of osteoporosis. Data collected from cells treated with serum from subjects who had sustained a fracture were placed in the CASE group and data collected from cell treated with serum from subjects who had not sustained a fracture were placed in the CNTRL group. With the groups identified, data were analyzed using the Origin Statistical Software (Version 6.0).

  The serum samples were collected from patients between the ages of 50 and 75, who are otherwise healthy. Although based upon the patient information provided, it is not clear whether the subjects were matched for co-morbidities, share similar medical profiles with no history of cancer, diabetes mellitus, kidney disease, chronic liver disease, unstable angina, uncontrolled hypertension, or recent infarction. Their pharmacologic profiles were similar in that none had been treated with bisphosphonates or other bone active agents, calcitonin, estrogen or a selective estrogen-receptor modulator within the previous six months. In addition, none had recently received any corticosteroid therapy, or anticonvulsant agents. The patient information provided included their age as well as results of a dual energy x-ray absorptiometry (DXA) of their lumbar spine (T-Spine), and of their hip (T-Hip). This information is presented in Table 2.

Table 2. *Descriptive Characteristics, Fracture Status Groups. Comparison of fracture status groups, descriptive characteristics. At the 0.05 level, the two means are not significantly different with regard to any of the parameters listed.*

	Fracture Status, CNTRL Group			Fracture Status, CASE Group			
	Mean	**SE**	**Range**	**Mean**	**SE**	**Range**	**p-value**
Age (years)	63.16	2.37	21.3 (52.3 to 73.6)	64.18	2.30	20.1 (50.7 to 70.8)	0.76373
T-Spine	-0.44	0.35	2.703 (-1.948 to 0.755)	-0.93	0.34	3.220 (-2.389 to 0.831)	0.33627
T-Hip	-0.75	0.18	1.703 (-1.780 to -0.077)	-1.11	0.37	0.934 (-1.506 to -0.572)	0.13564
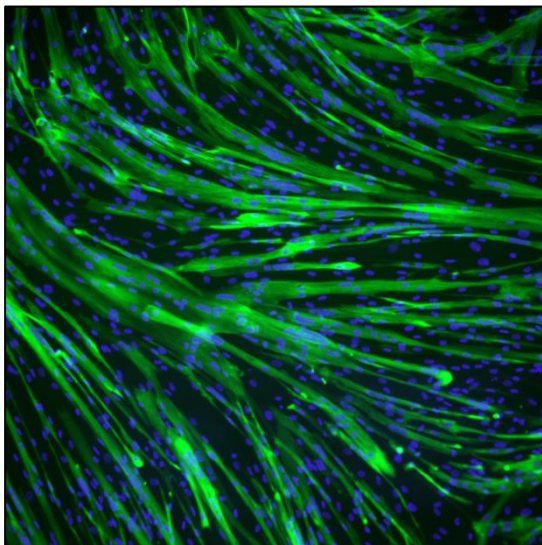
Figure10a .
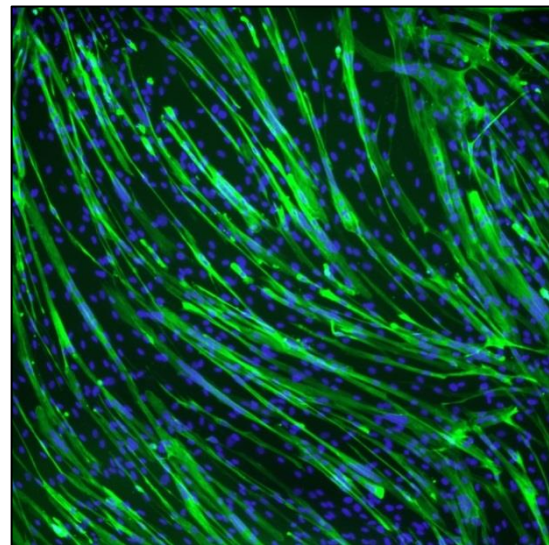
Figure 10b .

Figure 10. Immunostaining of HSMM Cells. Immunostaining with DAPI (blue) for nuclei and with anti-MHC Antibody (green) for myotubes. 10a. HSMM cells treated with media containing 1.0% serum (sample 495). 10b. HSMM cells treated with media containing 1.0% serum (sample 391).

Myogenic Differentiation. Figure 10 presents images of the HSMM cells upon immunostaining and are representative of each of the fracture status groups, Figure 10a is from the CNTRL group and Figure 10b from the CASE group. After normalizing the data, independent t-tests were performed comparing the two groups with regard to myotubes nuclei, total nuclei, and fusion indexes. At the 0.05 level, the two groups were shown to be significantly different for all three of these myogenic differentiation parameters. Table 3 presents the results of these statistical analyses.

Table 3. *Myogenic Differentiation, Fracture Status Groups. Comparison of fracture status groups, myogenic differentiation. *At the 0.05 level, the two means are significantly different with respect to myotube nuclei, total nuclei, and fusion index.*

Myotube Nuclei	CNTRL (n=39)	CASE (n=37)	p-value
Mean	1121	1012	p = 0.00273*
Total Nuclei	**CNTRL** (n=38)	**CASE** (n=38)	**p-value**
Mean	1412	1342	p = 0.03708*
Fusion Index	**CNTRL** (n=37)	**CASE** (n=40)	**p-value**
Mean	81%	76%	p = 0.00036*

These data are represented graphically in Figures 11 and 12.
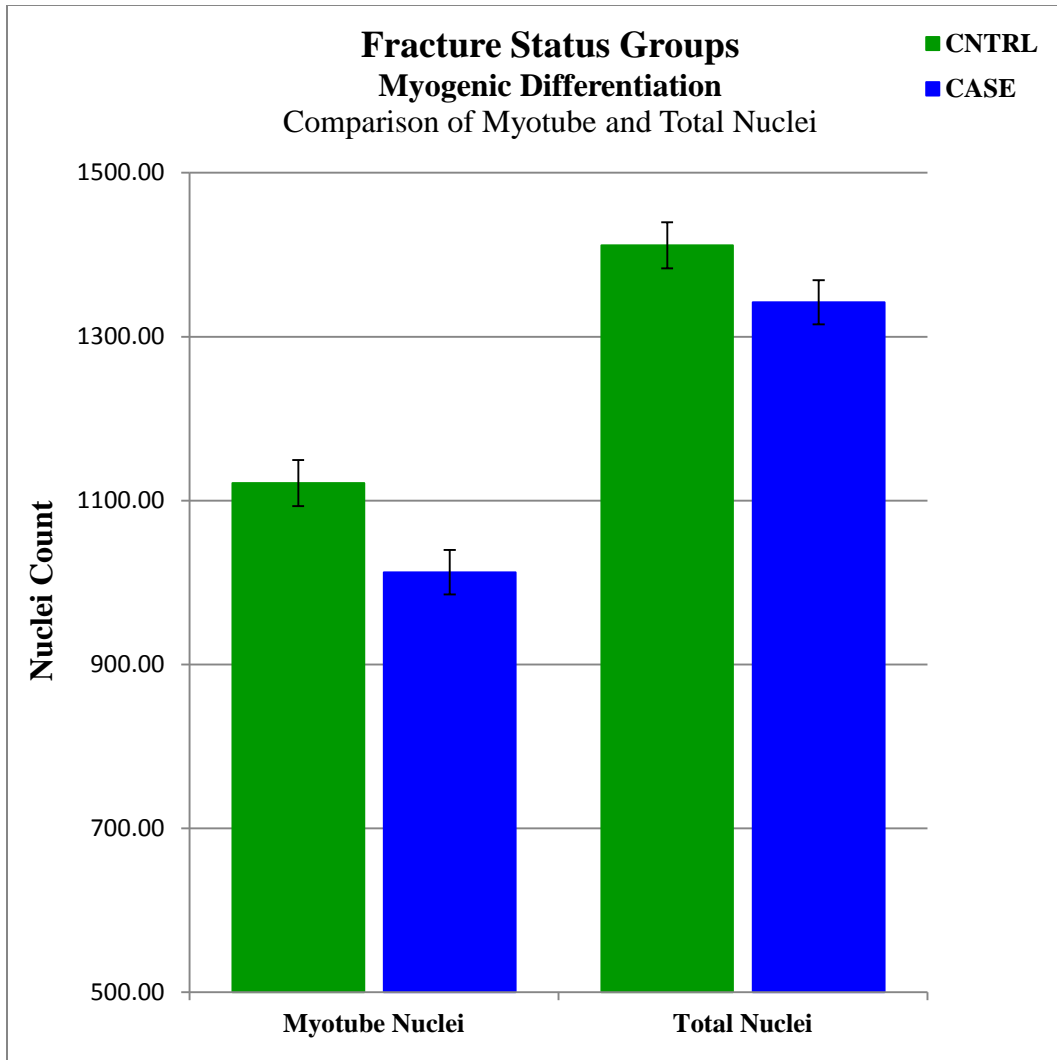
Figure 11. Myogenic Differentiaion, Myotube and Total Nulcei, Fracture Status Groups. Immunostaining of HSMM cells treated with 1% serum from either the CNTRL or CASE group. Graphic depiction of the significantly different means between the Fracture Status Group means.
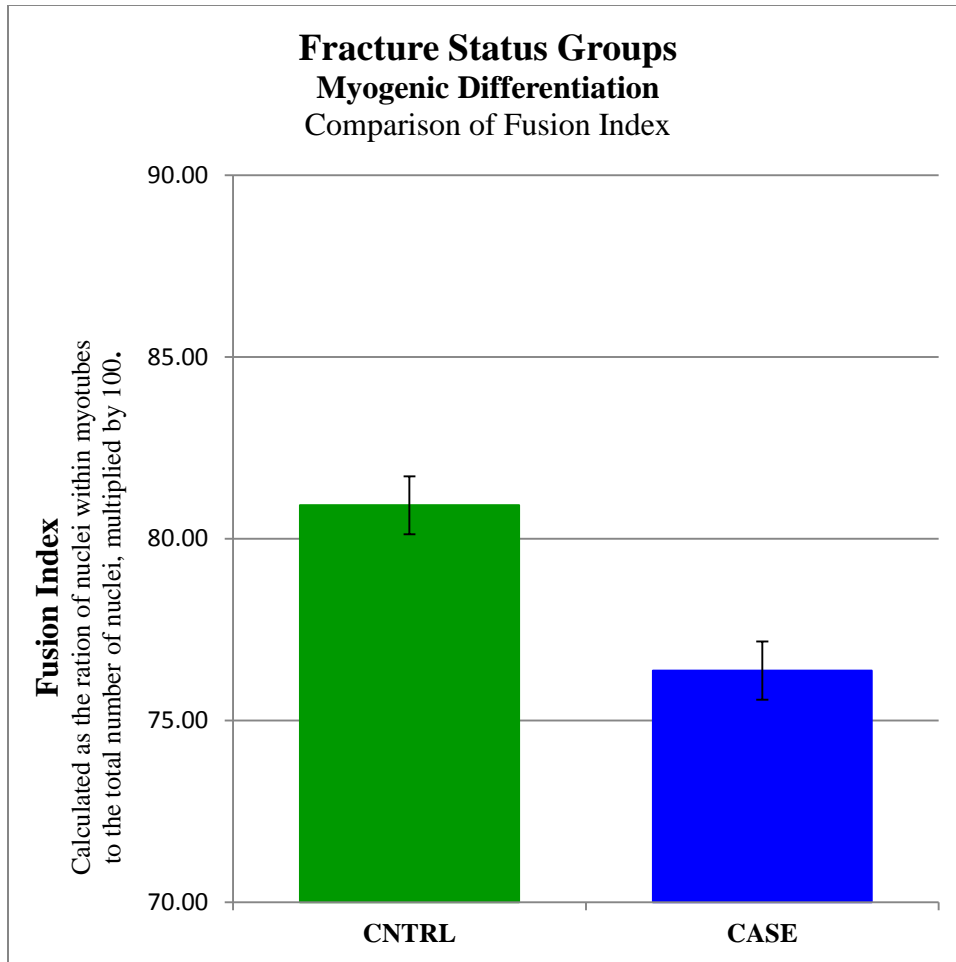
Figure 12. Myogenic Differentiaion, Fusion Index, Fracture Status Groups.
Immunostaining of HSMM cells treated with 1% serum from either the CNTRL or CASE
group. Graphic depiction of the significantly different means between the Fracture Status
Group means.

As the immunostained images were analyzed, there appeared an undeniable

difference in the size of myotubes treated with different serum samples. For that reason, it

was decided to also collect data with regard to the diameter of the myotubes captured in the

images taken. To do this, selected for each image were two (2) larger myotubes, two (2)

myotubes of medium size, and two (2) smaller myotubes as representatives. The lengths of measurements were first collected as pixels using Image J. These images had all been taken at 10X magnification using the inverted Leica microscope and were saved as 1125 X 1125 pixel images. Next, an image also at 10X magnification that had a scale of 100 micrometers (μm) on it was selected and sized to match these images at 125 X 1125 pixels. Matching this to the immunostained images, it was possible to calculate the measured lengths in micrometers.

The data were grouped first according to Fracture Status and next according to T-Score. After normalizing the data, independent t-tests were performed comparing the two groups with regard to myotube diameter. At the 0.05 level, when grouped according to Fracture Status, the two groups were shown to be significantly different for all with regard to myotube diameter. Table 4 presents the results of these statistical analyses.

Table 4. *Myotube Diameter, Fracture Status Groups. Comparison of fracture status groups, myotube diameter. *At the 0.05 level, the two means are significantly different with respect to myotube diameter.*

Myotube Diameter	CNTRL (n=225)	CASE (n=229)	p-value
Mean $\pm$ SEM (μm)	73 $\pm$ 3.5	54 $\pm$ 2.8	p = 0.00002*

Intracellular Calcium Homeostasis. Figure 13 presents representative images from the calcium imaging performed on each of the fracture status groups, Figure 13a from the CNTRL group and Figure 13b from the CASE group. After normalizing the data, independent t-tests were performed comparing the two groups with regard to resting intracellular calcium levels, peak levels, time to peak, and area under the curve. At the 0.05 level, the two groups were not significantly different for any of these parameters of intracellular calcium homeostasis. Table 4 presents the results of these statistical analyses.
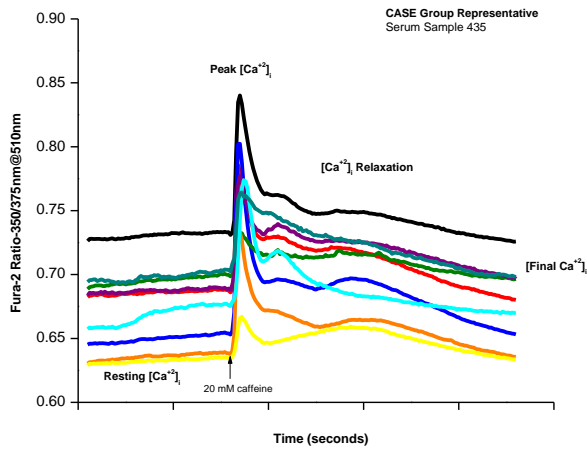
Figure 13a
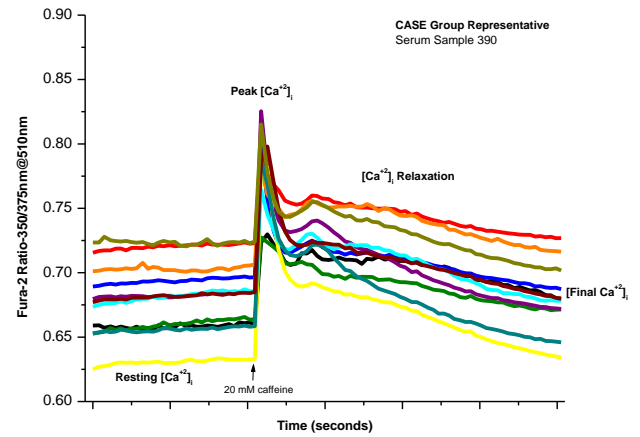
Figure 13b
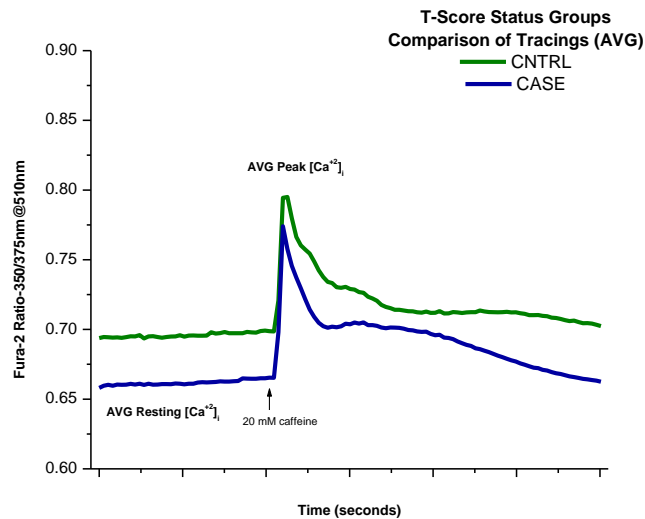
Figure 13c

Figure 13. Calcium Imaging, Representative Tracings. 13a. Calcium imaging performed on nine myotubes bathed in media containing 1% serum from one of the serum samples from the CNTRL group (sample # 435). This tracing also includes a tracing of the background for validation. 13b. Calcium imaging performed on eleven myotubes bathed in media containing 1% serum from one of the serum samples from the CASE group (sample # 390). This tracing also includes a tracing of the background for validation. Figure 13c. Representative tracings of the averages for CNTRL and CASE of T-Score Status Groups illustrate well the relative differences between the two groups.

Table 5. *Intracellular Calcium Homeostasis, Fracture Status Groups. Comparison of fracture status groups, intracellular calcium homeostasis. At the 0.05 level, the two means were not significantly different with regard to any of the parameters listed.*

Average Resting Levels	CNTRL (n=81)	CASE (n=86)	p-value
Mean	0.68111	0.68039	p = 0.91482

Average Peak Levels	CNTRL (n=83)	CASE (n=87)	p-value
Mean	0.78559	0.78325	p = 0.72496

Average Δ Level	CNTRL (n=86)	CASE (n=88)	p-value
Mean	0.10112	0.09810	p = 0.62337

Average Time to Peak (seconds)	CNTRL (n=81)	CASE (n=84)	p-value
Mean	8.923	10.47924	p = 0.06424

Calcium Transients (Area Under the Curve)	CNTRL (n=75)	CASE (n=85)	p-value
Mean	282.63261	282.32682	p = 0.90002

Cell Cycle Analysis. Figure 14 presents representative images from the cell cycle analysis performed on each of the fracture status groups, Figure 14a from the CNTRL group and Figure 14b from the CASE group. After normalizing the data, independent t-tests were performed comparing the two groups with regard to the number of cells in each phase of the cell cycle, G0/G1, S, and G2/M. At the 0.05 level, the two groups were not significantly

different for any of these parameters of cell cycle analysis. Table 6 presents the results of this statistical analysis.
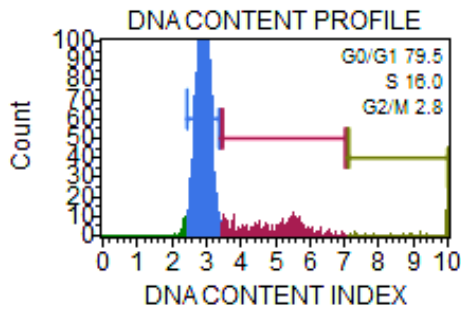
Figure 14a
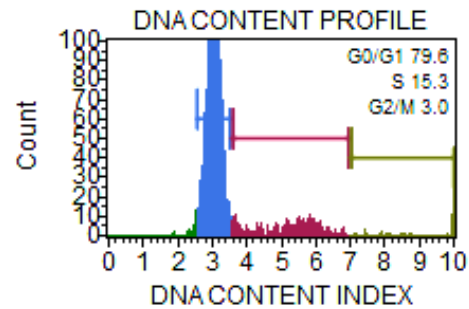
Figure 14b

Figure 14. Cell Cycle Analysis, Representative Graphs. 14a. Cell cycle analysis of HSMM cells treated with 1% of serum from the CNTRL group (sample #428). Figure 14b. Cell cycle analysis of HSMM cells treated with 1% of serum from the CASE group (sample #403).

Table 6. *Cell Cycle Analysis, Fracture Status Groups. Comparison of fracture status groups, cell cycle analysis. At the 0.05 level, the two means were not significantly different with regard to any of the parameters listed.*

G0/G1 phase	CNTRL (n=8)	CASE (n=8)	p-value
Mean	80.6075	82.3825	$p = 0.28816$
S phase	**CNTRL** (n=8)	**CASE** (n=8)	**p-value**
Mean	14.71125	13.71625	$p = 0.37149$
G2/M phase	**CNTRL** (n=8)	**CASE** (n=8)	**p-value**
Mean	2.8525	2.30625	$p = 0.33852$

Data Analysis: T-Score Status Groups Compared

       This researcher explored the research question also by evaluating the differences

between groups according to the T-Scores. Cells treated with media containing serum from

patients who had a T-Score less than -1.0 of either the lumbar spine or the hip were placed in

the T-Score status, CASE group. Cells treated with media containing serum from patients

with T-Scores of both their lumbar spines and hip above -1.0 were placed in the T-Score

status, CNTRL group. With these new groups defined, the data were analyzed using the

Origin Statistical Software. In addition to comparing the groups with regard to their

descriptive characteristics, differences between the groups were evaluated by performing

independent t-tests with regard to Myogenic Differentiation, Intracellular Calcium

Homeostasis, and Cell Cycle Analysis.

Table 7. *Descriptive Characteristics, T-Score Status Groups. Comparison of T-Score status groups, descriptive characteristics. *At the 0.05 level, the two means are significantly different with regard to T-Scores of the lumbar spine.*

	T-Score Status, CNTRL Group			T-Score Status, CASE Group			
	Mean	**SE**	**Range**	**Mean**	**SE**	**Range**	**p-value**
Age	67.7	1.7	15.8 (57.7 to 73.5)	61.6	2.2	20.1 (50.7 to 70.8)	0.06086
T-Spine	0.21	0.17	1.48 (-0.65 to 0.83)	-1.34	0.23	2.18 (-2.39 to -0.21)	5.14155E-5*
T-Hip	-0.85	0.06	0.54 (-0.97 to -0.43)	-1.01	0.20	1.70 (-1.78 to -0.08)	0.44969

Myogenic Differentiation. When the data were grouped according to T-Scores, independent t-tests were performed. With these data groups, analysis resulted in no significant difference between the means regarding any of the parameters for myogenic differentiation.

Table 8. *Myogenic Differentiation, T-Score Status Groups. Comparison of T-score status group means. At the 0.05 level, the two means were not significantly different.*

Myotube Nuclei	CNTRL (n=34)	CASE (n=43)	p-value
Mean	1051	1108	p = 0.15114

Total Nuclei	CNTRL (n=35)	CASE (n=41)	p-value
Mean	1361	1393	p = 0.35732

Fusion Index	CNTRL (n=35)	CASE (n=44)	p-value
Mean	78%	79%	p = 0.46511

As mentioned in the previous section there appeared an undeniable difference in the size of myotubes treated with different serum samples. After measuring representative myotubes for each image, the data were analyzed using the Origin Statistical Software. After

normalizing the data, independent t-tests were performed comparing the two groups with regard to myotube diameter. At the 0.05 level, when grouped according to T-Score Status, the two groups were shown not to be significantly different for all with regard to myotube diameter. Table 5 presents the results of these statistical analyses.

Table 9. *Myotube Diameter, T-ScoreStatus Groups. Comparison of fracture status groups, myotube diameter. At the 0.05 level, the two means were NOT significantly different with respect to myotube diameter.*

Myotube Diameter	CNTRL (n=197)	CASE (n=258)	p-value
Mean $\pm$ SEM (µm)	66 $\pm$ 3.6	62 $\pm$ 2.9	p = 0.41552

Intracellular Calcium Homeostasis. When these data were grouped according to T-Scores, independent t-tests were once again performed. With these data groups, analysis resulted in significant differences between the means regarding several of the parameters for intracellular calcium homeostasis.

Table 10. *Intracellular Calcium Homeostasis, T-Score Status Groups. *At the 0.05 level, the two means were significantly different with regard to average resting level, average peak level and calcium transients.*

Average Resting Levels	CNTRL (n=69)	CASE (n=94)	p-value
Mean	0.69278	0.67352	p = 0.00293*

Average Peak Levels	CNTRL (n=70)	CASE (n=99)	p-value
Mean	0.79903	0.77474	p = 0.00025*

Average Δ Level	CNTRL (n=70)	CASE (n=97)	p-value
Mean	0.09528	0.09592	p = 0.91133

Average Time to Peak (seconds)	CNTRL (n=70)	CASE (n=95)	p-value
Mean	10.29399	9.43535	p = 0.32098

Calcium Transients (Area Under the Curve)	CNTRL (n=71)	CASE (n=88)	p-value
Mean	285.6046	279.40629	p = 0.01126*
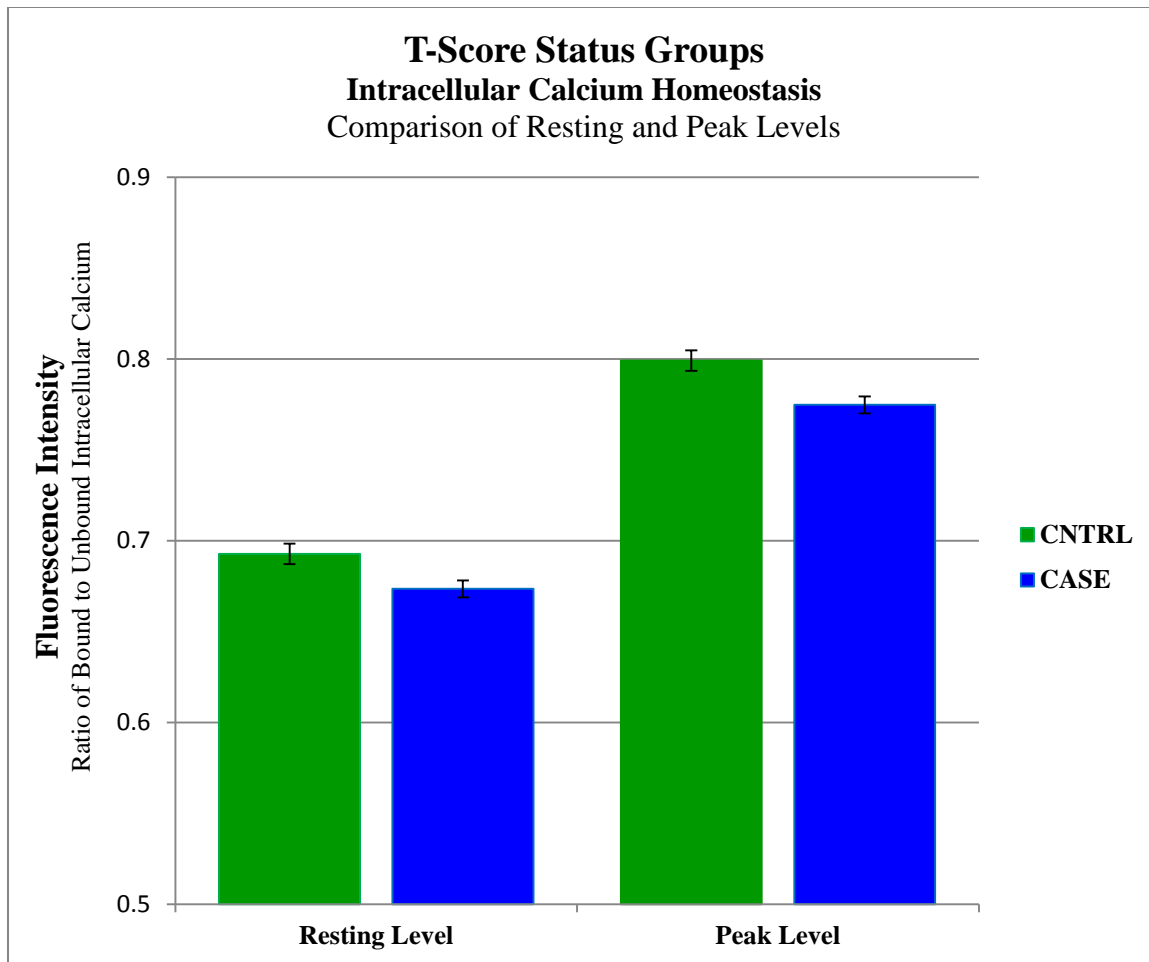
Figure 15. Calcium Imaging, Resting and Peak Levels, T-Score Status Groups. Calcium Imaging of HSMM cells treated with 1% serum from either the CNTRL or CASE group. Graphic depiction of the significant difference between means of the T-Score Status Groups.
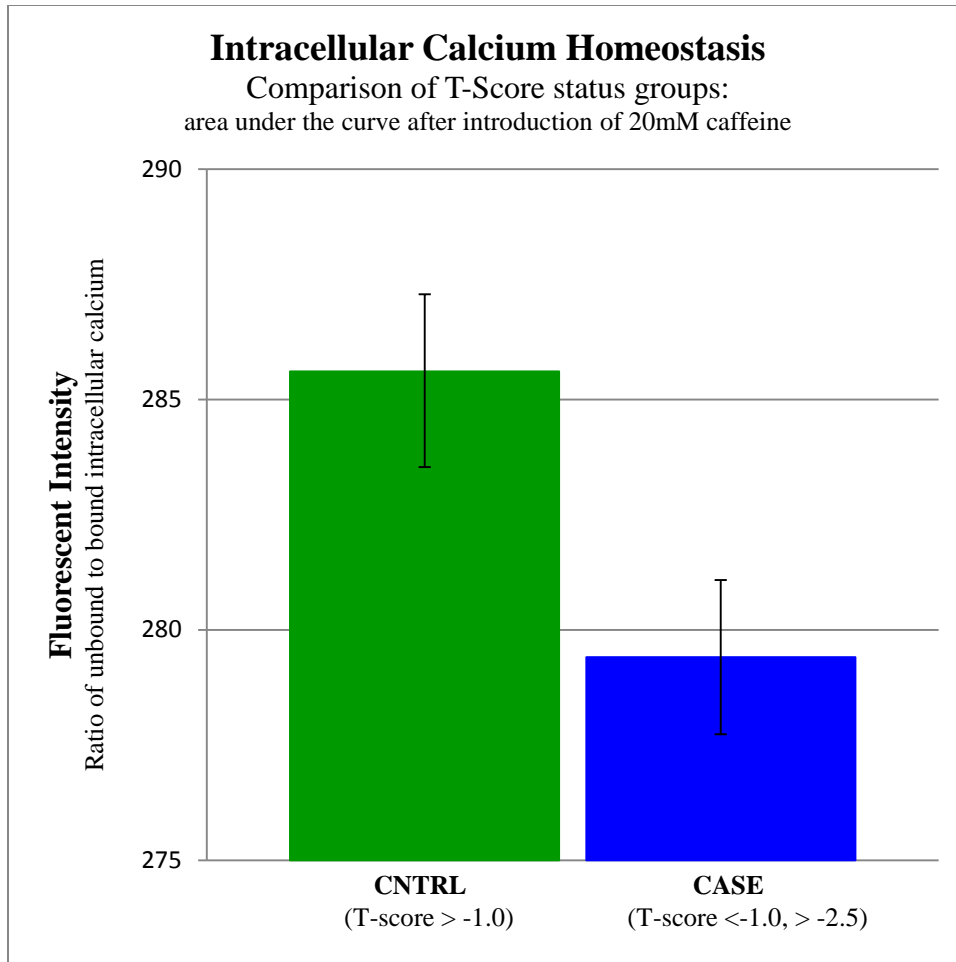
Figure 16. Calcium Imaging, Calcium Trasients, T-Score Status Groups. Calcium Imaging of HSMM cells treated with 1% serum from either the CNTRL or CASE group. Graphic depiction of the significant difference between means of the T-Score Status Groups.

Cell Cycle Analysis. When these data were grouped according to T-Scores,

independent t-tests were once again performed. With these data groups, there were no

significant differences between the means regarding parameters for cell cycle analysis.

Table 11. *Cell Cycle Analysis, T-Score Status Groups. Comparison of T- Score status groups, cell cycle analysis. At the 0.05 level, the two means were not significantly different for any of the parameters listed.*

G0/G1 phase	CNTRL (n=7)	CASE (n=9)	p-value
Mean	80.62143	82.17444	p = 0.35904

S phase	CNTRL (n=7)	CASE (n=9)	p-value
Mean	14.68143	13.8500	p = 0.46086

G2/M phase	CNTRL (n=7)	CASE (n=9)	p-value
Mean	3.03143	2.22778	p = 0.15391

Two tables have been prepared presenting these data collected on cells treated with each of the serum samples provided. Table 10 provides the information organized by Fracture Status Groups and Table 11 provides the information organized by T-Score Status Groups. These Tables can be found in Appendix J.

CHAPTER 5

DISCUSSION

Aging brings about a decline in physical strength and functioning that leads to disability and loss of independence. Osteoporosis and sarcopenia are two conditions associated with aging that contribute directly to this decline in function. Bones and muscles are connected anatomically and functionally, and over the years, research has demonstrated that the connection between these two systems is more complex than first believed. The objective of this dissertation study was to add to the growing body of knowledge related to the multifaceted relationship between bones and muscles. The working hypothesis was that human skeletal muscle cells treated with media containing serum from patients with osteoporosis will experience decreased differentiation and function than cells treated with media containing serum from patients without osteoporosis. This led to the specific aim, which was to investigate the biochemical, histomorphometric and functional differences in human skeletal muscle cells treated with conditioned media containing serum from patients with and without osteoporosis. The question this researcher set out to answer was: What is the extent of difference in biochemical, histomorphometric, and functional adaptations in HSMM cells treated with conditioned media containing serum from subjects with and without osteoporosis? The study results provided some insight into this research question, and raised additional questions to be explored.

All of the experiments were performed with this researcher blinded to the patient information associated with each of the serum samples. A member of the research team at Creighton University's Osteoporosis Research Center selected serum samples for this dissertation study from patients enrolled in their ongoing Bone Quality (BQ) Study. Eight

serum samples were selected that had been collected from patients with osteoporosis

(CASE), and eight serum samples were selected from patients without osteoporosis

(CNTRL). Even before the patient information was received, this researcher observed that

serum from different patients effected in distinct ways the differentiation and function of

human skeletal muscle (HSMM) cells. These differences came about in spite of the fact that

every effort was made to maintain the same environments, media components, and

procedures for all HSMM cells throughout each phase of the study. The observation that

differences occurred supports the premise that factors are present in serum that influence the

growth, development, and function of human skeletal muscle cells.

Myogenic Differentiation

After the experiments were completed, patient information was provided to this

researcher by the research team at Creighton University. The information provided on each

patient from whom serum samples had been used included the patient's age, fracture status,

and results of dual-energy X-ray absorptiometry (DXA) performed on their lumbar spine (T-

Spine) and hip (T-hip). First the data were grouped according to their fracture status:

whether or not the patient had sustained a non-traumatic fracture within the previous five

years, as this is the definition used by the Osteoporosis Research Group for

osteoporosis. When the data were grouped according to fracture status, the means of the two

groups were found by independent t-tests to be significantly different with regard to myotube

nuclei, total nuclei and fusion index. This analysis supports the proposed hypothesis and

indicates that the presence of osteoporosis negatively impacts the myogenesis of human

skeletal muscle cells. A decline in muscle mass and strength (sarcopenia) leads to decreased

protection from falls, and therefore leads to an increased risk of fracture among older

adults. The data suggest there is a reciprocated relationship. In other words, a decreased

bone mass (osteoporosis), as evidenced by non-traumatic fractures, contributes to a decline in

muscle mass. This provides support for another dimension to the relationship that exists

between bones and muscles.

The significant difference observed in myotube diameter when the data were grouped

according to fracture status is an important finding, especially with the growing appreciation

of muscle mass loss in older adults as a meaningful predictor of mortality (Brotto & Abreu,

2012; Chen et al., 2012; Kamel, 2003). Researchers are even suggesting that in older adults,

muscle mass index is a more reliable predictor of longevity than body mass index (BMI)

(Srikanthan & Karlamangla, 2014). As discussed in Chapter 2, skeletal muscle is a dynamic

tissue; constantly experiencing growth and repair. A key player in muscle regeneration and

repair is the muscle satellite cell. There is growing evidence that with aging, there is a

decline in the ability of these satellite cells to proliferate and differentiate into mature muscle

fibers (Karakelides & Naiar, 2005). Findings from this study suggests that factors in the

conditioned media of osteoporotic patients may inhibit the development of skeletal muscle

mass, further increasing the health risks of these aging individuals.

Clinicians are aware of the significant disability as well as the psychologic and

financial burden of osteoporotic fractures. For this reason, clinicians are motivated to assess

accurately the risk of fracture in their aging patients. One of the diagnostic criteria that

clinicians rely on most heavily to assess the risk of osteoporotic fractures is the dual-energy

X-ray absorptiometry (DXA). Since the early 1990s, osteoporosis has been defined as a T-

score of -2.5 or less performed at the lumbar spine, femoral neck, total hip, or one-third

radius sites (Baim, 2011; National Osteoporosis Foundation, 2010; World Health

Organization, 1994). The findings of several large epidemiologic studies that the majority of low-trauma fractures occur in women in the osteopenic range compared with those in the range of osteoporosis (Pasco, J. A. et al. 2006; Sornay-Rendu, E., Munoz, F., Garnero, P., Duboeuf, F., & Delmas, P. D., 2005; Wainwright, S. A. et al., 2006). Due to the important role that T-Scores play in determining the course of treatment related to fracture risk, this researcher grouped these data again; this time according to T-Scores. When grouped in this manner, the CASE group was comprised of patients with T-Scores less than -1.0. None of these patients had a T-Score below -2.5, but all had T-scores between -1.0 and -2.5, which categorizes them as osteopenic. The remaining seven patients had T-scores greater than -1.0, categorizing them as normal. When the data were grouped in this way, the means of the two groups were not found by independent t-tests to be significantly different. From this, it can be concluded that the presence of a non-traumatic fracture reflects a decrease in myogenic differentiation more accurately than a T-Score in the osteopenic range. The clinical goal, however, is to accurately forecast the risk of fracture rather than to treat it after is has occurred. Evidence uncovered in this portion of the dissertation study indicates that the determination of fracture risk, and therefore, the proper course of treatment for aging patients' needs to be based on more than just bone mineral density (BMD) as reflected by T-Scores.

With the revelation that BMD, as reflected in DXA scan T-Scores, is not the definitive measure of fracture risk, the WHO Fracture Risk Assessment Tool (FRAX) was developed (McCloskey, 2009). In addition to T-Scores, this tool includes a number of parameters to calculate a patient's 10-year probability of fracture including age, gender, and body mass index, family history of hip fracture, smoking, alcohol intake, and rheumatoid

arthritis. As more information is uncovered about the biochemical relationship between bones and muscles, it may be prudent to begin to include in the list of parameters a measure of the patient's muscle mass and strength.

<div align="center">**Intracellular Calcium Homeostasis**</div>

Skeletal muscle uses calcium (Ca^{2+}) as an important regulatory and signaling molecule. Fluctuations in intracellular Ca^{2+} determine to a large degree the force and speed of muscle contraction.   It is for these reasons that calcium imaging was employed as one of the methods to evaluate the impact of different serum samples on the function of differentiated HSMM cells. Within skeletal muscle cells, through the process of excitation-contraction coupling (ECC), depolarization of the external membrane and T-tubules lead to the release of Ca^{2+} from the sarcoplasmic reticulum (SR) into the cytosol. This release of Ca^{2+} overwhelms the contractile myofilaments, myosin and actin, and leads to the induction of muscle contraction. Key to this process is the ryanodine receptors (RyR1), which serve as gatekeepers to the release of Ca^{2+} from the SR.   For the calcium imaging experiments in this study, a solution of 20mM caffeine was introduced to the cells to sensitize the RyR1 to Ca^{2+} and to trigger SR Ca^{2+} release from the SR into the cytosol that can be accurately measured by the ratiometric dye Fura-2. From these calcium-imaging experiments, data on the intracellular calcium homeostasis were collected as resting levels, peak levels, time to peak, and calcium transients.

When the data gathered were grouped according to fracture status, the means of the two groups were not found by independent t-tests to be significantly different with regard to resting intracellular calcium level, peak intracellular calcium level, time to peak, or calcium transients, as measured by area under the curve. This analysis would seem to indicate that,

while factors present in the serum of patients with osteoporosis do influence the myogenesis of skeletal muscle cells, they do not affect the function of those cells. However, when the data gathered from calcium imaging were grouped according to T-Scores, the two means were significantly different with regard to resting intracellular calcium levels (100 vs 80nM in CNTRL vs CASE), peak intracellular calcium levels (~300nM vs ~260nM in CNTRL vs CASE), and calcium transients. The T-Score status CNTRL group mean had higher resting and peak levels, as well as higher calcium transients than the T-Score status CASE group mean. This would appear to contradict the indication of the first analysis. When the calcium imaging data were grouped according to T-Scores, it would appear that factors in the serum do affect the function of skeletal muscle cells. One observation that can be made from these two analyses of the data would again be that the parameters of T-Scores and fracture status are not consistent in their reflection of bone and muscle health; at least with regard to the intracellular calcium homeostasis of skeletal muscle cells. The T-Scores reflect the density of bones, which may be a good surrogate for calcium measurements.

Much has been learned about the role of intracellular calcium in the health and function of skeletal muscles. Recent research demonstrated in murine myoblasts that the inhibition of calcium channels, and therefore a decrease in intracellular calcium levels, inhibits myoblast differentiation (Porter, Makuck, & Rivkees, 2002). This is supported by the data from this dissertation study, which when grouped according to fracture status, revealed a significant difference in fusion index, or myogenic differentiation. The resting and peak intracellular calcium levels were also lower with this group, and although not significantly different when grouped according to fracture status, may provide a partial explanation for the decline in myoblast differentiation. These data support the research that

demonstrated a correlation between a decrease in intracellular calcium level and myoblast inhibition.

It is generally accepted that aging brings with it a reduction in size and number of muscle fibers, especially Type II (fast-twitch) muscle fibers (Andersen, 2003; Deschenes, 2004). Research has also shown that the amount of calcium that is released in fast twitch muscle fibers is three-to four-fold greater than the amount released in slow twitch fibers (Baylor & Hollingworth, 2012). It would then follow that with aging skeletal muscle cells would experience a decrease in the amount of resting intracellular calcium. This is consistent with the data obtained from this dissertation study, and significantly when these data were grouped according to T-Score status.

While many factors impact the aging of skeletal muscle, recent research has demonstrated, in murine models, that mitochondrial dysfunction, oxidative stress, and impaired RyR1 may all play a role in age-related muscle weakness (Andersson, et al., 2011; Berchtold, Brinkmeier, & Muntener, 2000). Of special clinical significance, researchers have also come to believe that the magnitude of the Ca^{2+} released from the SR is related to the force of contraction (Berchtold, Brinkmeier, & Muntener, 2000; Capes, Loaiza, & Valdivia, 2011). The data obtained in this dissertation study suggest that the group with lower intracellular calcium levels would be the group with decreased muscle strength and increased risk for injury. An additional layer to this physiologic conundrum is that calcium also regulate/modulate genetic function, and therefore may be influencing many signaling pathways. The overall calcium transient in the control group was characterized by higher resting level, higher peak, and higher post-peak levels of calcium. Thus, calcium-induced gene regulation may be enhanced in the control group as compared to the case group.

88

Additional research is needed to better understand the role of intracellular calcium homeostasis in skeletal muscle cell function, bone density, and the overall health of the aging patient.

Cell Cycle Analysis

As myoblasts proliferate, they proceed through the two phases of the cell cycle: interphase and mitosis. G1 is the first and typically, the longest part of interphase, as components of the cell grows. A sub-portion of this is the G0 phase, for those cells in G1 that are not ready to progress along the cell cycle. Cells in the G0 phase are in holding pattern. The second part of interphase is the S phase, during which DNA is duplicated. The third and final portion of interphase is the G2 as cells ready themselves for mitosis. The shorter phase of the cell cycle is mitosis, during which the cells divide. Myoblasts continually travel through this process as they proliferate and until they enter differentiation.

Flow cytometry was performed using the MUSE™ Cell Analyzer for HSMM cells treated with media containing 1% of each of the serum samples. One of the features of the MUSE™ Cell Analyzer is a graphic representation of the DNA content of each run. Although myocytes exit the cell cycle when they enter differentiation, it was believed that the myotubes, or differentiated cells, would be observed along the far right of the graph, having increased DNA as the myocytes fuse together to form myotubes.

Data were collected and then analyzed to evaluate the differences between the CASE and CNTRL groups with regard to the number of cells in each phase of the cell cycle as well as the magnitude of DNA content. The data were grouped and independent t-tests were performed to compare the group means. Whether the data were grouped according fracture

status or T-Score status, there was no significant difference observed between the group means.

With regard to the DNA Content Profile, it was expected that an increased amount of myogenic differentiation would be reflected in a greater number of cells toward the far right of the graph, representing the increased DNA content associated with myotubes. Unfortunately, the graphic representation of DNA Content Profile provided a limited range of DNA content index along the x-axis. For this reason, the amount of DNA content exceeded the limits of the scale provided, thus there was no evidence of it on the graph. It is believed that more myotubes would have been represented, had it been possible to expand the range of the horizontal axis. Until this technical issue is resolved, the use of Flow Cytometry for cell cycle analysis will be limited to research focused on myoblast proliferation.

Limitations

One of the limitations of this preliminary study was the inability to match perfectly the profiles of patients from case and control groups. As described, the participants were matched according to age, gender, and general health. However, for this dissertation study, there was no match for environmental and other potentially confounding factors such as nutritional intake, genetic profiles or emotional status. Health of bones and muscles are dependent upon multiple variables, and the more variables that can be examined in studies, the greater the likelihood of clarifying the magnitude of the impact each variable has on patient outcomes.

The World Health Organization (WHO) has established criteria for making a diagnosis of osteoporosis based upon bone mineral density as determined by DXA scan

results, or T-Scores. Patients with T-Scores that fall below -2.5 are diagnosed as

osteoporotic; those with T-Scores between -1.0 and -2.5 are diagnosed with osteopenia; and

those with T-Scores greater than -1.0 are considered normal. Another potential limitation of

this dissertation study is that none of the serum samples included in this study was from

patients with T-Scores below -2.5, or according to the WHO definition, osteoporotic. It

would be interesting to repeat these experiments with the CASE group comprised of patients

who had not only experienced a non-traumatic fracture, but who also had evidence of

osteoporosis based upon DXA scan results.

Although the serum samples are collected *in vivo*, another limitation of this proposed

study was that the experiments will be performed *in vitro*. The behavior of cells is altered

when *in vivo* due to dynamic conditions of the individual and their environment. These

dynamic conditions cannot be replicated in the setting of a cell culture. Additionally, two of

the three phases of this study supported the hypothesis that myogenesis is impacted by

factors present in the serum of patients with and without osteoporosis. No specific

information was collected that clearly identified which the factor(s) altered the samples.

Thus, additional studies will need to be performed to determine this.

Future Directions

Data collected in this study will contribute to the growing body of knowledge related

to bone-muscle interactions. Insight was gained into the differing effects of serum from

patients with and without osteoporosis on human skeletal muscle cell differentiation and

function.   In addition to repeating Phases I and II of the study, this researcher is interested in

performing a factor analysis of elements that have shown to increase the aging patient's risk

for injury. Elements such as age, gender, level of activity, body mass index (BMI), T-Score,

muscle strength as measured by grip strength, medication profile and co-morbidities. It will also be essential to identify genes/proteins that are responsible for the effects observed by the serum samples of patients with osteoporotic fractures, since they could lead into new therapeutic targets to perhaps treat both osteoporosis and sarcopenia.

The ultimate goal of this research is at least two-pronged: first, to accurately identify those who are at greatest risk for fractures and other injuries that are so often the consequence of aging, and second, to identify biochemical factors that influence bone and muscle health. In so doing, interventions can be developed to make a meaningful difference in the quality of life for each member of our aging population.

Observations made throughout this study support the biochemical communication that exists between bones and muscles. However, the observations made have also led to more questions. For example, with regard to myogenic differentiation, what specific signaling pathways are involved that lead to muscle wasting and/or a decline in muscle repair with aging? What is the role of satellite cells in this process? What activities or exercises could reduce muscle wasting with age? Moreover, with regard to intracellular calcium homeostasis, what level of intracellular calcium correlates with optimal function of skeletal muscles cells? At what point is an increased resting level of intracellular calcium due to impaired myogenesis, and when is it the result of defective release from the SR?

Additional studies will also need to be performed related to changes that occur in bone-derived factors with aging, comparing the effect on myogenesis in human skeletal muscle cells of serum collected from patients ranging from young adults (20 to 40 years of age), from middle-aged adults (41 to 65 years of age), and from older adults (age 65 and older). That information would provide additional insight into the bone-muscle crosstalk,

and the degree to which age versus disease (e.g. osteoporosis) impacts human skeletal muscle formation and function.

Further research opportunities exist in the expansion of this work to include other tissues in the bone-muscle unit: cartilage, ligaments, and tendons. Advances are being made in these areas, but are becoming even more important to bridge the gap between bench research and clinical practice. The dynamic and ongoing interplay between bones and muscles must be embraced and inculcated into all aspects of biomedical research, if it is to translate into meaningful therapeutic and preventive approaches to patient care.

Appendix A

IRB Authorization Agreement

Creighton
UNIVERSITY

August 28, 2013

Janalee Isaacson
17120 Penrose Lane
Lenexa, KS 66219

RE: Implementing Letter and IRB Approval Letter

Dear Janalee

Enclosed you will find two copies of the UBMTA Implementing Letter for your use of serum samples from our BQ study. Please obtain the appropriate signatures on both copies and send one fully executed copy back to my attention at the following address:

Karla Melcsker
Creighton University
Osteoporosis Research Center
601 North 30th Street, Suite 4820
Omaha, NE 68131

My telephone number is (402) 280-4293 if you need it.

Also, I am enclosing a copy of the IRB approval for the use of these serum specimens.

Let me know if questions.

Thank you.

Sincerely

Karla Malesker
Grants Administrator

Enclosure

Creighton
UNIVERSITY

☑ Expedited Review
☐ Convened Meeting Review

August 20, 2013

Robert Recker, M. D.
School of Medicine
Department of Medicine/Osteoporosis Research Center

RE:
IRB #:   07-14738
TITLE: A STUDY OF REDUCED BONE QUALITY AS A CAUSE OF
              FRACTURES

Dear Dr. Recker,

The IRB office has received the following documents for the above project:

1. Application for Request for Modification of Approved Research signed August 16, 2013
2. Protocol amendment #7 dated August 8, 2013

This amendment concerns the use of stored specimens to be sent to a lab at the University of Missouri Kansas City (UMKC). A Consent Addendum for the Storage of Unused Blood Serum and/or Bone Samples has previously been approved for this study. The contents of this amendment are administrative in nature and do not appear to adversely affect the risk/benefit ratio of this study or the process of obtaining informed consent. Therefore, amendment #7 is approved for use at this site. This amendment did not require a change to the consent document.

The approvals conditions are as follows:

1. A Material Transfer Agreement for this project will be signed by both institutions. In the agreement it should include that the UMKC site will not be given any identifying information with the specimen. A signed copy of this agreement should be submitted to be kept in the IRB file.
2. The only specimens that may be sent to UMKC are those in which the participant signed the Consent Addendum for the Storage of Unused Blood Serum and/or Bone Samples without limiting the conditions on the use of their specimen.

Sincerely,

Mary Kimes-Connell, Ph.D.
Chair, Institutional Review Board

UBMTA Implementing Letter

The purpose of this letter is to provide a record of the biological material transfer, to memorialize the agreement between the PROVIDER SCIENTIST (identified below) and the RECIPIENT SCIENTISTS (identified below) to abide by all terms and conditions of the Uniform Biological Material Transfer [[Page 12775]] Agreement ("UBMTA") March 8, 1995, and to certify that the RECIPIENT (identified below) organization has accepted and signed an unmodified copy of the UBMTA. The RECIPIENT organization's Authorized Official also will sign this letter if the RECIPIENT SCIENTISTS are not authorized to certify on behalf of the RECIPIENT organization. The RECIPIENT SCIENTISTS (and the Authorized Official of RECIPIENT, if necessary) should sign both copies of this letter and return one signed copy to the PROVIDER. The PROVIDER SCIENTIST will forward the material to the RECIPIENT SCIENTISTS upon receipt of the signed copy from the RECIPIENT organization.

Please fill in all of the blank lines below:

1. PROVIDER: Organization providing the ORIGINAL MATERIAL:

   Organization: Creighton University

   Address: 2500 California Plaza

   Omaha, NE 68178

2. RECIPIENT: Organization receiving the ORIGINAL MATERIAL:

   Organization: University of Missouri-Kansas City

   Address: 2464 Charlotte St

   Kansas City, MO 64108

3. ORIGINAL MATERIAL (Enter description): serum samples from the sixteen [16] BQ study participants identified as follows: BQ ID #228, 368, 380, 390, 391, 397, 403, 428, 435, 439, 463, 480, 482, 488, 495, 496

4. Termination date for this letter (optional): None

5. Transmittal Fee to reimburse the PROVIDER for preparation and distribution costs (optional). Amount: None

This Implementing Letter is effective when signed by all parties. The parties executing this Implementing Letter certify that their respective organizations have accepted and signed an unmodified copy of the UBMTA, and further agree to be bound by its terms, for the transfer specified above.

PROVIDER SCIENTIST

Name: _Robert Recker, M.D._____
Professor of Medicine
Osteoporosis Research Center
Creighton University
2500 California Plaza
Omaha, NE 68178

Signature: _Robert R. Becker_____

Date: _____

RECIPIENT SCIENTISTS

Name: _Maren Butin, BSN, MS, Ph.D._____
Associate Professor of Nursing and Medicine
University of Missouri-Kansas City
Health Sciences Building
Suite 2217
2464 Charlotte St.
Kansas City, MO 64108

Signature: _MouRotts_____
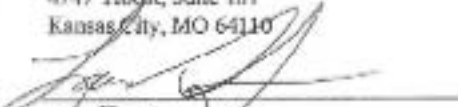
Date: _09/04/2013_____

Name: _Janelee Isaacson, RN MSN_____
PhD Student
University of Missouri-Kansas City
Health Sciences Building
Suite 2217
2464 Charlotte St.
Kansas City, MO 64108

Signature: _Janelee Isaacson_____
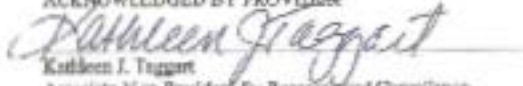
Date: _09/04/2013_____
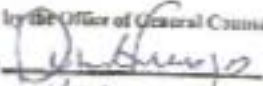
RECIPIENT ORGANIZATION CERTIFICATION

Certification: I hereby certify that the RECIPIENT organization has accepted and signed an unmodified copy of the UBMTA (May be the RECIPIENT SCIENTIST if authorized by the RECIPIENT organization):

Authorized
Official: Lawrence Dreyfus

Title: Vice Chancellor for Research and Economic Development

Address: 4747 Troost, Suite 101
                 Kansas City, MO 64110

Signature:

Date: 9-6-13

ACKNOWLEDGED BY PROVIDER:

Kathleen J. Taggart
Associate Vice President for Research and Compliance
Creighton University

Date   8/27/13

Reviewed by the Office of General Counsel

Signature

Date   6/27   20   13

98

Appendix B

List of Identified Factors:
Exploring the biochemical relationship between bones, muscles and other tissues.

Factor Full Name/ Abbreviation	Tissues/ Cells Secreted From	Actions/ Information	References
Adiponectin	adipocytes *Secrete > 50 adipokines!*	The only known adipokine that is downregulated in obesity. Positively influences insulin sensitivity. Low plasma levels used as an indicator/ predictor of insulin resistance and diabetes. Possibly an autocrine regulator of adipocytes secretion?	Sell, Dietz-Schroeder & Eckel, 2006
Adenosine triphosphate/ ATP	osteocytes	"molecular currency" transports chemical energy within cells for metabolism	
Brain-derived neurotrophic factor/ BDNF	Myocytes	Plays a role in peripheral metabolism, myogenesis and muscle regeneration. Levels of this protein increase with exercise.	Matthews et al., 2009 Sakuma & Yamaguchi, 2011
Dickkopf-related/ DKK-1	osteocytes	Inhibits the Wnt signaling pathway. Elevated levels of this protein in bone marrow, plasma and peripheral blood are associated with osteolytic bone lesions in patients with multiple myeloma. One of the most up-regulated proteins in androgen-potentiated balding. In humans, is encoded by the *DKK1* gene.	

Dentin matrix acid phosphoprotein 1/ DMP-1	Found in bone and tooth tissue	An extracellular matrix protein; critical for the mineralization of bone and dentin. Diseases associated with this protein include osteomalacia and rickets.	
Chemokine CXC motif ligand-1/ CXCL-1 (also known as keratinocyte-derived chemokine/ KC)	Myocytes	Exercise induces a six-fold increase in mRNA and a 2.4 fold in serum.	Pedersen, Olsen, Pedersen, & Hojman, 2012
Free fatty acids/ FFA		Become elevated in non-adipose tissue in obesity. Lipotoxic effects on skeletal muscle and other peripheral tissues (Sell, 2006) Interfere with insulin signaling in skeletal muscle as the level of IRS-1 serine phosphorylation	
Fibroblast growth factor 23/ FGF-23	osteocytes	Regulates phosphorous and vitamin D metabolism	Bonewald & Wacker, 2012
	osteoblasts and osteoclasts – in response to calcitrol	Regulation of serum phosphate levels; site of action is the kidneys	Shimada et al., 2004 Yamashita et al., 2000
Interleukin-5	Myocytes	Role in muscle fat crosstalk?	Pedersen, Akerstrom, Neilsen & Fischer, 2007
Interleukin 6/ IL-6	adipocytes	Pro-inflammatory cytokine	
	myocytes	Biomarker for low grade inflammation; Upregulated in obesity	Duzova, 2012
		Increases with exercise. Increases insulin sensitivity in skeletal muscle cells. Activates lipolysis in adipose tissue	
Interleukin-7/ IL-7	myocytes	Role in satellite cell recruitment in muscle regeneration	Pedersen, Akerstrom, Neilsen & Fischer, 2007

Interleukin-15/ IL-15	myocytes	Alters muscle protein metabolism. In rodents, influences lipid partitioning by limiting free fatty acid uptake and favoring oxidations – resulting in the reduced mass of white adipose tissue. Increases adiponectin secretion in 3T3 adipocytes.	
Leptin	adipocytes	Crucial role in regulation of body weight. Increases insulin sensitivity Impairs action of insulin in hepatocytes, adipocytes and myocytes *in vitro*.	
Leukemia inhibitory factor/ LIF	myocyte	Associated with increased myocyte differentiation after injury	Kurek, Bower, Romanella, Koentgen, Murphy, & Austin, 1997
Monocyte chemotactic protein/ MCP-1	monocytes endothelial cells adipocytes	Can induce insulin resistance in adipocytes and myocytes. Elevated expression of MCP-1 is believed to increase the inflammatory processes in heart and arteries.	
Matrix extracellular phosphoglycoprotein/ MEPE	osteocytes	Regulation of phosphate homeostasis and mineralization	
Nitric oxide/ NO	osteocytes	Increased production is associated with rheumatoid arthritis, inflammation Pro-inflammatory cytokines such as IL-1 and TNF cause activation of the iNOS pathway in bone cells and NO derived from this pathway potentiates cytokine and inflammation induced bone loss. Relevant to the pathogenesis of osteoporosis in inflammatory diseases such	

		as rheumatoid arthritis, which are characterized by increased NO production and cytokine activation.	
Neurtrophin-3/ NT-3; NT-4/5	Myocytes	Protein growth factor known to have activity with neurons of the central nervous system	
Osteoprotegerin/ OPG	osteocytes	Traffic regulator of RANKL – possibly as a decoy receptor? Critical for osteoclastogenesis.	
osteocalcin (also known as the bone gamma-carboxyglutamate acid-containing protein/ BGLAP)	osteoblasts	Involved in regulation of metabolism Acts on beta cells of pancreas to secrete insulin Acts on fat cells to secrete adiponectin Possible role in male fertility? In humans, encoded by the *BGLAP* gene	Karsenty, Gerard, & Wagner, 2002
Prostaglandins/ PG Especially E- and F-series (PGE and PGF)	osteocytes myocytes	Bone homeostasis Inflammation Pain mediation Platelet aggregation Smooth muscle contraction	Agas, Marchetti, Hurley, & Sabbieti, 2013
Receptor activator of nuclear factor kappa-B ligand/ RANKL (also known as tumor necrosis factor ligand superfamily member 11/ TNFSF11) (also known as TNF-related activation-induced cytokine/ TRANCE) (also known as osteoprotegerin ligand/ OPGL)	osteocytes	A <u>protein</u> that in humans is encoded by the *TNFSF11* <u>gene</u>. Found on osteoblasts; critical for activation of osteoclasts. Overproduction is associated with bone degenerative diseases, such as rheumatoid arthritis; osteoporosis	Karsenty, Gerard, & Ferron, 2012

(also known as
osteoclast
differentiation factor/
ODF)

Retinol-binding protein/ RBP-4	adipocytes	Contributes to insulin resistance *in vivo*.	
Sclerostin	osteocytes	Inhibition of bone formation.	Winkler et al., 2003
Tissue growth factor α/ TGFα	myocytes	Secreted by injured skeletal muscle	Kurek, Bower, Romanella, Koentgen, Murphy, & Austin, 1997 Li & Huard, 2002
Tissue growth factor β1/ TGFβ1	myocytes	Secreted by injured skeletal muscle	Kurek, Bower, Romanella, Koentgen, Murphy, & Austin, 1997 Li & Huard, 2002
Tissue inhibitor of metalloproteinases/ TIMP-1	adipocytes	May play a role in maintaining adipose tissue mass in obesity?	
Tumor necrosis factor/ TNFα	Adipocytes	Biomarker for low grade inflammation; Upregulated in obesity Induces insulin resistance in hepatocytes and adipose *tissue in vitro*.	Dyck, et al., 2011
	myocytes		Castellano, V., 2006

Appendix C

HSMM Protocols

PROTOCOL C1: Media Preparation, Skeletal Muscle Growth Media-2

Gather supplies
- SkGM™-2 Basal Medium
- SkGM™-2 SingleQuots™ Kit (Catalog # CC-3244), which contains
  - human Epidermal Growth Factor (hEGF) *(0.5ml)*
  - Dexamethasone *(0.5ml)*
  - L-glutamine *(10ml)*
  - Fetal Bovine Serum (FBS) *(50ml)*
  - Gentamicin/ Amphotericin-B (GA) *(0.5ml)*
- Pipettes

Working in the cell culture hood and observing aseptic technique,
1. Spray external surfaces of all vials, medium bottle and reagent bottles with 70% ethanol.
2. Using pipette, transfer contents of the SkGM™-2 SingleQuots Kit to the SkGM™-2 Basal Medium
3. Rinse the vial with medium to recover as much of the contents as possible.
4. Transfer the label provided to the Basal Medium bottle, taking care not to obscure the lot # and expiration date.
5. Store in 4° C refrigerator.

PROTOCOL C2: Thawing of HSMM Cells/ Initiation of Culture Process

The recommended seeding density for HSMM is 3500 cells/cm^2. Therefore, to thaw a cryovials containing $\geq$ 500,000 cells, I will use two (2) T75 flasks, since each T75 flask would accommodate approximately 250, 000 cells (3500 cells/cm^2 X 75 cm^2 =262,500 cells)

Also, the manufacturer recommends the appropriate amount of medium to be 1ml/ 5 cm^2, so for each T75 flask, I will plan to use 15ml (1ml/5cm^2 X 75 cm^2 = 15ml)

One last point to note: the manufacturer reports that centrifugation should not be performed to remove cells from the "cryoprotectant cocktail," as this action is more damaging than the effects of DMSO residue in the culture.

Gather supplies
- Cryovial (Normal HSMM, $\geq$500,000 cells; Catalog # CC-2580)
- T75 flasks (2)
- Skeletal Muscle Growth Medium-2
- Pipettes
- Beaker for discard

Working in the cell culture hood and observing aseptic technique,
1. Spray external surfaces of all vials, medium bottle and reagent bottles with 70% ethanol.
2. Transfer 15 ml of the Skeletal Muscle Growth Medium-2 into each of two T75 flasks.
3. Place in incubator at 37° C and 5% CO$_2$.

4. In the cell culture hood, briefly twist the cap of the cryovials a quarter turn to relieve pressure, and then retighten.
5. Thaw cryovials in a 37° C warm water bath, taking care not to submerge the vial.
   (Note: thawing the cells for longer than 2 minutes may yield less than optimal results)
   As soon as ice crystals disappear, swab the outside of the vial with 70% ethanol.
6. Resuspend the cells in the cryovial, gently pipetting up and down to distribute evenly.
7. Using a pipette, transfer half the contents of the cryovial into each of the T75 flasks.
8. Gently rock the flasks to evenly distribute the cells and return to the incubator at 37° C and 5% CO_2.
9. Let cells recover for 16 hours in the incubator at 37° C and 5% CO_2 for 16 hours.
10. The next morning, aspirate out the diluted DMSO-containing shipping cryopreservation medium from the cell layer and discard.
11. Add 15 ml Skeletal Muscle Growth Medium-2 into each of two T75 flasks.

PROTOCOL C3: Subculturing HSMM cells

Subculture the cells when they are 50% to 70% confluent.

Gather supplies
- Solutions
    a. Dulbecco's Phosphate Buffered Saline (DPBS)
    b. Trypsin/ EDTA
    c. Trypsin Neutralizing Solution (TNS)
    d. SkGM-2 Growth Medium
- 15ml conical tube(s)
- Culture vessel(s) of choice: T75 flasks, six-well plates, optic dishes
- Pipettes
- Beaker for waste

1. Propagate cells until they reach 50% to 70% confluence.
2. Allow solutions to come to room temperature.
    a. Dulbecco's Phosphate Buffered Saline (DPBS)
    b. Trypsin/ EDTA
    c. Trypsin Neutralizing Solution (TNS)
    d. SkGM-2 Growth Medium
3. Aspirate and discard medium from T75 flask.
4. Wash cells with 15 ml DPBS.
5. Aspirate and discard DPBS wash.
6. Cover cells with 2 ml of Trypsin/ EDTA solution.
7. Incubate for 2 to 6 minutes at 37°C and 5% CO_2.
8. Examine cells using microscope. When ~ 90% of cells are rounded up, rap the flask against the palm of hand to release majority of cells from the surface of the flask.
9. Add 4 ml Trypsin Neutralizing Solution.
10. Using pipette, wash the bottom of the flask several times.
11. Quickly transfer contents to 15 ml conical tube.
12. Rinse flask with 2 to 5 ml of PBS, add this to 15 ml conical tube.
13. Observe harvested flask under the microscope to assure fewer than 5% of cells left behind Centrifuge at 220 x g for five (5) minutes.

NOTE: The centrifuge we use has a radius of 8 cm, therefore, using the G-Force to rpm conversion calculator retrieved from: http://www.geneinfinity.org/sp/sp_rotor.html

$220 \, x \, g = 1569 \, rpm$

14. Aspirate and discard the supernatant, leaving 100 to 200 μL
15. Flick the tube to loosen the pellet
16. Dilute the cells to a final volume of 2 to 5 ml of growth medium, pipetting up and down gently to ensure uniform suspension. (be certain to note the total volume of the diluted cell suspension)
17. After performing cell count, prepare flasks/ plates/ dishes in which to transfer/ seed the cells.
18. Carefully transfer growth medium to new culture vessels by adding 1 ml/ 5 cm^2 surface area of the flask (e.g. Add 15ml growth medium to each T75 flask; or 2ml/well of a 6-well plate)
19. Plate the cells at the recommended seeding density of 3500/ cm^2. (e.g. 35K/ well in a 6 well plate or optic dish)

PROTOCOL C4: Cryopreservation of HSMM cells

Clonetics™ HSMM Cryopreserved cultures are assured for experimental use for 10 population doublings. I would like to store as many cells as possible from the initial purchase of 1 cryovial, containing ≥ 500,000 cells.

Desired Volume of Cryopreservation Media	Base Media	DMSO	FBS
Clonetics™ (Lonza) suggestions	70% SkGM-2 base media	10% DMSO	20% FBS
20ml	14ml	2ml	4ml
10ml	7ml	1ml	2ml
5ml	3.5ml	0.5ml	1ml

Gather supplies
- Solutions:
  a. Dulbecco's Phosphate Buffered Saline (DPBS)
  b. Trypsin/ EDTA
  c. Trypsin Neutralizing Solution (TNS)
  d. SkGM-2 Growth Medium
  e. Cryopreservation Medium components
- Filters, 0.2micron
- 15ml conical tube(s)
- Cryovials
- Styrofoam or propanol freezing canister
- Pipettes
- Beaker for waste

1. Prepare the cryopreservation media as described in the Table above.

2. Sterile filter the cryopreservation media using a 0.2 micron filter.
3. Harvest and centrifuge cells to pellet. (see Protocol C: Sub culturing HSMM cells)
4. Aspirate and discard supernatant.
5. Resuspend cells in cold cryopreservation media at 500,000 cells/ml
6. Pipette aliquots of 1ml each into cryopreservation vials and seal.
7. Place in styrofoam or propanol freezing canister (?)
8. Store the cells at -80° C overnight
9. Within 12 to 24 hours, place cells in liquid nitrogen for long-term storage.

PROTOCOL C5: Differentiation to Form Myotubes

Gather supplies
- T75 flasks with HSMM cultured to approximately 50% to 60% confluence.
- Fusion Medium
  DMEM: F-12 supplemented with 2% horse serum

Total Volume	DMEM	Horse Serum
500ml	490ml	10ml
250ml	245ml	5ml
100ml	98ml	2ml
50ml	49ml	1ml

- Beaker to receive discarded medium
- Pipettes

Working in the cell culture hood and observing aseptic technique,
1. Spray external surfaces of all vials, medium bottle and reagent bottles with 70% ethanol.
2. Remove the growth medium and discard.
3. Replace with an equal volume of Fusion Medium (DMEM F-12 supplemented with 2% horse serum)
4. Replace with fresh Fusion Medium every other day for about 3 to 5 days or until myuotubes are observed throughout the culture.

NOTE: If the myotubes are to be used in assays that require an extended period in culture, following differentiation, remove the fusion medium and add growth medium. For best performance, replace growth medium every other day to maintain the culture for ~2 to 3 weeks post differentiation. Myotube cultures are best used by 2 weeks post differentiation.

Appendix D

Protocol: HSMM, Immunostaining for Fusion Index Calculations

Fixation of cells
1. Working in the chemical hood, discard media from wells.
2. Gently add 2ml PBS to each well, adding slowly at the side of the well.
3. Incubate at room temperature for 5 minutes
4. Repeat for a total of three (3) washings with PBS.
5. Fix cells by adding 1ml/well of 10% NPF (Neutral Buffered Formalin)
6. Incubate at room temperature for 7 to 8 minutes (Do not exceed 10minutes!)
7. Discard 10% NPF in special container in chemical hood.
8. Gently add 2ml PBS to each well, adding slowly at the side of the well.
9. Incubate at room temperature for 5 minutes
10. Repeat for a total of three (3) washings with PBS, making certain all the NBF is removed.

   NOTE: If not staining immediately, may store cells by adding 2ml/well of 70% ETOH; wrap the plate in saran wrap and store in chemical hood at room temperature.

Staining of cells, (Solution Preparation for two (2) six-well plates)

Prepare 0.1% Trition X -100 from the 100% Triton stock:

$$C1V1 = C2V2$$
$$100V1 = 0.1(30ml)$$
$$(0.03ml)V1 = 30\mu L \text{ of } 100X \text{ Triton}$$

Therefore, add 30 µL of 100X Triton to 29.97 ml PBS for a total of 30 ml 0.1% Triton X-100.

   NOTE: Take care to aspirate Triton <u>very</u> slowly, as it is incredibly viscous and difficult to work with. Also, mix slowly with PBS for the same reason.

Working in the cell culture hood, transfer 29.97 ml PBS into a 50 ml Conical tube. Then, moving to the PTI room, and working under red light, carefully withdraw 30 µL 100X Triton X-100. It is extremely important to do this slowly to be accurate (d/t to the viscosity and surface tension of the Triton X-100). Then, add this to the tube containing 29.97 ml PBS. Again, inject this slowly and rinse the pipette tip several times to remove as much of the Triton X-100 as possible.

Prepare 1X TBST, which is PBS with 0.1% Triton and 0.1% Tween

   Prepare 12 ml of 1X TBST, anticipating 0.8ml / well for 12 wells.
   (TIP – I learned the importance of making a little extra to account for pipetting error, etc….)

The TWEEN I am using is 20 TWEEN, and Julian shared with me that I am to calculate it as it if is 100X—just like the Triton. Therefore

```
      12  µL 100X Triton
       12  µL  40TWEEN
  +   11976 µL PBS            .
    12000 µL 1X TBST (12 ml, total of 1X TBST)
```

To this, add 20 µL/ ml MHC$_{Ab}$; 20 µL/ml X 12 ml = 240 µL MHC Ab
Remember to document the Lot# of the MHC$_{Ab}$ used

1. Permeabilization on the shaker, with 1ml/ well 0.1% TritonX-100 for 12 minutes (use setting 1 on the shaker)
2. Repeat PBS wash steps – total of three times, incubating for 5 minutes each time at RT
3. Stain the cells by adding just 800 µL of this MHC$_{Ab}$/ 1X TBST solution to each well. This should just cover the bottom surface of the well. Wrap the plate in foil and place of the shaker for 30 minutes.
4. At 30 minutes, go back into the PTI room and, under red light, add 1 µL DAPI-1 µg/µL (1:1000, or 10mg/ml)) to each well. Mix solution well. Cover again with foil and place on shaker for another 5 minutes on shaker.
5. Wash cells three times in 1X PBS, working in red light.
6. Add 2ml/well of 1X PBS and place on microscope for visualization/ photography.

Taking photos of cells
- Turned on components in order: #2-fluorescent light source, #4 - microscope, #5 – camera attached to microscope, computer.
- Clicked on µManager icon on Desktop
- PTI-Config\Hamamatsu-PTI-Leica.cfg
- OKAY
- Select Multi channel, and make certain that DAPI and MHC are selected.

Appendix E

Protocol: HSMM, Calcium Imaging

1. Remove media and discard.

2. Turn the oven on allowing plenty of time for it to warm up to the desired 37°C.

3. Wash three (3) times with 1 ml Ringers with 2.5mM Ca^{2+}, adding drops to side of the dish to avoid dropping fluid directly onto the cells. Leave the last 1ml solution in dish while preparing Fura 2 solution.
   Note: When working with the fluorescent dye, Fura-2AM, take care to only work in red light.

4. Prepare the Fura 2 solution: Add 500 µL Ringers with 2.5mM Ca^{2+} to a 1.5ml eppendorf tube. Then add 4 µL of the Fura, pipetting up and down several times to mix. Sonicate for at 30 to 40 seconds to further mix. Then add 500 µL Ringers with 2.5mM Ca^{2+} to the tube for a total of 1ml solution.

5. Remove last wash of Ringers with Ca^{2+} from optic dish containing cells. Then add Fura-2 solution to the dish. Cover completely with foil.

6. Incubate in an oven preheated to 37°C for 30 minutes to allow the Fura time to enter the cytoplasm of the cells. (See PTI System below for steps to turn on components at this time.)
   Note: If cells are plated at high densities, increasing the loading period to 40-45 minutes would be helpful.

7. After the 30-minute loading period, remove the Fura 2 solution and discard. Wash three (3) times with 1 ml Ringers with 2.5mM Ca^{2+}, to remove any residual Fura 2. Leave the last 1ml solution in dish while preparing Fura 2 solution.

8. Cover with foil and incubate at room temperature for 30 minutes for desterification.

9. Just prior to removing dish from the oven, prepare **BTS solution** – Add 1 ml Ringers with 2.5mM Ca2+ to an eppendorf tube; To this add 2µL of 10mM BTS (for a final concentration of 20µM) no need to sonicate this BTS preparation, simply mix using the pipette several times

10. After the 30 minutes incubation at room temperature, still working in room with only red light, mount the dish on the microscope stage and locate area of interest at 10X magnification on TL PH.

11. Once area is identified, increase magnification to 40X on TL PH, making sure myotubes are visible in field as well as an area to use for background.

PTI System

- While the dish is incubating at room temperature for 30 minutes or more, it is a good time to turn on the PTI system, following the numbers on the red tape:

#1 – Lamp Power Supply, waiting for it to reach 75 watts prior to

#3 -- Xenon Lamp

(30K volts or 6 amps go to the lamp – so be certain to have everything else off when this is turned on….);

5 -- the power to the camera;

#6 -- Photon Technology International;   Make certain it is switched to 'C' and that the switch on the back of the microscope to 'X' (turn knob to the right)

#7 -- *there is no #7*

#8 – *only if you wish to use this board as your control for images (did not turn on)*

#9 – computer tower; the computer is the last one to be turned on to decrease the risk of a power surge to the computer.

#11 controls the perfusion system that has been developed….

Computer:

Select the PTI/Leica Programs icon on the Desktop.

Click on the "Easy Pro-Ratio" program, then

Click on Fura-2 from the menu along the top of the screen.

OK or continue.

Select 'Open Session/Template' as file type to open

Go to E Drive → Janalee → Calcium Imaging

Select drop down to select Template; Fura2.est will appear. Open this file.

*** Important*** save file in proper folder, and name file to include cell type, treatment, sample and date…

- Use the 10X magnification (TL PH or fluorescence) to find fibers – then, switch to 40X before changing to Furo PH by depressing top button on right side of the microscope.

Note: To preserve the fluorescence, look for area in the dish using fluorescence setting on microscope. Again, look first at 10X magnification – then change to 40X, adjust the focus, set the perfusion system and then pull the lever on the left side of the microscope to send the image to the computer screen.   Note the exposure – and keep it consistent between samples. I like to focus on the grey scale palette and then select the green scale to run the imaging. (The rainbow palette is helpful to identify areas that are overexposed.)

- Pull the lever to direct the image to the computer screen; making sure the Shutter is open on the microscope.
- Using the mouse, click on the "R" for each column fura 350 (fura bound to calcium), fura 375 (unbound fura) and ratio. Also highlight the bottom bar on each of these columns. Then, when ready to get image to appear, click on small round icon to record. Select 'S' on 380 column.
- Once the image is set, locate regions of interest (ROI) including one from the background. Use polygon to identify tubes, and rectangle to identify background.
- Click on the Run button to begin (blue arrow).   I like to toggle visibility of the fura 350 and the fura 375 so that just the ratio is streaming on the graph. I also toggle the visibility of the background ratio, once I determine there is a difference between that and the ROIs from within the cells/ fibers selected.

Appendix F

Protocol: HSMM, Flow Cytometry, MUSE™ Cell Cycle Assay

Muse™ Product Specifications

Input Cell Numbers   • User selected; Cell concentration range of 10,000-500,000/mL *(Craig recommends 300K to 500K/ml)*

Sample format   • Single loader, <2 minutes per sample
                                • Sample volume and number of cells counted can be specified

Cell Types   • Homogeneous or heterogeneous,
                           suspension or adherent, primary cells
                           or cell lines

Cell Size   • 2-60+ microns (μm) in diameter

Data handling   • Data analyzed on system, with USB export of graphs, CSV files, and raw data files

Synchronize cells

After seeding cells at appropriate density (35K/ well for six-well plates). Allow to acclimate for 24 hours in SkGM-2 Growth Media, incubating at 37 °C and 5% CO_2.

Then,to synchronize the HSMM cells to G0/G1, prepare the SkGM-2 Growth Media with no hEGF (human epidermal growth factor) and with only 1% FBS. The reason for omitting the hEGF, which is a component of SkGM-2, is due to the mitogenic role it plays. Since I was hoping to 'stall the cell cycle', it seemed prudent to withhold this component as well as providing only 1% FBS, compared to the 10% FBS that is normally present in the SkGM-2 Growth Media.

Working under the cell culture hood and observing aseptic technique, add the following to the 500ml of SkBM Basal Media:
  • 10 ml L-Glutamine, Cat. #: CC-4422W; Lot #: 0000428210; Expires, 25 Jul 2015
  • 0.5ml Gentamycin Sulfate/ Amphotericin B, Cat. #: CC-4419W; Lot #: 0000428205; Expires, 29 Jul, 2015
  • 0.5 ml Dexamethasone, Cat. #: CC-4421W; Lot #: 0000428209; Expires, 24 Jul 2015
  • 5 ml FBS, Cat. # CC-4423W; Lot #: 0000428211; Expires, 25 Jul 2015

Once the Synchronization Media is prepared,
  • remove and discard the media on the cells.

- wash the cells with DPBS.
- add 2 ml of this SkGM-2 with only 1% FBS (Synchronization Media) to each well
- incubate at 37 °C and 5% CO2 for up to 24hours (I left it on for 18 hours)
- After incubation with Synchronization Media, remove and discard before adding 2ml SkGM-2 (with all components again) to cells.

Grow cells to optimal myogenesis, DAY 6 or 7 following synchronization

Preparing Fixative Solution

Prepare fresh 70% ethanol. ***NOTE:*** *Due to the stability of 70% ethanol, it is recommended that fresh, cold 70% ethanol using high-grade absolute ethanol be prepared on the cell fixation day.*

1. Mix the cold absolute ethanol (200 proof) with cold DI water. See the following table for amounts. Store 70% ethanol at −20°C until use. Keep 70% ethanol on ice at all times during usage. ***NOTE:*** *It is essential to keep the fixative very cold for optimal fixation and high quality cell cycle resolution.*

2. Proceed to "Fixing Samples" in the following section.

Fixing Samples
It is important to have a single cell suspension prior to ethanol fixation. Otherwise, the ethanol fixation process will result in a high percentage of aggregated cells and/or debris, affecting the accuracy of your results.

1. Transfer the cell sample to a 12 x 75-mm polystyrene tube or 15-mL or 50-mL conical tube (depending on the total cell number) if the cells are not already in a tube. The minimum recommended number of cells for fixation in a tube is 1×10^6 cells.
2. Centrifuge the tube at 300 x g for 5 minutes.
3. Remove and discard the supernatant without disturbing the cell pellet. After centrifugation, the cell pellet forms either a visible pellet or a white film on the bottom of the tube.
4. Add appropriate volume of PBS to each tube (ie, 1 mL of PBS per 1×10^6 cells). Mix the cells well by pipetting several times or gently vortexing.
5. Centrifuge the cells at 300 x g for 5 minutes.
6. Remove and discard the supernatant without disturbing the cell pellet. Leave approximately 50 μL of PBS per 1×10^6 cells.
7. Resuspend the cell pellet in the residual PBS by repeated pipetting several times or gently vortexing.
8. Add the resuspended cells drop-wise into the tube containing 1mL of ice cold 70% ethanol while vortexing at medium speed.
9. Cap and freeze the tube at −20°C for at least 3 hours prior to staining. Fixed cells are stable for 2 to 3 months at -20°C.
10. Proceed to the "Staining Protocol" protocol in the following section.

Staining Protocol

1. Obtain a uniform ethanol-fixed cell suspension for staining. For more information on cell preparation and fixation see "Cell Sample Fixation in Tubes" above and Cell Preparation section in Appendix A.
   NOTE: If cells appear to be in clumps, see "Troubleshooting" page to determine how to proceed.
2. Add 200 µL of ethanol-fixed cells to a 12 x 75-mm polystyrene test tube. The cell concentration should be between 5 x 10^5 to 1 x 10^6 cells/mL.
   NOTE: The manufacturer recommends using 12 x 75-mm polystyrene tubes to minimize cell loss.
3. Centrifuge ethanol-fixed cells at 300 x g for 5 minutes at room temperature.
4. Remove and discard the supernatant.
5. Resuspend the cell pellet in 0.25 mL PBS per 5 x 10^5 cells.
6. Centrifuge cells at 300 x g for 5 minutes at room temperature.
7. Remove and discard the supernatant.
8. Resuspend the cell pellet in 200 µL of Muse™ Cell Cycle Reagent.
9. Incubate for 30 minutes at room temperature, protected from light.
10. Transfer cell suspension sample to a 1.5-mL microcentrifuge tube prior to analysis on Muse™ Cell Analyzer.

Prepare the Muse Cell Analyzer

1. Make sure the tubes on the back of Muse are not pressed and/or squeezed up against anything
   a. Red bottle: waste, blue bottle: wash.

2. Place flow cell (*if using for the first time like during the training*). This should need to be replaced infrequently – only if it becomes clogged and none of the trouble shooting works to clear it or if it gets broken. (Note: there is an extra one of these that came with the system – just in case!)
   a. Open the lid on the top.
   b. Flip the notch on the left side.
   c. Make sure that the sample arm is down.
   d. Connect the fluid tube of the probe.

3. On the touch screen, select "Complete System Clean."
   a. Need to run each time when we use Muse.

4. Select, "Run Complete Clean."

5. Place the Instrument Cleaning Fluid (ICF) in a 1.5 ml tube (<u>without lid</u>) till the top. Place the tube onto the sample holder. *The ICF is stored at RT in a green topped squeeze bottle on the counter next to the Muse Cell Analyzer*.

6. Raise the sample arm.

7. Click "Run."
    a. Make sure no bubbles in the flow cell tube of the probe (inside the lid).
        i. If bubbles are formed, it means that the solution is low, the connection screw is loose, or the tube is not intact. <u>Continuous bubbles in ICF mean something is wrong.</u>

8. Run DI water (*Craig suggested to use Nanopure H$_2$O unless we can 100% trust DI H$_2$O*).
    a. Place Nanopure H$_2$O in 1.5 ml tube (<u>without lid</u>) till the top. Place the tube onto the sample holder.

9. Click "Continue."

Priming

1. Thaw system check beads & system check diluent (bring them to room temp). Mix well. *These are kept at 4 ° C in the common area in the refrigerator, in the Muse System Check Kit.*

2. Add 380 μl of diluent into 1.5ml centrifuge tube.

3. Vortex beads.

4. Add 20 μl of beads into the tube.

5. Place the tube onto the sample holder. Raise the sample arm.

6. Select "System → Close → Run System Check."

7. Type: bead lot #, expiration date, and check code.

8. Click "Next."

9. Mix the tube by flicking the tube (or pipetting up/down).

10. Click "Close," then "Run."

11. Run 3 replicates. Each time mix the tube by flicking or pipetting up/down.

12. If it says PASS, proceed to the samples
    <5%CV = ok. *(Today, our %CV was 2.95%)*

Sample preparation

1. After the incubation, add 150 μl of diluted 7-AAD into each cell suspension tube. Mix by pipetting up/down, and then vortex.
   a. Can use dark color tube (so we don't need to wrap with foil).
2. Incubate in dark (room temp, 5 min) by placing them in a drawer.
3. During the incubation, place H_2O tube in the tube holder.
4. After the 5min incubation, click "eject" and remove the H_2O tube.
5. Cut the lid of cell suspension tube off.
6. Select "test," then "run assay."
7. Flick and mix the sample.
8. Place the tube on the tube holder.

Clean up

1. Select "complete system clean."
2. Run ICF.
3. Raise the sample arm, run.
4. Place Nanopure H_2O tube in the sample holder.
   a. Keep the probe in H_2O.

Saving the experiment

- Option → save as current settings.
  - So next time we don't need to set up again (e.g. day 1, day 2…)
  - Next time, "retrieve settings." Select the previous setting, and "run."

NOTES
- To use Muse, ~15 min to start, ~10 min to finish cleaning up, and ~1 hour experiment (depends on # of experiments).
- System check → clean -→
  - Cap rinse – actually nothing it does.
  - Quick – DI H_2O
  - Back flush – empty tube and flush ICF back
  - Complete – 10% bleach/DI H_2O.
- If flow tubes clogged,
  - Use syringe (that came with Muse) to flush out.
  - Flush the tube with 10% bleach using syringe. (Place bleach in a syringe, connect to the tube, flush).
  - Place the tip of probe in 10% bleach for overnight.

Appendix G

Data Collected: HSMM, Immunostaining for Fusion Index Calculations

Impact of Osteoporosis on Myogenesis Study
HSMM, P2, DAY 7
CNTRL
Immunostaining with MHC$_{Ab}$ and DAPI

September 13, 2014

HSMM, P2, D7, CNTRL A, 2,
20140913

913/1229
0.74
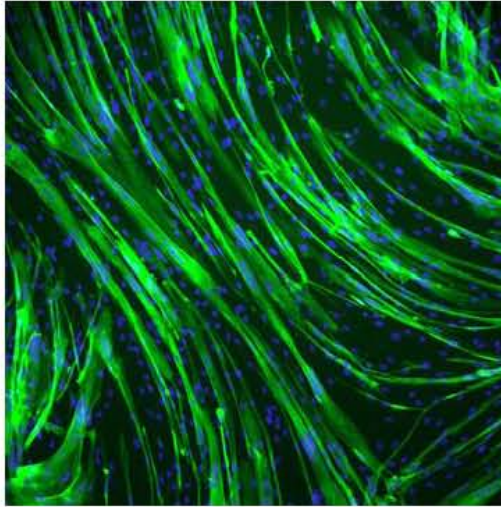
HSMM, P2, D7, CNTRL A, 4,
20140913

901/1190
0.76
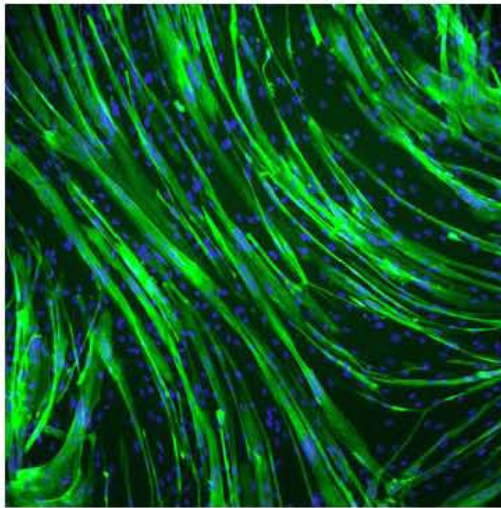
HSMM, P2, D7, CNTRL A, 5, 20140913

852/1085
0.79
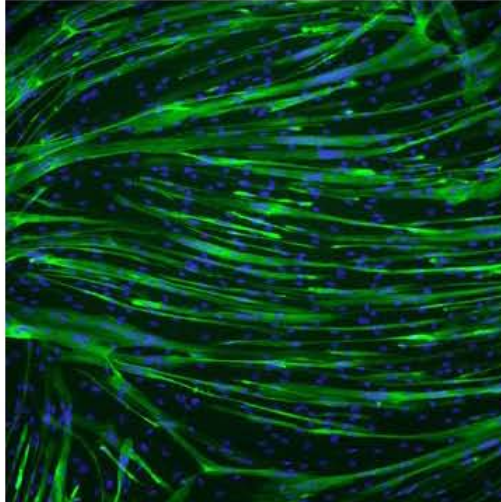
HSMM, P2, D7, CNTRL C, 20140913

846/1068
0.79
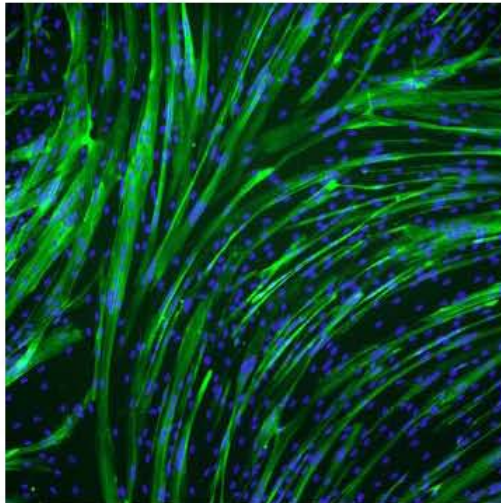
HSMM, P2, D7, CNTRL C, 2 20140913

746/1000
0.75
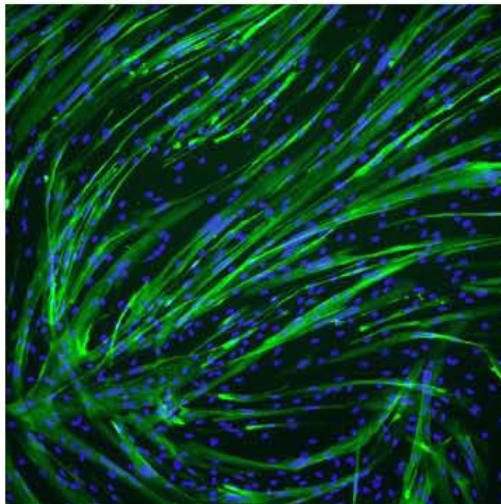
Impact of Osteoporosis on Myogenesis Study
HSMM, P2, DAY 7
Serum Sample, 228
Immunostaining with MHC$_{Ab}$ and DAPI

September 13, 2014

HSMM, P2, D7, 228,
20140913

888/1254
0.71
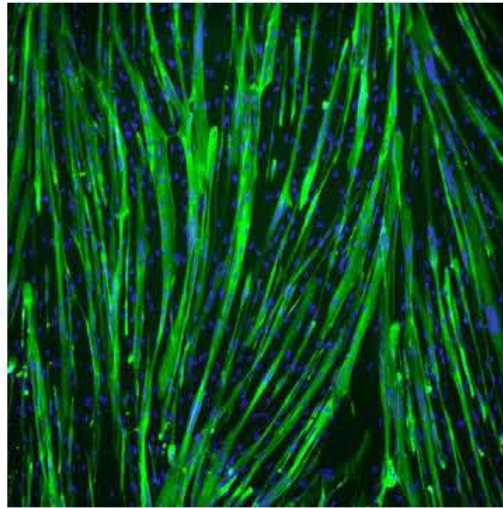
HSMM, P2, D7, 228, B,
20140913

835/1173
0.71
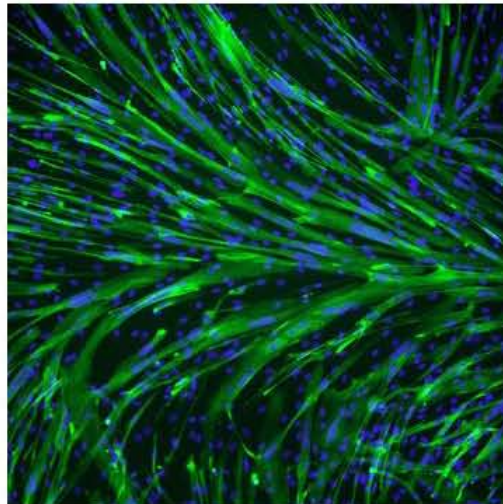
HSMM, P2, D7, 228, C,
20140913

814/1175
0.69
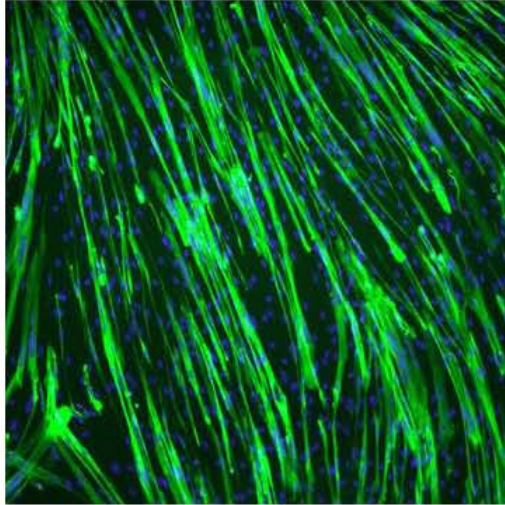
HSMM, P2, D7, 228, D,
20140913

868/1265
0.69
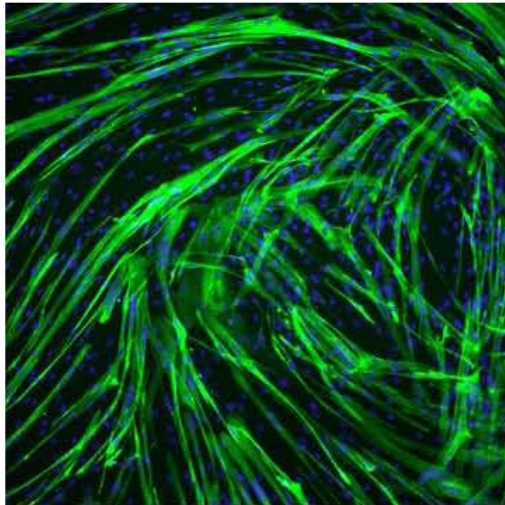
HSMM, P2, D7, 228, E,
20140913

876/1300
0.67
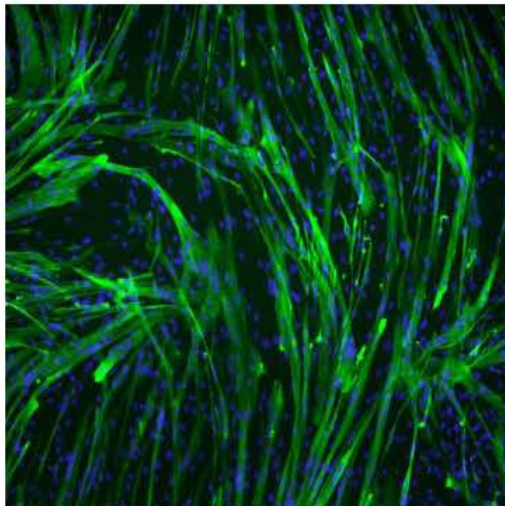
Impact of Osteoporosis on Myogenesis Study
HSMM, P2, DAY 7
Serum Sample, 368
Immunostaining with MHC$_{Ab}$ and DAPI

September 13, 2014

HSMM, P2, D7, 368,
20140913

969/1223
0.79
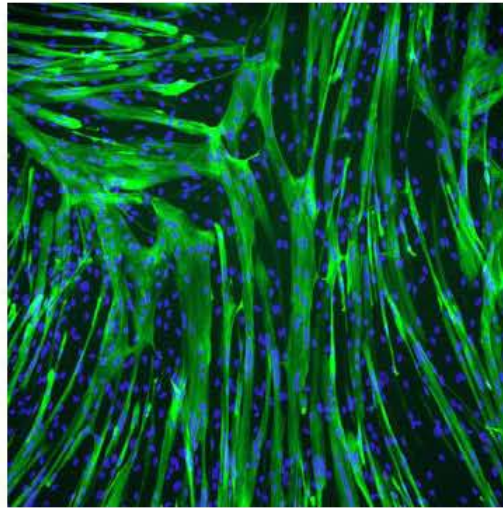
HSMM, P2, D7, 368, B,
20140913

913/1209
0.76
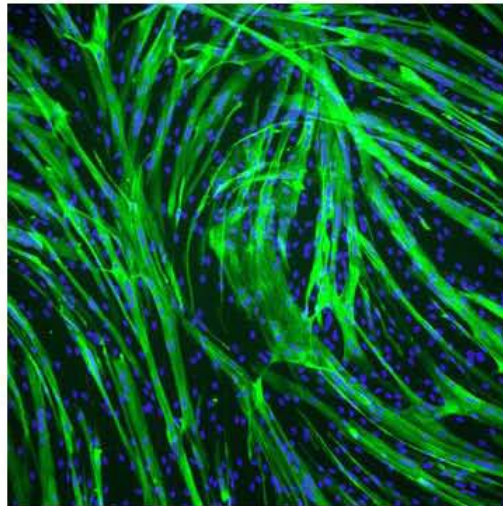
HSMM, P2, D7, 368, C,
20140913

1099/1336
0.82
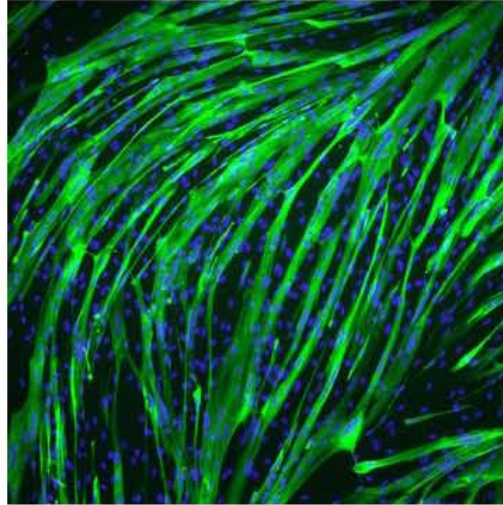
HSMM, P2, D7, 368, D,
20140913

899/1260
0.71
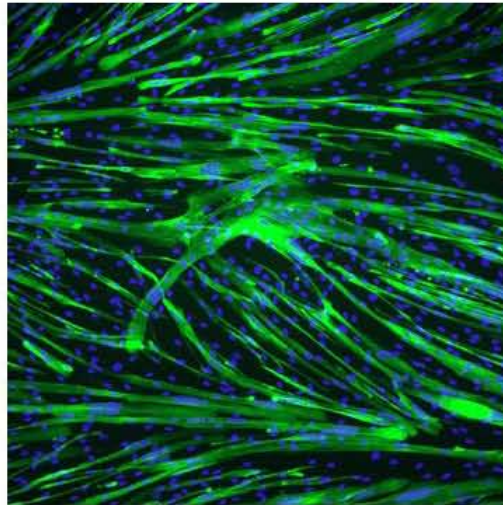
HSMM, P2, D7, 368, E,
20140913

973/1469
0.66
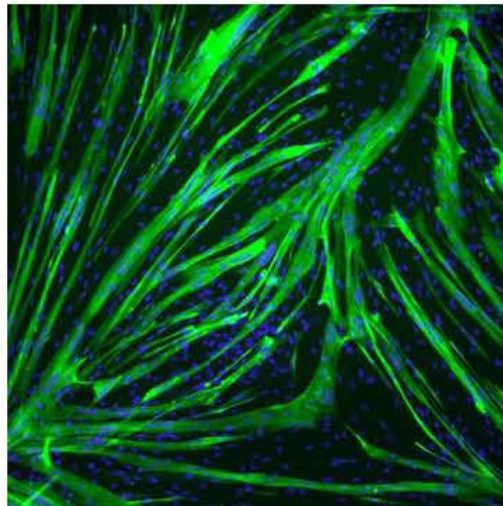
Impact of Osteoporosis on Myogenesis Study
HSMM, P2, DAY 7
Serum Sample, 380
Immunostaining with MHC_{Ab} and DAPI

September 13, 2014

HSMM, P2, D7, 380,
20140913

794/ 1069
0.74
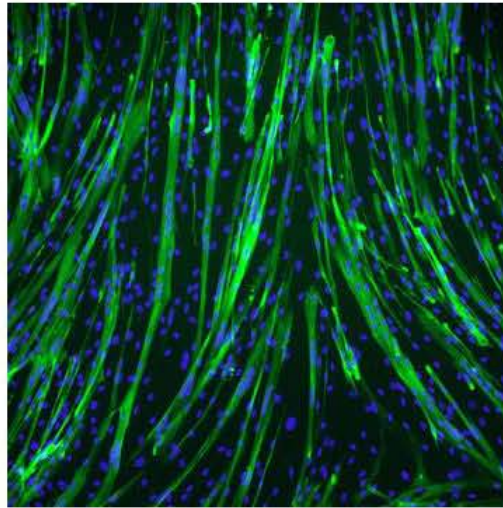
HSMM, P2, D7, 380, B,
20140913

951/ 1347
0.71
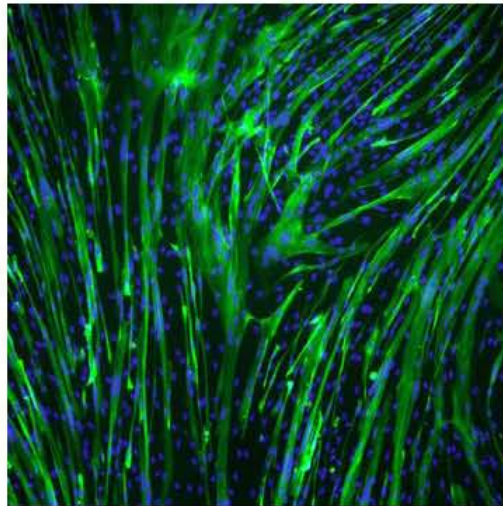
HSMM, P2, D7, 380, C,
20140913

906/1239
0.73
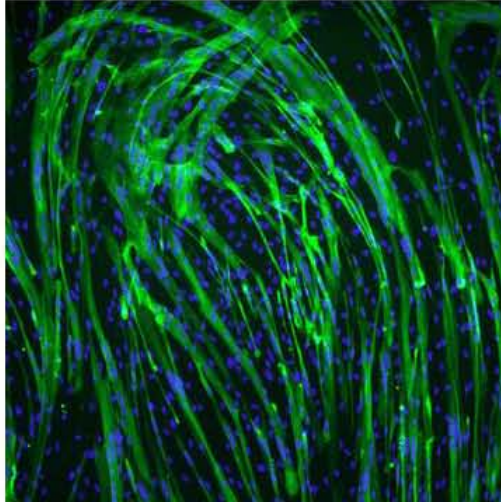
HSMM, P2, D7, 380, D,
20140913

944/1256
0.75
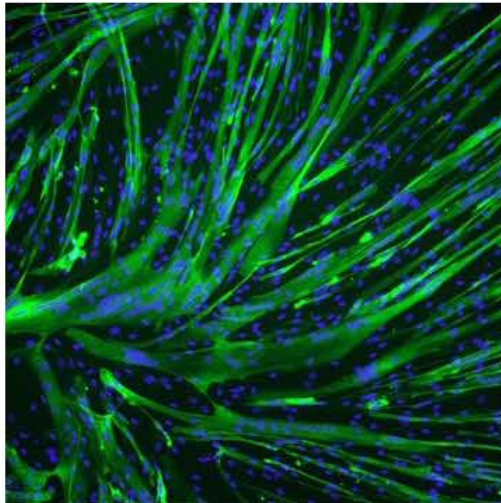
HSMM, P2, D7, 380, E,
20140913

1096/1385
0.79
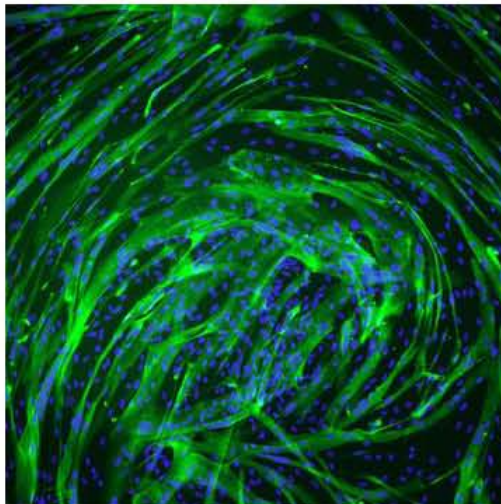
Impact of Osteoporosis on Myogenesis Study
HSMM, P2, DAY 7
Serum Sample, 390
Immunostaining with MHC_{Ab} and DAPI

September 13, 2014

HSMM, P2, D7, 390,
20140913

966/ 1410
0.69
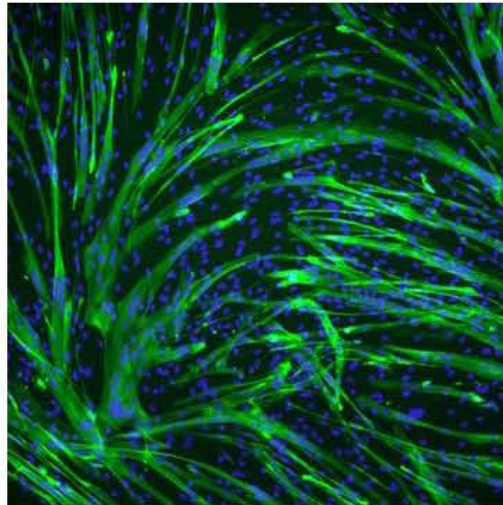
HSMM, P2, D7, 390, B,
20140913

1053/ 1356
0.78
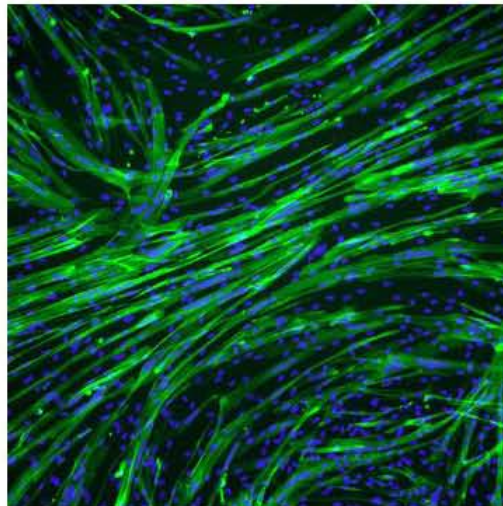
HSMM, P2, D7, 390, C,
20140913

973/1394
0.70
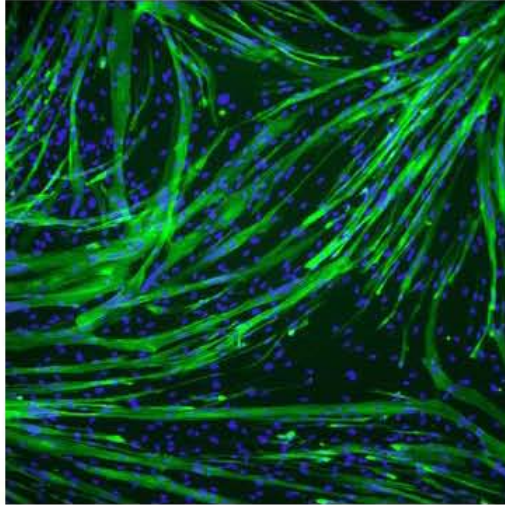
HSMM, P2, D7, 390, D,
20140913

1052/1392
0.76
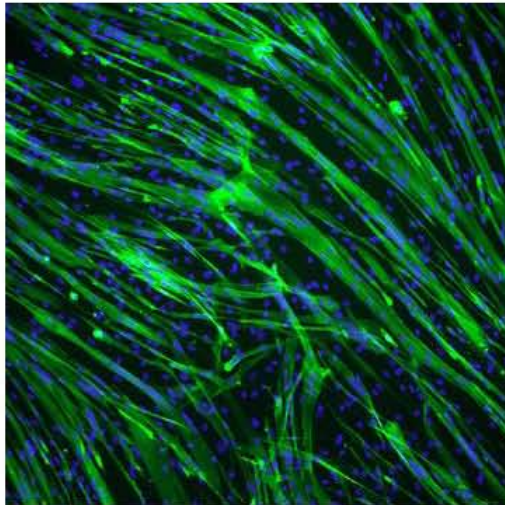
HSMM, P2, D7, 390, E,
20140913

970/1272
0.76
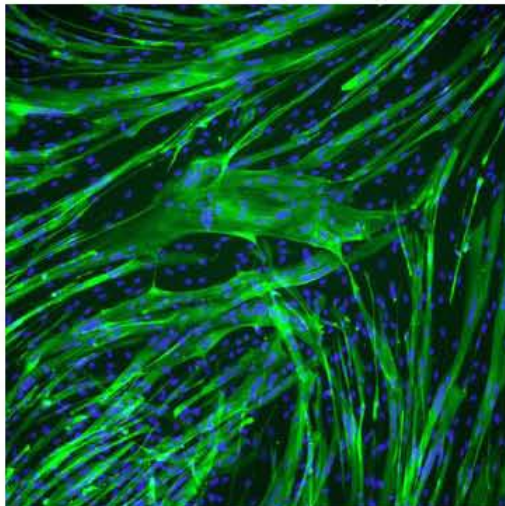
Impact of Osteoporosis on Myogenesis Study
HSMM, P2, DAY 7
Serum Sample, 391
Immunostaining with MHC$_{Ab}$ and DAPI

September 13, 2014

HSMM, P2, D7, 391,
20140913

914/1332
0.69
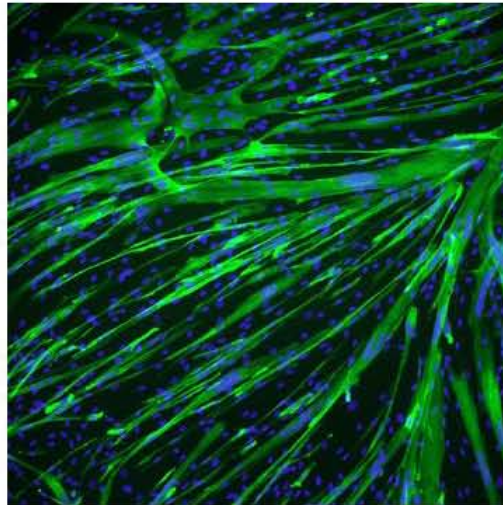
HSMM, P2, D7, 391, B,
20140913

950/1450
0.66
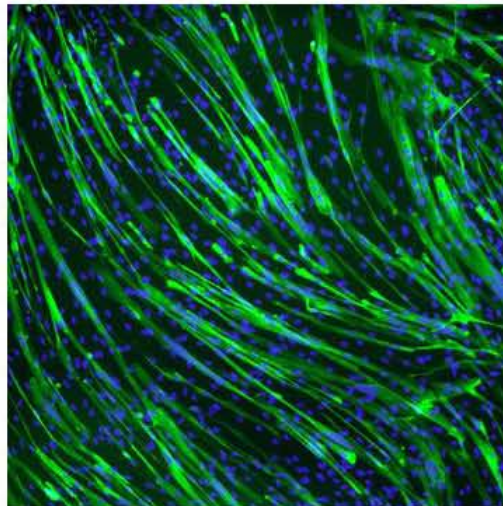
HSMM, P2, D7, 391, C,
20140913

865 / 1321
0.65
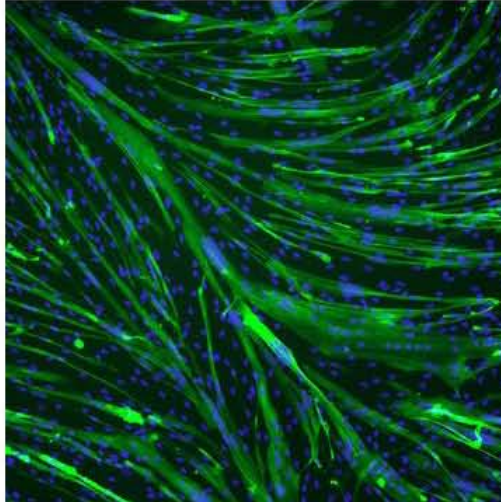
HSMM, P2, D7, 391, D,
20140913

813 / 1197
0.68
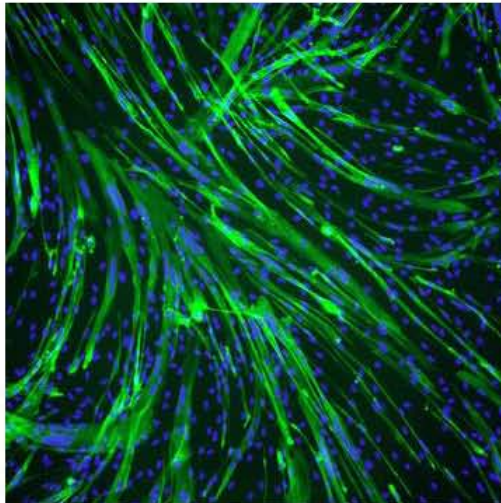
HSMM, P2, D7, 391, E,
20140913

967 / 1386
0.70
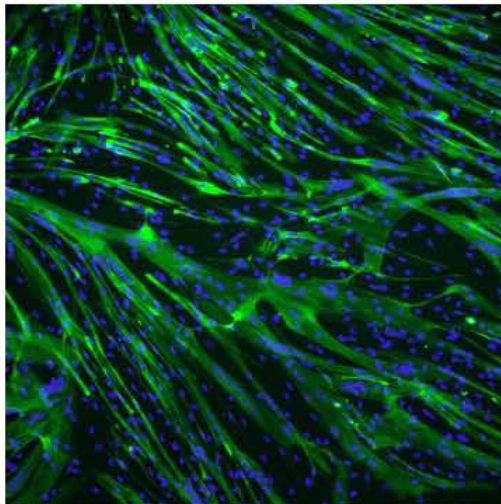
Impact of Osteoporosis on Myogenesis Study
HSMM, P2, DAY 7
Serum Sample, 397
Immunostaining with MHC$_{Ab}$ and DAPI

September 13, 2014

HSMM, P2, D7, 397,
20140913

881/1158
0.76
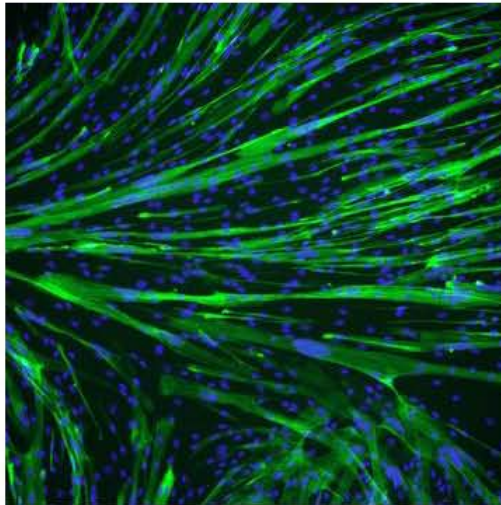
HSMM, P2, D7, 397, B,
20140913

1004/1297
0.77
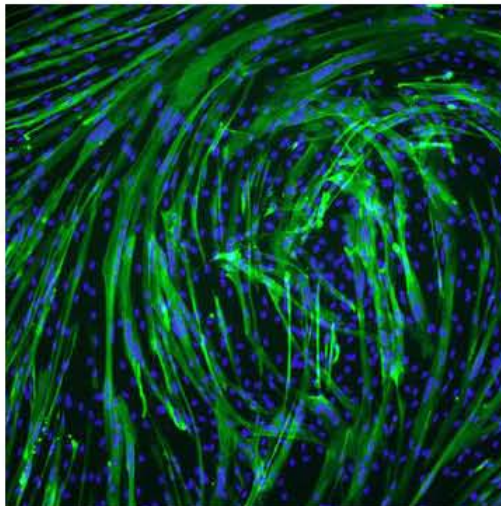
HSMM, P2, D7, 397, C,
20140913

966/1359
0.71
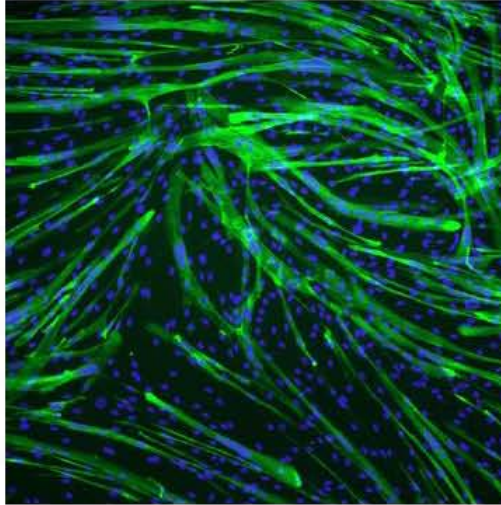
HSMM, P2, D7, 397, D,
20140913

989/1319
0.75
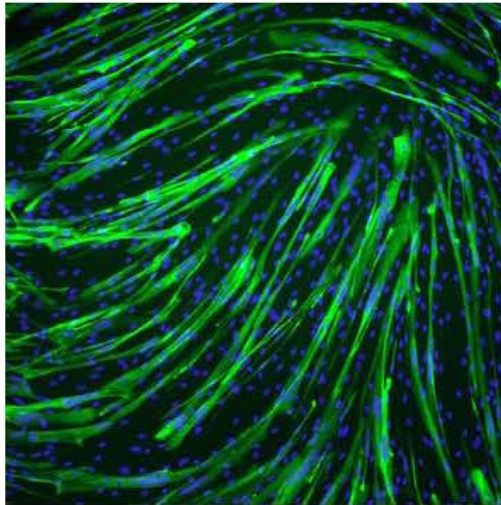
HSMM, P2, D7, 397, E,
20140913

1061/1323
0.80
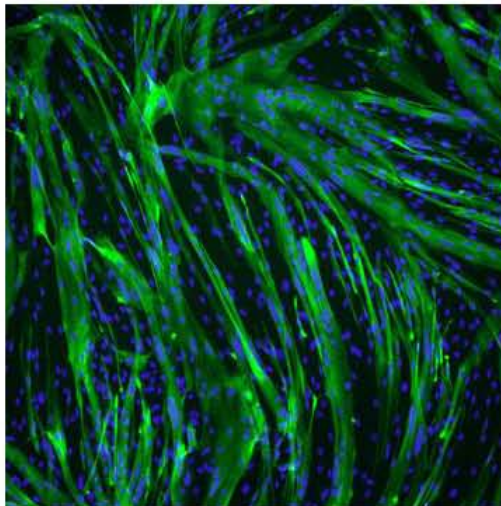
Impact of Osteoporosis on Myogenesis Study
HSMM, P2, DAY 7
Serum Sample, 403
Immunostaining with MHC_{Ab} and DAPI

September 13, 2014

HSMM, P2, D7, 403,
20140913

922/1147
0.80
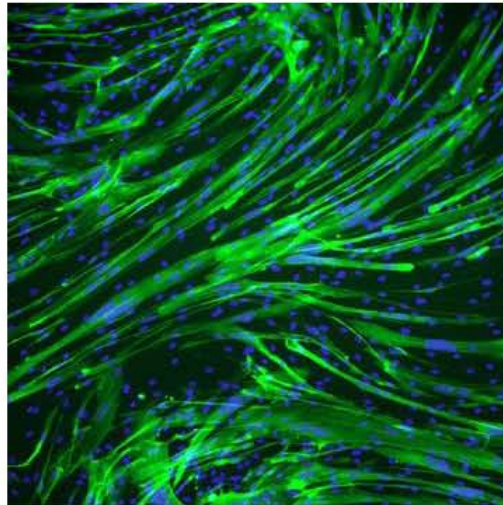
HSMM, P2, D7, 403, B,
20140913

1202/1529
0.79
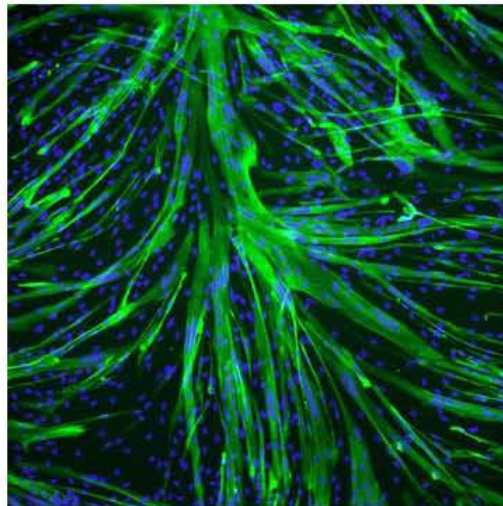
HSMM, P2, D7, 403, C,
20140913

1107 / 1442
0.70
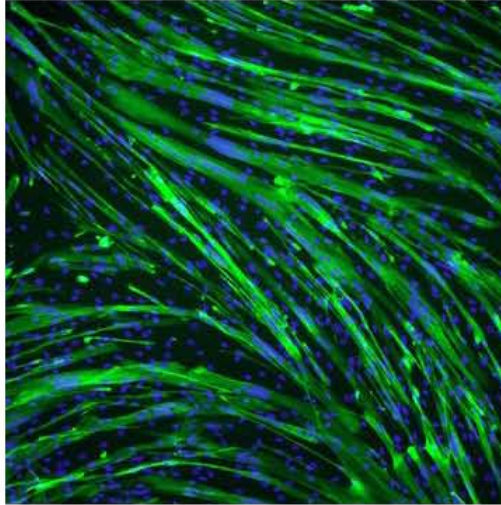
HSMM, P2, D7, 403, D,
20140913

989 / 1310
0.76
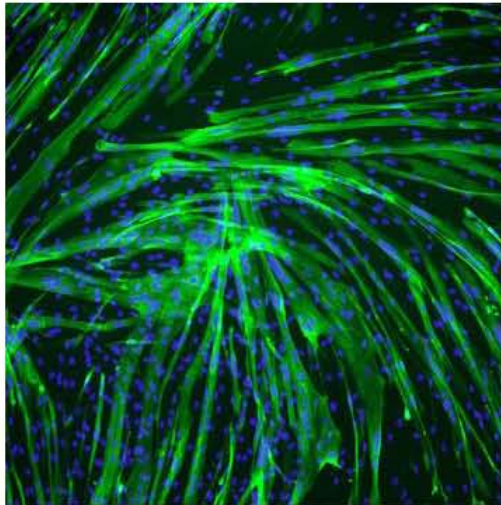
HSMM, P2, D7, 403, E,
20140913

963 / 1253
0.77
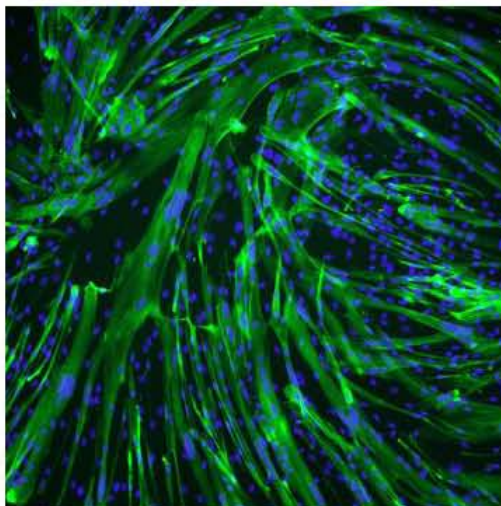
Impact of Osteoporosis on Myogenesis Study
HSMM, P2, DAY 7
Serum Sample, 428
Immunostaining with MHC_{Ab} and DAPI

September 13, 2014

HSMM, P2, D7, 428,
20140913

1080/ 1466
0.74
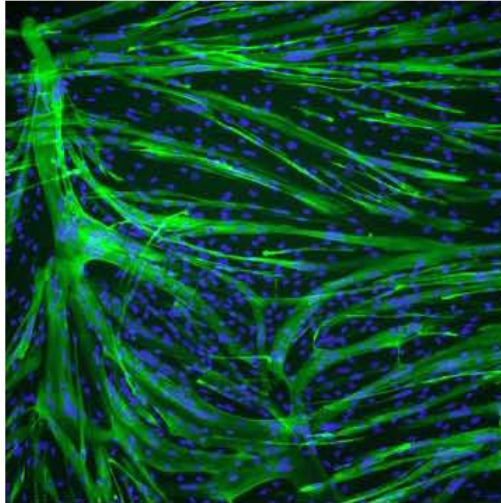
HSMM, P2, D7, 428, B,
20140913

851/ 1169
0.73
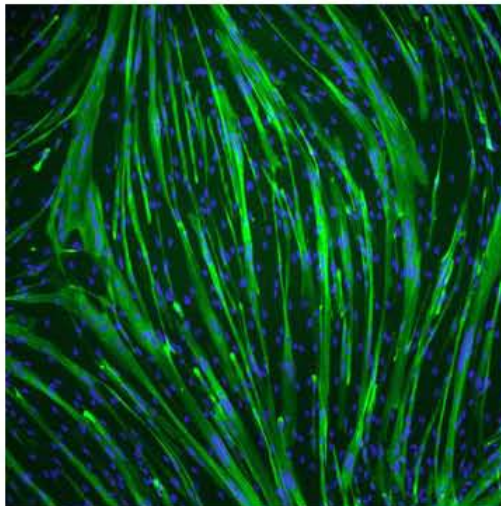
HSMM, P2, D7, 428, C,
20140913

1276/ 1632
0.78
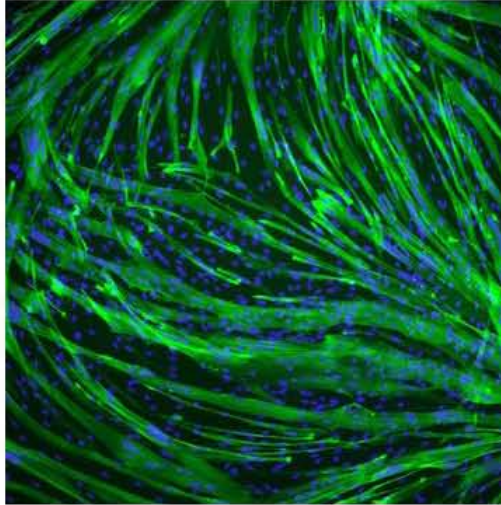
HSMM, P2, D7, 428, D,
20140913

1292/ 1600
0.81

HSMM, P2, D7, 428, E,
20140913
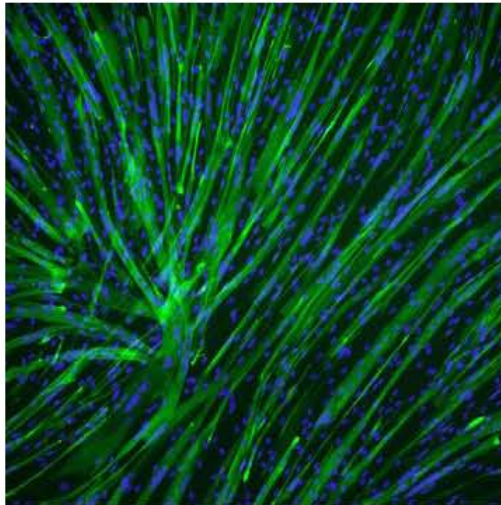
1014/ 1335
0.76
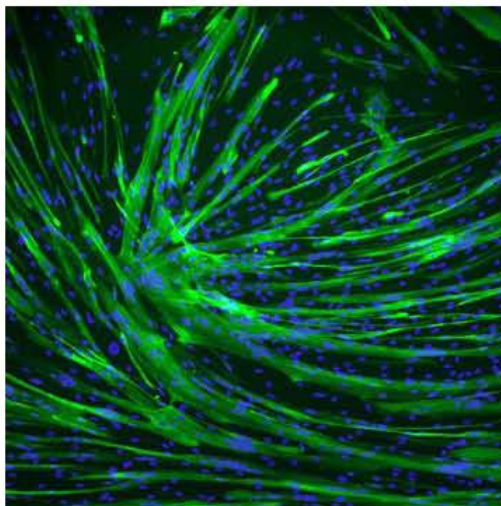
Impact of Osteoporosis on Myogenesis Study
HSMM, P2, DAY 7
Serum Sample, 435
Immunostaining with MHC$_{Ab}$ and DAPI

September 13, 2014

HSMM, P2, D7, 435,
20140913

1134/1357
0.84
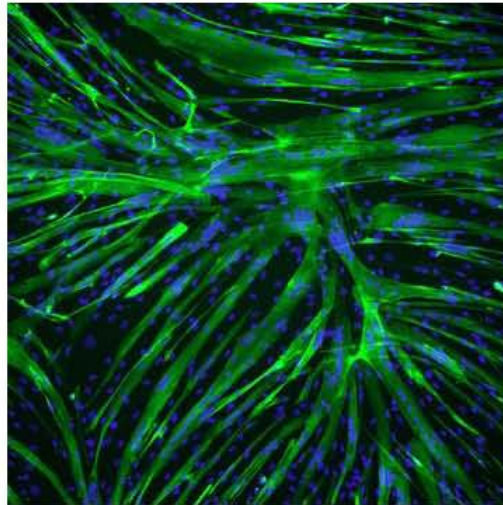
HSMM, P2, D7, 435, B,
20140913

1246/1463
0.85
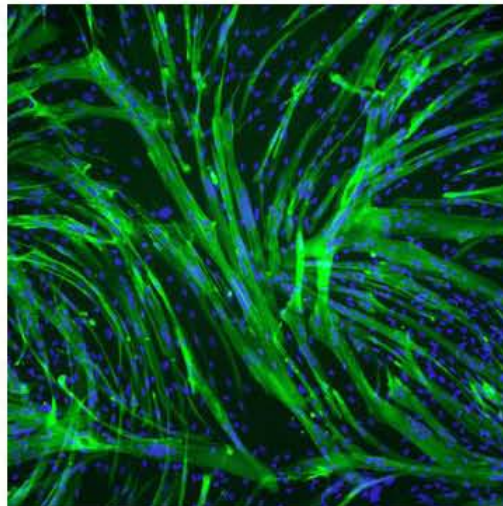
HSMM, P2, D7, 435, C,
20140913

1135/1366
0.83
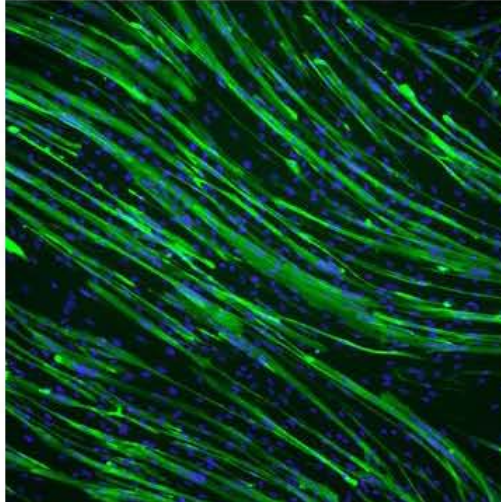
HSMM, P2, D7, 435, D,
20140913

1200/1415
0.85
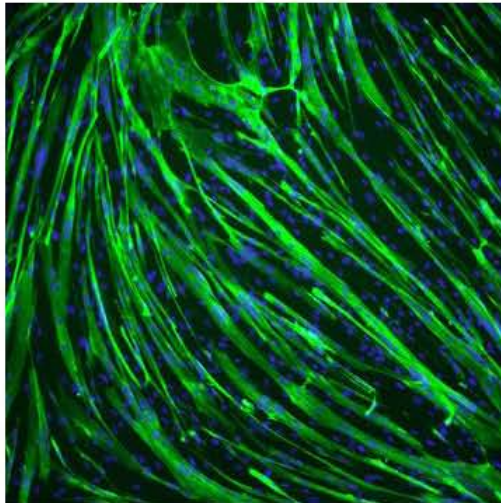
HSMM, P2, D7, 435, E,
20140913

955/1141
0.84
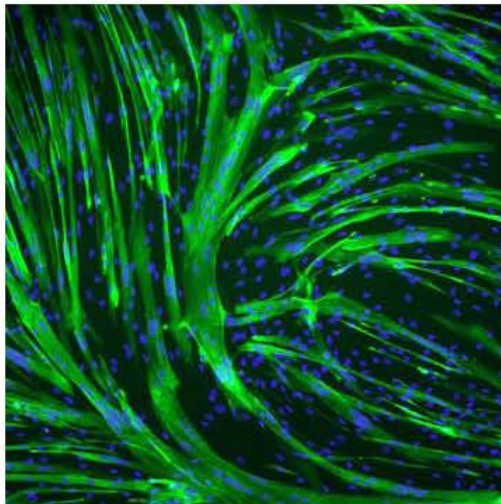
Impact of Osteoporosis on Myogenesis Study
HSMM, P2, DAY 7
Serum Sample, 439
Immunostaining with MHC$_{Ab}$ and DAPI

September 13, 2014

HSMM, P2, D7, 439,
20140913

1272/ 1544
0.82
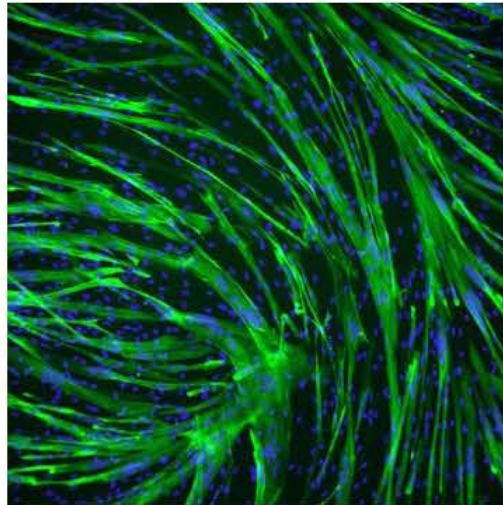
HSMM, P2, D7, 439, B,
20140913

1357/ 1585
0.86
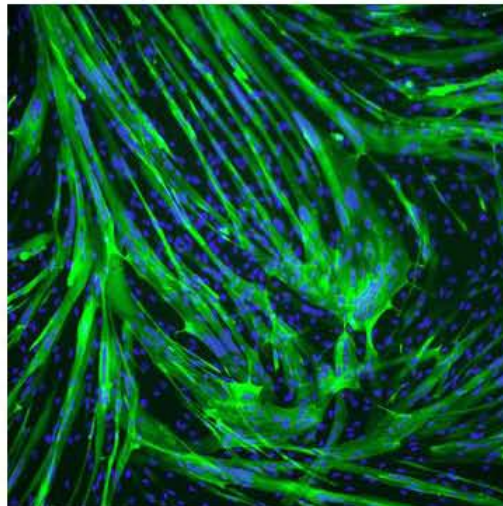
HSMM, P2, D7, 439, C,
20140913

1120/ 1379
0.81
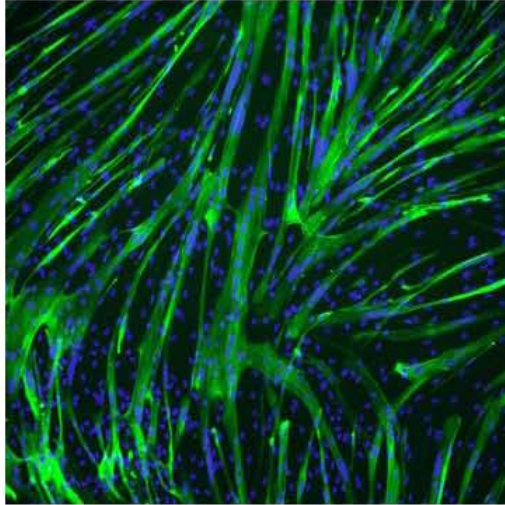
HSMM, P2, D7, 439, D,
20140913

858/ 1027
0.84
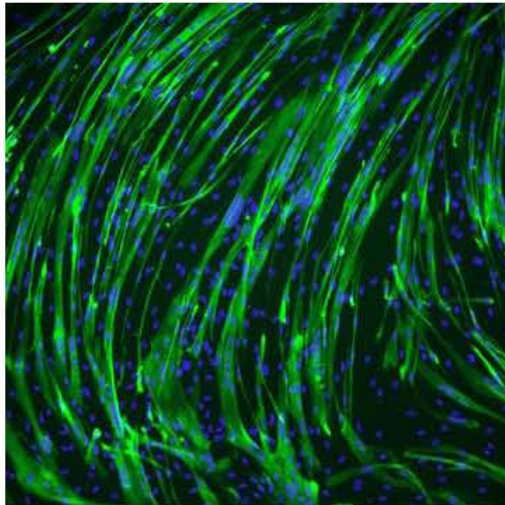
HSMM, P2, D7, 439, E,
20140913

1000/ 1182
0.85
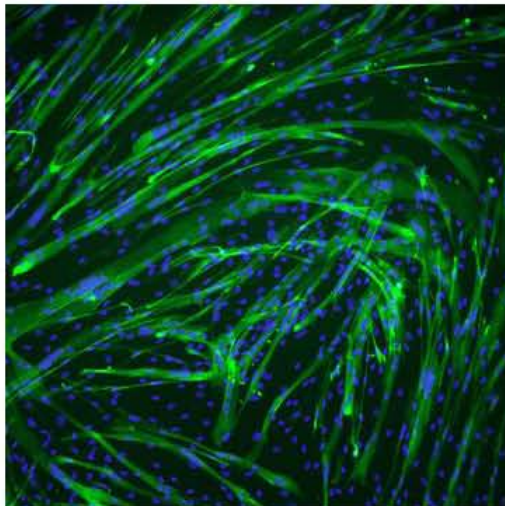
Impact of Osteoporosis on Myogenesis Study
HSMM, P2, DAY 7
Serum Sample, 463
Immunostaining with MHC_{Ab} and DAPI

September 13, 2014

HSMM, P2, D7, 463,
20140913

1277/ 1481
0.86
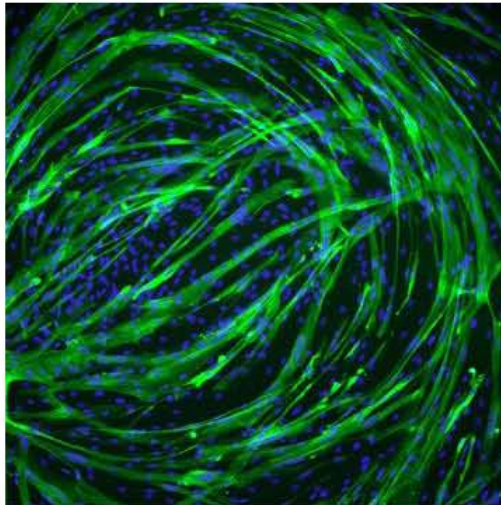
HSMM, P2, D7, 463, B,
20140913

1228/ 1455
0.84
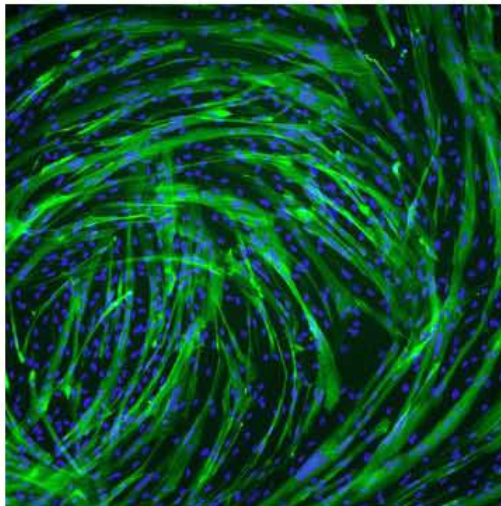
HSMM, P2, D7, 463, C,
20140913

1005/1255
0.80
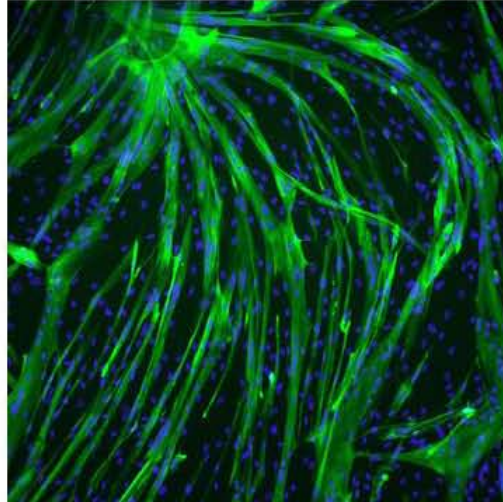
HSMM, P2, D7, 463, D,
20140913

1195/1455
0.82
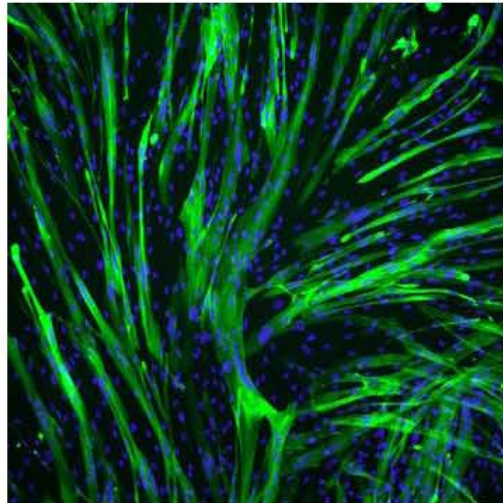
HSMM, P2, D7, 463, E,
20140913

994/1182
0.84
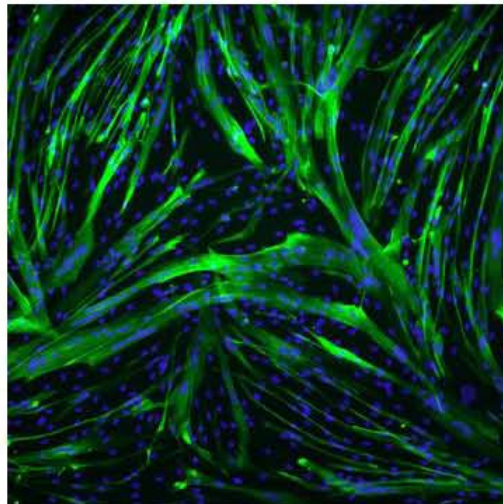
Impact of Osteoporosis on Myogenesis Study
HSMM, P2, DAY 7
Serum Sample, 480
Immunostaining with MHC_{Ab} and DAPI

September 13, 2014

HSMM, P2, D7, 480,
20140913

1373/1591
0.86
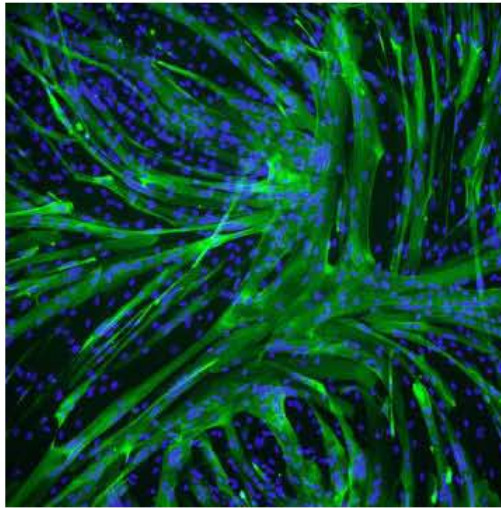
HSMM, P2, D7, 480, B,
20140913

1491/1787
0.83
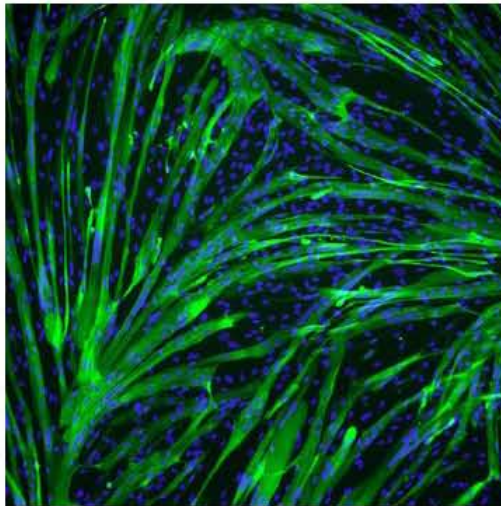
HSMM, P2, D7, 480, C,
20140913

1409/ 1660
0.85
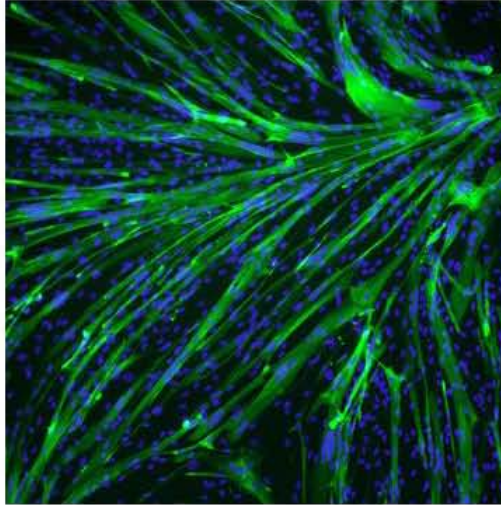
HSMM, P2, D7, 480, D,
20140913

1244/ 1476
0.84
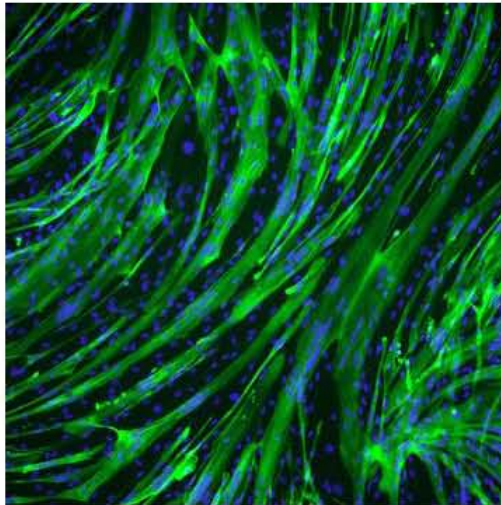
HSMM, P2, D7, 480, E,
20140913

1504/ 1733
0.87
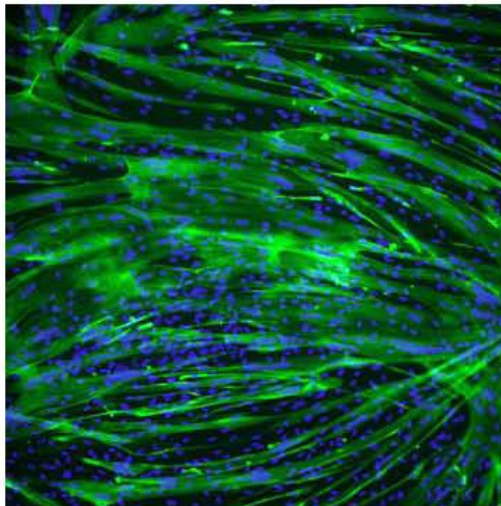
Impact of Osteoporosis on Myogenesis Study
HSMM, P2, DAY 7
Serum Sample, 482
Immunostaining with MHC_{Ab} and DAPI

September 13, 2014

HSMM, P2, D7, 482,
20140913

1451/1736
0.84
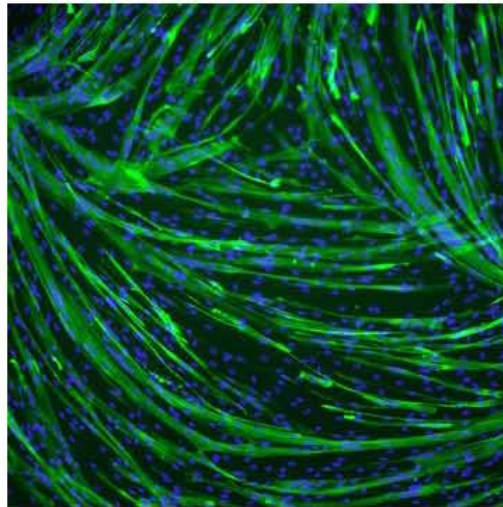
HSMM, P2, D7, 482, B,
20140913

1026/1267
0.81
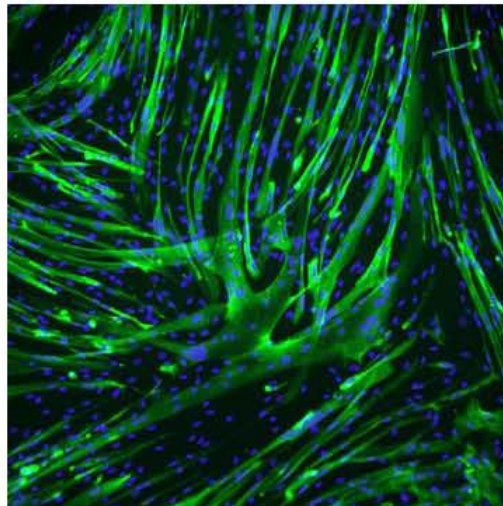
HSMM, P2, D7, 4B2, C,
20140913

1220/ 1408
0.87
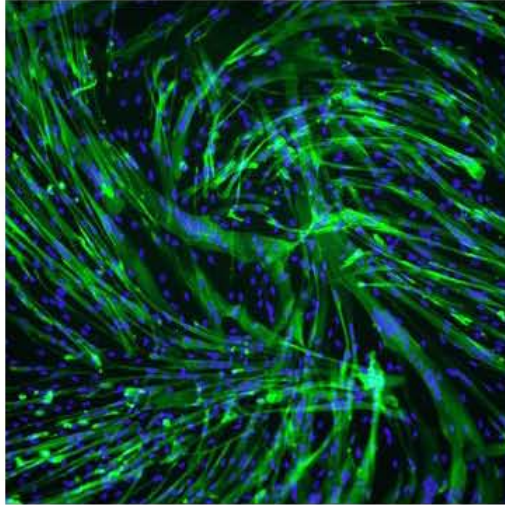
HSMM, P2, D7, 4B2, D,
20140913

1118/ 1394
0.80
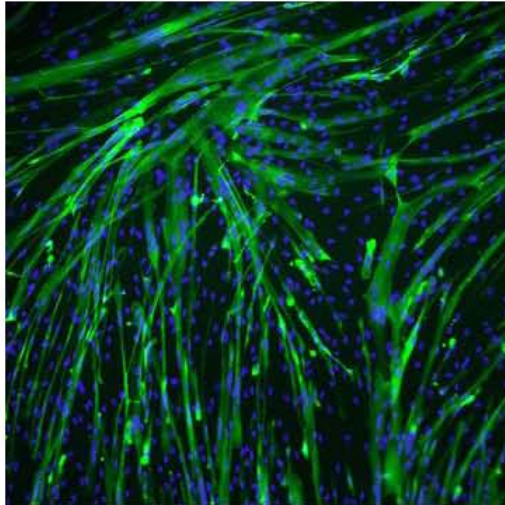
HSMM, P2, D7, 4B2, E,
20140913

1289/ 1534
0.84
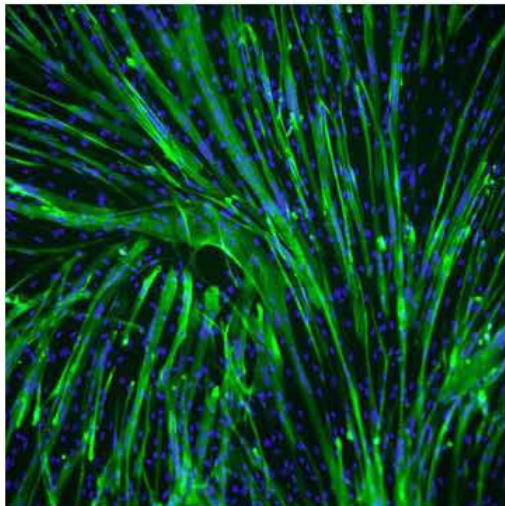
Impact of Osteoporosis on Myogenesis Study
HSMM, P2, DAY 7
Serum Sample, 489
Immunostaining with MHC_{Ab} and DAPI

September 13, 2014

HSMM, P2, D7, 489,
20140913

999/1240
0.81
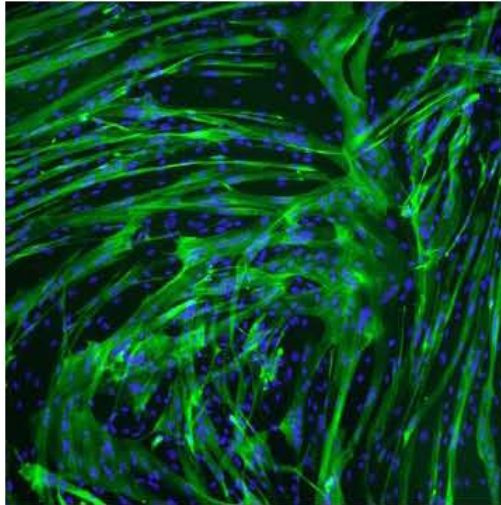
HSMM, P2, D7, 489, B,
20140913

1265/1477
0.86
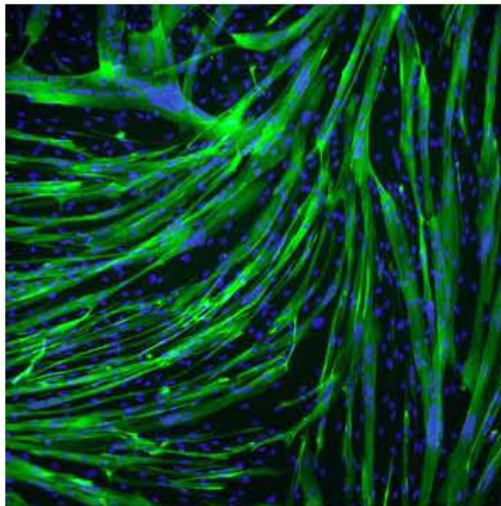
HSMM, P2, D7, 489, C,
20140913

1155/ 1439
0.80
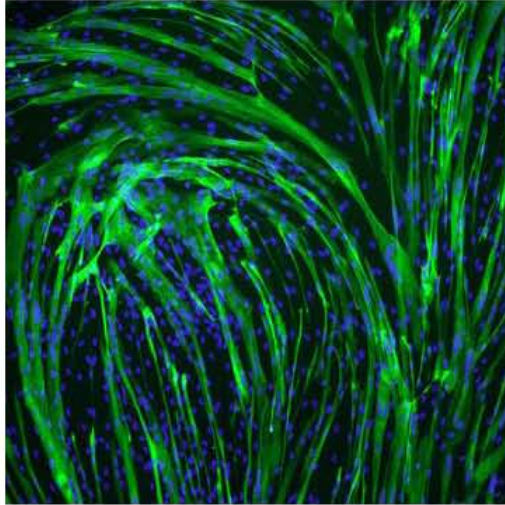
HSMM, P2, D7, 489, D,
20140913

1284/ 1517
0.85
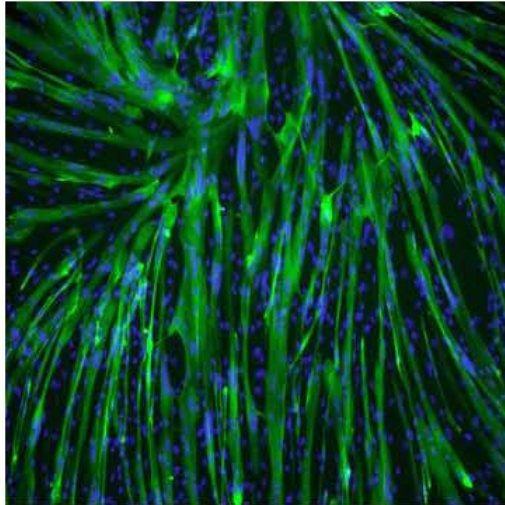
HSMM, P2, D7, 489, E,
20140913

1394/ 1663
0.84
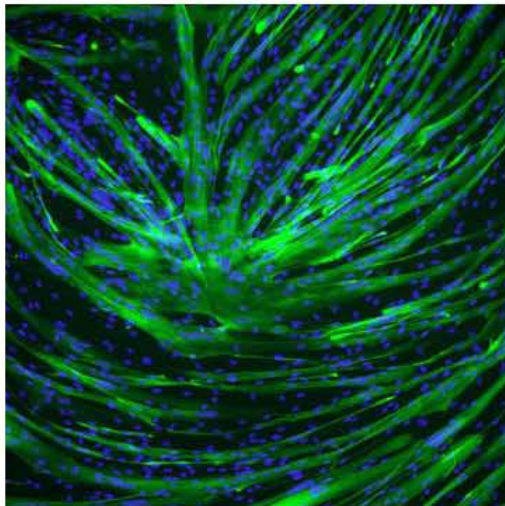
Impact of Osteoporosis on Myogenesis Study
HSMM, P2, DAY 7
Serum Sample, 495
Immunostaining with MHC_{Ab} and DAPI

September 13, 2014

HSMM, P2, D7, 495,
20140913

1541/1868
0.83
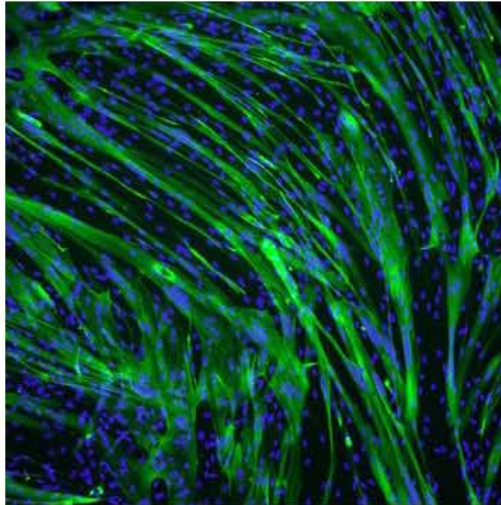
HSMM, P2, D7, 495, B,
20140913

1387/1754
0.79
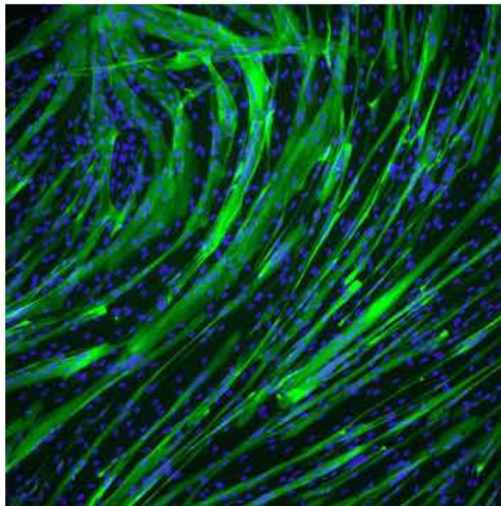
HSMM, P2, D7, 495, C,
20140913

1182/ 1514
0.78
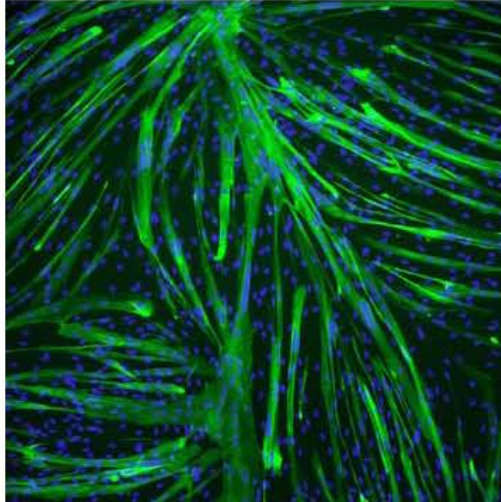
HSMM, P2, D7, 495, D,
20140913

1088/ 1313
0.83
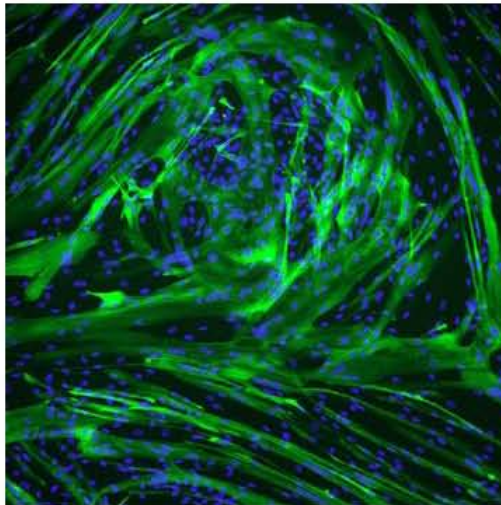
HSMM, P2, D7, 495, E,
20140913

1247/ 1511
0.83
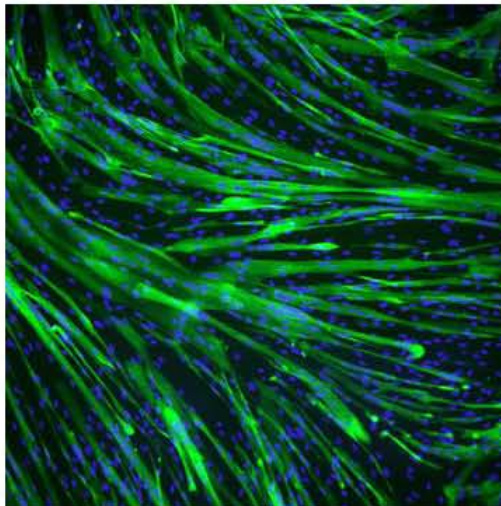
Impact of Osteoporosis on Myogenesis Study
HSMM, P2, DAY 7
Serum Sample, 496
Immunostaining with MHC$_{Ab}$ and DAPI

September 13, 2014

HSMM, P2, D7, 496,
20140913

998/ 1325
0.75
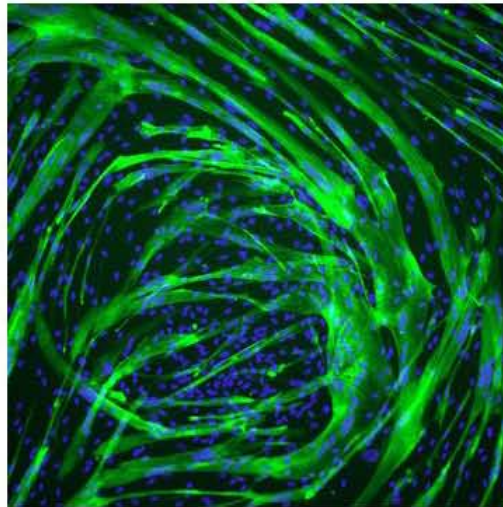
HSMM, P2, D7, 496, B,
20140913

1110/ 1397
0.80
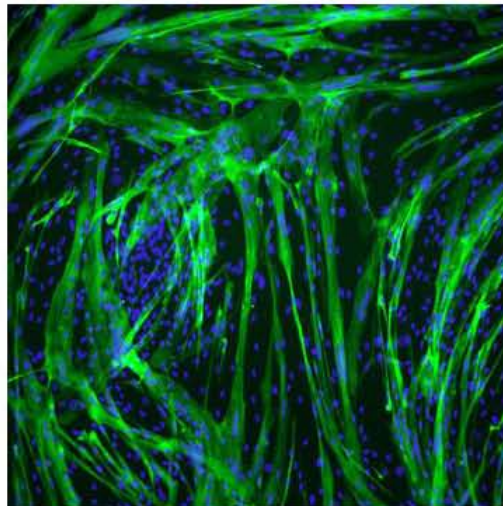
HSMM, P2, D7, 496, C,
20140913

1174/ 1429
0.82
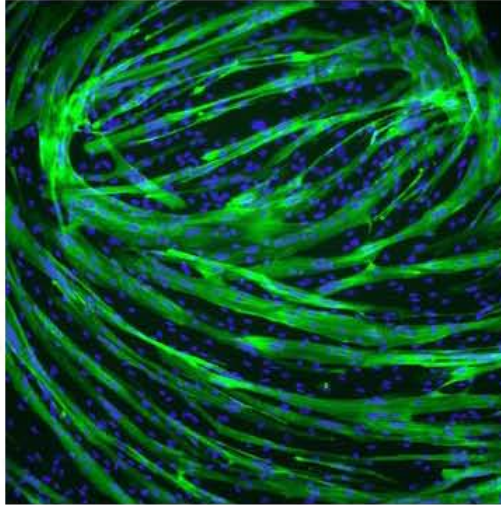
HSMM, P2, D7, 496, D,
20140913

1057/ 1412
0.75
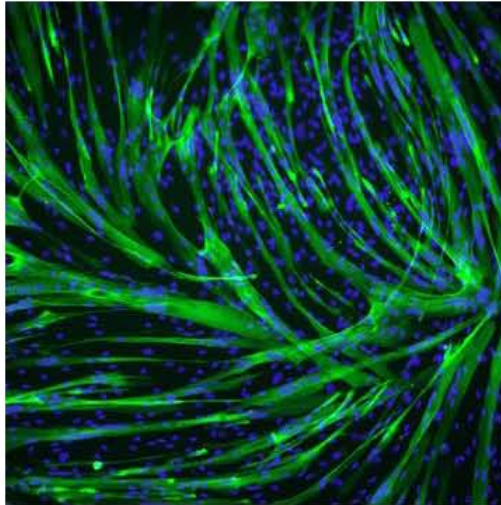
HSMM, P2, D7, 496, E,
20140913

1220/ 1506
0.81
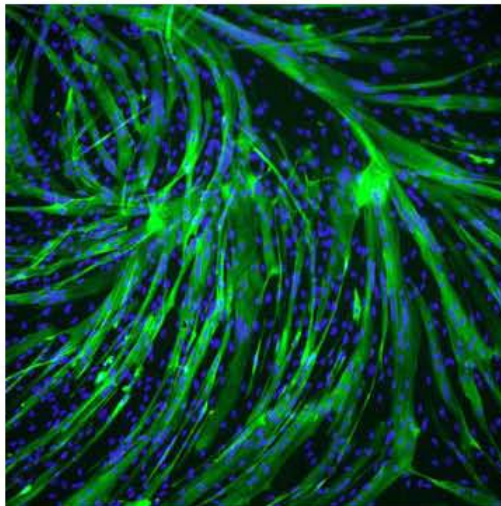
Appendix H

Data Collected: HSMM, Calcium Imaging
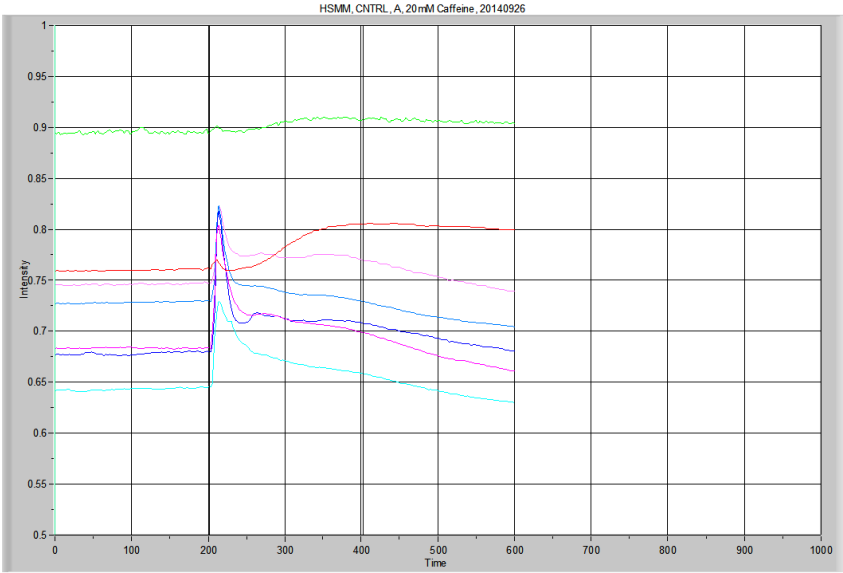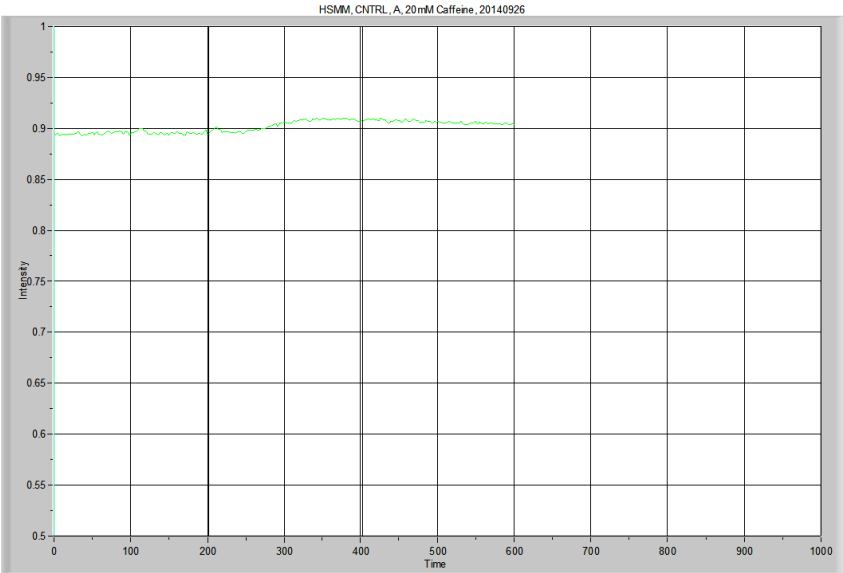
Overview

	Average resting level	Peak	Δ Level	Time to Peak	Area Under the Curve Low X: 201.278 High X: 598.467	Peak Area
CNTRL A, BG	0.894929	0.909999	0.01507	NA	359.27763	2.26281
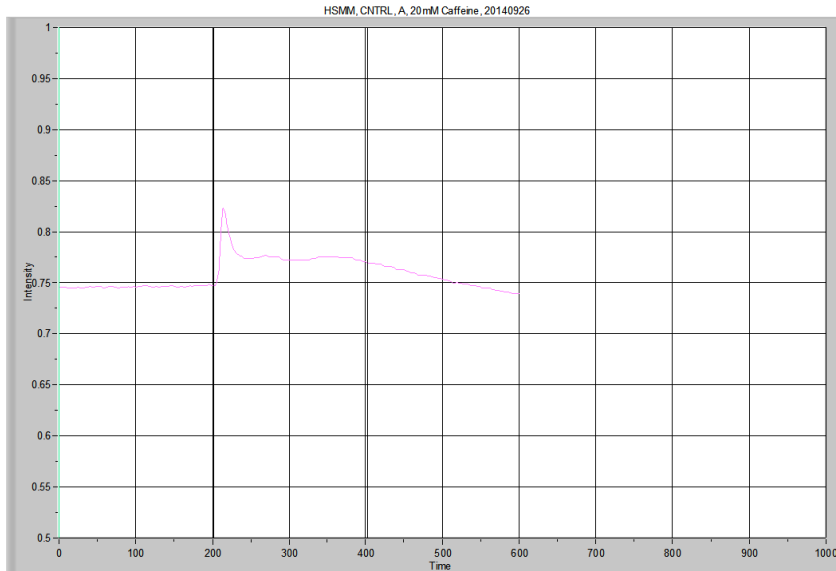
154

HSMM, CNTRL, A, 20mM Caffeine, 20140926

	Average resting level	Peak	Δ Level	Time to Peak	Area Under the Curve Low X: 201.278 High X: 598.467	Peak Area
CNTRL A, P1	0.745651	0.822826	0.077175	8.051103	303.67829	8.77822
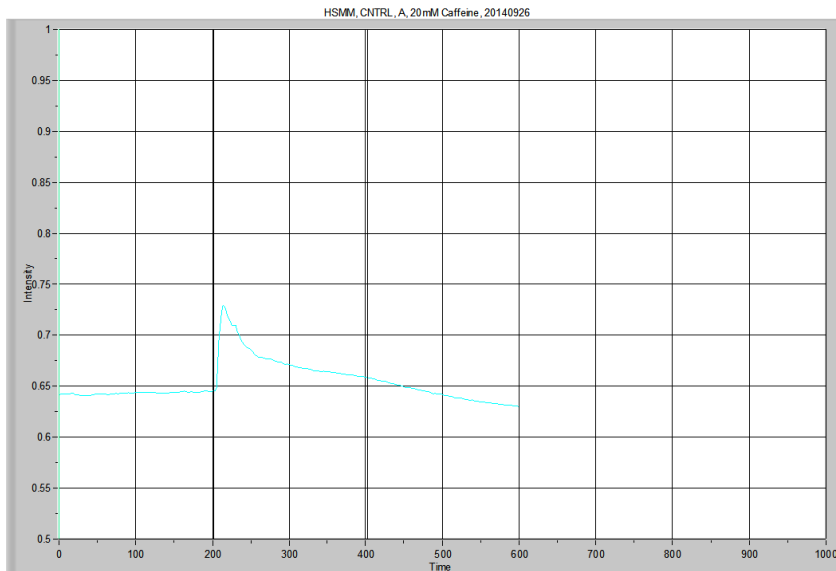
HSMM, CNTRL, A, 20mM Caffeine, 20140926

	Average resting level	Peak	Δ Level	Time to Peak	Area Under the Curve Low X: 201.278 High X: 598.467	Peak Area
CNTRL A, P3	0.642623	0.729303	0.08668	8.051103	261.62826	8.44850
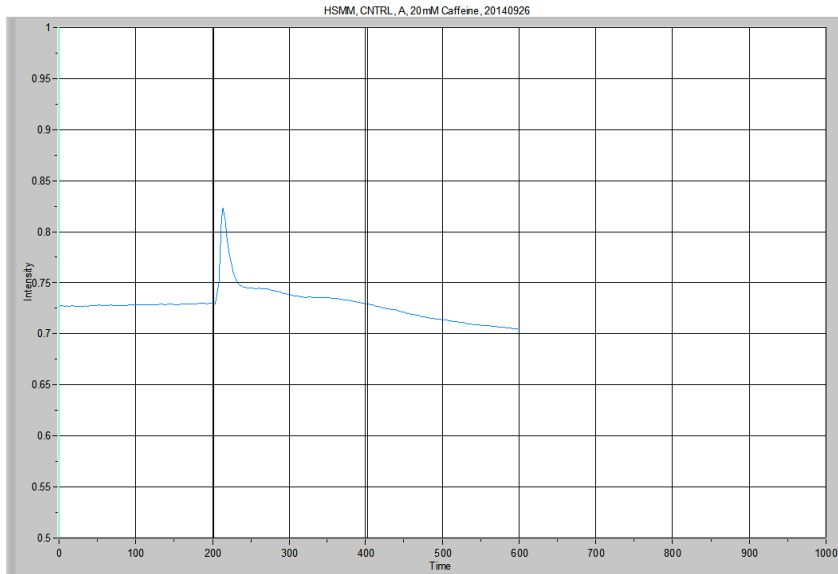
155

	Average resting level	Peak	Δ Level	Time to Peak	Area Under the Curve Low X: 201.278 High X: 598.467	Peak Area
CNTRL A, P5	0.727718	0.822909	0.095192	8.051103	289.47561	4.64138
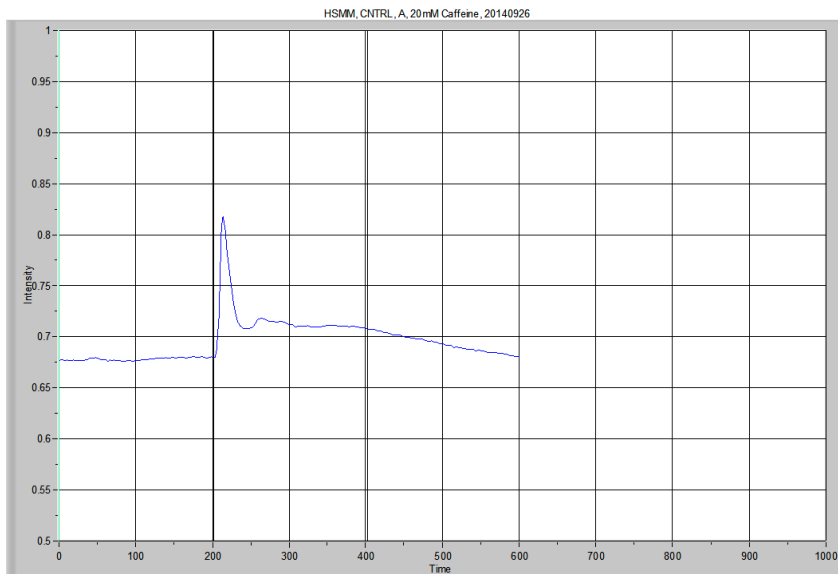
	Average resting level	Peak	Δ Level	Time to Peak	Area Under the Curve Low X: 201.278 High X: 598.467	Peak Area
CNTRL A, P6	0.677588	0.817368	0.13978	10.73468	280.04012	10.08337
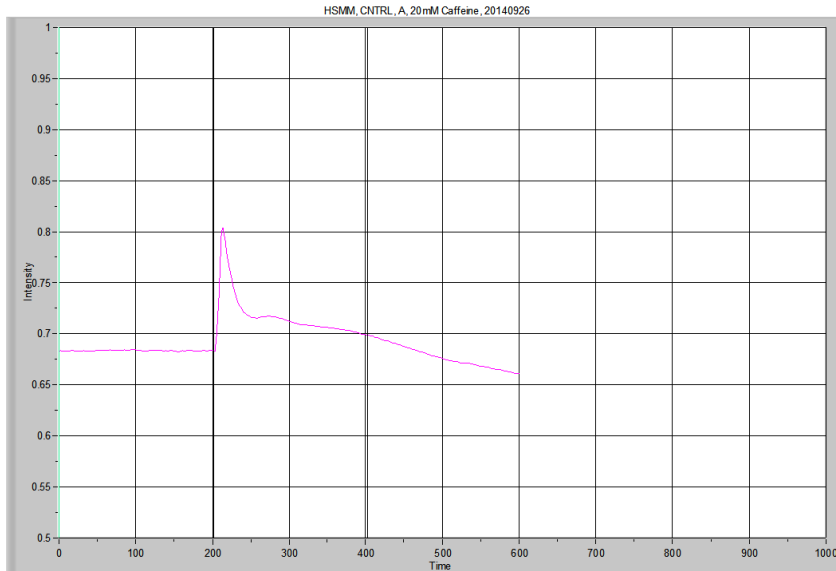
HSMM, CNTRL, A, 20mM Caffeine, 20140926

	Average resting level	Peak	Δ Level	Time to Peak	Area Under the Curve Low X: 201.278 High X: 598.467	Peak Area
CNTRL A, P7	0.682992	0.803704	0.120711	8.051103	276.90563	9.97577

HSMM, CNTRL, A, 20mM Caffeine, 20140926
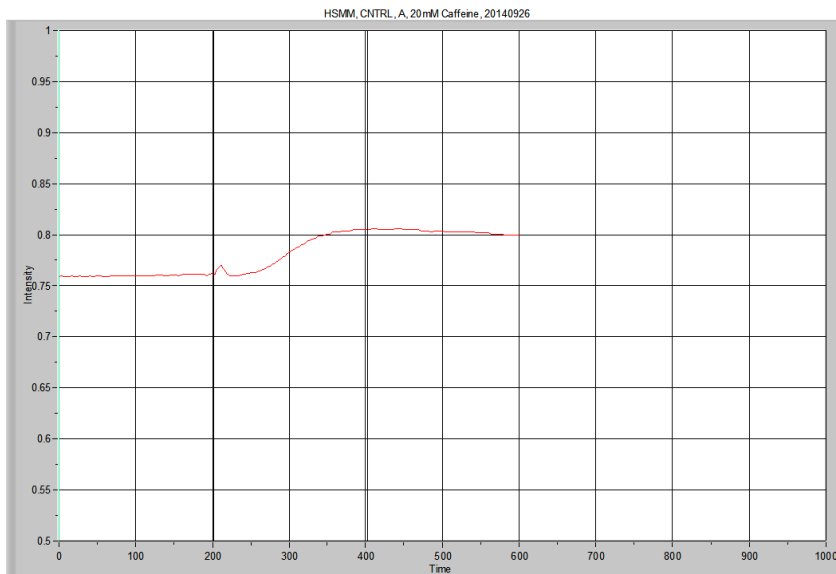
I do not plan to use data from this tracing, as the myotube must have moved out of range upon stimulation with the 20mM caffeine.

	Average resting level	Peak	Δ Level	Time to Peak	Area Under the Curve	Peak Area
CNTRL A, P8	0.759535	0.805633	0.046334	Unable to measure	NA	NA

Calcium Imaging, HSMM
CNTRL C, 20140927
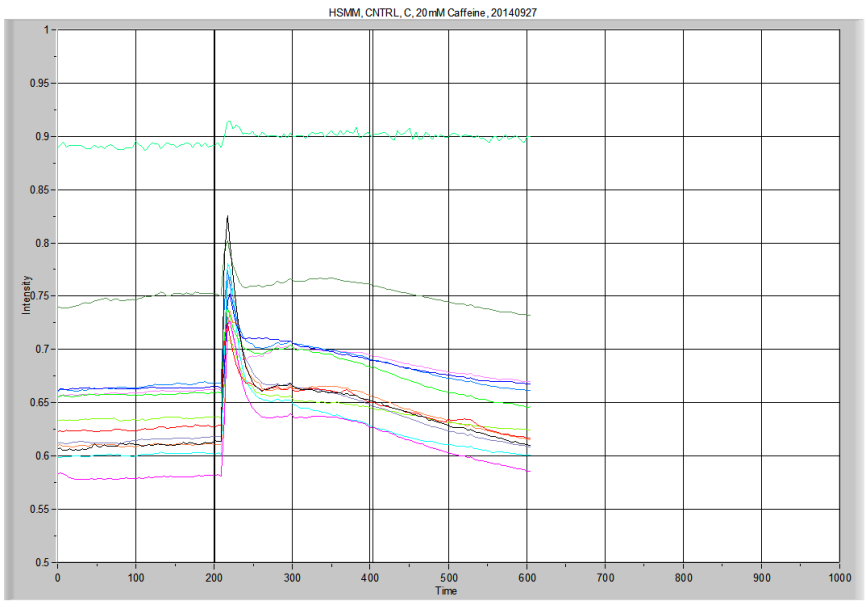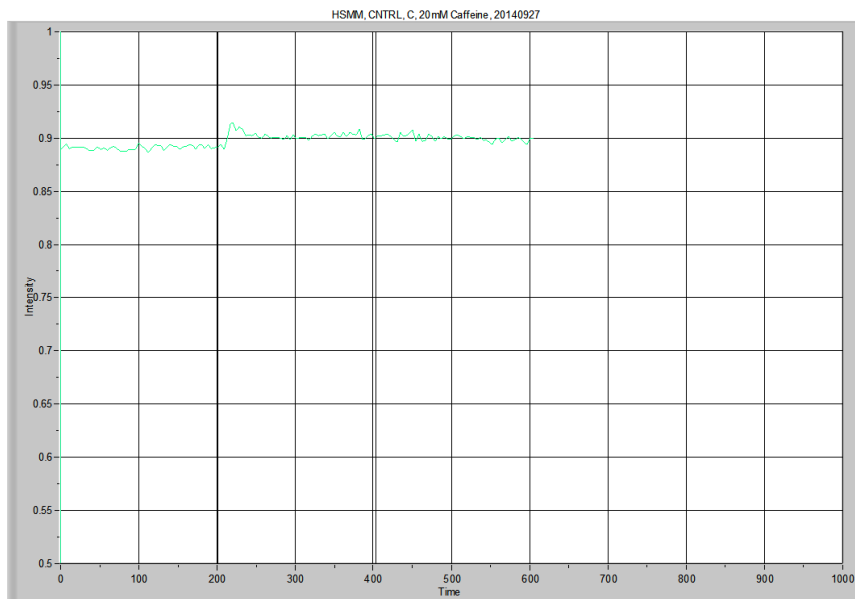
157

Overview

	Average resting level	Peak	Δ Level	Time to Peak	Area Under the Curve Low X: 201.279 High X: 597.13	Peak Area
CNTRL C, BG	0.890472	0.913951	0.023479	NA	356.60390	3.30095
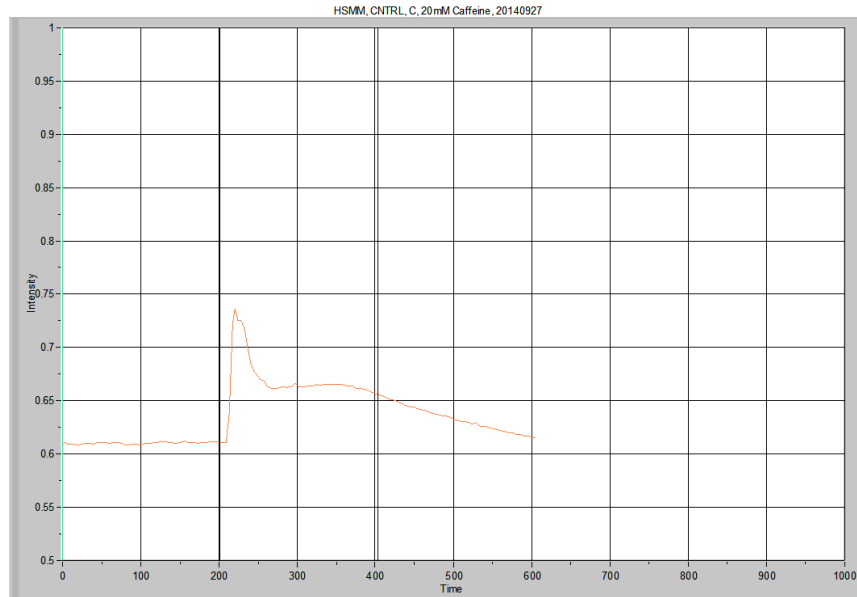
158

HSMM, CNTRL, C, 20mM Caffeine, 20140927

	Average resting level	Peak	Δ Level	Time to Peak	Area Under the Curve Low X: 201.279 High X: 597.13	Peak Area
CNTRL C, P1	0.609661	0.736234	0.126573	8.051138	257.70647	14.94170
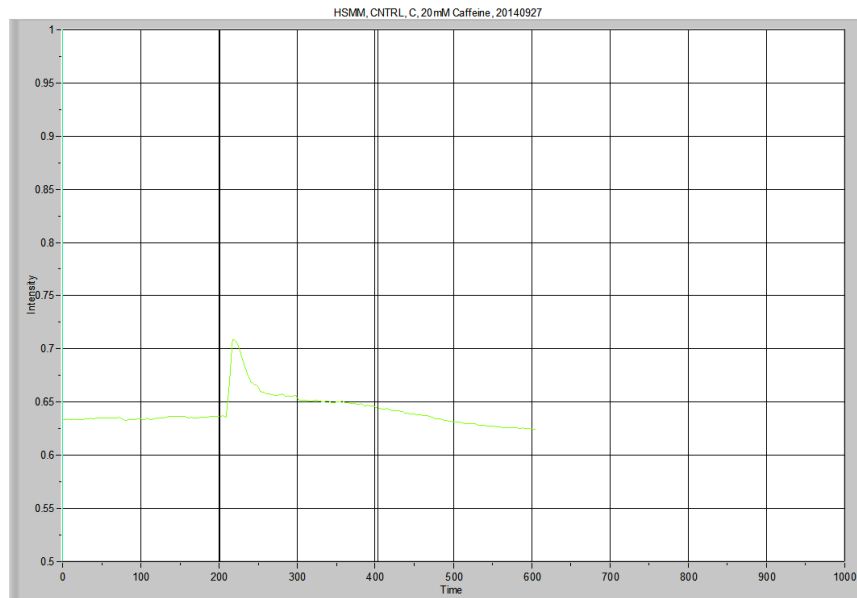
HSMM, CNTRL, C, 20mM Caffeine, 20140927

	Average resting level	Peak	Δ Level	Time to Peak	Area Under the Curve Low X: 201.279 High X: 597.13	Peak Area
CNTRL C, P2	0.634226	0.708983	0.074757	4.025553	255.36600	5.91512
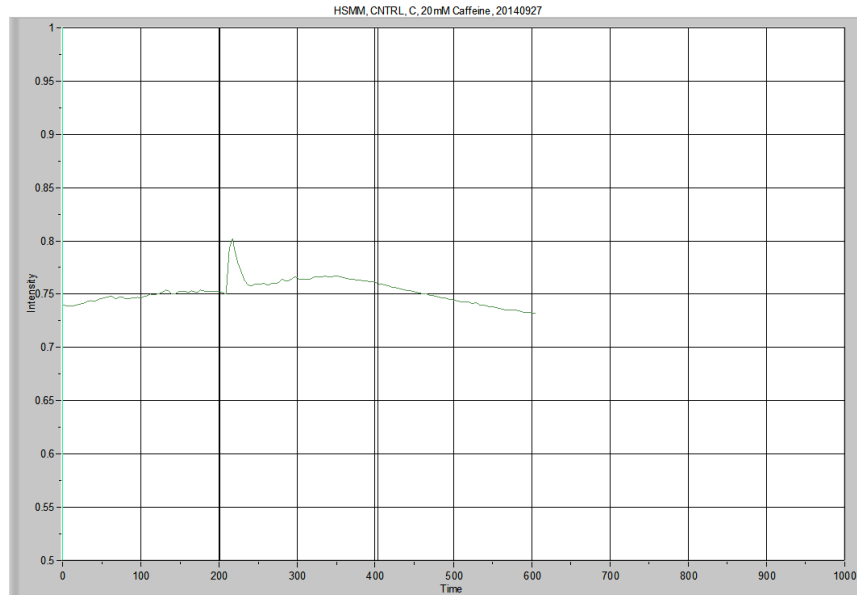
HSMM, CNTRL, C, 20mM Caffeine, 20140927

	Average resting level	Peak	Δ Level	Time to Peak	Area Under the Curve Low X: 201.279 High X: 597.13	Peak Area
CNTRL C, P3	0.746669	0.801659	0.05499	4.025553	298.79073	5.06828
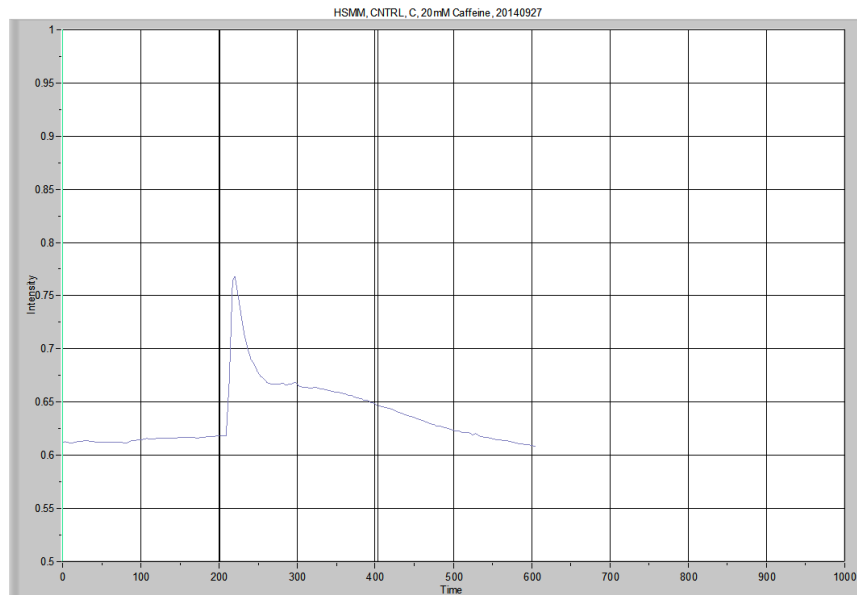
HSMM, CNTRL, C, 20mM Caffeine, 20140927

	Average resting level	Peak	Δ Level	Time to Peak	Area Under the Curve Low X: 201.279 High X: 597.13	Peak Area
CNTRL C, P4	0.613649	0.767619	0.15397	8.051138	256.47530	13.59520
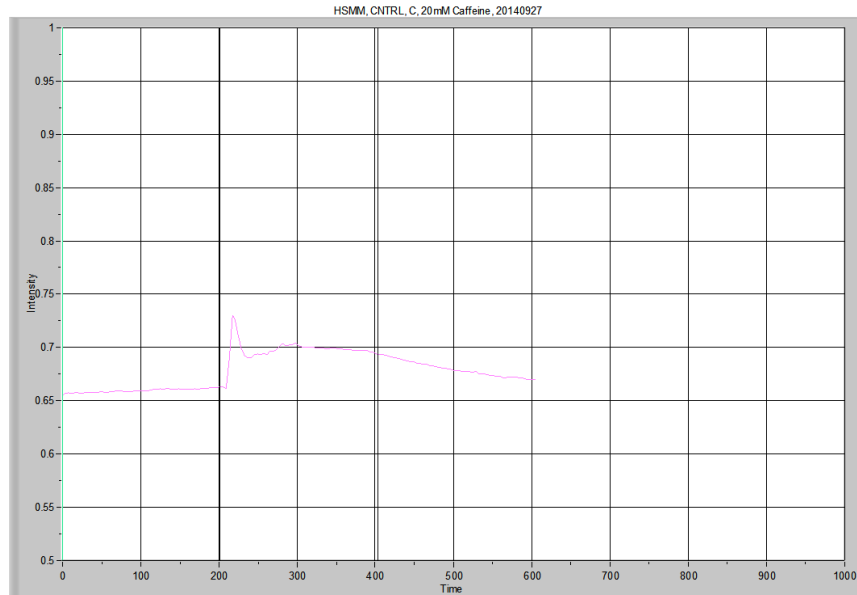
160

HSMM, CNTRL, C, 20mM Caffeine, 20140927

	Average resting level	Peak	Δ Level	Time to Peak	Area Under the Curve Low X: 201.279 High X: 597.13	Peak Area
CNTRL C, P5	0.658719	0.729933	0.071214	4.025553	272.57786	9.01723
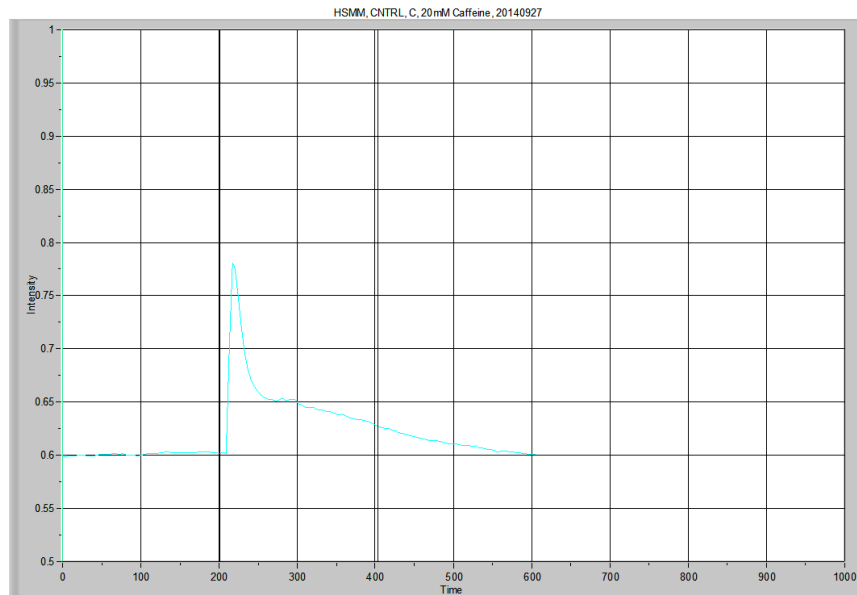
HSMM, CNTRL, C, 20mM Caffeine, 20140927

	Average resting level	Peak	Δ Level	Time to Peak	Area Under the Curve Low X: 201.279 High X: 597.13	Peak Area
CNTRL C, P6	0.600577	0.780981	0.180404	4.025553	250.64563	12.71607
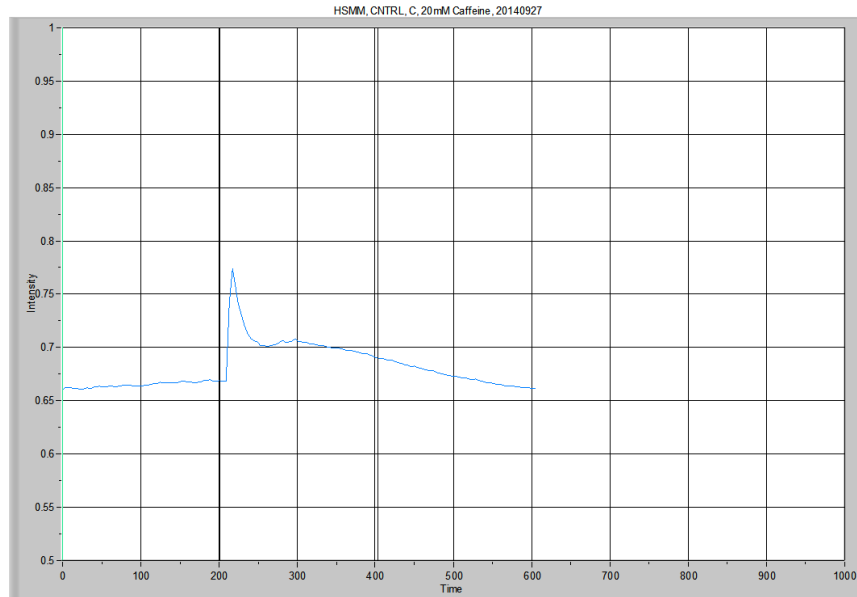
161

HSMM, CNTRL, C, 20mM Caffeine, 20140927

	Average resting level	Peak	Δ Level	Time to Peak	Area Under the Curve Low X: 201.279 High X: 597.13	Peak Area
CNTRL C, P7	0.664071	0.77412	0.110049	4.025553	272.91870	9.67276
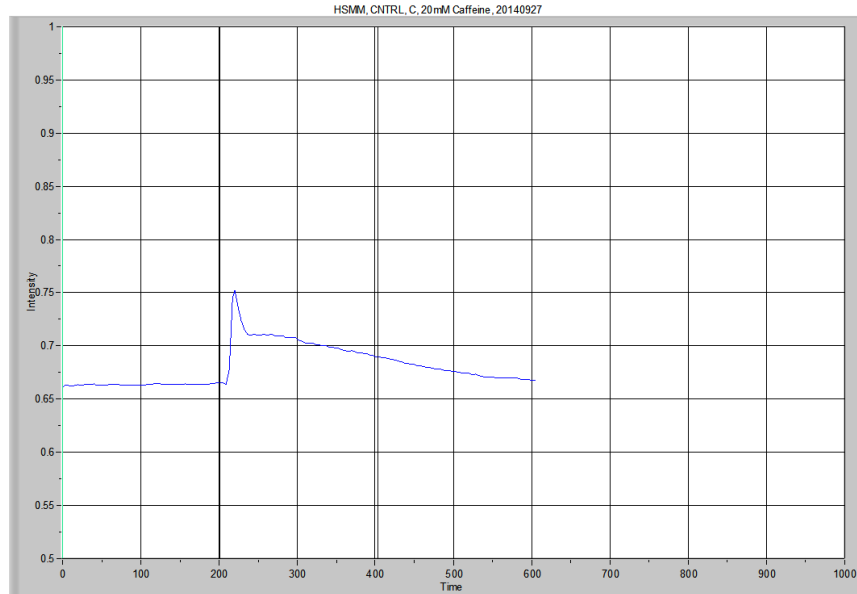
HSMM, CNTRL, C, 20mM Caffeine, 20140927

	Average resting level	Peak	Δ Level	Time to Peak	Area Under the Curve Low X: 201.279 High X: 597.13	Peak Area
CNTRL C, P8	0.663004	0.751822	0.088818	8.051138	273.08709	9.35460
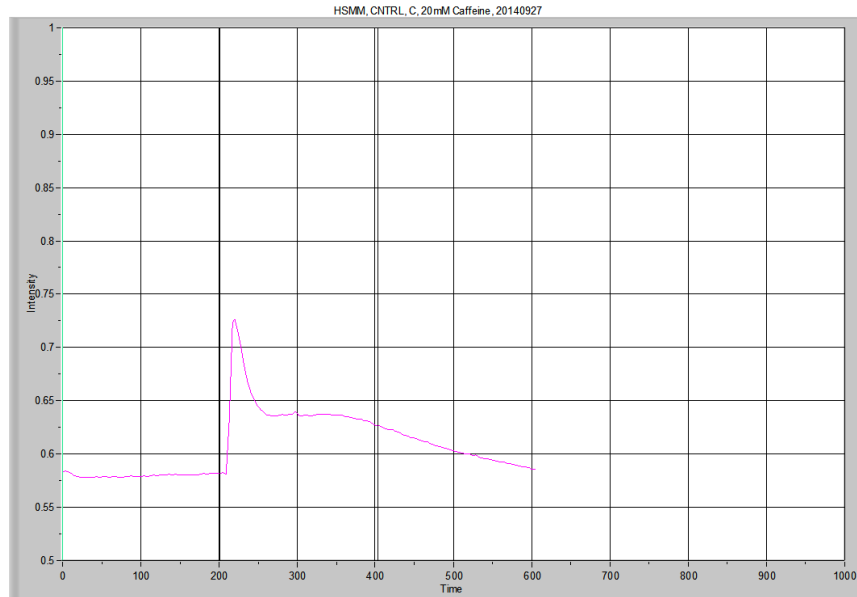
HSMM, CNTRL, C, 20mM Caffeine, 20140927

	Average resting level	Peak	Δ Level	Time to Peak	Area Under the Curve Low X: 201.279 High X: 597.13	Peak Area
CNTRL C, P9	0.579244	0.72626	0.147016	8.051138	246.69825	15.55078
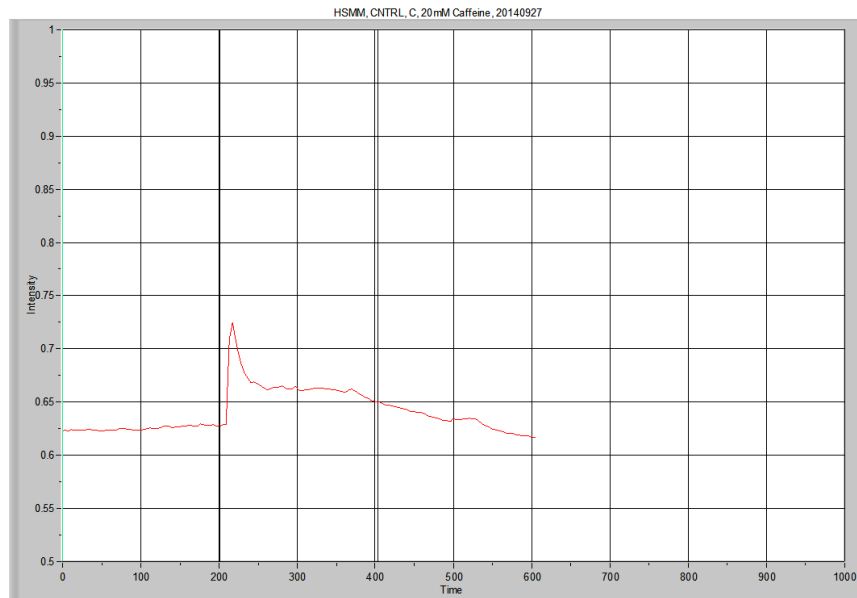
HSMM, CNTRL, C, 20mM Caffeine, 20140927

	Average resting level	Peak	Δ Level	Time to Peak	Area Under the Curve Low X: 201.279 High X: 597.13	Peak Area
CNTRL C, P10	0.624523	0.724571	0.100048	12.07676	256.86649	10.53180
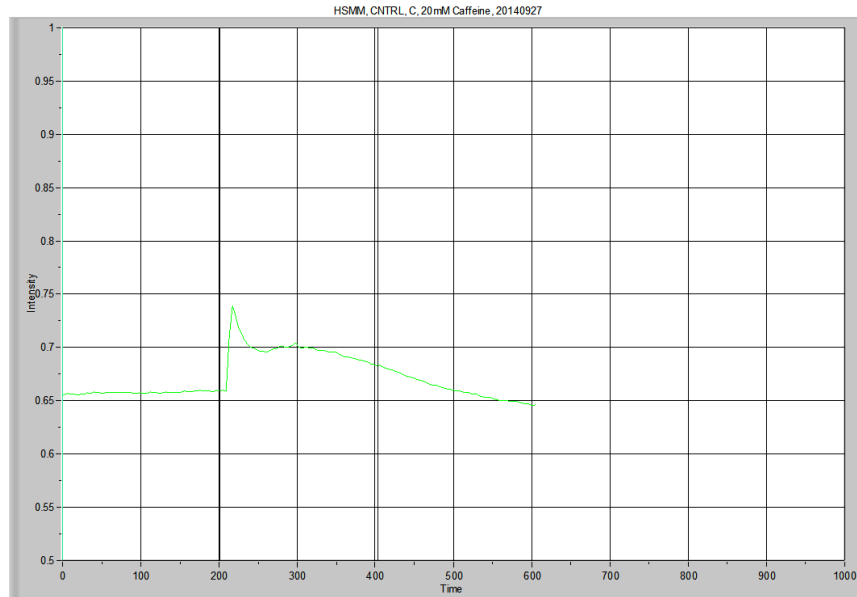
163

HSMM, CNTRL, C, 20mM Caffeine, 20140927

	Average resting level	Peak	Δ Level	Time to Peak	Area Under the Curve Low X: 201.279 High X: 597.13	Peak Area
CNTRL C, P11	0.65709	0.739034	0.081944	4.025553	268.90175	10.55403
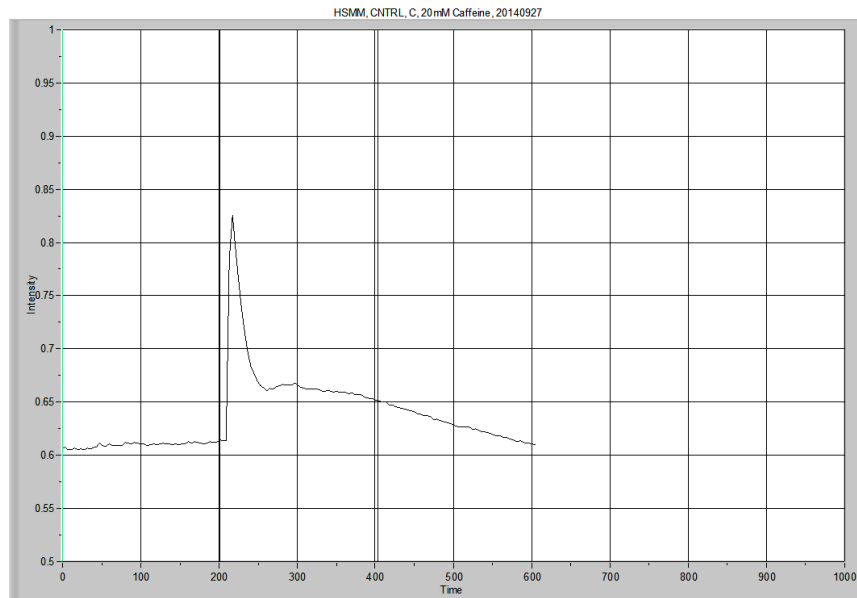
HSMM, CNTRL, C, 20mM Caffeine, 20140927

	Average resting level	Peak	Δ Level	Time to Peak	Area Under the Curve Low X: 201.279 High X: 597.13	Peak Area
CNTRL C, P12	0.609097	0.825425	0.216327	4.025553	258.00132	15.57382
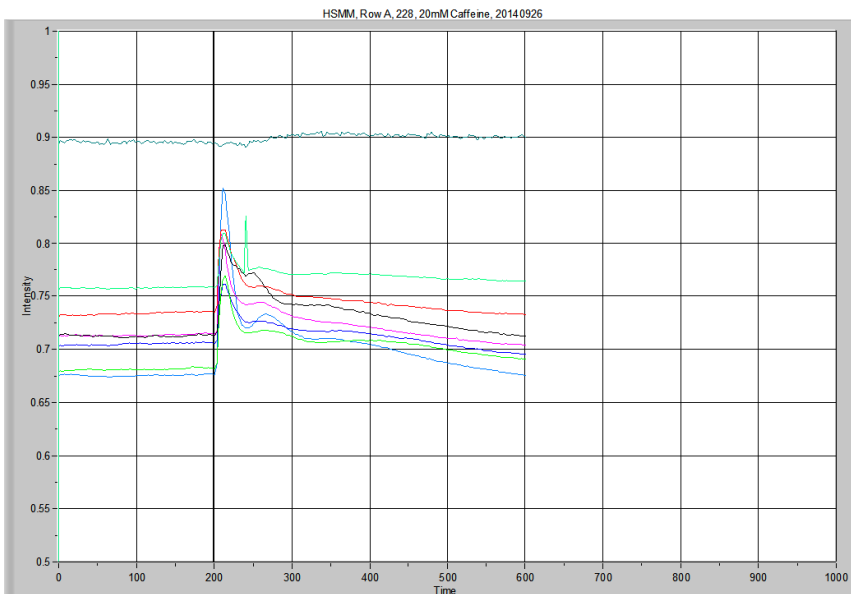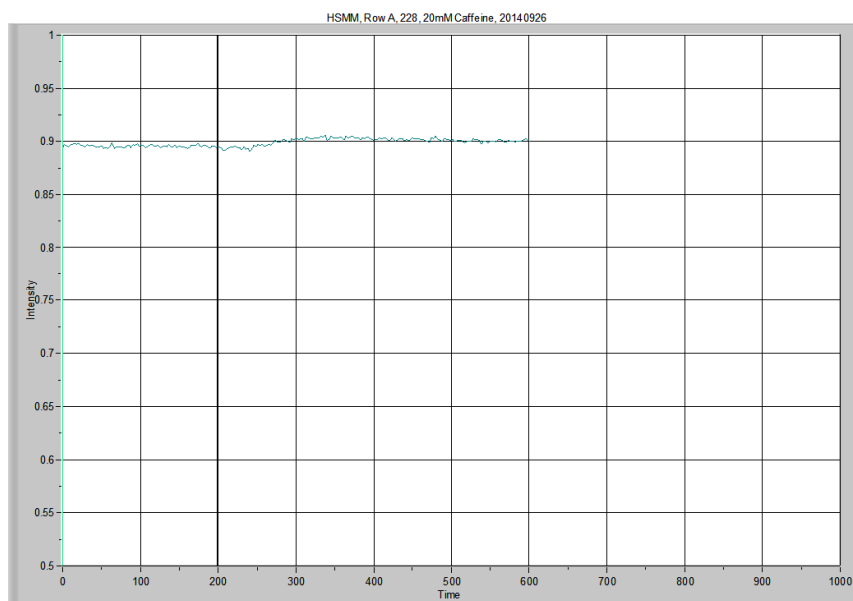
164

Overview

	Average resting level	Peak	Δ Level	Time to Peak	Area Under the Curve Low X: 201.278 High X: 598.467	Peak Area
228, BG	0.895094	0.904952	0.009859	NA	357.46819	0.93483
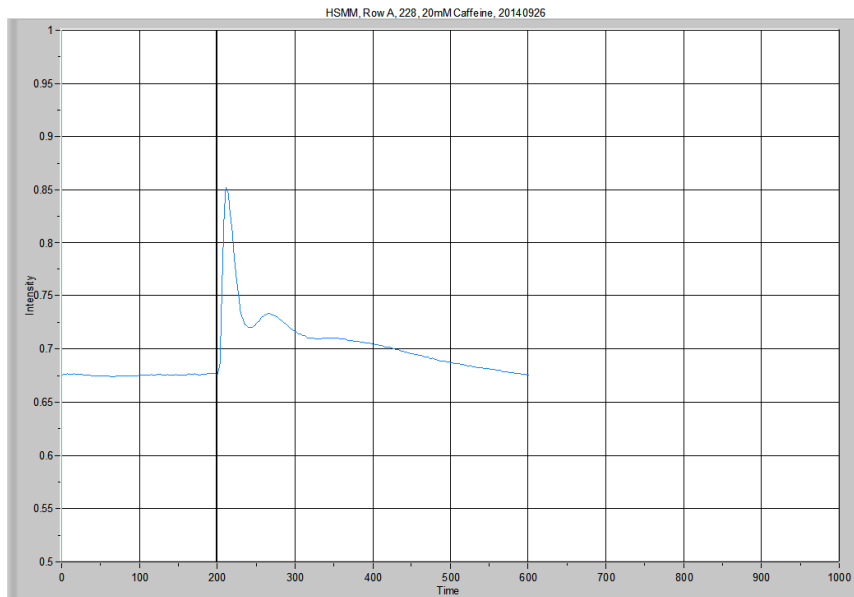
165

	Average resting level	Peak	Δ Level	Time to Peak	Area Under the Curve Low X: 201.278 High X: 598.467	Peak Area
228, P1	0.675183	0.851763	0.176581	8.05102	280.87457	12.45487
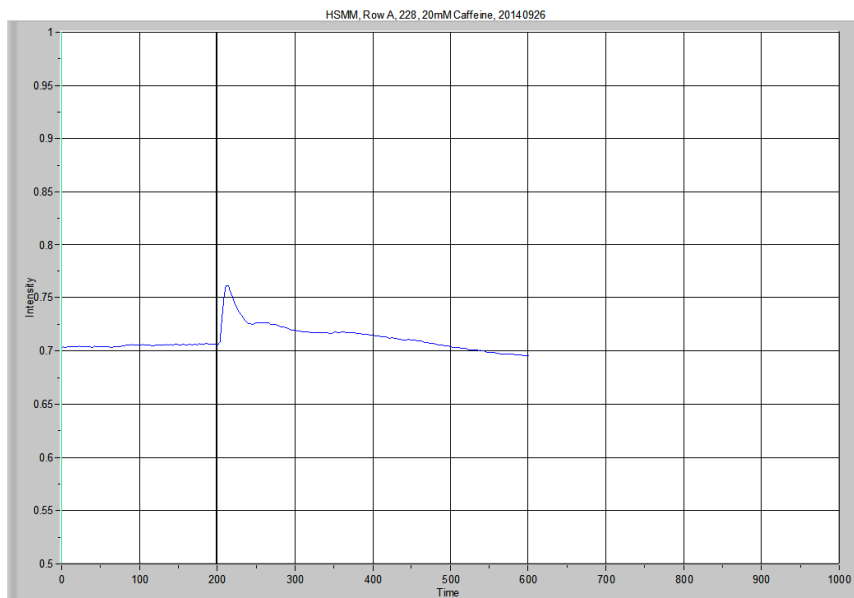
	Average resting level	Peak	Δ Level	Time to Peak	Area Under the Curve Low X: 201.278 High X: 598.467	Peak Area
228, P2	0.704742	0.761679	0.056937	10.73474	283.54444	5.42949
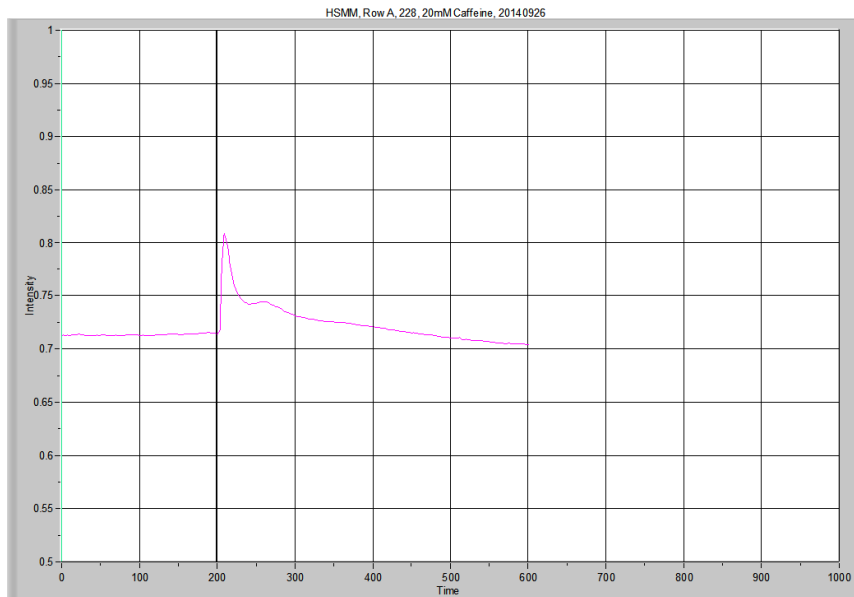
HSMM, Row A, 228, 20mM Caffeine, 20140926

	Average resting level	Peak	Δ Level	Time to Peak	Area Under the Curve Low X: 201.278 High X: 598.467	Peak Area
228, P3	0.713041	0.808925	0.095883	5.367426	287.54207	6.05005
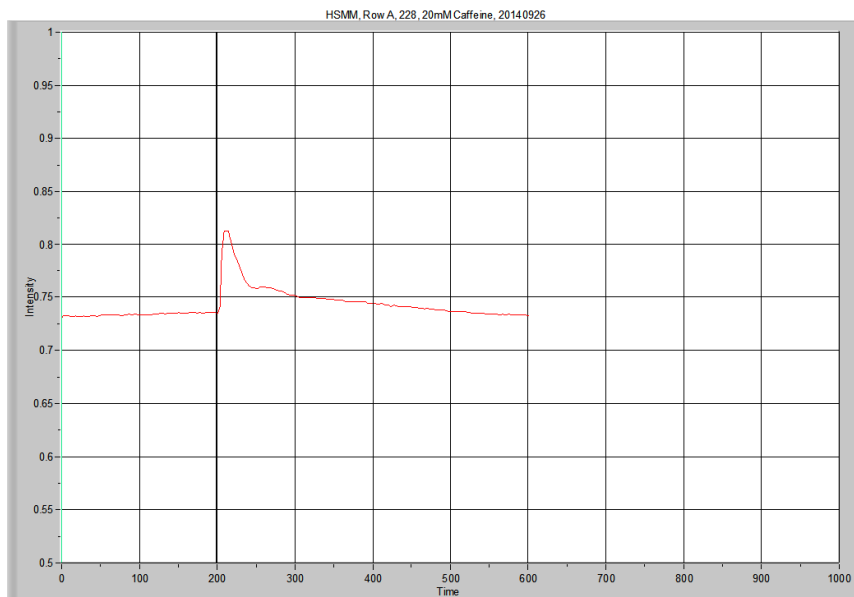
HSMM, Row A, 228, 20mM Caffeine, 20140926

	Average resting level	Peak	Δ Level	Time to Peak	Area Under the Curve Low X: 201.278 High X: 598.467	Peak Area
228, P4	0.733512	0.812356	0.078844	10.73474	296.88430	5.36465
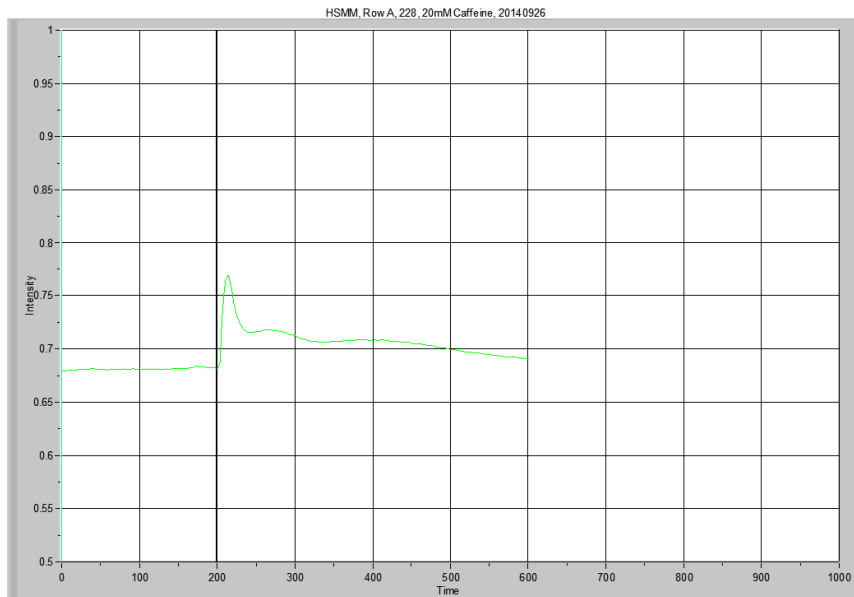
167

HSMM, Row A, 228, 20mM Caffeine, 20140926

	Average resting level	Peak	Δ Level	Time to Peak	Area Under the Curve Low X: 201.278 High X: 598.467	Peak Area
228, P5	0.680908	0.76959	0.088683	10.73474	281.00744	8.52524
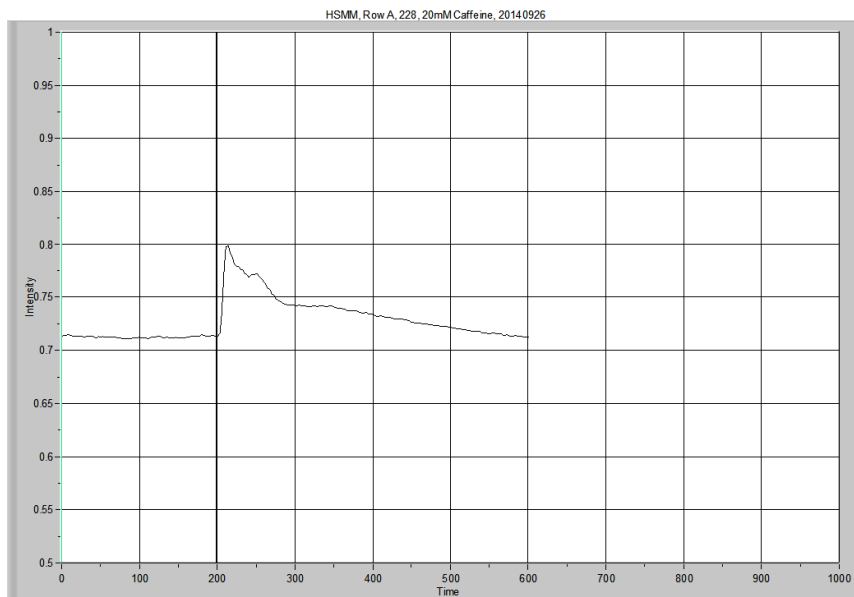
HSMM, Row A, 228, 20mM Caffeine, 20140926

	Average resting level	Peak	Δ Level	Time to Peak	Area Under the Curve Low X: 201.278 High X: 598.467	Peak Area
228, P6	0.712359	0.798712	0.086353	10.73474	292.45145	9.36121
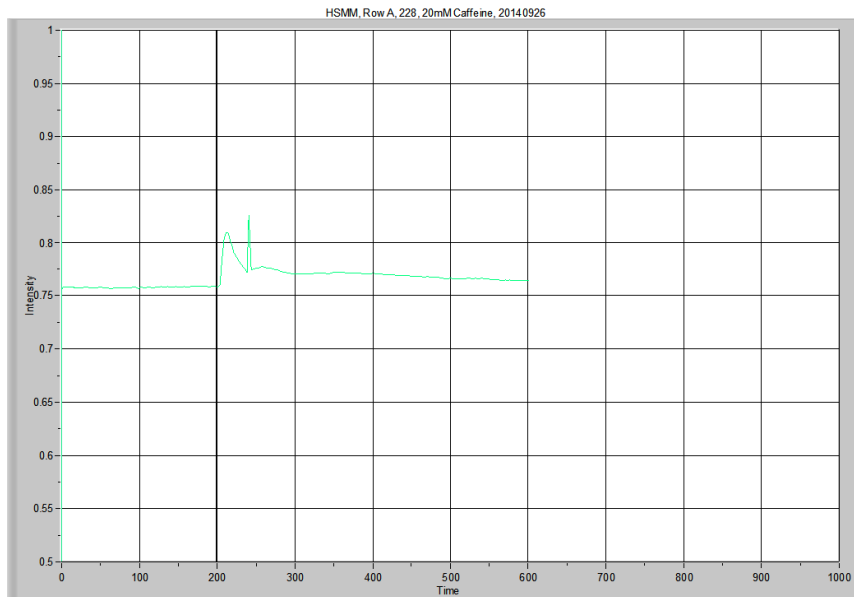
168

HSMM, Row A, 228, 20mM Caffeine, 20140926

	Average resting level	Peak	Δ Level	Time to Peak	Area Under the Curve Low X: 201.278 High X: 598.467	Peak Area
228, P9	0.757595	0.825766	0.068171	Unable to detect	306.23825	4.03008

Calcium Imaging, HSMM

169
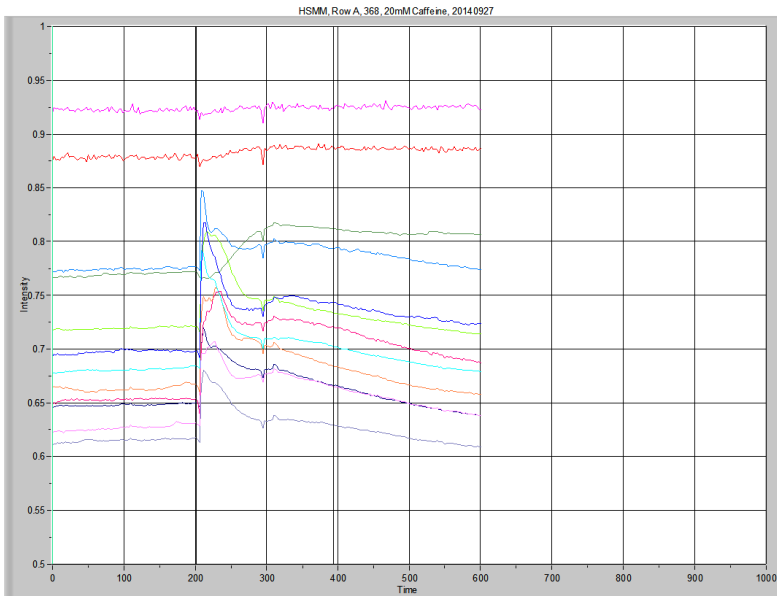
Overview
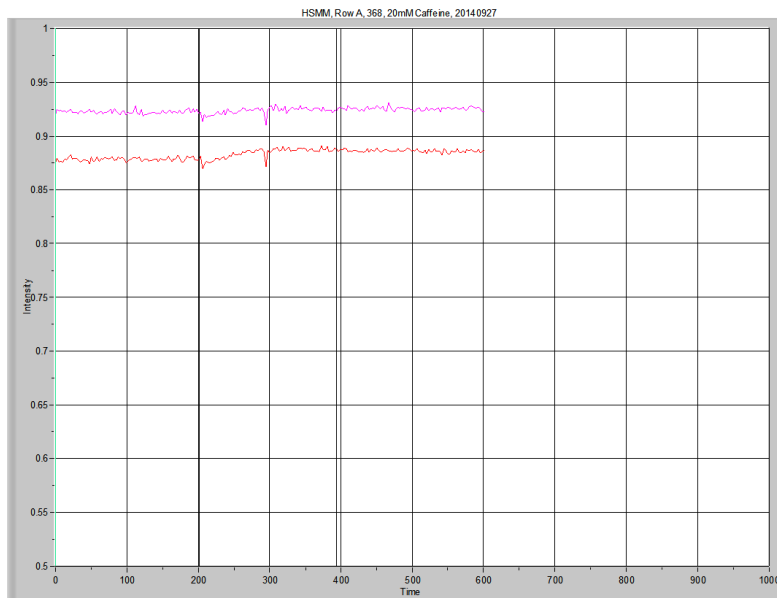
I did not keep this data on the Excel file – because I have so many other tracings of Background…
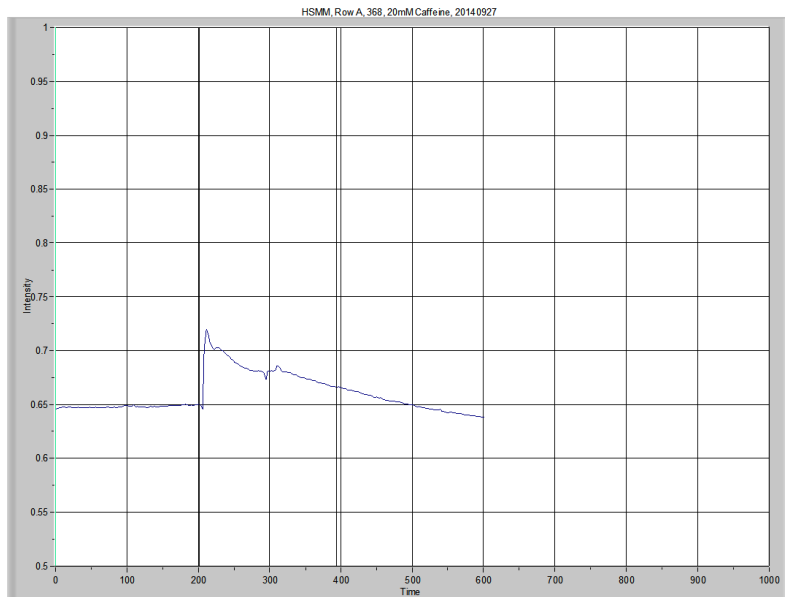
HSMM, Row A, 368, 20mM Caffeine, 20140927

	Average resting level	Peak	Δ Level	Time to Peak	Area Under the Curve Low X: 201.28 High X: 598.475	Peak Area
368, P1	0.647625	0.719902	0.072277	2.683591	264.36438	8.59591
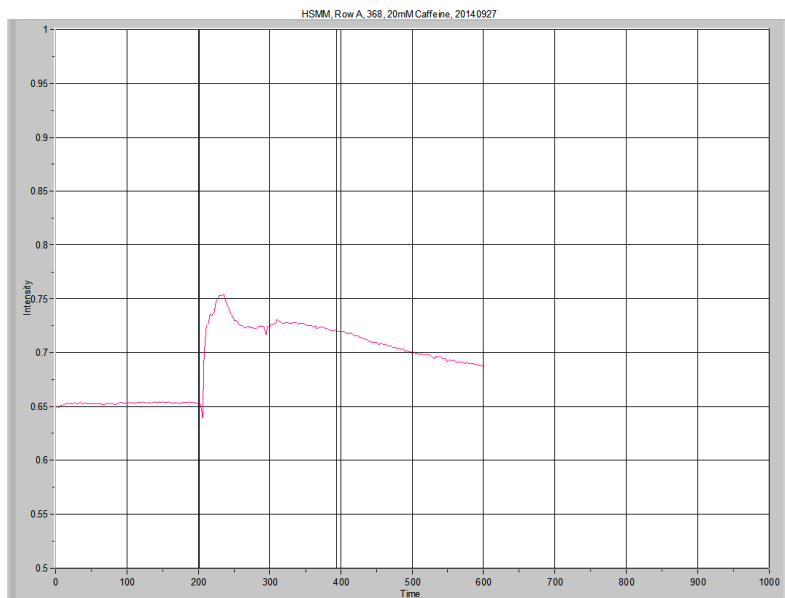
HSMM, Row A, 368, 20mM Caffeine, 20140927

	Average resting level	Peak	Δ Level	Time to Peak	Area Under the Curve Low X: 201.28 High X: 598.475	Peak Area
368, P2	0.652673	0.753595	0.100921	26.83716	283.28749	16.96522
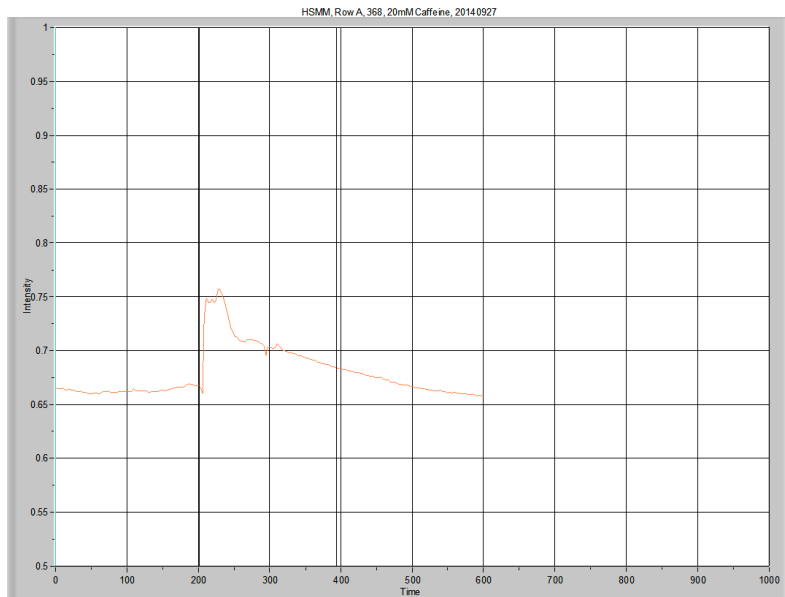
171

	Average resting level	Peak	Δ Level	Time to Peak	Area Under the Curve Low X: 201.28 High X: 598.475	Peak Area
368, P3	0.662877	0.756867	0.09399	21.46966	272.95525	9.88087
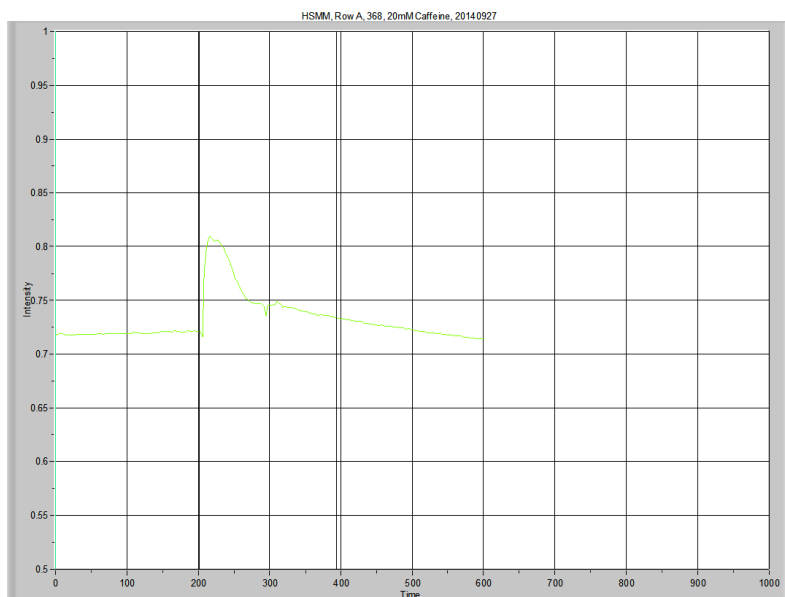
	Average resting level	Peak	Δ Level	Time to Peak	Area Under the Curve Low X: 201.28 High X: 598.475	Peak Area
368, P4	0.719001	0.809502	0.0905	8.050969	293.23553	8.23952

172
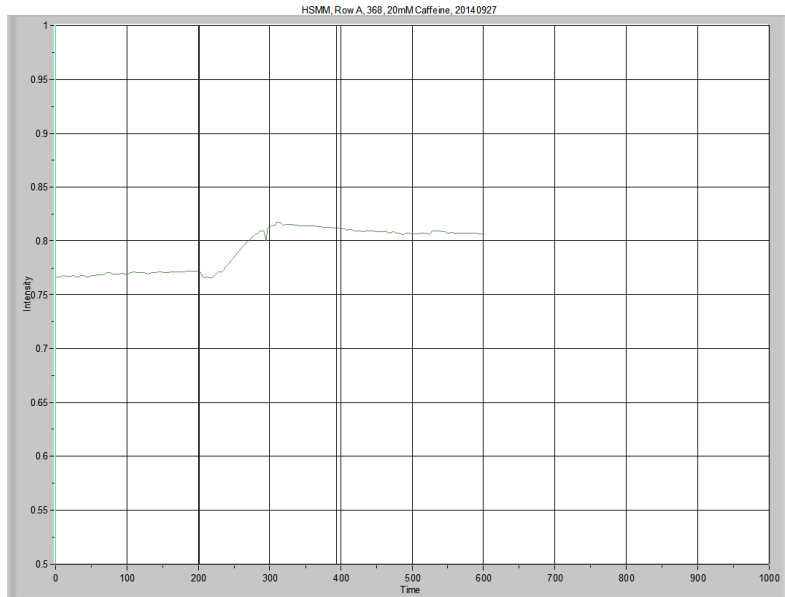
Did not include in analysis, because this myotube drifted away upon contraction….
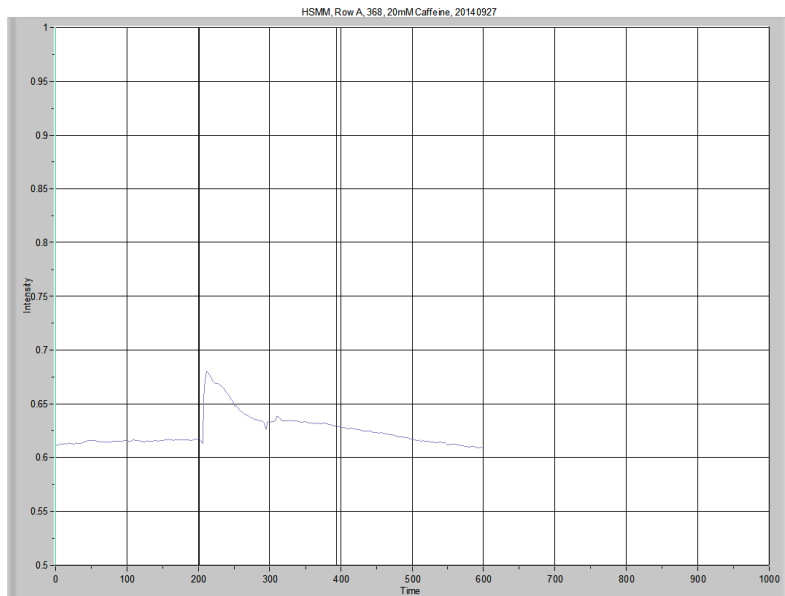
	Average resting level	Peak	Δ Level	Time to Peak	Area Under the Curve Low X: 201.28 High X: 598.475	Peak Area
368, P6	0.614816	0.679626	0.064809	18.78625	249.88525	6.35996
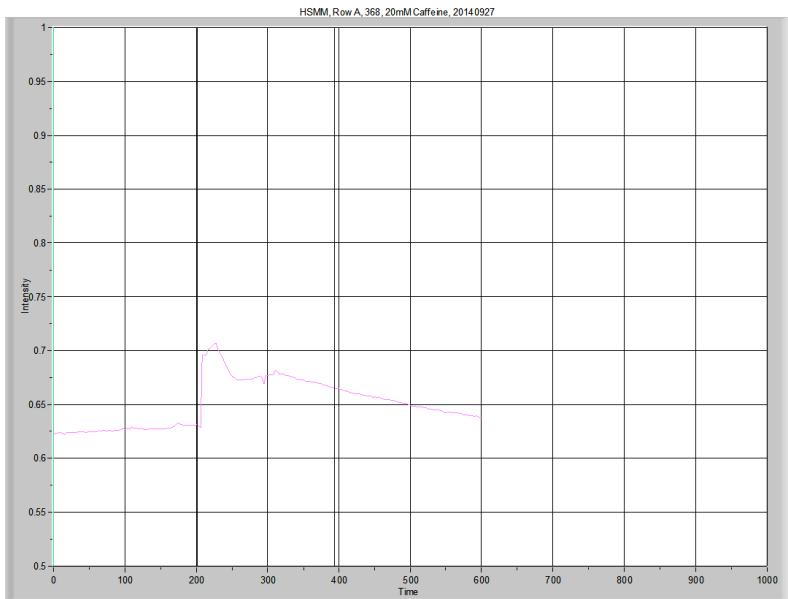
HSMM, Row A, 368, 20mM Caffeine, 20140927

	Average resting level	Peak	Δ Level	Time to Peak	Area Under the Curve Low X: 201.28 High X: 598.475	Peak Area
368, P7	0.626432	0.707148	0.080716	13.41884	263.36239	11.40369
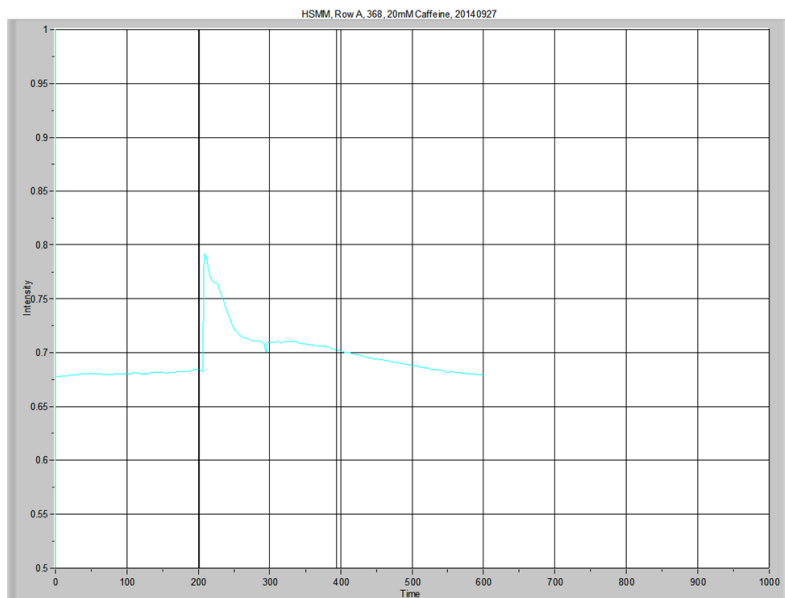
HSMM, Row A, 368, 20mM Caffeine, 20140927

	Average resting level	Peak	Δ Level	Time to Peak	Area Under the Curve Low X: 201.28 High X: 598.475	Peak Area
368, P8	0.680316	0.791707	0.111391	8.051455	279.33024	8.59806
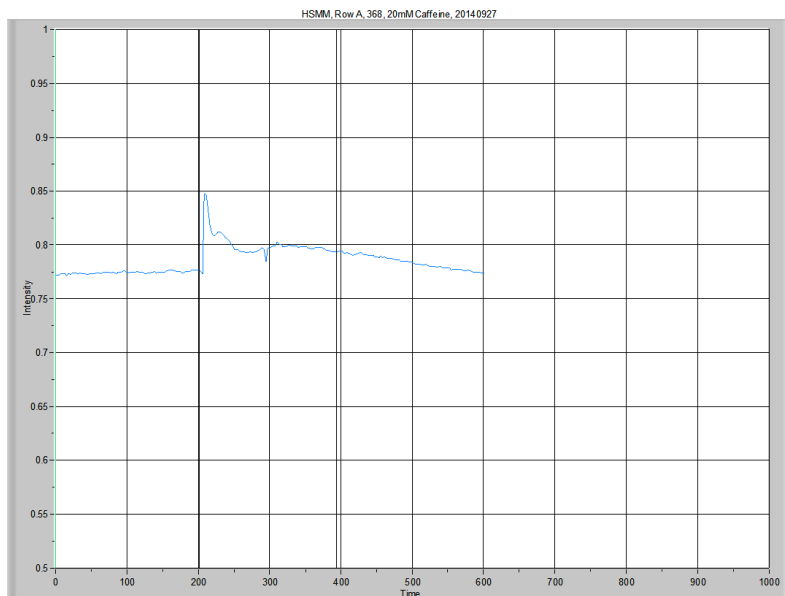
HSMM, Row A, 368, 20mM Caffeine, 2014 0927

	Average resting level	Peak	Δ Level	Time to Peak	Area Under the Curve Low X: 201.28 High X: 598.475	Peak Area
368, P9	0.774037	0.84717	0.073133	8.051455	314.31274	6.49135
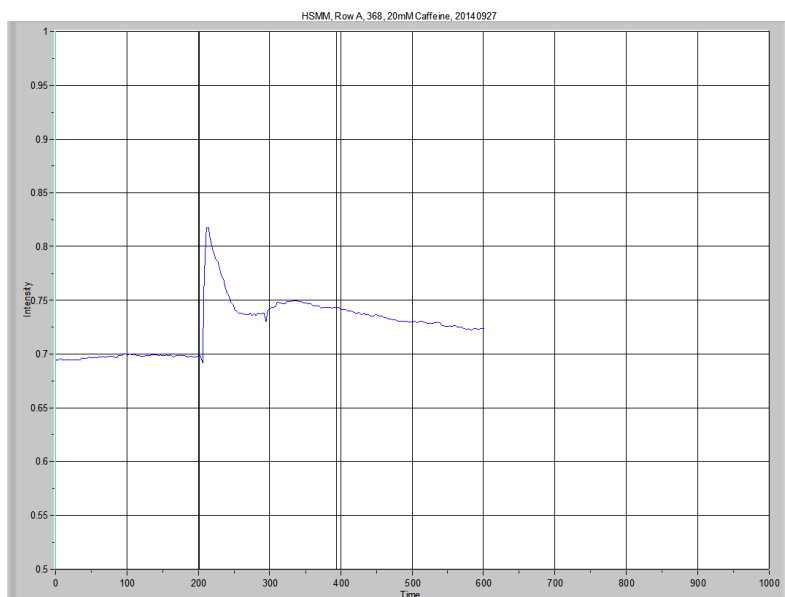
HSMM, Row A, 368, 20mM Caffeine, 2014 0927

	Average resting level	Peak	Δ Level	Time to Peak	Area Under the Curve Low X: 201.28 High X: 598.475	Peak Area
368, P10	0.697172	0.817674	0.120502	5.367265	293.84289	11.49776

Calcium Imaging, HSMM
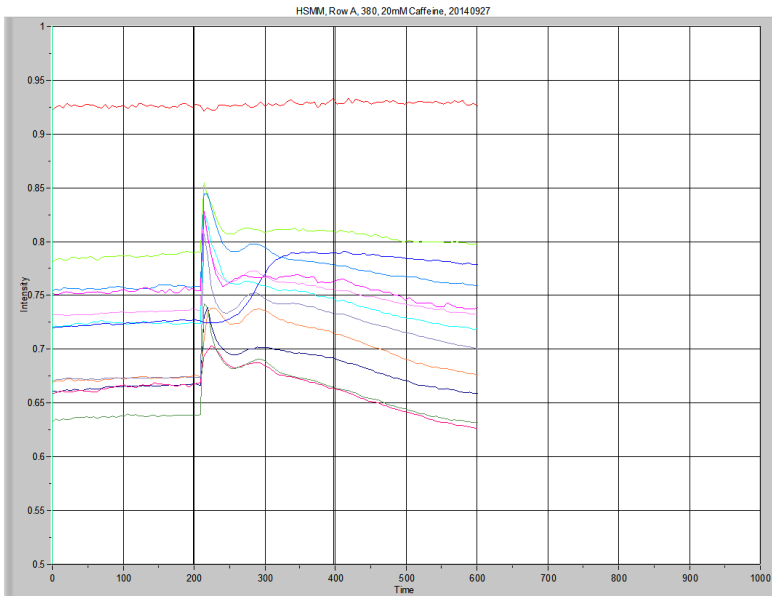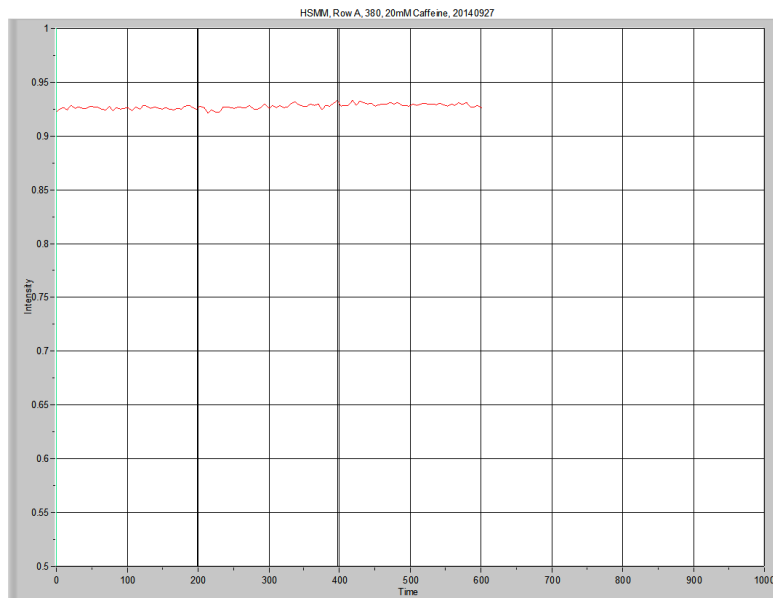
175

Overview

	Average resting level	Peak	Δ Level	Time to Peak	Area Under the Curve Low X: 203.964 High X: 601.158	Peak Area
380, BG	0.925621	0.932803	0.007183	NA	368.56308	0.42837
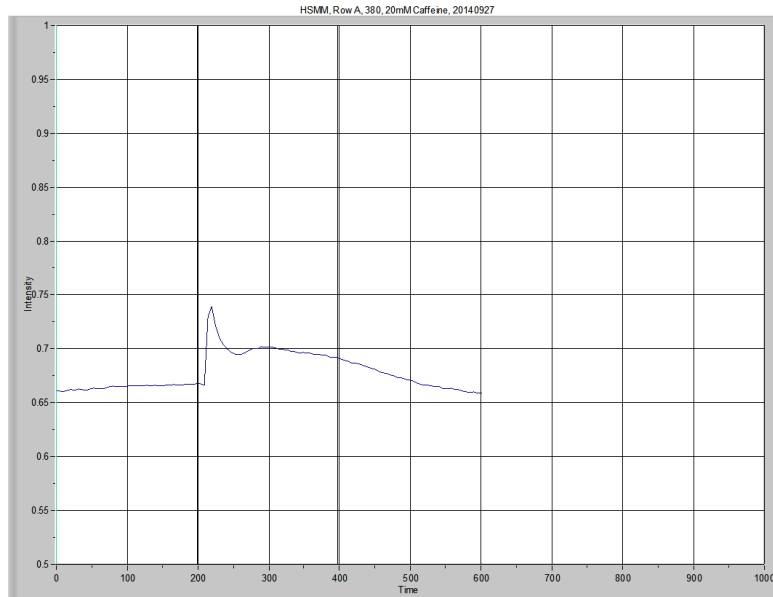
HSMM, Row A, 380, 20mM Caffeine, 20140927

	Average resting level	Peak	Δ Level	Time to Peak	Area Under the Curve Low X: 203.964 High X: 601.158	Peak Area
380, P1	0.664107	0.738742	0.074636	16.10246	272.12901	8.76775
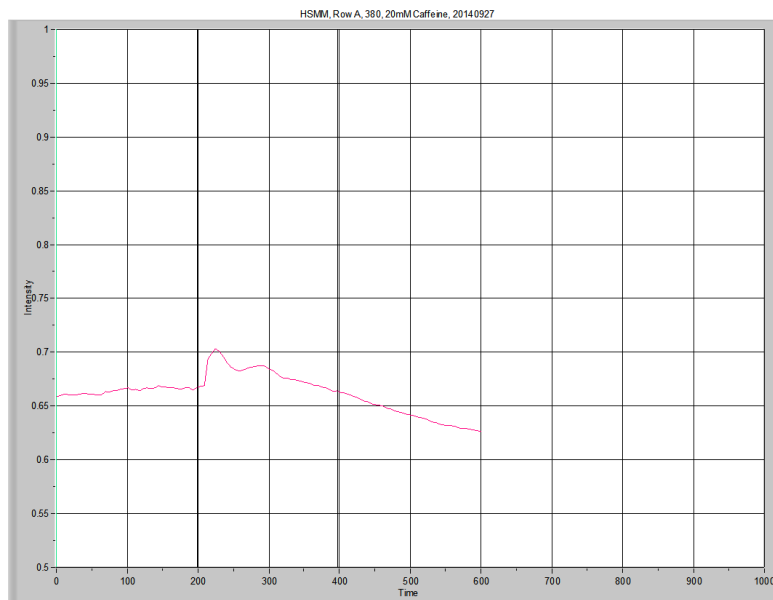
HSMM, Row A, 380, 20mM Caffeine, 20140927

	Average resting level	Peak	Δ Level	Time to Peak	Area Under the Curve Low X: 203.964 High X: 601.158	Peak Area
380, P2	0.663651	0.703156	0.039505	21.46992	262.43486	5.47867
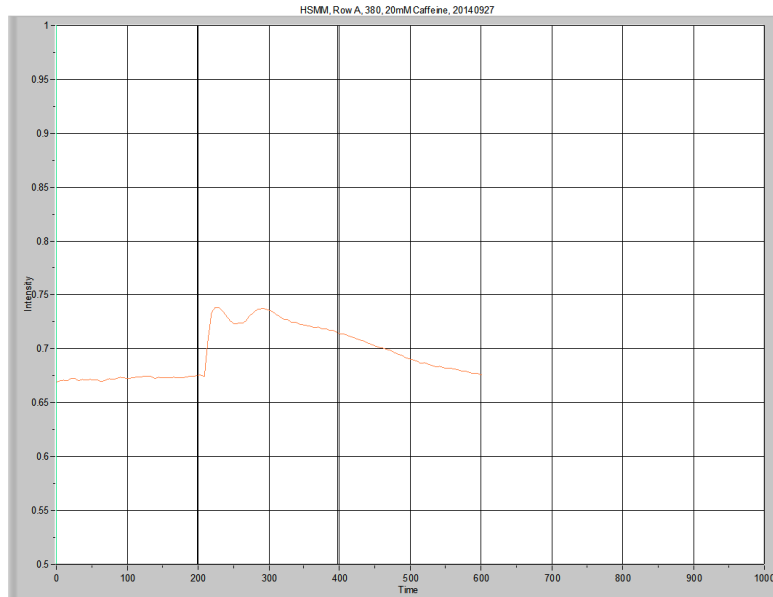
177

HSMM, Row A, 380, 20mM Caffeine, 20140927

	Average resting level	Peak	Δ Level	Time to Peak	Area Under the Curve Low X: 203.964 High X: 601.158	Peak Area
380, P3	0.672032	0.738216	0.066184	10.73498	281.23388	13.00693
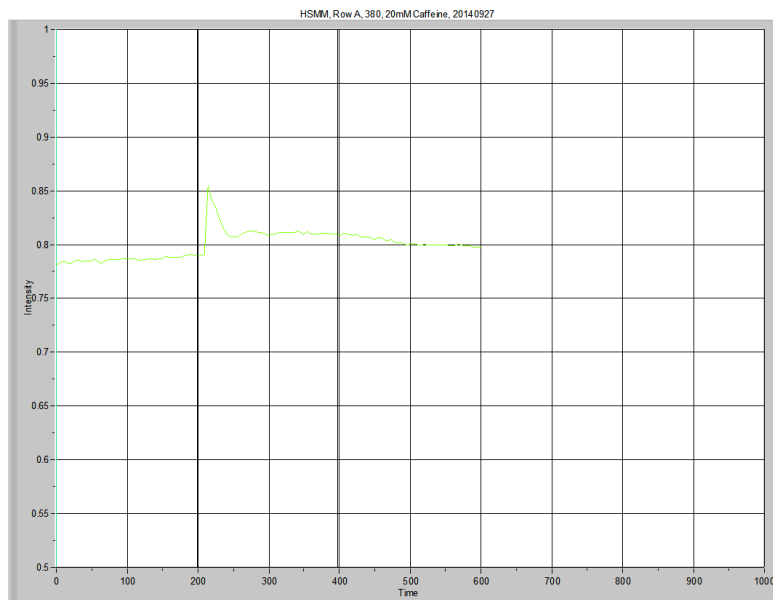
HSMM, Row A, 380, 20mM Caffeine, 20140927

	Average resting level	Peak	Δ Level	Time to Peak	Area Under the Curve Low X: 203.964 High X: 601.158	Peak Area
380, P4	0.785737	0.85455	0.068813	10.73495	320.64774	5.60320
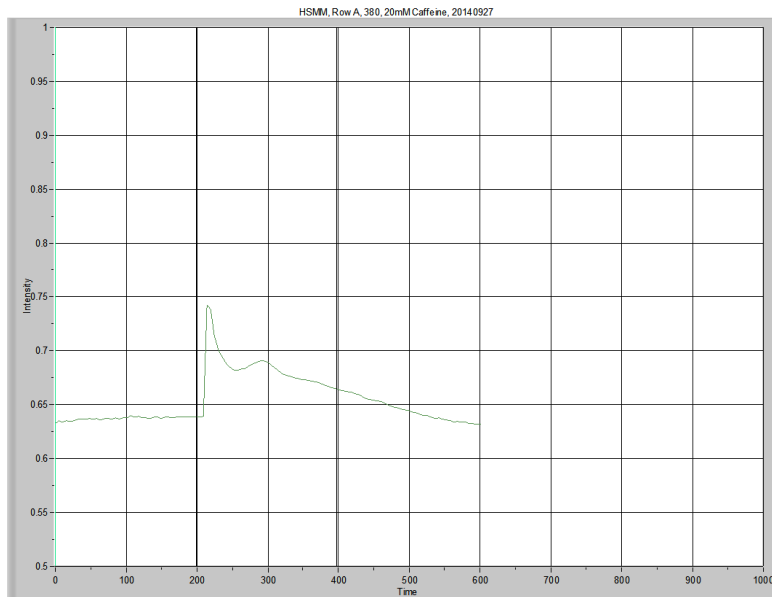
HSMM, Row A, 380, 20mM Caffeine, 20140927

	Average resting level	Peak	Δ Level	Time to Peak	Area Under the Curve Low X: 203.964 High X: 601.158	Peak Area
380, P5	0.636808	0.742035	0.105227	10.73495	263.47590	11.26519
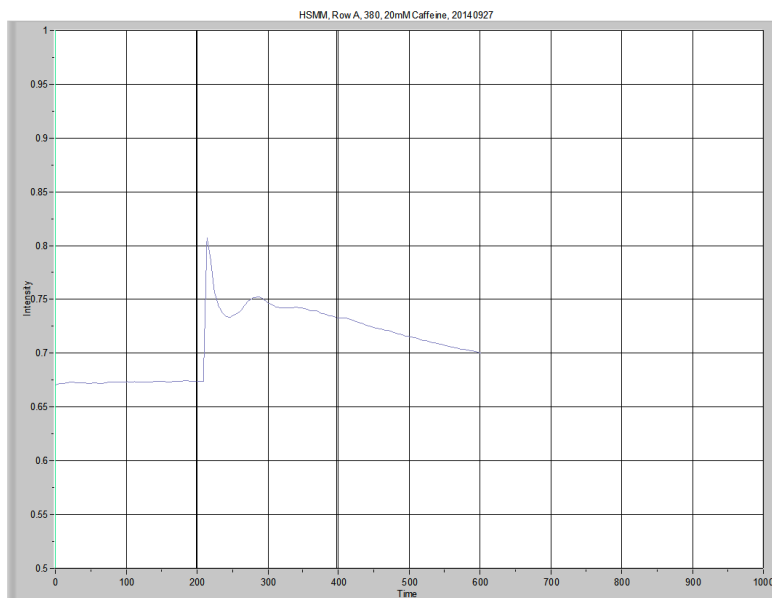
HSMM, Row A, 380, 20mM Caffeine, 20140927

	Average resting level	Peak	Δ Level	Time to Peak	Area Under the Curve Low X: 203.964 High X: 601.158	Peak Area
380, P6	0.672548	0.807031	0.134484	10.73495	289.37347	16.64545
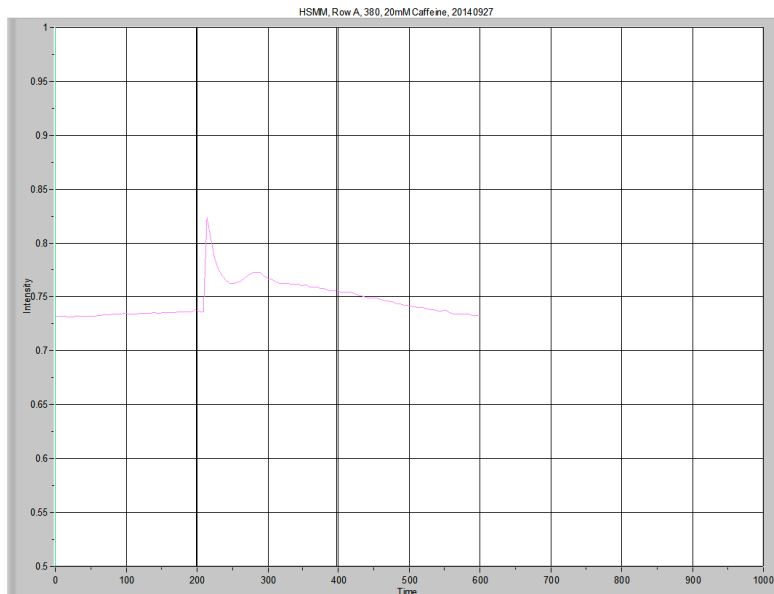
179

HSMM, Row A, 380, 20mM Caffeine, 20140927

	Average resting level	Peak	Δ Level	Time to Peak	Area Under the Curve	Peak Area
					Low X: 203.964 High X: 601.158	
380, P7	0.733344	0.823623	0.090279	5.367451	299.42321	7.77508
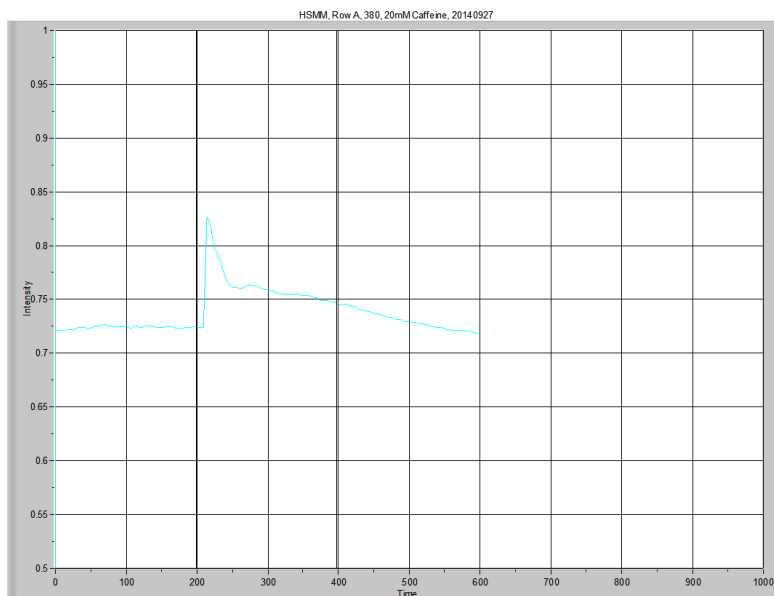
HSMM, Row A, 380, 20mM Caffeine, 20140927

	Average resting level	Peak	Δ Level	Time to Peak	Area Under the Curve Low X: 203.964 High X: 601.158	Peak Area
380, P8	0.7236	0.826956	0.103356	5.367451	296.02820	9.56682
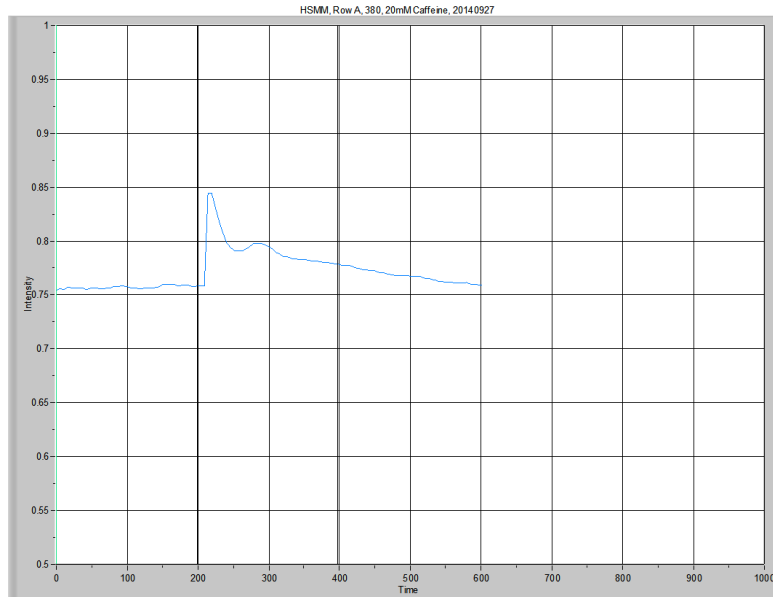
180

HSMM, Row A, 380, 20mM Caffeine, 20140927

	Average resting level	Peak	Δ Level	Time to Peak	Area Under the Curve Low X: 203.964 High X: 601.158	Peak Area
380, P9	0.756679	0.844523	0.087844	5.367451	309.52542	8.40852

HSMM, Row A, 380, 20mM Caffeine, 20140927
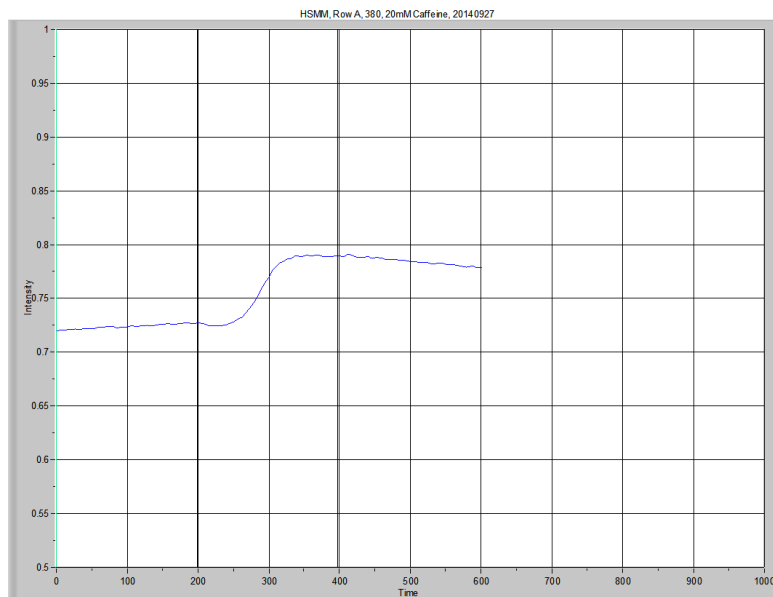
I do not plan to include this data in my analysis, as it looks as though the myotube moved so that the ROI was no longer true….

	Average resting level	Peak	Δ Level	Time to Peak	Area Under the Curve	Peak Area
380, P10	*0.723359*	*0.790576*	*0.067218*	*177.127*		
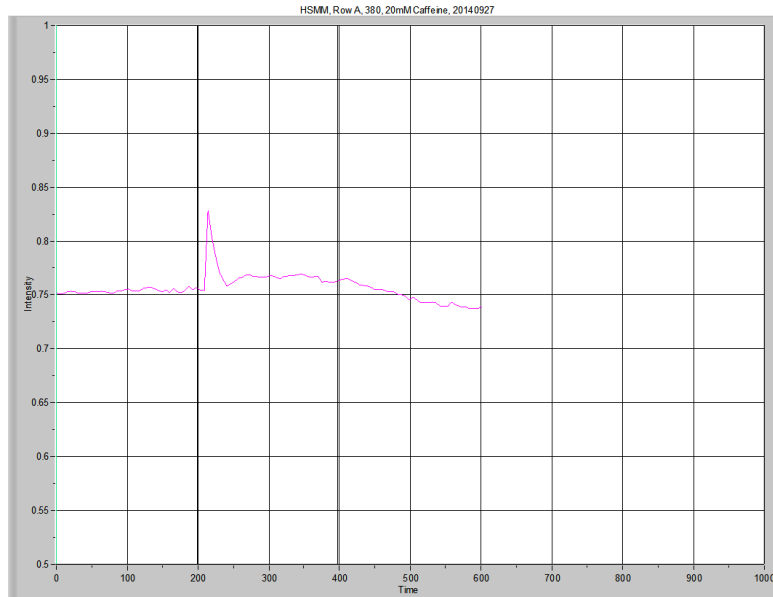
181

HSMM, Row A, 380, 20mM Caffeine, 2014 0927

	Average resting level	Peak	Δ Level	Time to Peak	Area Under the Curve Low X: 203.964 High X: 601.158	Peak Area
380, P11	0.753215	0.827809	0.074594	5.367451	301.12695	4.65324
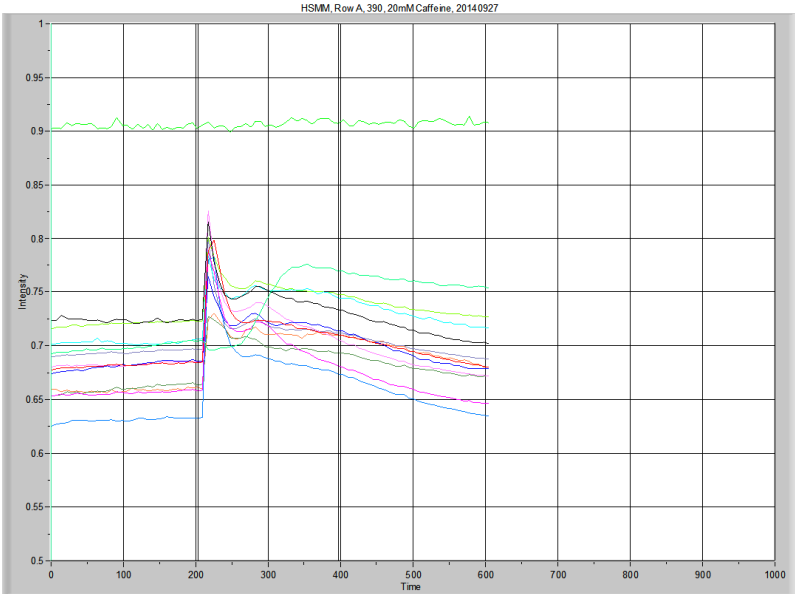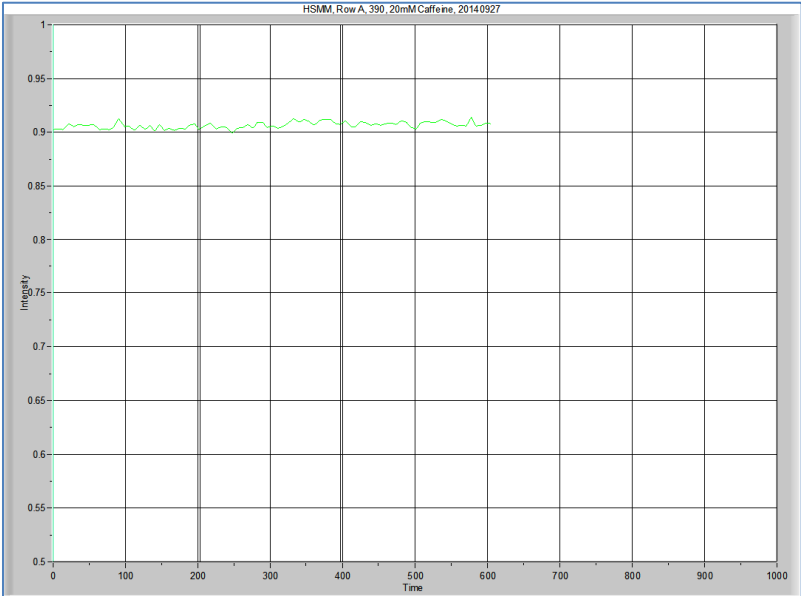
Overview

	Average resting level	Peak	Δ Level	Time to Peak	Area Under the Curve Low X: 202.625 High X: 598.475	Peak Area
390, BG	0.904409	0.913479	0.00907	NA	359.11677	0.80679
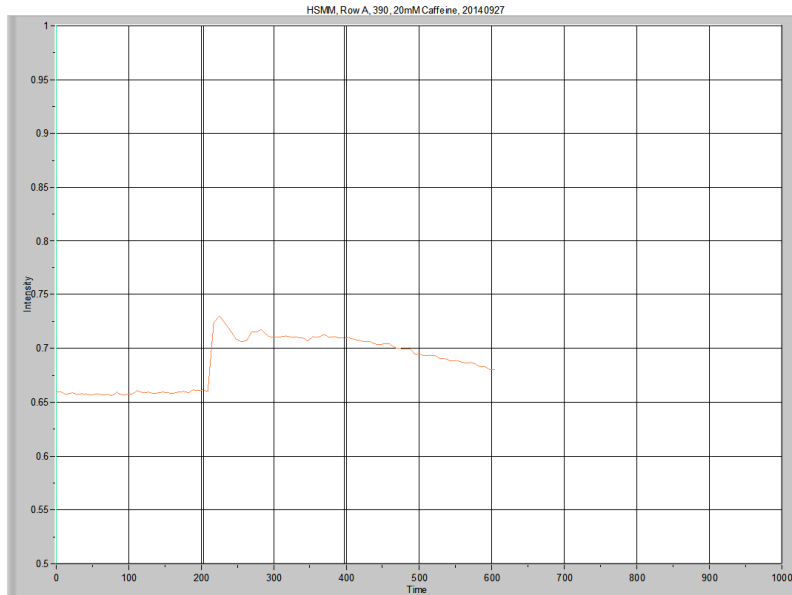
183

	Average resting level	Peak	Δ Level	Time to Peak	Area Under the Curve Low X: 202.625 High X: 598.475	Peak Area
390, P1	0.658304	0.729773	0.07147	8.051234	278.24481	12.71425
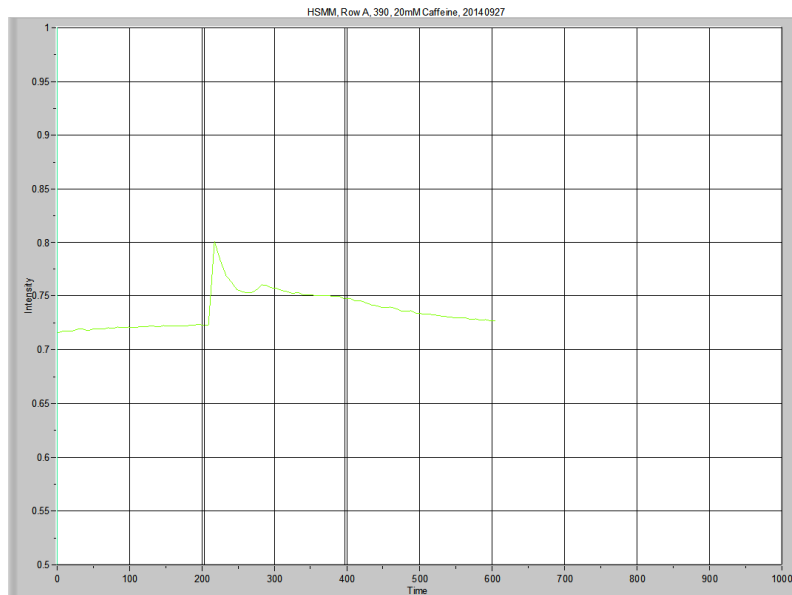
	Average resting level	Peak	Δ Level	Time to Peak	Area Under the Curve Low X: 202.625 High X: 598.475	Peak Area
390, P2	0.720274	0.800628	0.080354	8.051215	295.12265	8.26396
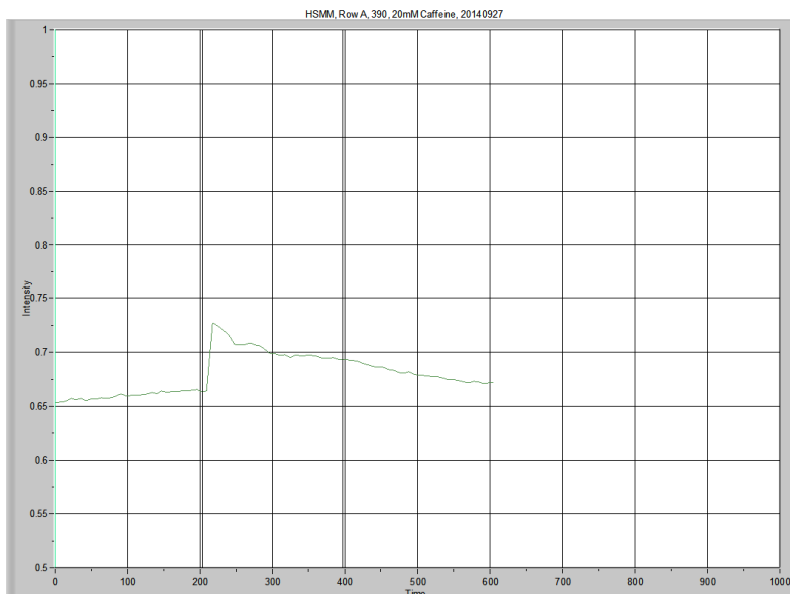
184

HSMM, Row A, 390, 20mM Caffeine, 2014 0927

	Average resting level	Peak	Δ Level	Time to Peak	Area Under the Curve Low X: 202.625 High X: 598.475	Peak Area
390, P3	0.659591	0.727412	0.067821	8.051215	273.42330	9.23176
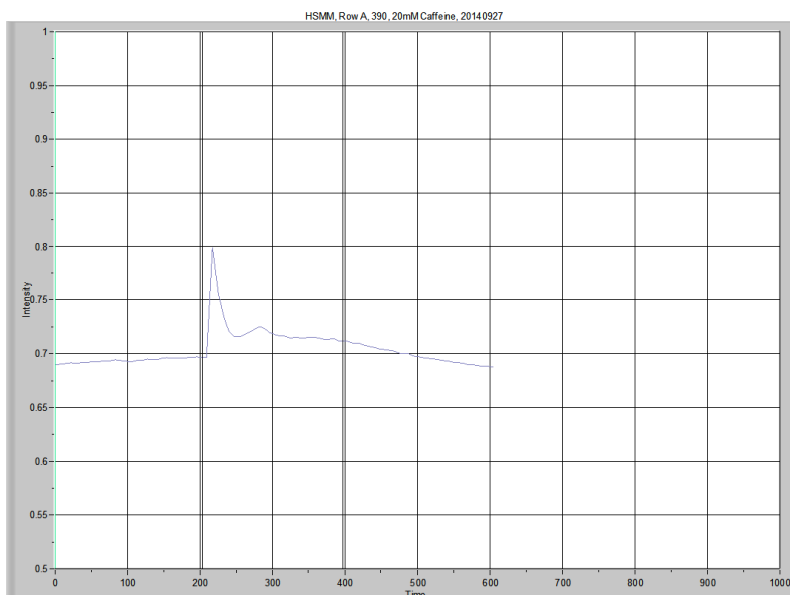
HSMM, Row A, 390, 20mM Caffeine, 2014 0927

	Average resting level	Peak	Δ Level	Time to Peak	Area Under the Curve Low X: 202.625 High X: 598.475	Peak Area
390, P4	0.693513	0.798951	0.105439	8.051215	281.06191	7.02472
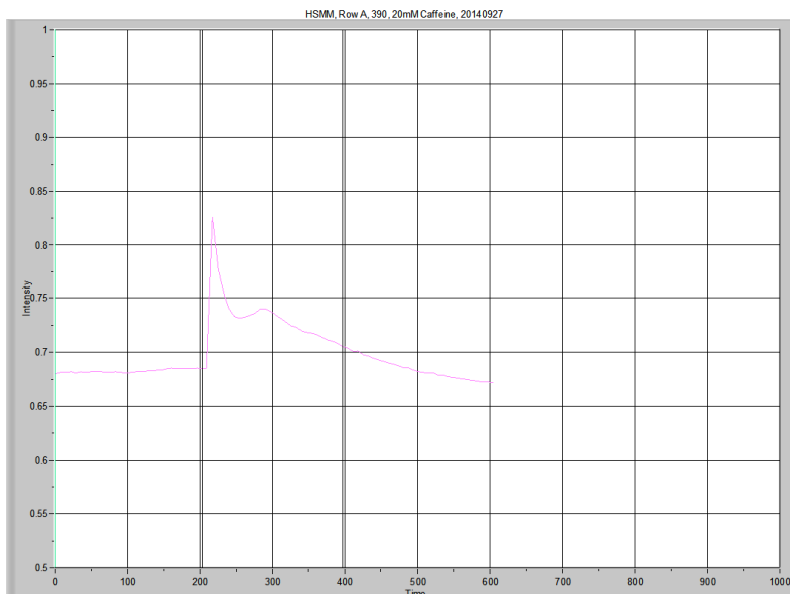
185

HSMM, Row A, 390, 20mM Caffeine, 2014 0927

	Average resting level	Peak	Δ Level	Time to Peak	Area Under the Curve Low X: 202.625 High X: 598.475	Peak Area
390, P5	0.682415	0.825374	0.142959	8.051215	280.27161	11.67871
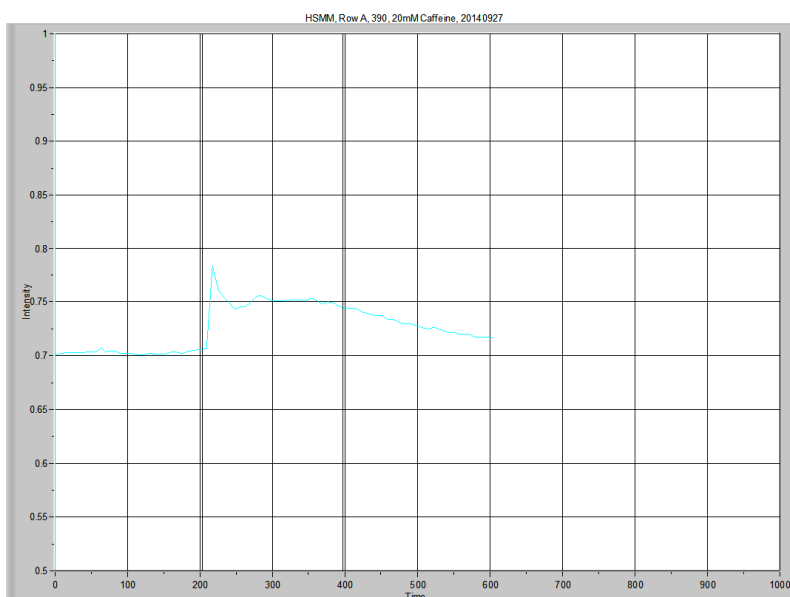
HSMM, Row A, 390, 20mM Caffeine, 2014 0927

	Average resting level	Peak	Δ Level	Time to Peak	Area Under the Curve Low X: 202.625 High X: 598.475	Peak Area
390, P6	0.702768	0.783631	0.080862	14.75776	292.71500	11.18713
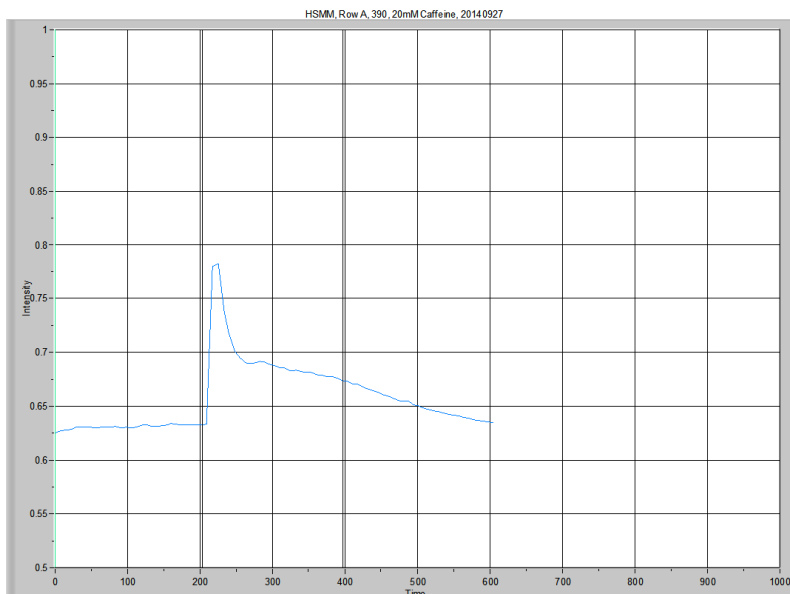
186

HSMM, Row A, 390, 20mM Caffeine, 20140927

	Average resting level	Peak	Δ Level	Time to Peak	Area Under the Curve Low X: 202.625 High X: 598.475	Peak Area
390, P7	0.630656	0.782134	0.151478	22.80899	266.22273	15.33531

HSMM, Row A, 390, 20mM Caffeine, 20140927

	Average resting level	Peak	Δ Level	Time to Peak	Area Under the Curve Low X: 202.625 High X: 598.475	Peak Area
390, P8	0.681262	0.764354	0.083092	8.051215	280.10416	10.15740
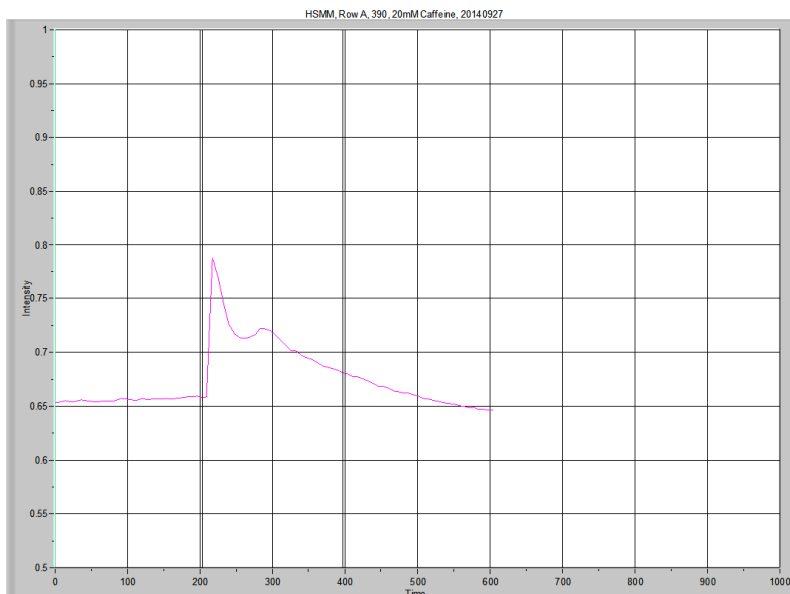
187

HSMM, Row A, 390, 20mM Caffeine, 20140927

	Average resting level	Peak	Δ Level	Time to Peak	Area Under the Curve Low X: 202.625 High X: 598.475	Peak Area
390, P9	0.655768	0.788037	0.132268	8.051215	271.21267	13.01252
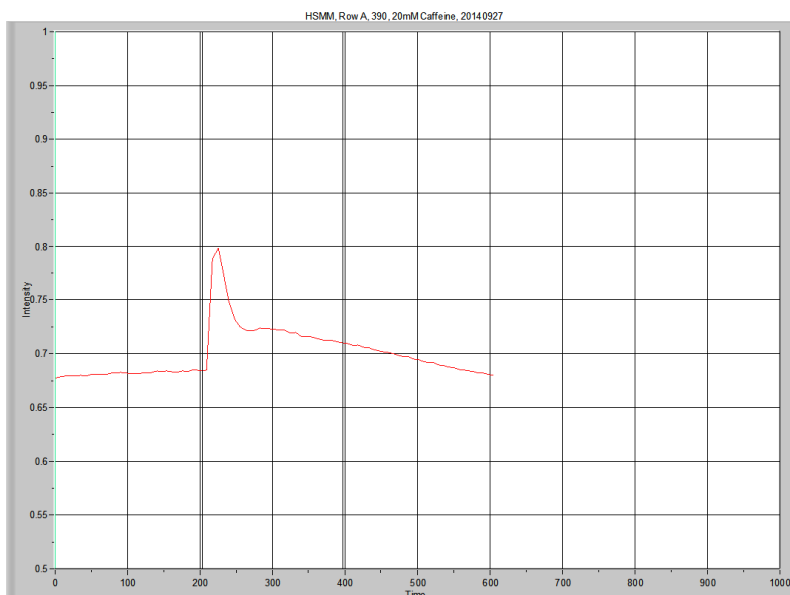
HSMM, Row A, 390, 20mM Caffeine, 20140927

	Average resting level	Peak	Δ Level	Time to Peak	Area Under the Curve Low X: 202.625 High X: 598.475	Peak Area
390, P10	0.681569	0.79803	0.116461	16.10245	281.26457	11.13052
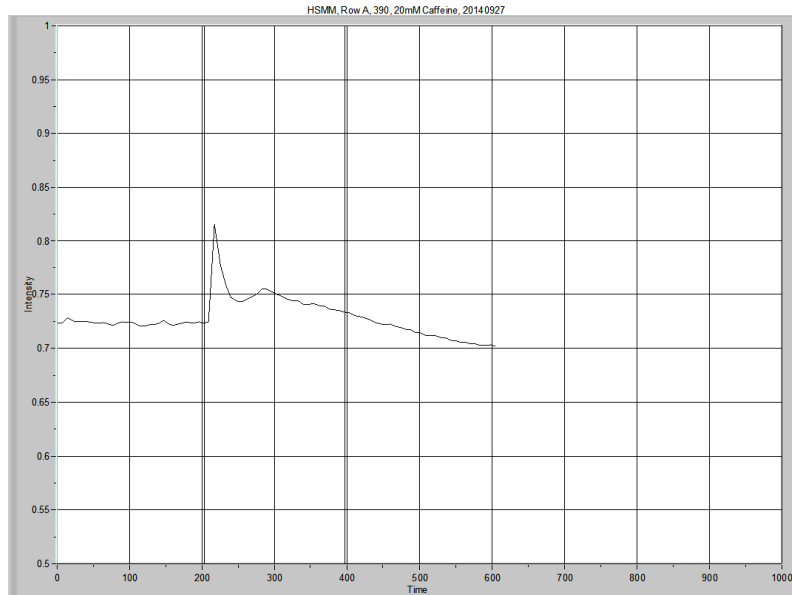
HSMM, Row A, 390, 20mM Caffeine, 20140927

	Average resting level	Peak	Δ Level	Time to Peak	Area Under the Curve Low X: 202.625 High X: 598.475	Peak Area
390, P11	0.72347	0.815189	0.091719	8.051215	289.65757	7.34744

HSMM, Row A, 390, 20mM Caffeine, 20140927
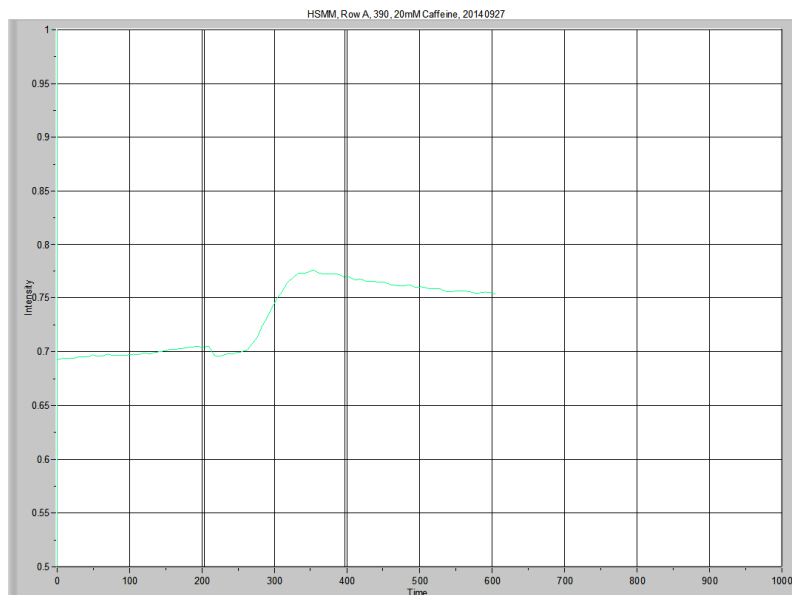
I plan to discard this data, as I believe the myotube floated away and/or moved with contraction.

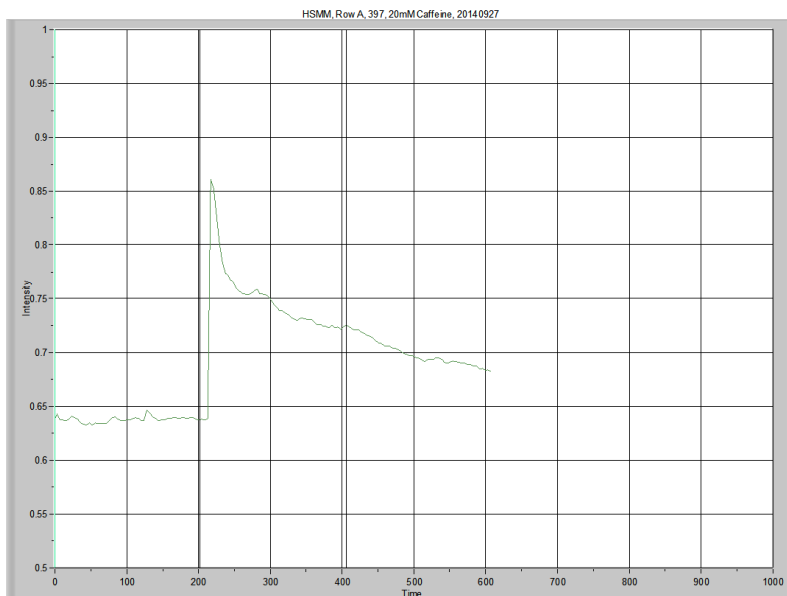|	Average resting level	Peak	Δ Level	Time to Peak	Area Under the Curve	Peak Area
390, P12	0.697541	0.775896	0.078355	120.7686		

Calcium Imaging, HSMM
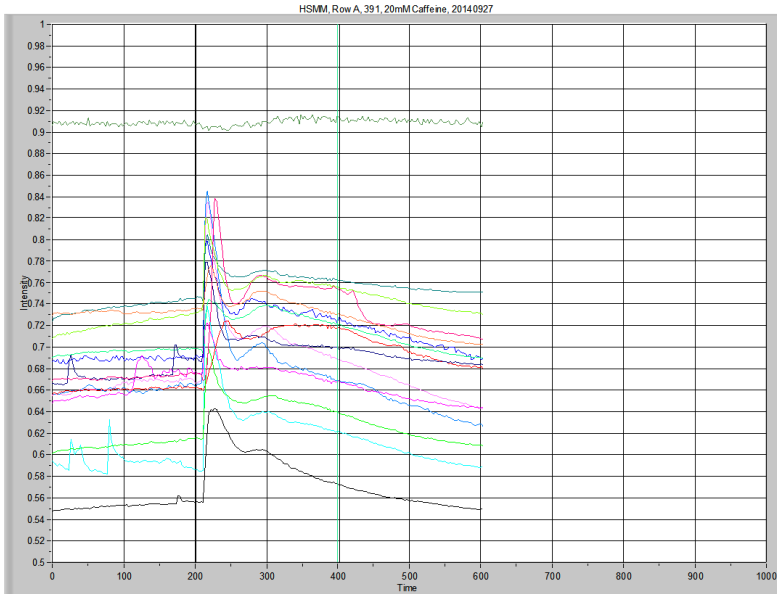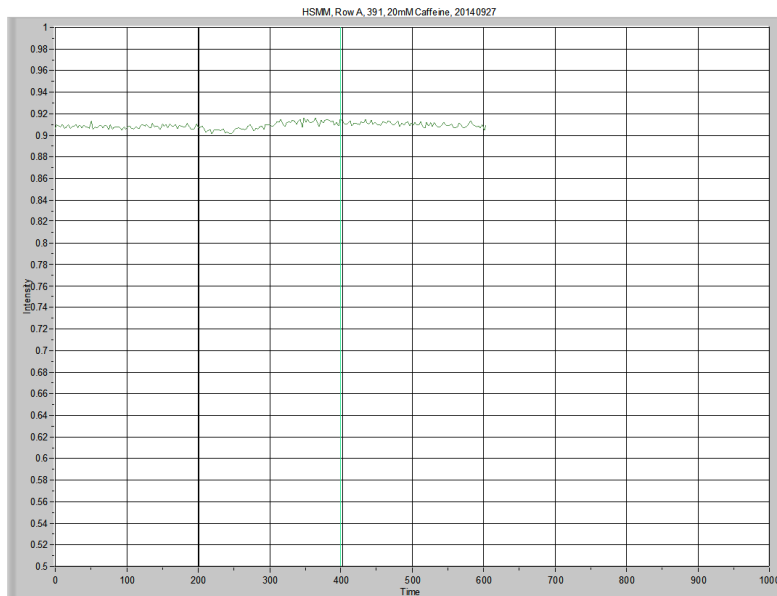
189

Overview

	Average resting level	Peak	Time to Peak	Area Under the Curve Low X: 201.28 High X: 598.475	Peak Area
391, BG	0.907616	0.915491037	NA	361.09957	0.60566
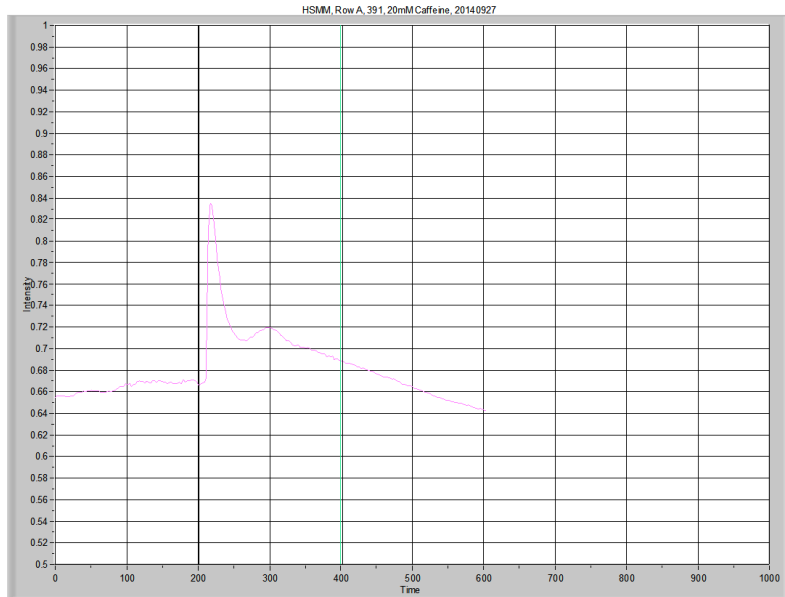
190

HSMM, Row A, 391, 20mM Caffeine, 20140927

	Average resting level	Peak	Δ Level	Time to Peak	Area Under the Curve Low X: 201.28 High X: 598.475	Peak Area
391, P1	0.663989	0.834853	0.170865	16.10237	274.02795	14.00249
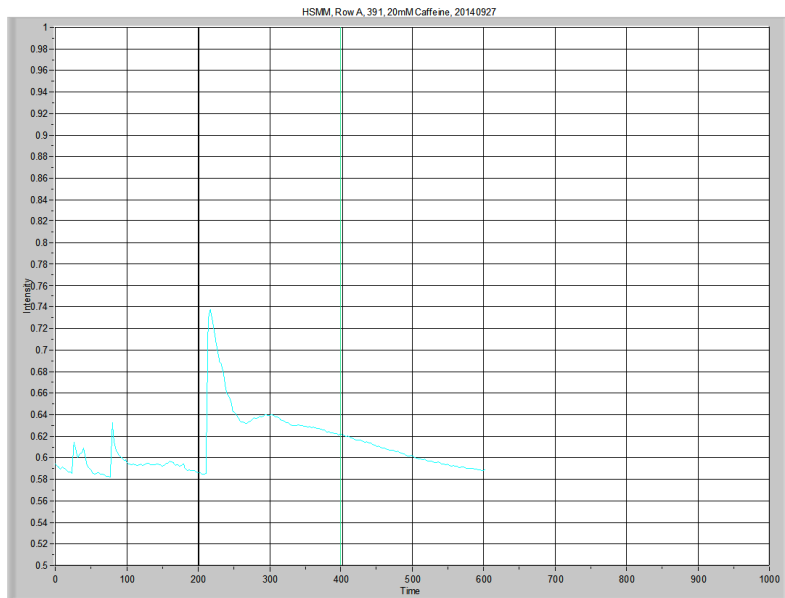
HSMM, Row A, 391, 20mM Caffeine, 20140927

	Average resting level	Peak	Δ Level	Time to Peak	Area Under the Curve Low X: 201.28 High X: 598.475	Peak Area
391, P2	0.593635	0.737571	0.143936	16.10237	246.70153	13.61755
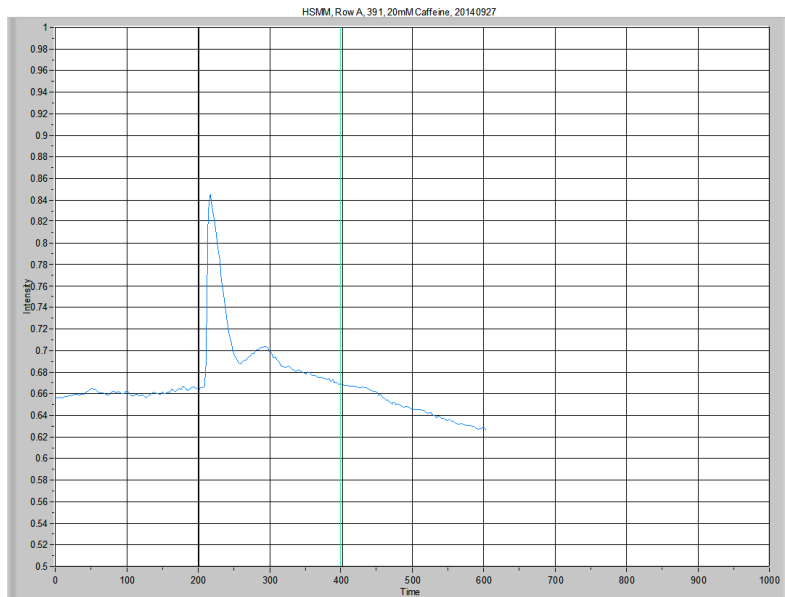
HSMM, Row A, 391, 20mM Caffeine, 20140927

	Average resting level	Peak	Δ Level	Time to Peak	Area Under the Curve Low X: 201.28 High X: 598.475	Peak Area
391, P3	0.660597	0.844989	0.184392	16.10237	267.88969	11.42192
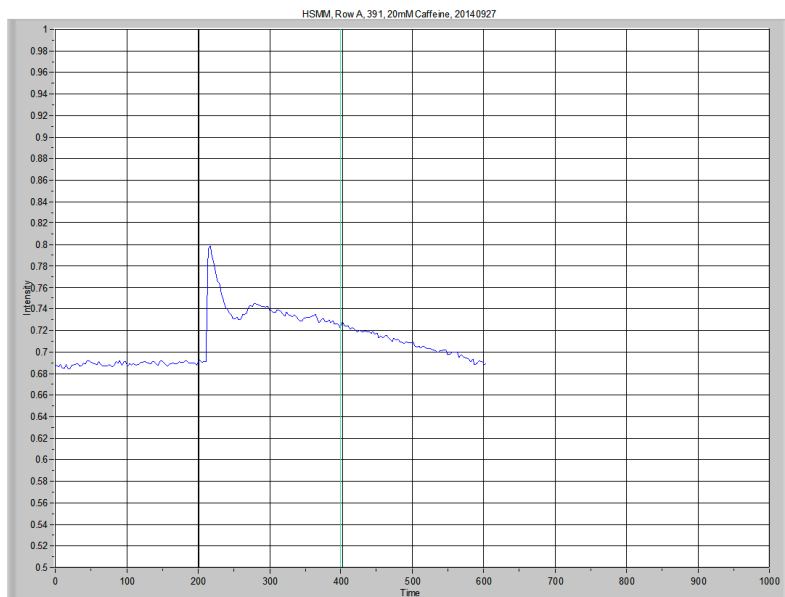
HSMM, Row A, 391, 20mM Caffeine, 20140927

	Average resting level	Peak	Δ Level	Time to Peak	Area Under the Curve Low X: 201.28 High X: 598.475	Peak Area
391, P4	0.688779	0.7983	0.109522	16.10237	286.82469	12.21385

192

HSMM, Row A, 391, 20mM Caffeine, 20140927
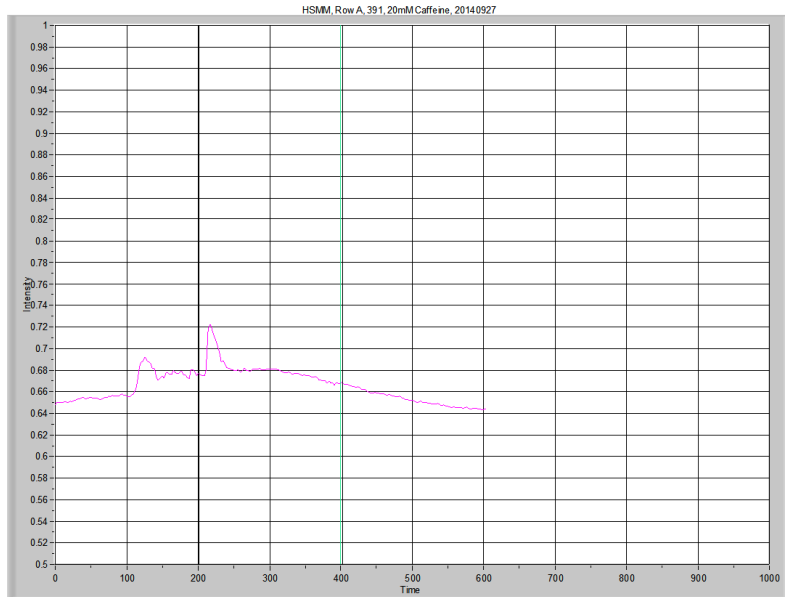
	Average resting level	Peak	Δ Level	Time to Peak	Area Under the Curve	Peak Area
					Low X: 201.28 High X: 598.475	
391, P5	0.664354	0.722538	0.058184	16.10237	264.83327	2.56588

HSMM, Row A, 391, 20mM Caffeine, 20140927

	Average resting level	Peak	Δ Level	Time to Peak	Area Under the Curve Low X: 201.28 High X: 598.475	Peak Area
391, P6	0.660386	0.724468	0.064082	Unable to assess	279.38954	12.62908
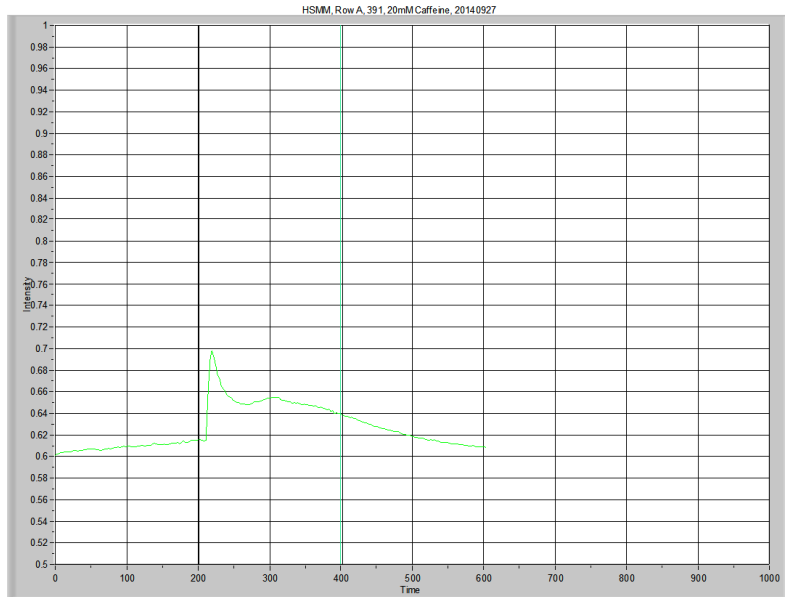
193

HSMM, Row A, 391, 20mM Caffeine, 20140927

	Average resting level	Peak	Δ Level	Time to Peak	Area Under the Curve Low X: 201.28 High X: 598.475	Peak Area
391, P7	0.608556	0.698025	0.089469	18.78611	252.42774	9.31762
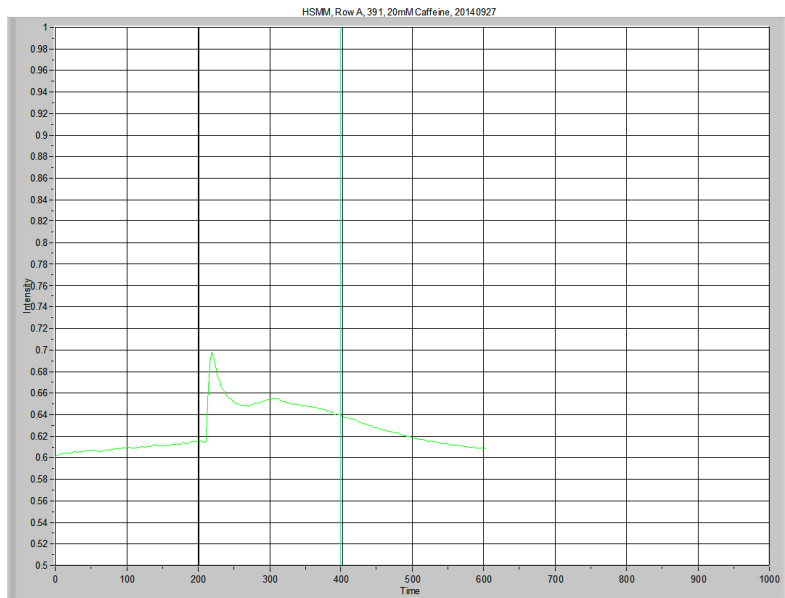
HSMM, Row A, 391, 20mM Caffeine, 20140927

	Average resting level	Peak	Δ Level	Time to Peak	Area Under the Curve Low X: 201.28 High X: 598.475	Peak Area
391, P8	0.552377	0.642797	0.09042	26.83737	229.39595	10.05722
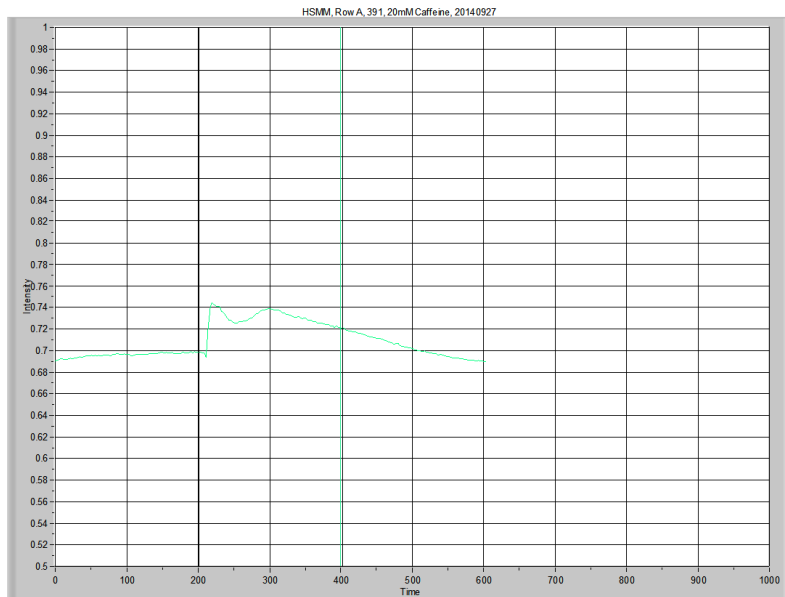
194

	Average resting level	Peak	Δ Level	Time to Peak	Area Under the Curve Low X: 201.28 High X: 598.475	Peak Area
391, P9	0.695681	0.744597	0.048917	18.78611	284.42673	8.64955
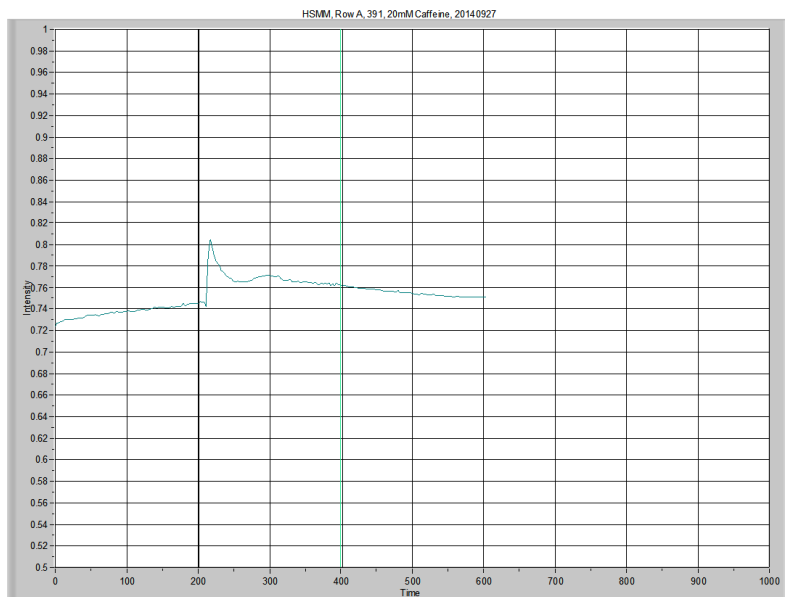
	Average resting level	Peak	Δ Level	Time to Peak	Area Under the Curve Low X: 201.28 High X: 598.475	Peak Area
391, P10	0.736837	0.804625	0.067788	16.10237	302.32587	5.30206
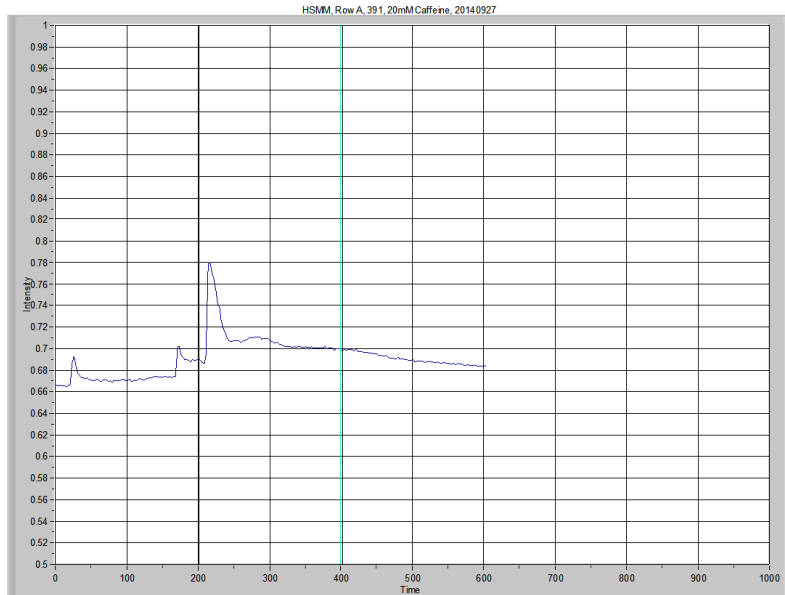
195

HSMM, Row A, 391, 20mM Caffeine, 20140927

	Average resting level	Peak	Δ Level	Time to Peak	Area Under the Curve Low X: 201.28 High X: 598.475	Peak Area
391, P11	0.674532	0.779226	0.104693	16.10237	277.93735	5.31181
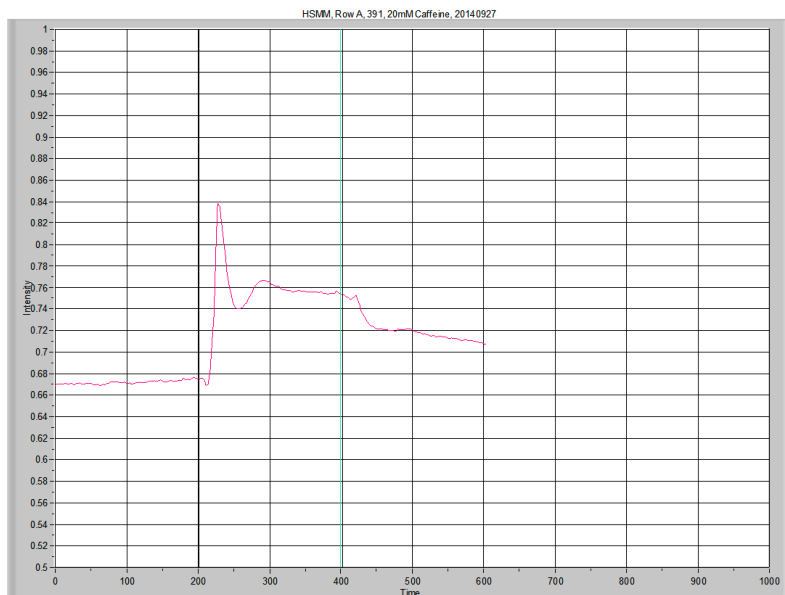
HSMM, Row A, 391, 20mM Caffeine, 20140927

	Average resting level	Peak	Δ Level	Time to Peak	Area Under the Curve Low X: 201.28 High X: 598.475	Peak Area
391, P12	0.671642	0.838306	0.166663	26.83737	292.86326	18.18648
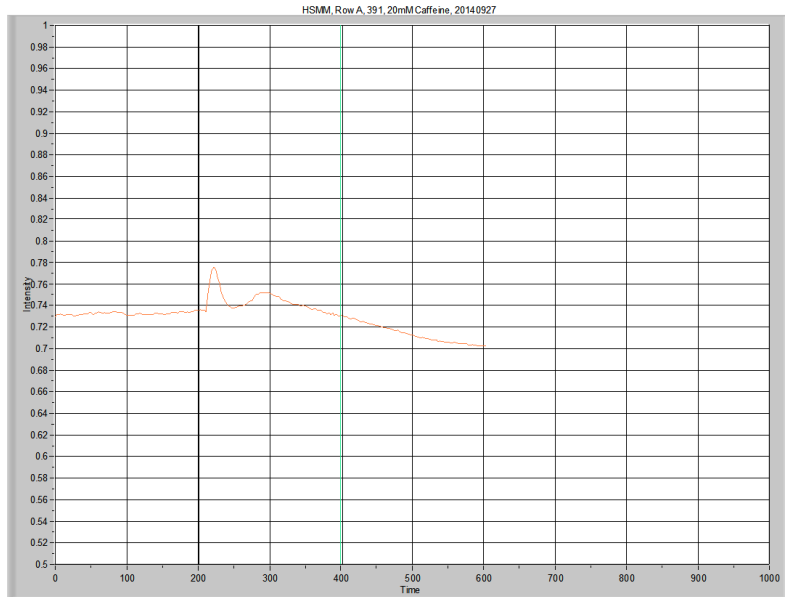
196

HSMM, Row A, 391, 20mM Caffeine, 20140927

	Average resting level	Peak	Δ Level	Time to Peak	Area Under the Curve Low X: 201.28 High X: 598.475	Peak Area
391, P13	0.732279	0.775309	0.04303	21.46989	289.42468	3.87444
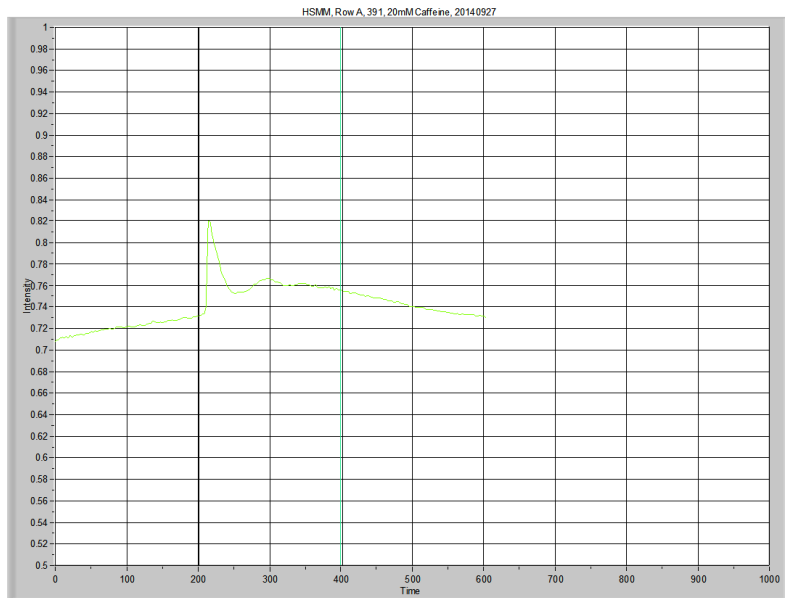
HSMM, Row A, 391, 20mM Caffeine, 20140927

	Average resting level	Peak	Δ Level	Time to Peak	Area Under the Curve Low X: 201.28 High X: 598.475	Peak Area
391, P14	0.720866	0.820043	0.099177	13.41865	298.65521	8.15479
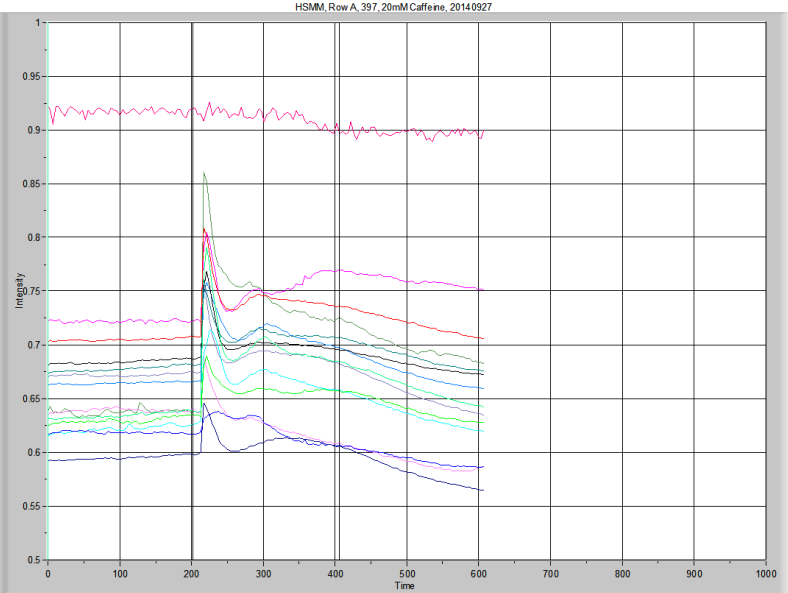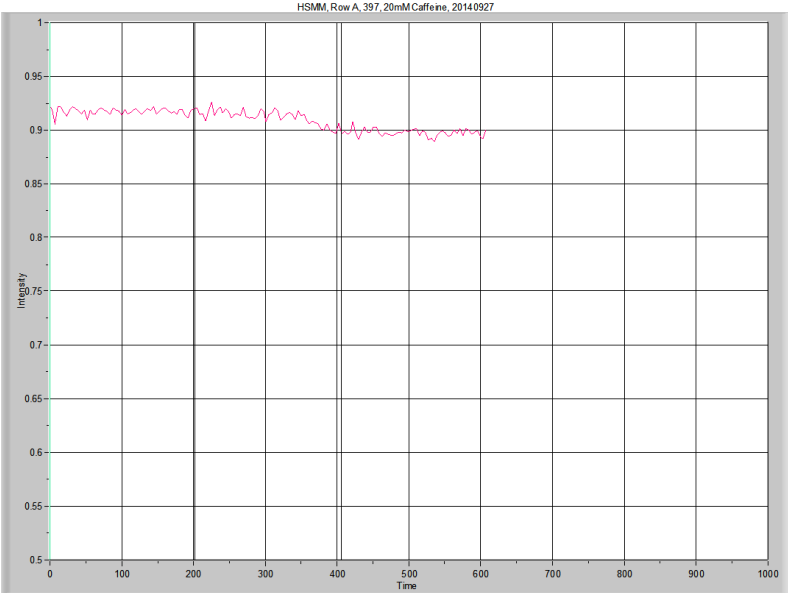
197

Overview

	Average resting level	Peak	Δ Level	Time to Peak	Area Under the Curve Low X: 201.279 High X: 599.813	Peak Area
397, BG	0.917101	0.926035	0.008934	NA	360.64185	-0.64068

HSMM, Row A, 397, 20mM Caffeine, 20140927

	Average resting level	Peak	Δ Level	Time to Peak	Area Under the Curve Low X: 201.279 High X: 599.813	Peak Area
397, P1	0.637608	0.861114	0.223506	8.051153	287.76858	24.70659
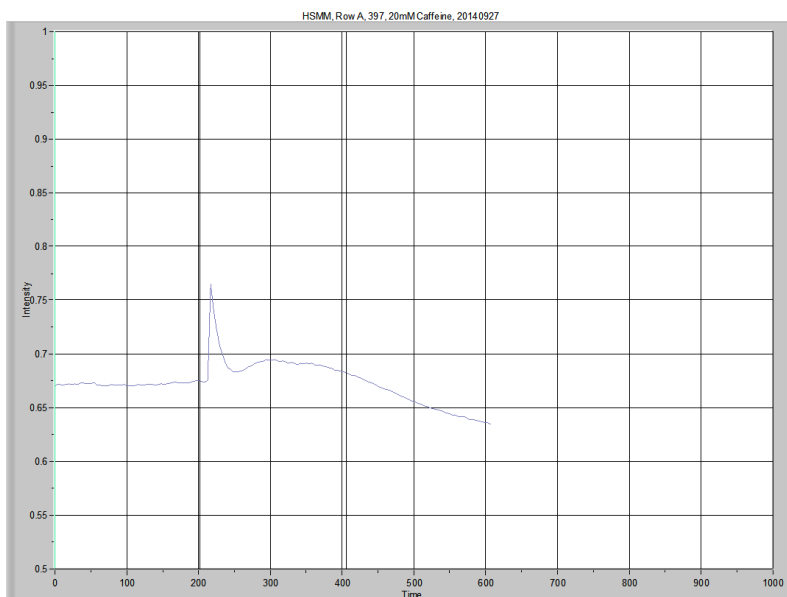
HSMM, Row A, 397, 20mM Caffeine, 20140927

	Average resting level	Peak	Δ Level	Time to Peak	Area Under the Curve Low X: 201.279 High X: 599.813	Peak Area
397, P2	0.671766	0.764842	0.093076	8.051153	268.95770	7.83936
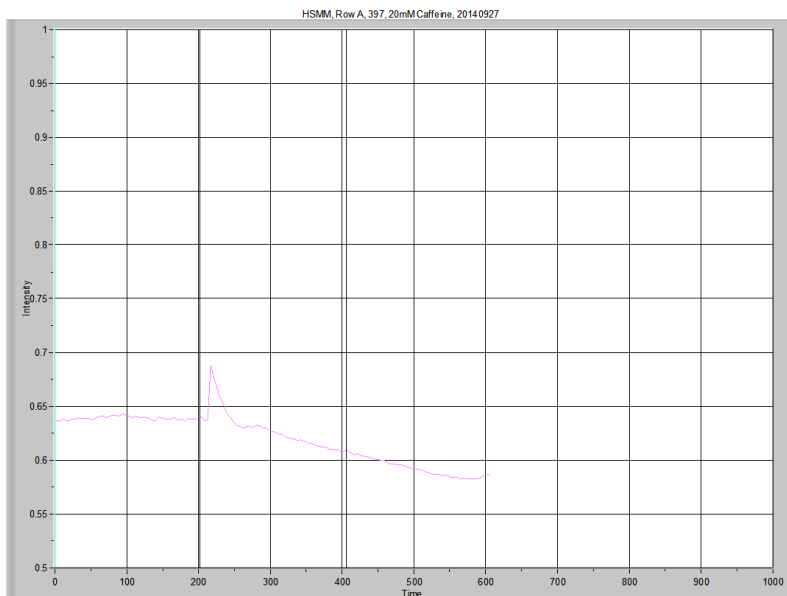
199

HSMM, Row A, 397, 20mM Caffeine, 20140927

	Average resting level	Peak	Δ Level	Time to Peak	Area Under the Curve Low X: 201.279 High X: 599.813	Peak Area
397, P3	0.638692	0.688595	0.049903	8.051153	243.50800	-0.82070
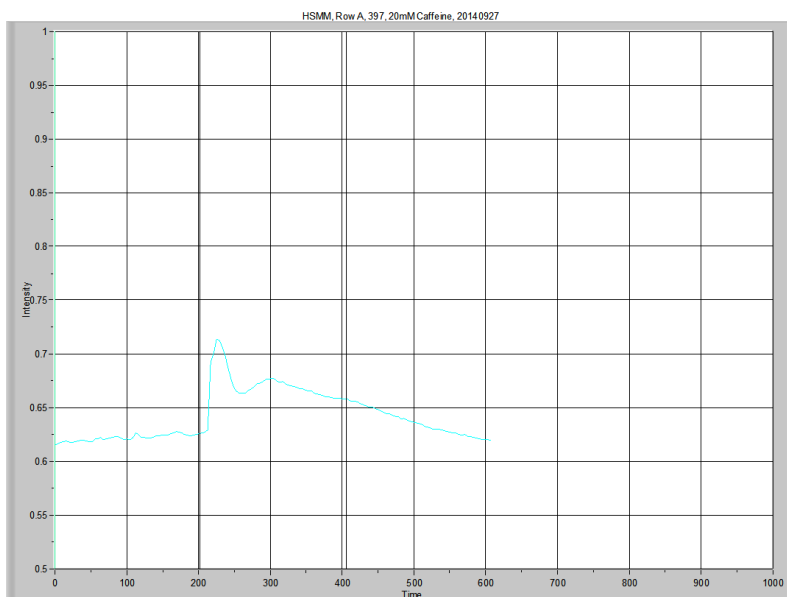
HSMM, Row A, 397, 20mM Caffeine, 20140927

	Average resting level	Peak	Δ Level	Time to Peak	Area Under the Curve Low X: 201.279 High X: 599.813	Peak Area
397, P4	0.621852	0.713885	0.092033	24.15355	260.45776	12.233572
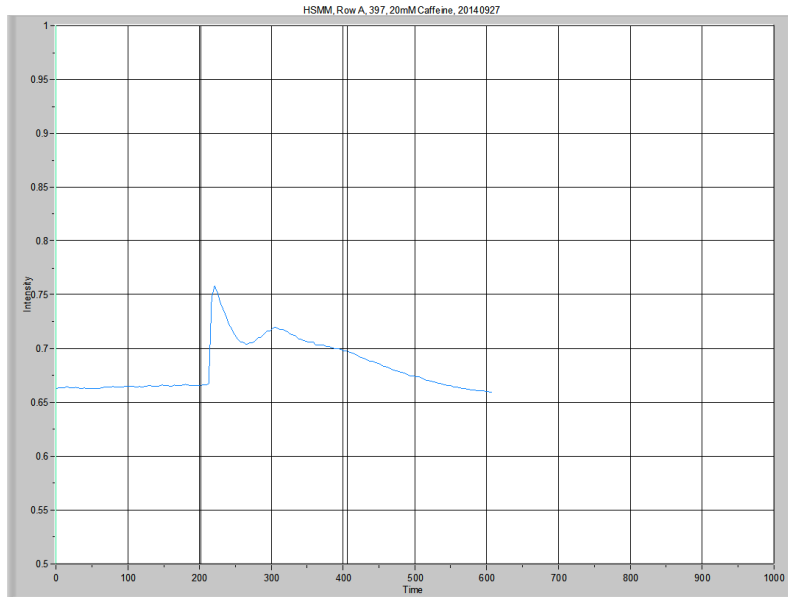
200

HSMM, Row A, 397, 20mM Caffeine, 20140927

	Average resting level	Peak	Δ Level	Time to Peak	Area Under the Curve Low X: 201.279 High X: 599.813	Peak Area
397, P5	0.664295	0.758091	0.093797	20.12795	276.16072	12.12479

HSMM, Row A, 397, 20mM Caffeine, 20140927
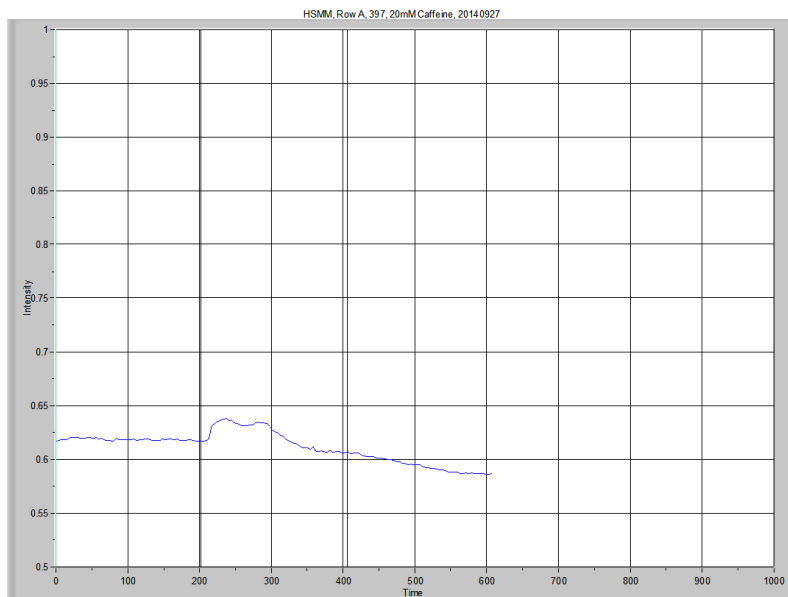
I do not plan to use this tracing, as it did not behave as the others. Perhaps my ROI was off a bit?

	Average resting level	Peak	Δ Level	Time to Peak	Area Under the Curve Low X: 201.279 High X: 599.813	Peak Area
397, P7	*0.618222*	*0.637635*	*0.019413*	28.17909	242.51549	2.89787
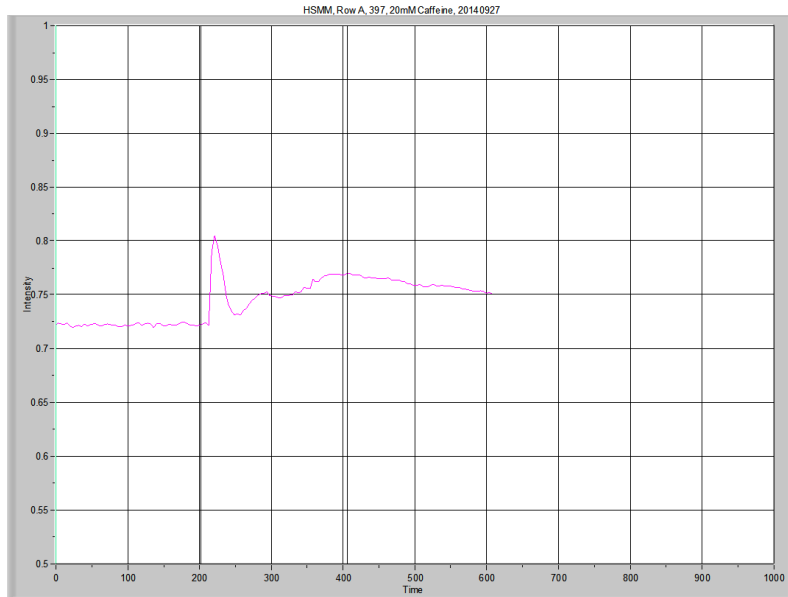
201

HSMM, Row A, 397, 20mM Caffeine, 20140927

	Average resting level	Peak	Δ Level	Time to Peak	Area Under the Curve Low X: 201.279 High X: 599.813	Peak Area
397, P8	0.72183	0.804515	0.082685	8.051121	301.63892	8.17591
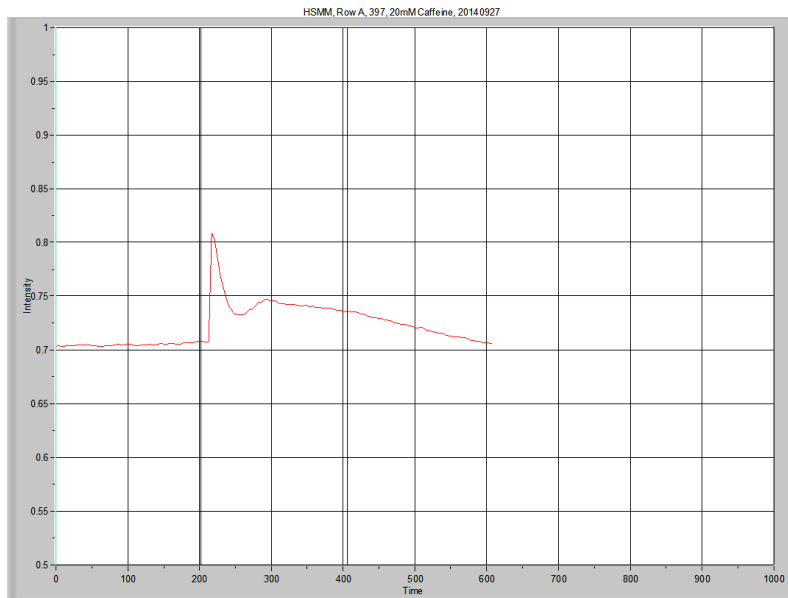
HSMM, Row A, 397, 20mM Caffeine, 20140927

	Average resting level	Peak	Δ Level	Time to Peak	Area Under the Curve Low X: 201.279 High X: 599.813	Peak Area
397, P9	0.704704	0.808753	0.104049	4.025537	291.65523	9.88994
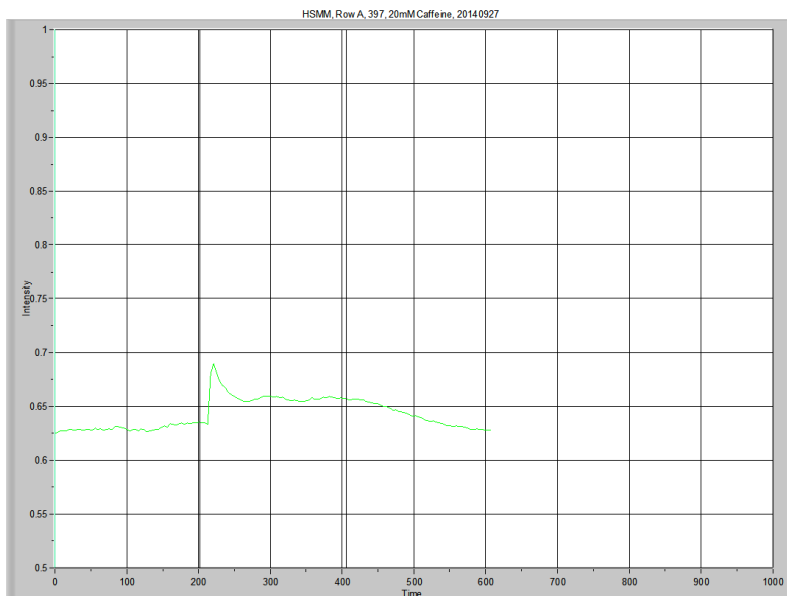
HSMM, Row A, 397, 20mM Caffeine, 20140927

	Average resting level	Peak	Δ Level	Time to Peak	Area Under the Curve Low X: 201.279 High X: 599.813	Peak Area
397, P10	0.629636	0.689708	0.060072	4.025584	259.01102	7.40709
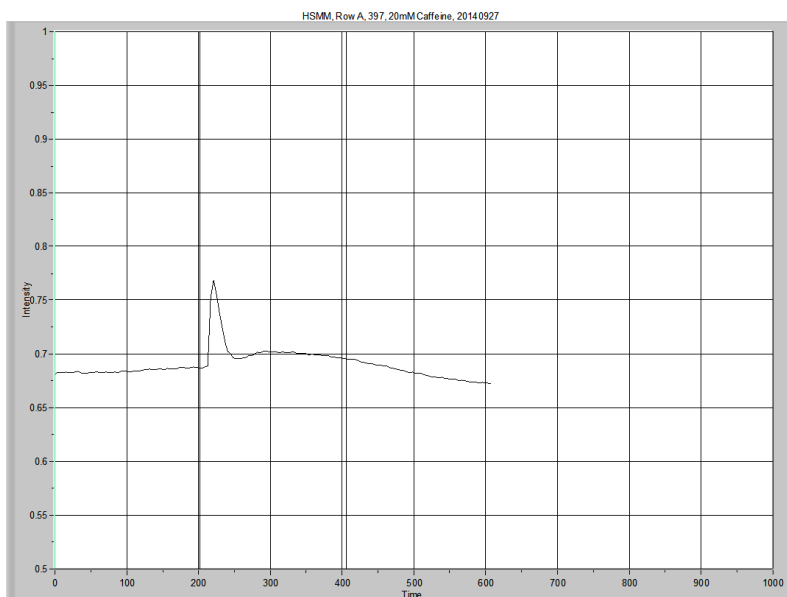
HSMM, Row A, 397, 20mM Caffeine, 20140927

	Average resting level	Peak	Δ Level	Time to Peak	Area Under the Curve Low X: 201.279 High X: 599.813	Peak Area
397, P11	0.684153	0.768352	0.084199	12.07674	276.32190	5.37847
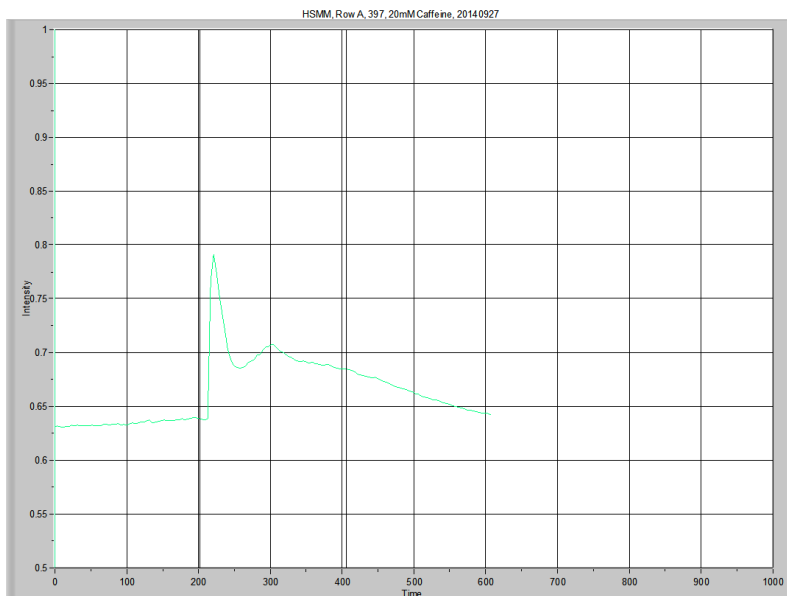
203

HSMM, Row A, 397, 20mM Caffeine, 20140927

	Average resting level	Peak	Δ Level	Time to Peak	Area Under the Curve Low X: 201.279 High X: 599.813	Peak Area
397, P12	0.634308	0.790793	0.156485	8.051121	271.06944	15.59008
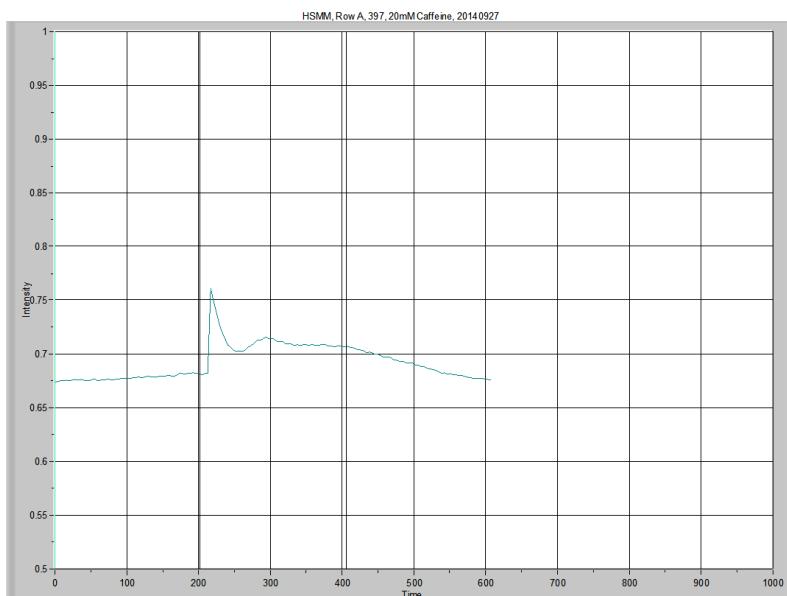
HSMM, Row A, 397, 20mM Caffeine, 20140927

	Average resting level	Peak	Δ Level	Time to Peak	Area Under the Curve Low X: 201.279 High X: 599.813	Peak Area
397, P13	0.677587	0.76088	0.083293	4.025537	279.03675	8.57676
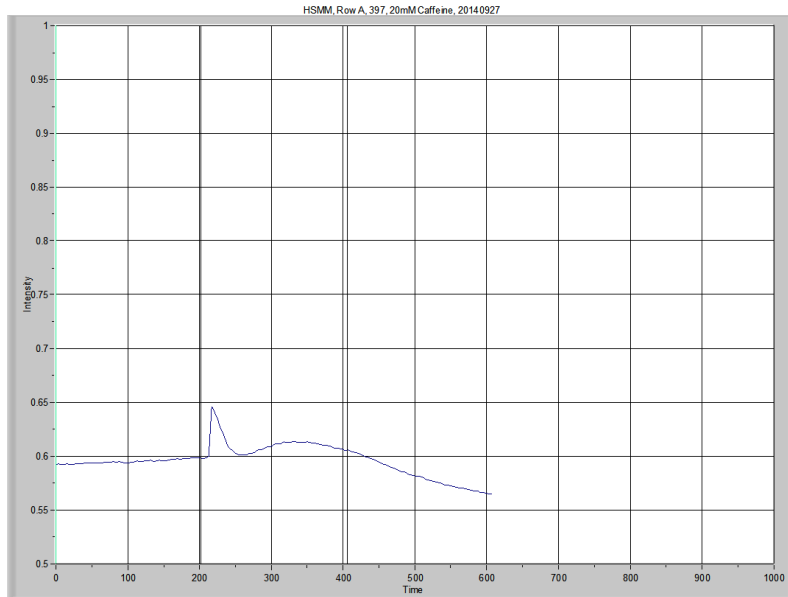
204

HSMM, Row A, 397, 20mM Caffeine, 20140927

	Average resting level	Peak	Δ Level	Time to Peak	Area Under the Curve Low X: 201.279 High X: 599.813	Peak Area
397, P14	0.5948	0.645781	0.050981	8.051153	237.90593	6.12087
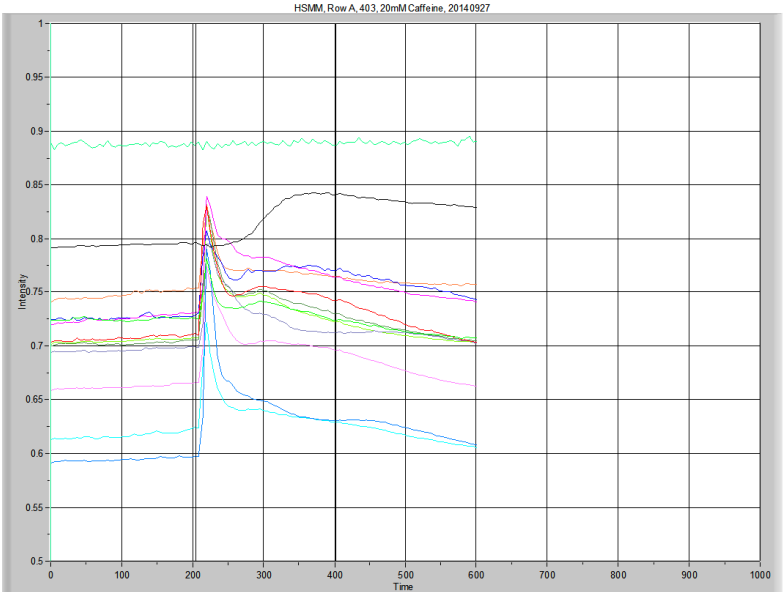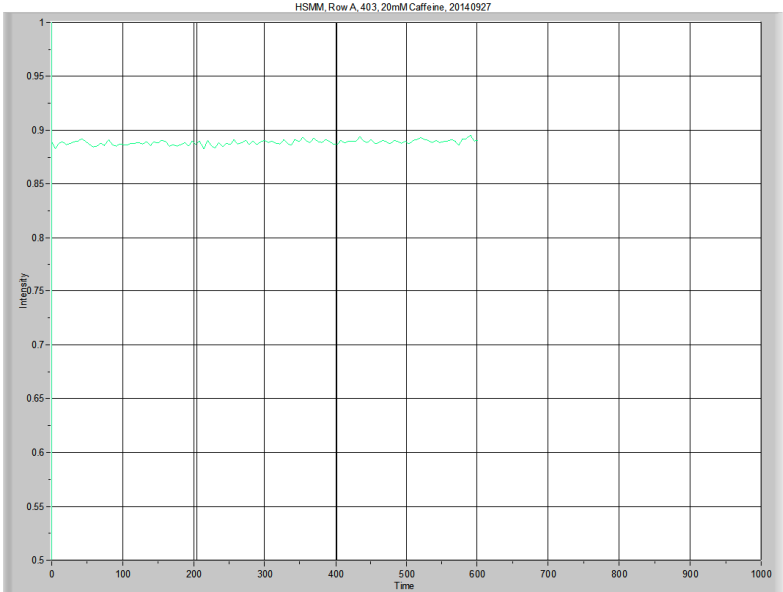
205

Overview

	Average resting level	Peak	Δ Level	Time to Peak	Area Under the Curve Low X: 203.963 High X: 601.155	Peak Area
403, BG	0.887064	0.895164	0.0081	NA	353.02003	0.36768
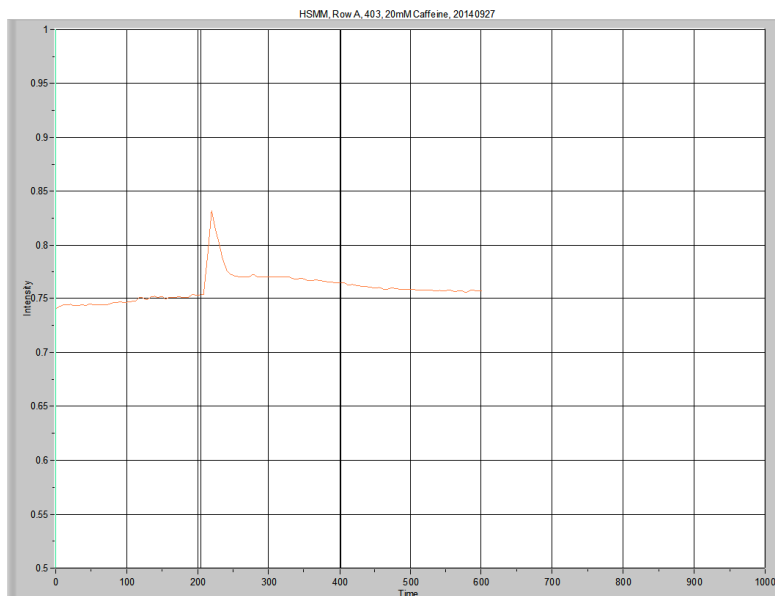
HSMM, Row A, 403, 20mM Caffeine, 20140927

	Average resting level	Peak	Δ Level	Time to Peak	Area Under the Curve Low X: 203.963 High X: 601.155	Peak Area
403, P1	0.746927	0.831495	0.084568	16.1023	304.22930	4.38179
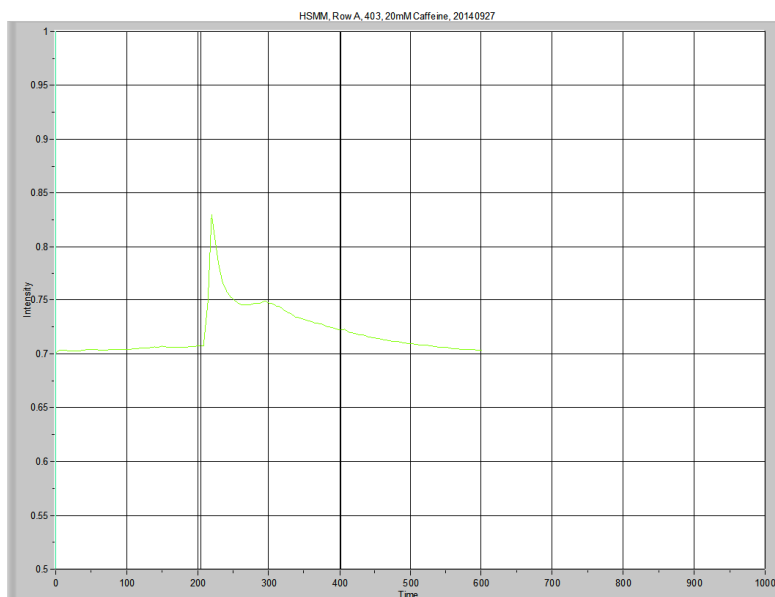
HSMM, Row A, 403, 20mM Caffeine, 20140927

	Average resting level	Peak	Δ Level	Time to Peak	Area Under the Curve Low X: 203.963 High X: 601.155	Peak Area
403, P2	0.704225	0.829883	0.125658	16.1023	288.77451	8.74654
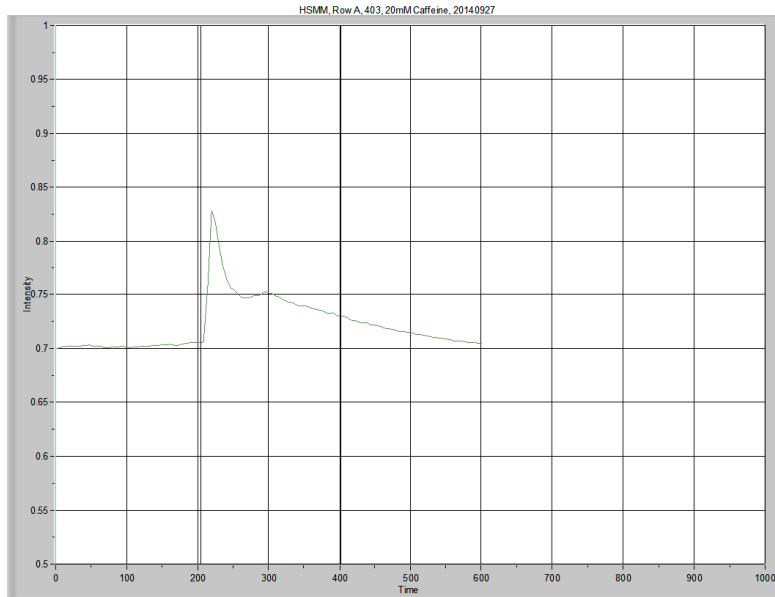
207

HSMM, Row A, 403, 20mM Caffeine, 20140927

	Average resting level	Peak	Δ Level	Time to Peak	Area Under the Curve Low X: 203.963 High X: 601.155	Peak Area
403, P3	0.701905	0.828117	0.126212	16.1023	290.76347	10.86140
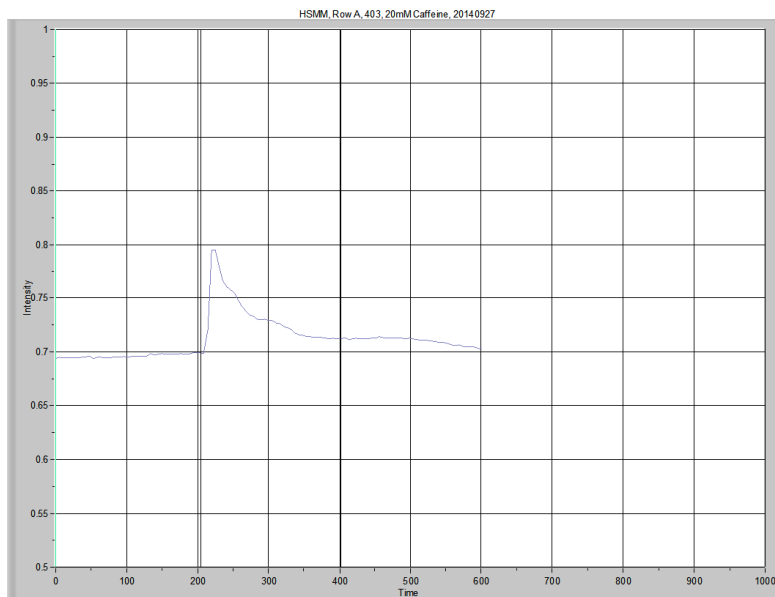
HSMM, Row A, 403, 20mM Caffeine, 20140927

	Average resting level	Peak	Δ Level	Time to Peak	Area Under the Curve Low X: 203.963 High X: 601.155	Peak Area
403, P4	0.695638	0.79502	0.099382	10.73492	286.20551	7.94899
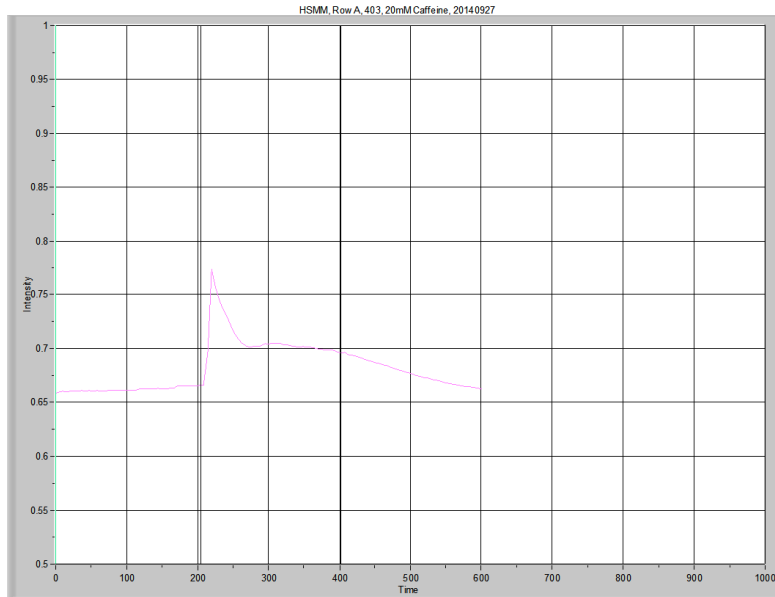
208

HSMM, Row A, 403, 20mM Caffeine, 20140927

	Average resting level	Peak	Δ Level	Time to Peak	Area Under the Curve Low X: 203.963 High X: 601.155	Peak Area
403, P5	0.661406	0.774056	0.11265	5.367463	274.99995	11.28649
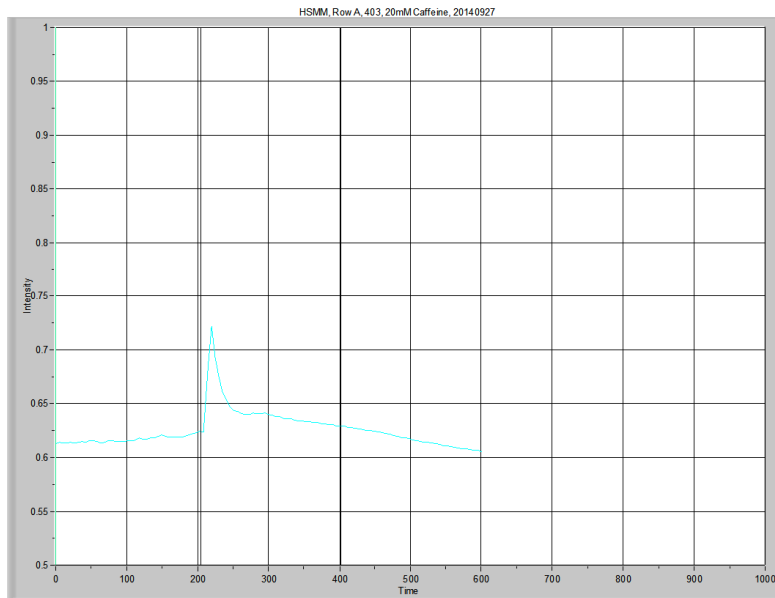
HSMM, Row A, 403, 20mM Caffeine, 20140927

	Average resting level	Peak	Δ Level	Time to Peak	Area Under the Curve Low X: 203.963 High X: 601.155	Peak Area
403, P6	0.615961	0.72211	0.10615	16.1023	250.22343	6.07411
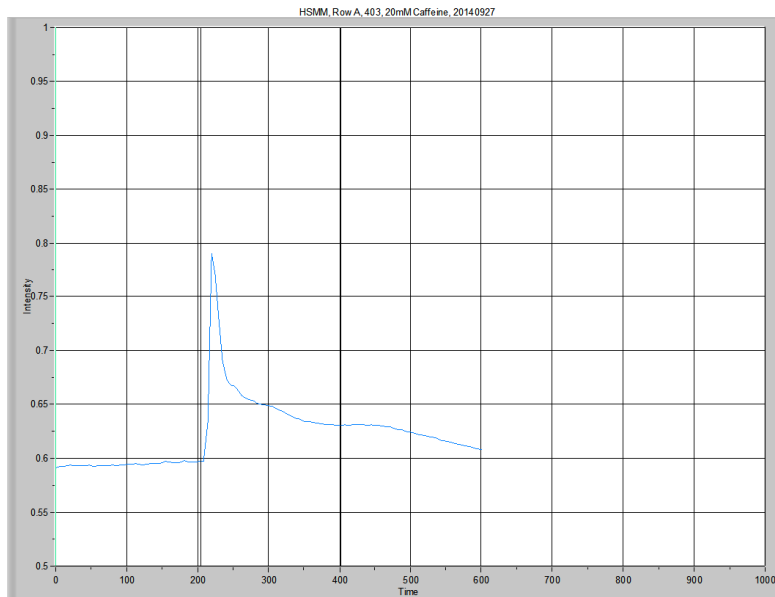
HSMM, Row A, 403, 20mM Caffeine, 20140927

	Average resting level	Peak	Δ Level	Time to Peak	Area Under the Curve Low X: 203.963 High X: 601.155	Peak Area
403, P7	0.593949	0.789955	0.196006	16.1023	253.22180	13.99581
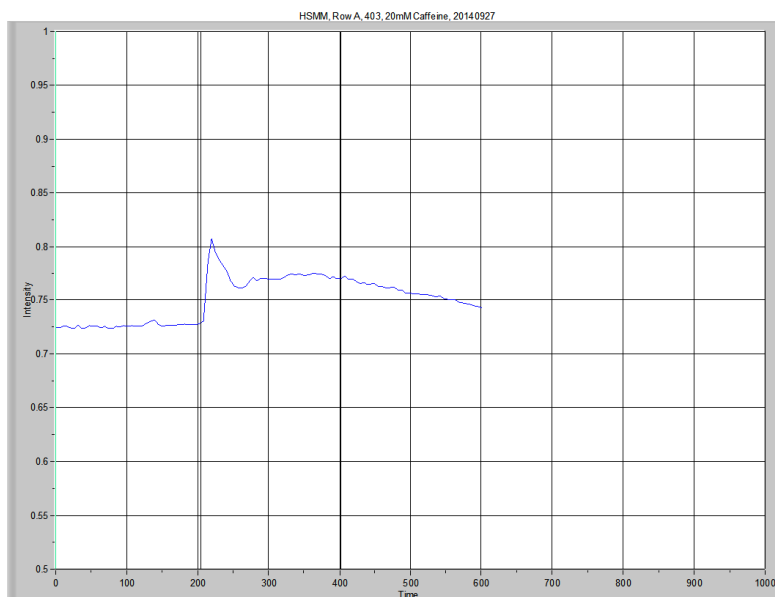
HSMM, Row A, 403, 20mM Caffeine, 20140927

	Average resting level	Peak	Δ Level	Time to Peak	Area Under the Curve Low X: 203.963 High X: 601.155	Peak Area
403, P8	0.725843	0.806851	0.081007	16.1023	303.59170	11.45349
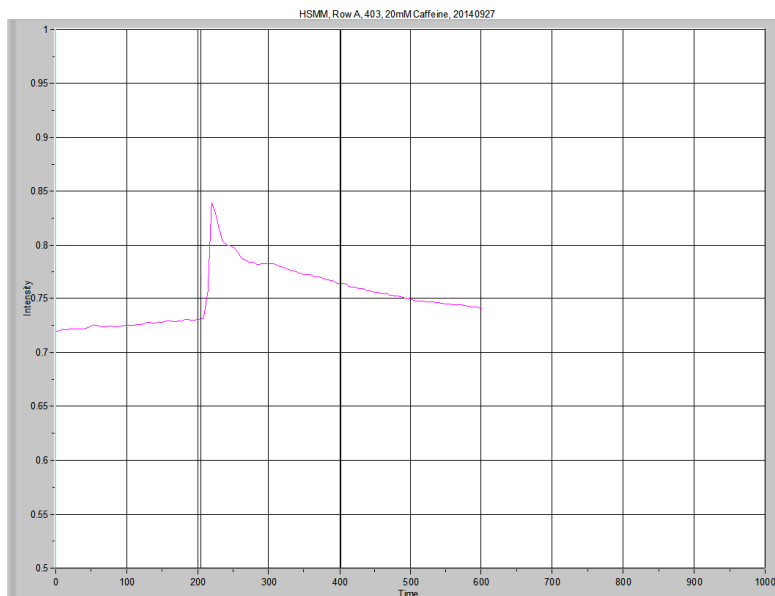
HSMM, Row A, 403, 20mM Caffeine, 20140927

	Average resting level	Peak	Δ Level	Time to Peak	Area Under the Curve Low X: 203.963 High X: 601.155	Peak Area
403, P9	0.724888	0.839221	0.114333	16.1023	304.11123	11.87683
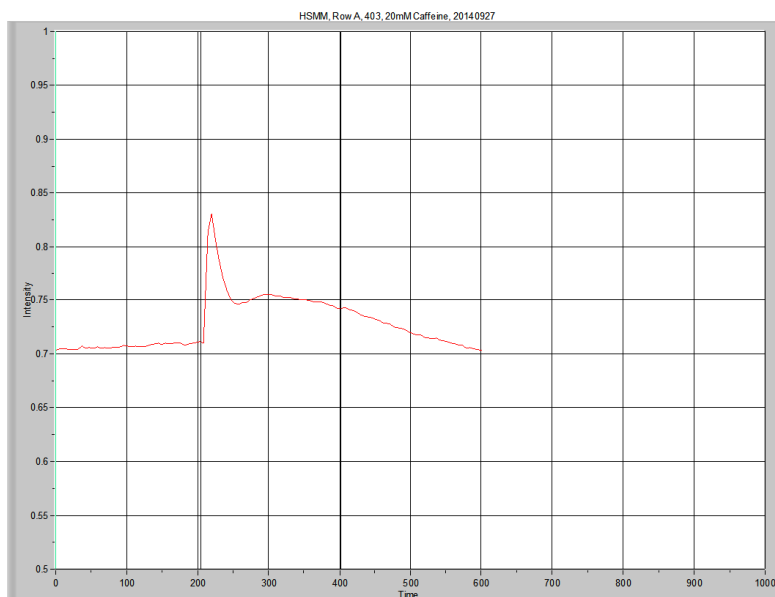
HSMM, Row A, 403, 20mM Caffeine, 20140927

	Average resting level	Peak	Δ Level	Time to Peak	Area Under the Curve Low X: 203.963 High X: 601.155	Peak Area
403, P10	0.706653	0.830469	0.123816	16.1023	293.27794	12.44882
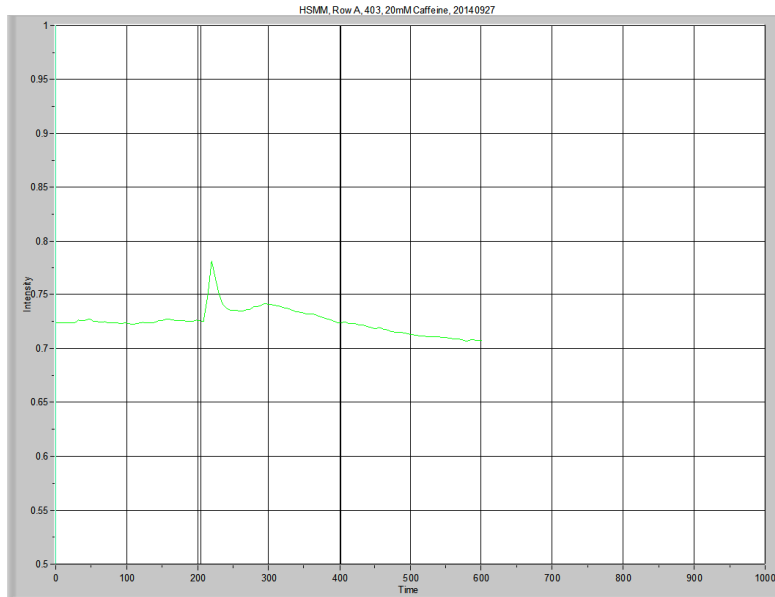
211

HSMM, Row A, 403, 20mM Caffeine, 20140927

	Average resting level	Peak	Δ Level	Time to Peak	Area Under the Curve	Peak Area
					Low X: 203.963 High X: 601.155	
403, P11	0.724526	0.781531	0.057005	5.367463	288.19091	3.69274

HSMM, Row A, 403, 20mM Caffeine, 20140927
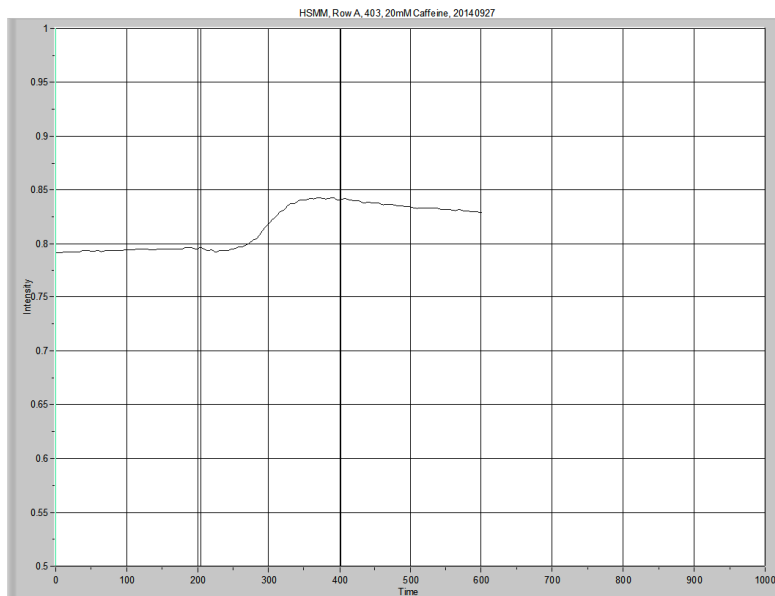
I will not use this tracing, as the myotube moved from the ROI with contraction.

	Average resting level	Peak	Δ Level	Time to Peak	Area Under the Curve	Peak Area
					Low X: 203.963 High X: 601.155	
403, P12	0.792582	0.84273	0.050148		328.17647	5.50077
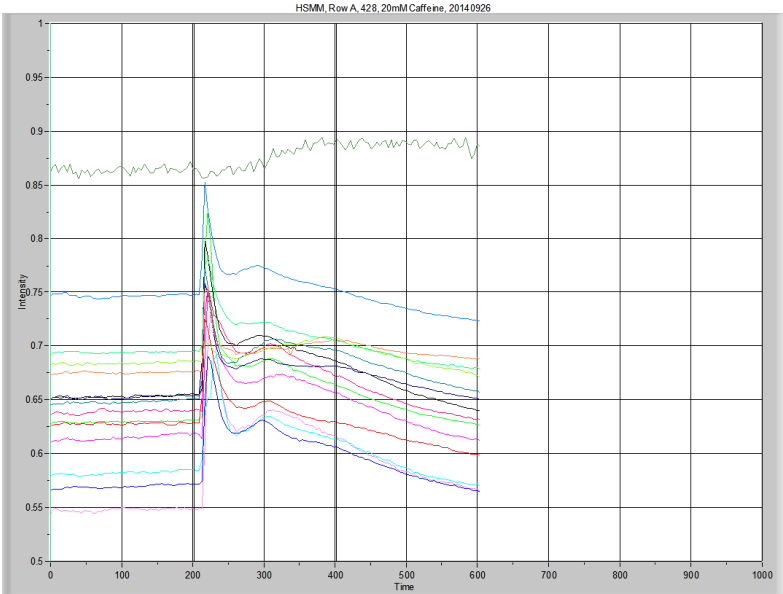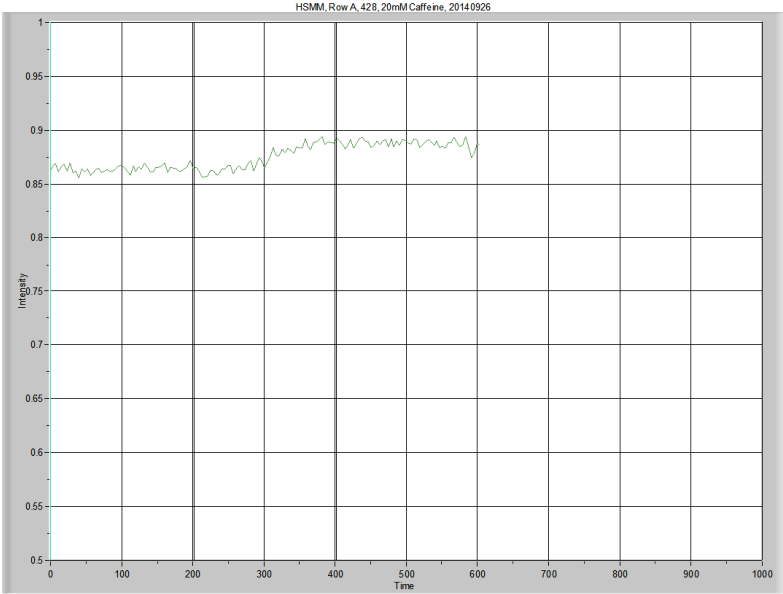
212

Overview

	Average resting level	Peak	Δ Level	Time to Peak	Area Under the Curve Low X: 201.279 High X: 599.813	Peak Area
428, BG	0.863276	0.893298	0.030022	NA	350.75964	1.78144
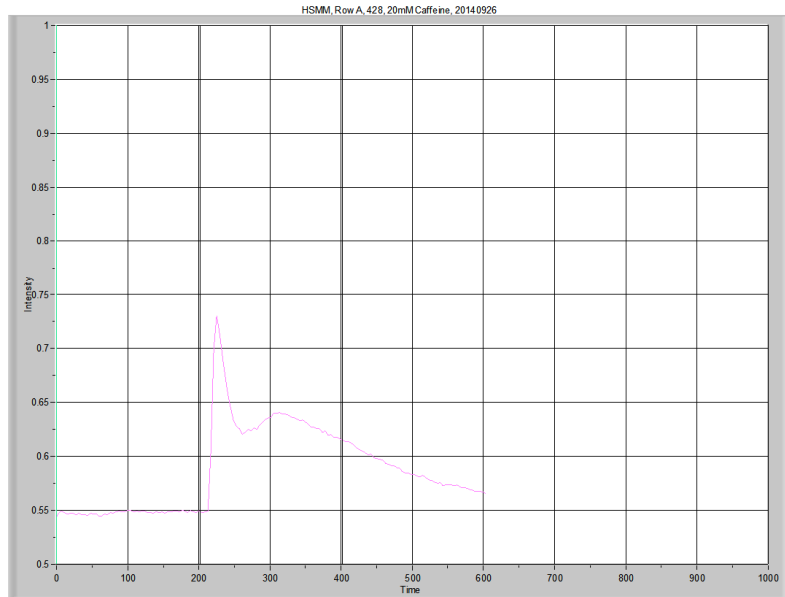
HSMM, Row A, 428, 20mM Caffeine, 2014 0926

	Average resting level	Peak	Δ Level	Time to Peak	Area Under the Curve Low X: 201.279 High X: 599.813	Peak Area
428, P1	0.547533	0.730508	0.182975	16.10236	242.61531	20.22137
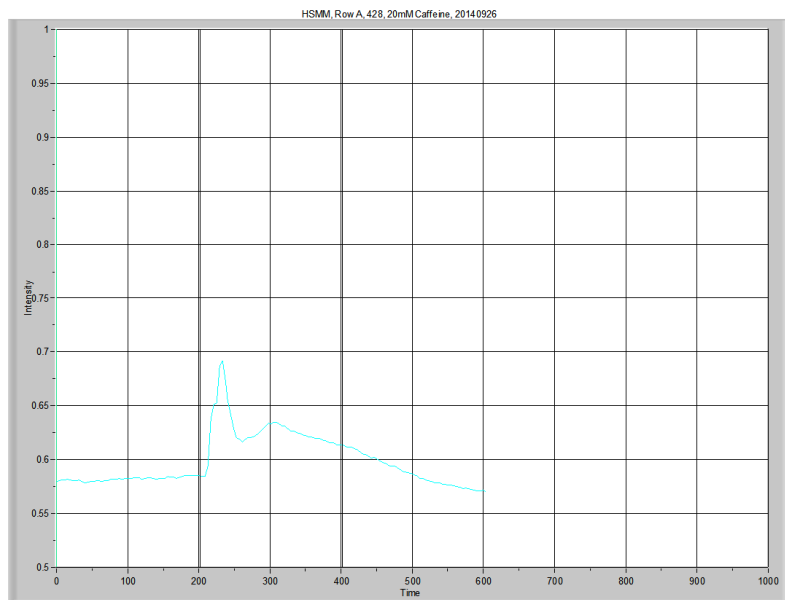
HSMM, Row A, 428, 20mM Caffeine, 2014 0926

	Average resting level	Peak	Δ Level	Time to Peak	Area Under the Curve Low X: 201.279 High X: 599.813	Peak Area
428, P2	0.581416	0.691618	0.110202	16.10237	242.21715	11.85322
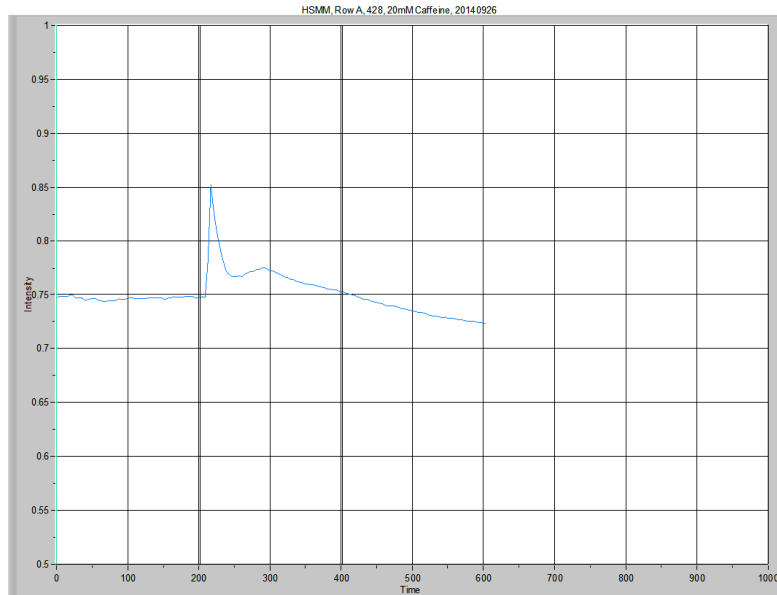
214

HSMM, Row A, 428, 20mM Caffeine, 2014 0926

	Average resting level	Peak	Δ Level	Time to Peak	Area Under the Curve Low X: 201.279 High X: 599.813	Peak Area
428, P3	0.746218	0.851979	0.105761	4.025575	299.90895	6.82660
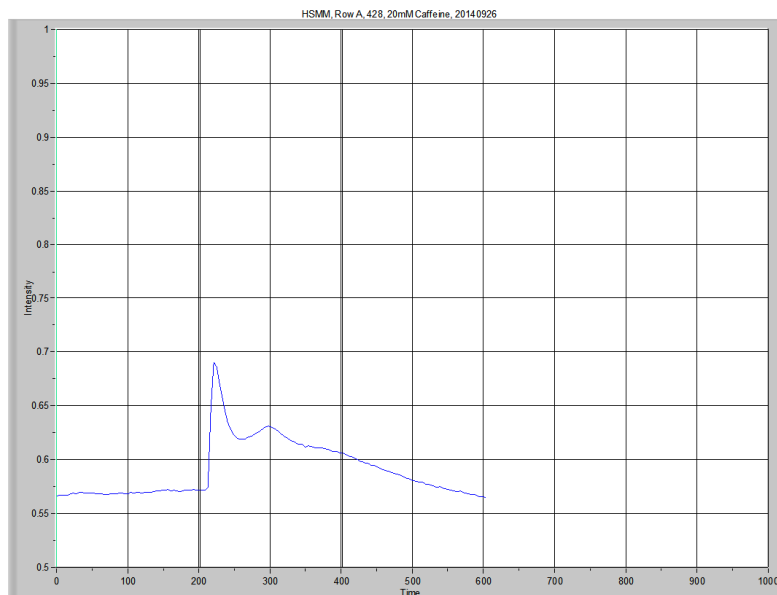
HSMM, Row A, 428, 20mM Caffeine, 2014 0926

	Average resting level	Peak	Δ Level	Time to Peak	Area Under the Curve Low X: 201.279 High X: 599.813	Peak Area
428, P4	0.568868	0.690528	0.12166	8.05119	239.94082	13.41411
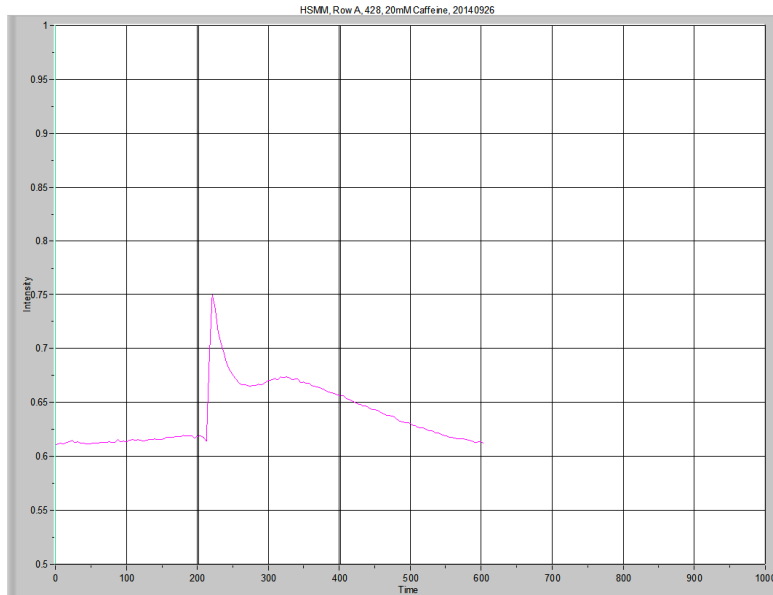
HSMM, Row A, 428, 20mM Caffeine, 20140926

	Average resting level	Peak	Δ Level	Time to Peak	Area Under the Curve Low X: 201.279 High X: 599.813	Peak Area
425, P5	0.614012	0.750171	0.136158	4.025615	259.43741	13.99989
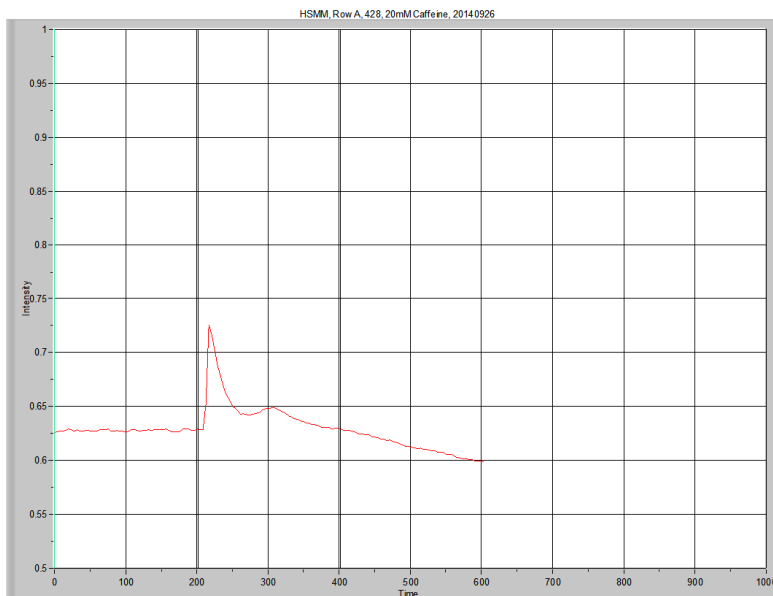
HSMM, Row A, 428, 20mM Caffeine, 20140926

	Average resting level	Peak	Δ Level	Time to Peak	Area Under the Curve Low X: 201.279 High X: 599.813	Peak Area
428, P6	0.627396	0.725547	0.098151	4.025575	251.24470	6.49882
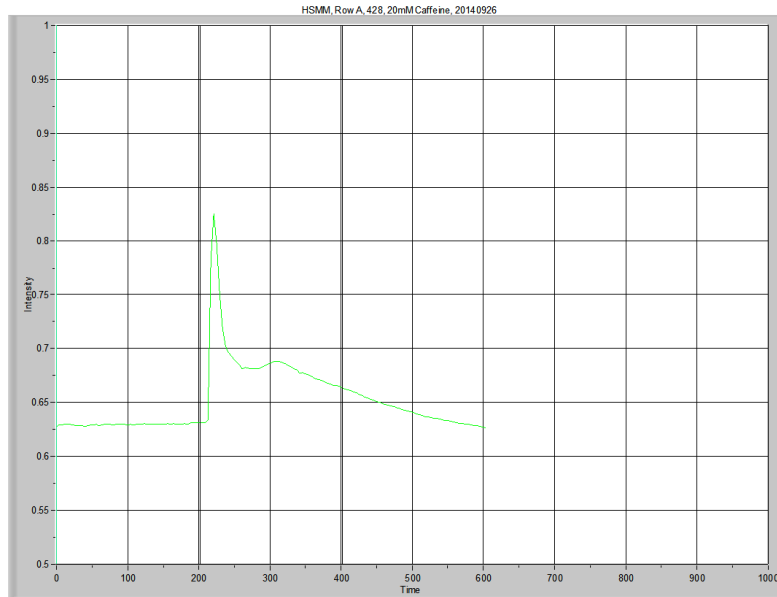
216

HSMM, Row A, 428, 20mM Caffeine, 2014 0926

	Average resting level	Peak	Δ Level	Time to Peak	Area Under the Curve Low X: 201.279 High X: 599.813	Peak Area
428, P7	0.629234	0.825151	0.195916	12.07679	264.84018	14.23565
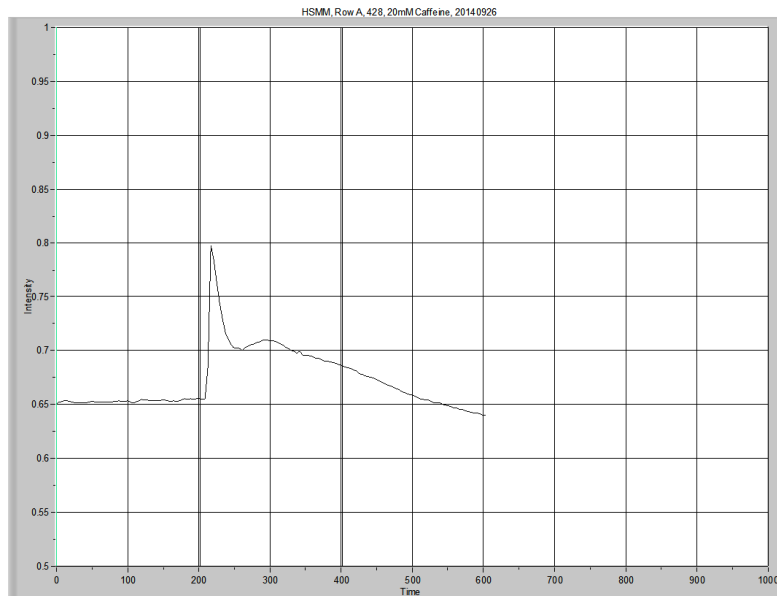
HSMM, Row A, 428, 20mM Caffeine, 2014 0926

	Average resting level	Peak	Δ Level	Time to Peak	Area Under the Curve Low X: 201.279 High X: 599.813	Peak Area
428, P8	0.652614	0.797607	0.144992	8.051176	272.01551	13.98259
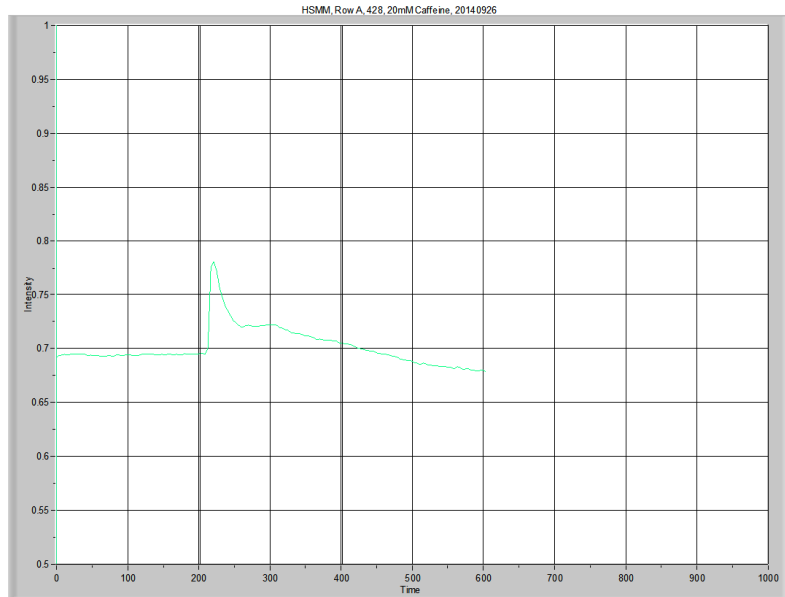
217

HSMM, Row A, 428, 20mM Caffeine, 2014 0926

	Average resting level	Peak	Δ Level	Time to Peak	Area Under the Curve Low X: 201.279 High X: 599.813	Peak Area
428, P9	0.693855	0.780592	0.086737	8.05119	281.02529	6.98890
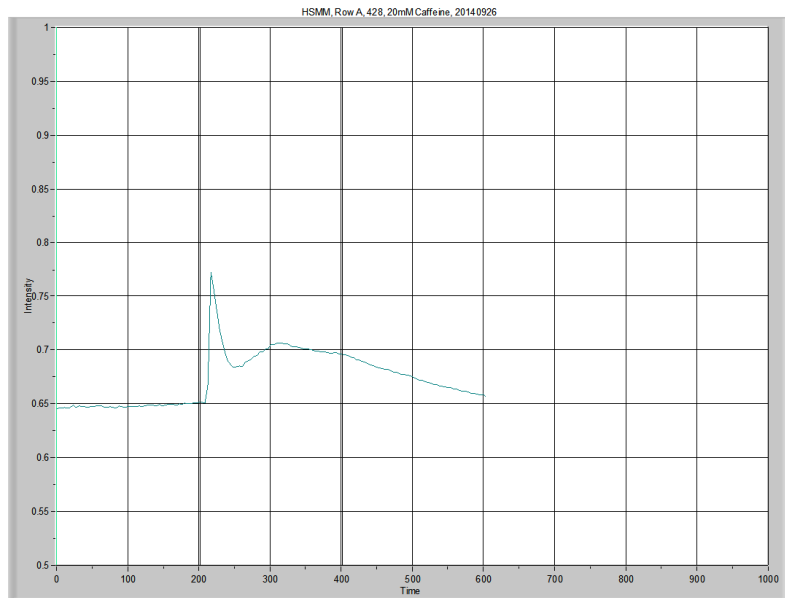
HSMM, Row A, 428, 20mM Caffeine, 2014 0926

	Average resting level	Peak	Δ Level	Time to Peak	Area Under the Curve Low X: 201.279 High X: 599.813	Peak Area
428, P10	0.647486	0.77246	0.124974	4.025575	273.78770	12.72328
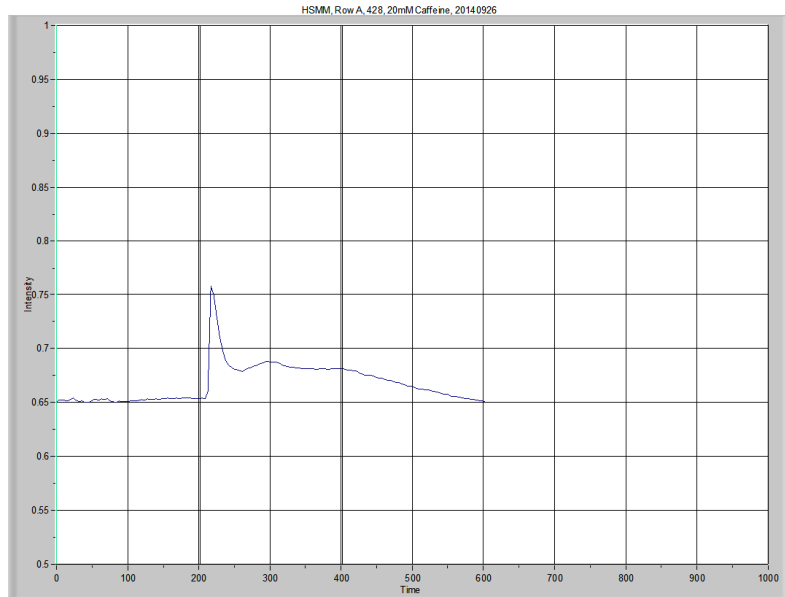
218

HSMM, Row A, 428, 20mM Caffeine, 2014 0926

	Average resting level	Peak	Δ Level	Time to Peak	Area Under the Curve Low X: 201.279 High X: 599.813	Peak Area
428, P11	0.652009	0.758368	0.10636	4.025575	269.21490	9.30972
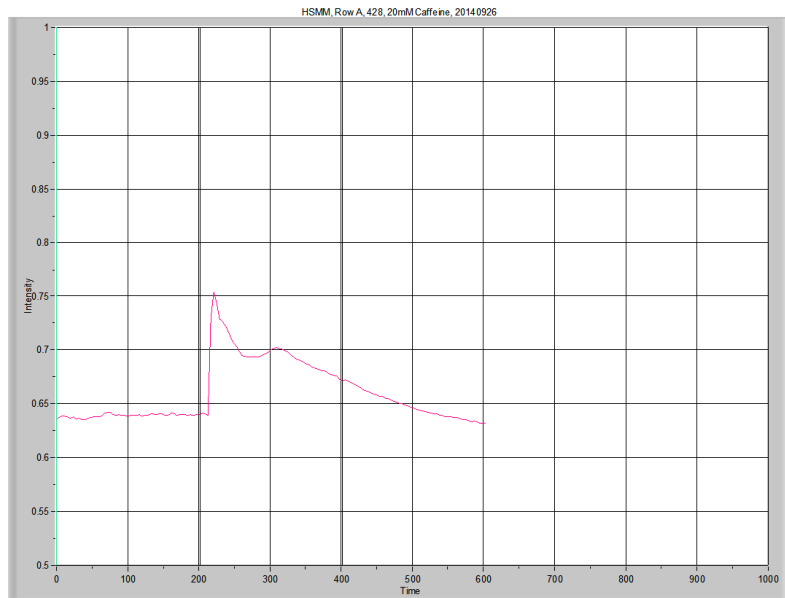
HSMM, Row A, 428, 20mM Caffeine, 2014 0926

	Average resting level	Peak	Δ Level	Time to Peak	Area Under the Curve Low X: 201.279 High X: 599.813	Peak Area
428, P12	0.638695	0.753905	0.11521	8.05119	267.51436	13.94986
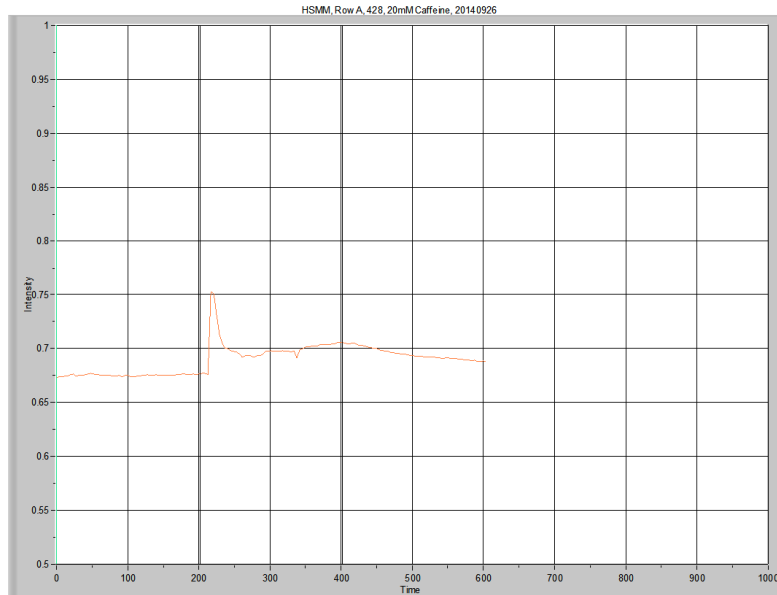
219

	Average resting level	Peak	Δ Level	Time to Peak	Area Under the Curve Low X: 201.279 High X: 599.813	Peak Area
428, P13	0.674849	0.75254	0.077691	4.025615	278.02638	6.09213
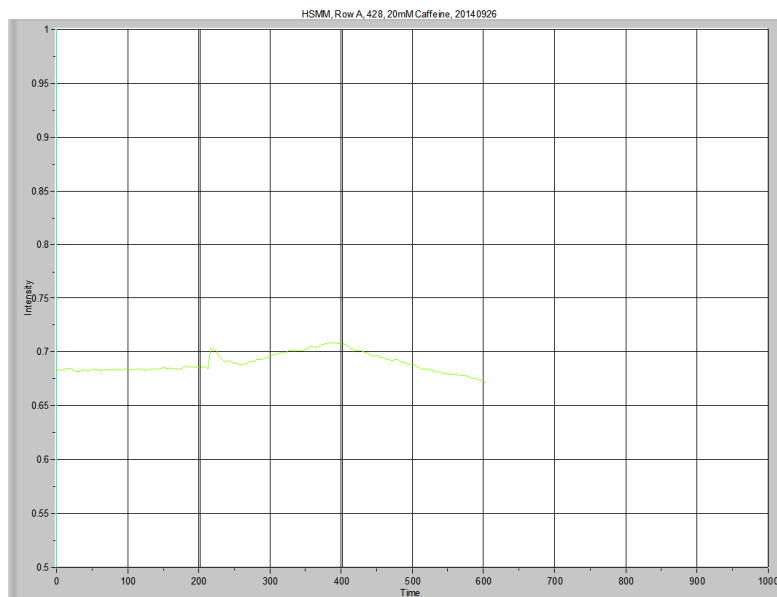
I do not plan to use this in my data, as it appears the myotube may have moved from ROI with stimulation.

	Average resting level	Peak	Δ Level	Time to Peak	Area Under the Curve Low X: 201.279 High X: 599.813	Peak Area
428, P14	*0.683495*	*0.708903*	*0.025408*	NA	276.16165	5.63700
		0.70812905	0.0247525			
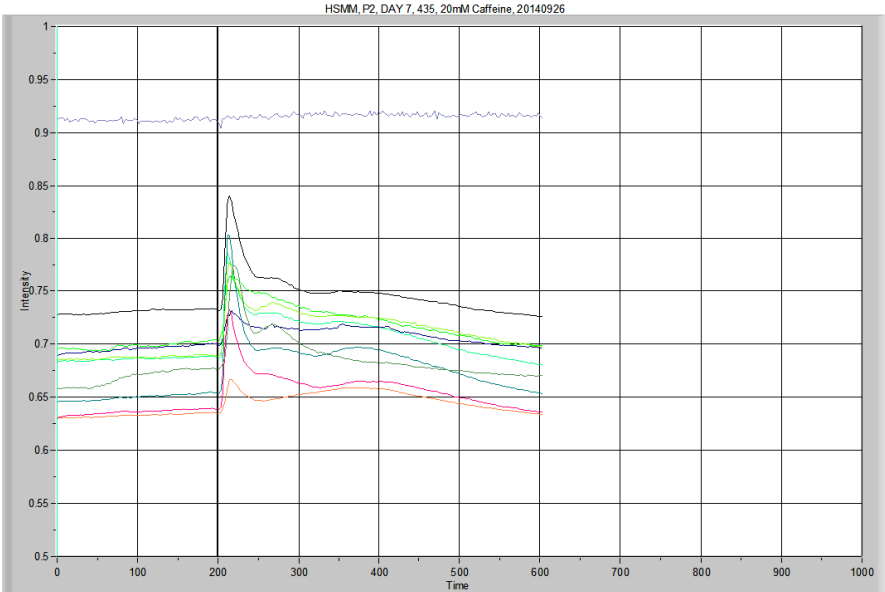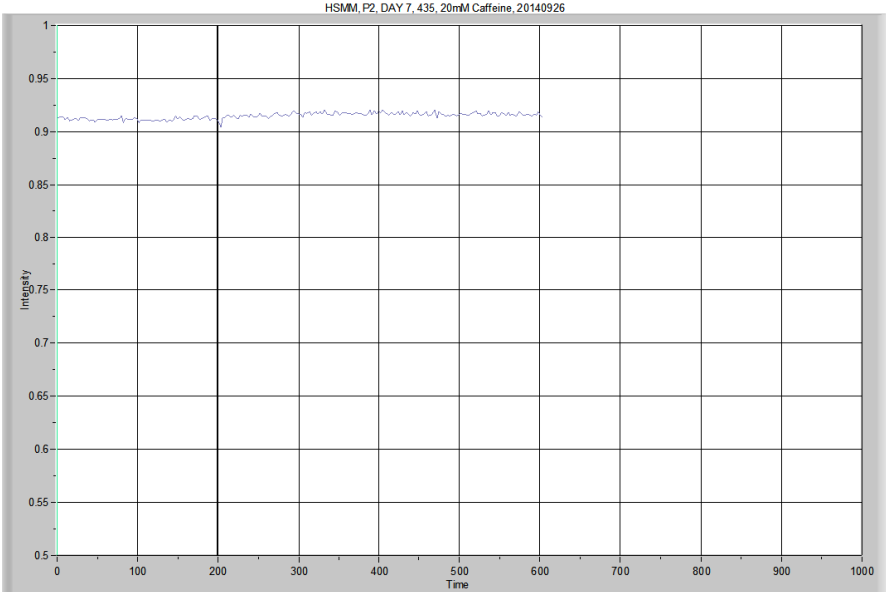
220

Overview

	Average resting level	Peak	Δ Level	Time to Peak	Area Under the Curve Low X: 201.278 High X: 598.467	Peak Area
435, BG	0.911124	0.919731	0.008606	NA	363.72147	0.95167
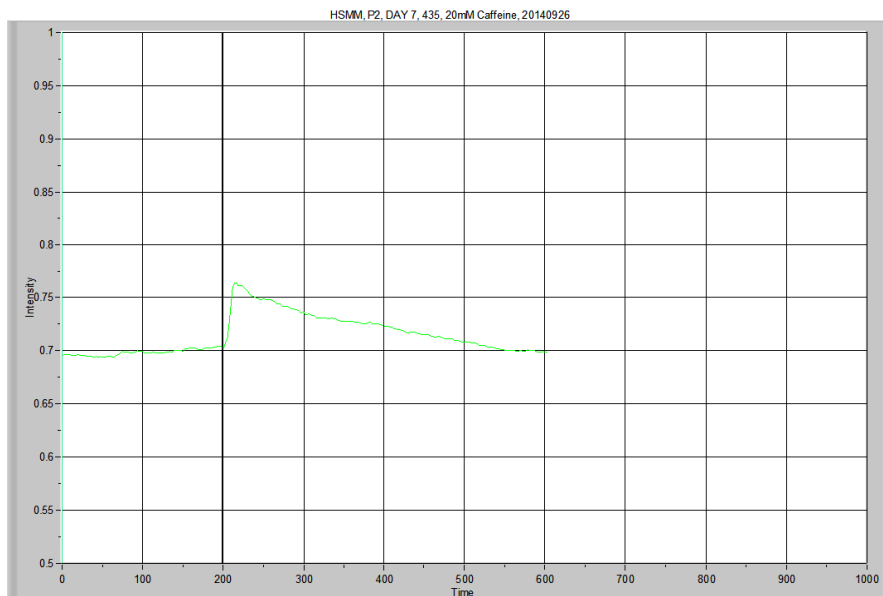
HSMM, P2, DAY 7, 435, 20mM Caffeine, 20140926

	Average resting level	Peak	Δ Level	Time to Peak	Area Under the Curve Low X: 201.278 High X: 598.467	Peak Area
435, P1	0.696259	0.764281	0.068022	13.41852	287.11666	8.75164
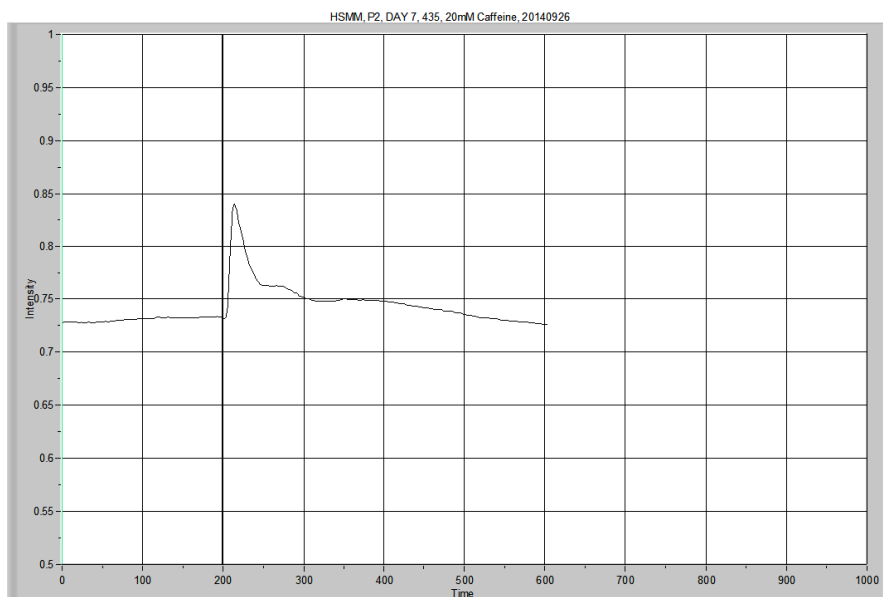
HSMM, P2, DAY 7, 435, 20mM Caffeine, 20140926

	Average resting level	Peak	Δ Level	Time to Peak	Area Under the Curve Low X: 201.278 High X: 598.467	Peak Area
435, P2	0.729299	0.840155	0.110856	10.73485	297.35723	7.98588
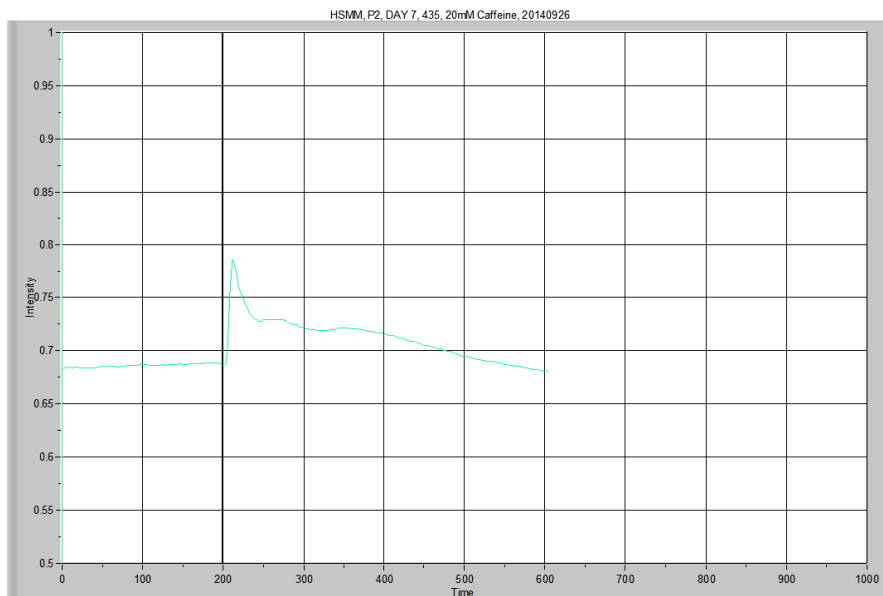
222

HSMM, P2, DAY 7, 435, 20mM Caffeine, 20140926

	Average resting level	Peak	Δ Level	Time to Peak	Area Under the Curve Low X: 201.278 High X: 598.467	Peak Area
435, P3	0.68497	0.785666	0.100696	5.36749	282.62434	11.24547
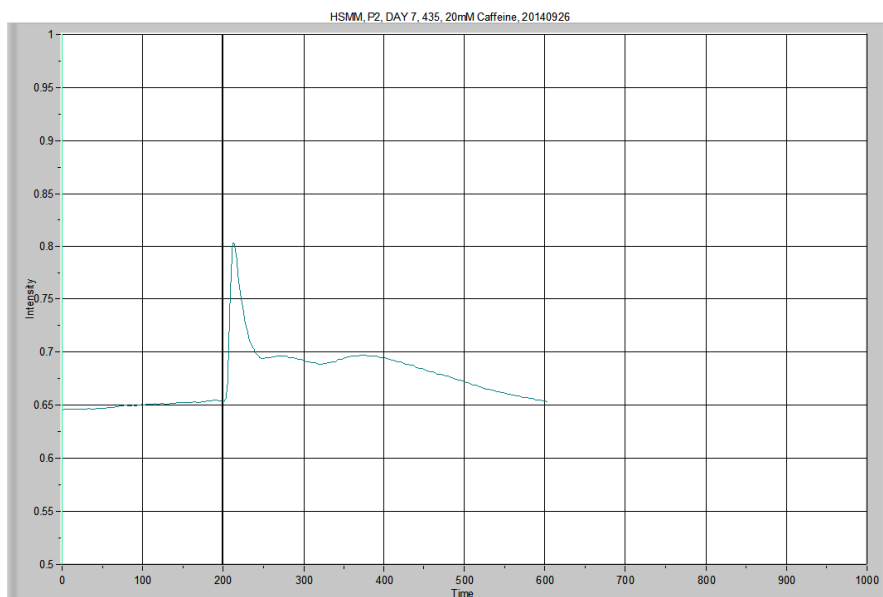
HSMM, P2, DAY 7, 435, 20mM Caffeine, 20140926

	Average resting level	Peak	Δ Level	Time to Peak	Area Under the Curve Low X: 201.278 High X: 598.467	Peak Area
435, P4	0.647937	0.80234	0.154403	10.73485	272.93763	13.40011
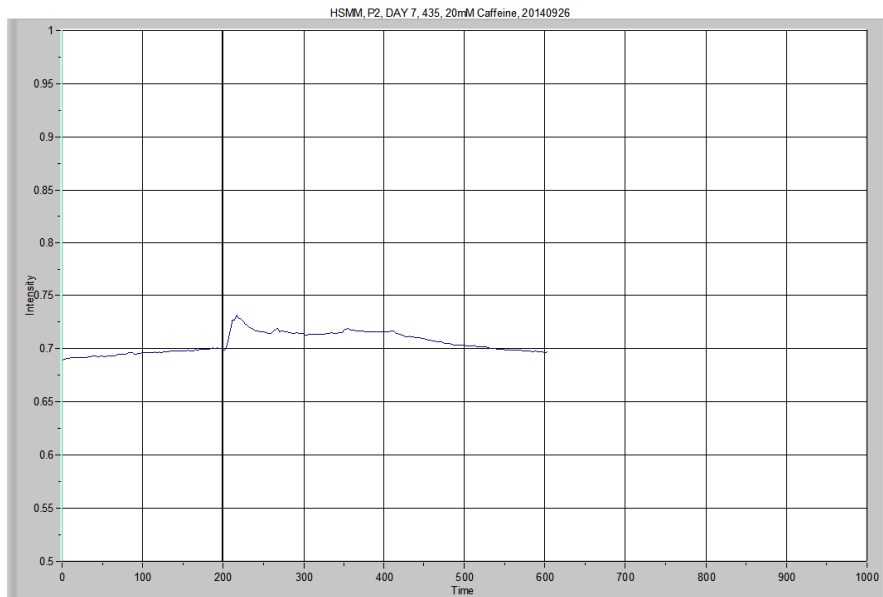
223

HSMM, P2, DAY 7, 435, 20mM Caffeine, 20140926

	Average resting level	Peak	Δ Level	Time to Peak	Area Under the Curve Low X: 201.278 High X: 598.467	Peak Area
435, P5	0.693425	0.732388	0.038964	13.41852	282.14702	5.11035
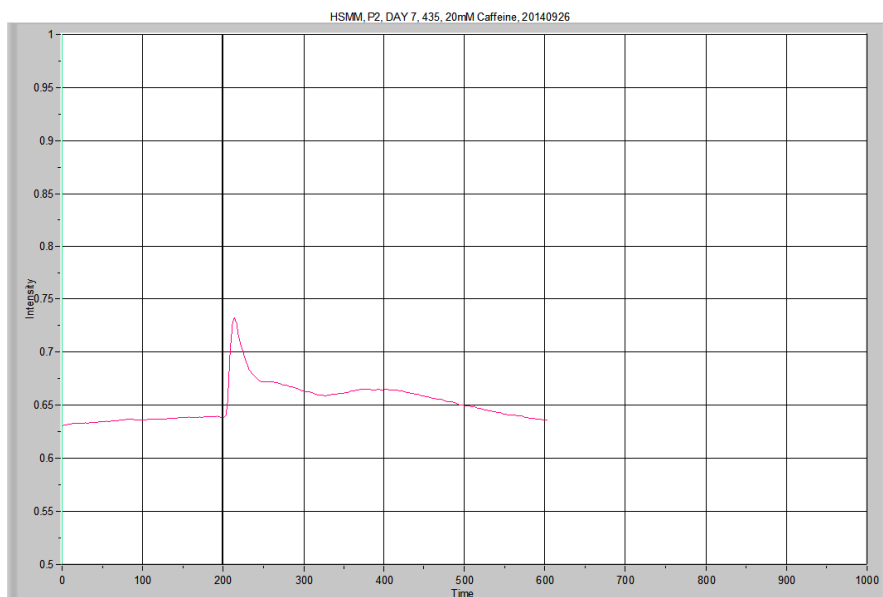
HSMM, P2, DAY 7, 435, 20mM Caffeine, 20140926

	Average resting level	Peak	Δ Level	Time to Peak	Area Under the Curve Low X: 201.278 High X: 598.467	Peak Area
435, P6	0.634478	0.732943	0.098464	10.73485	262.28835	9.31812
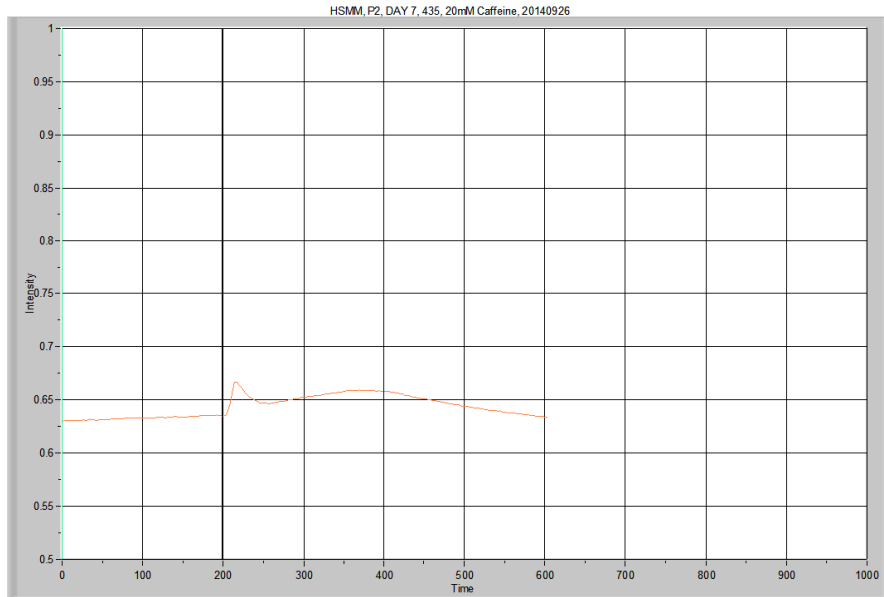
224

HSMM, P2, DAY 7, 435, 20mM Caffeine, 20140926

	Average resting level	Peak	Δ Level	Time to Peak	Area Under the Curve Low X: 201.278 High X: 598.467	Peak Area
435, P7	0.631535	0.66692	0.035385	13.41852	257.86755	6.05394
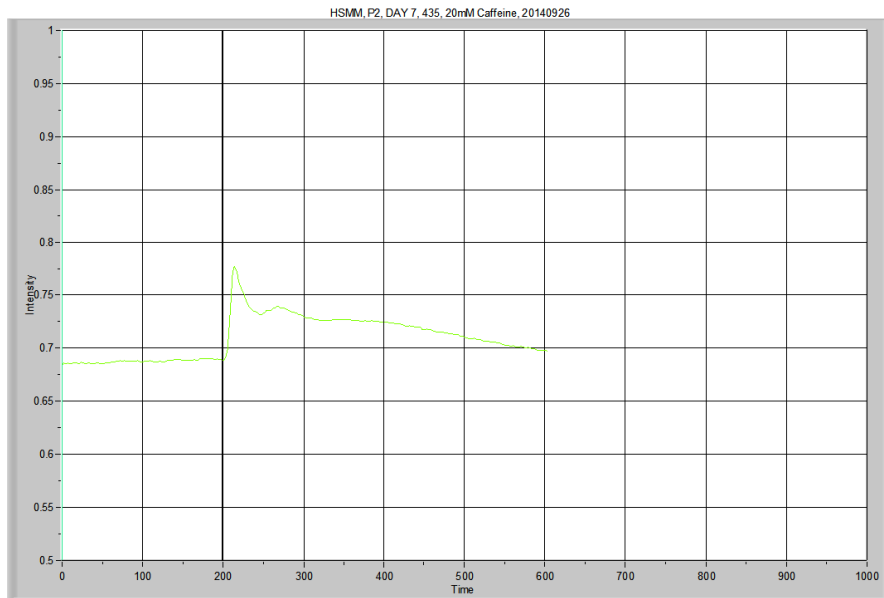
HSMM, P2, DAY 7, 435, 20mM Caffeine, 20140926

	Average resting level	Peak	Δ Level	Time to Peak	Area Under the Curve Low X: 201.278 High X: 598.467	Peak Area
435, P8	0.686478	0.77724	0.090762	10.73485	286.54606	11.41454
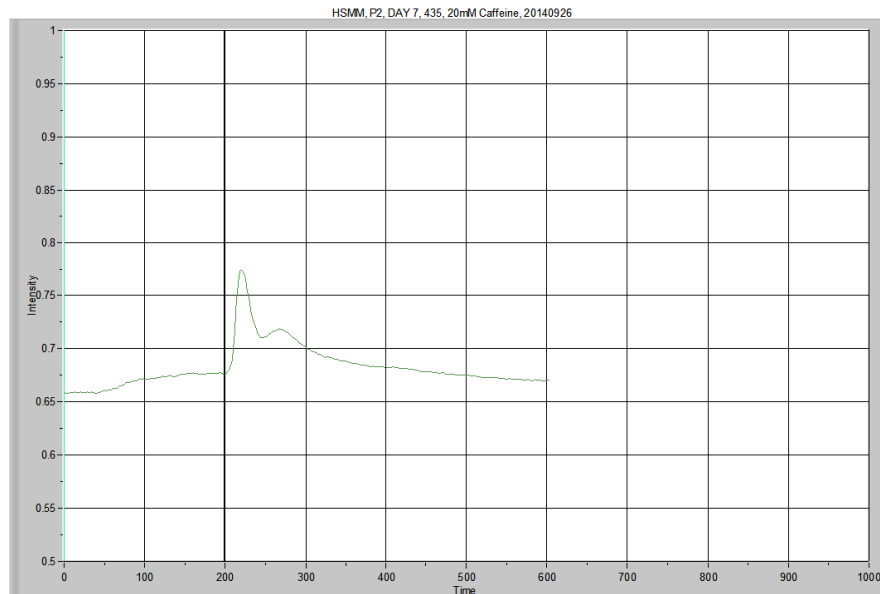
225

HSMM, P2, DAY 7, 435, 20mM Caffeine, 20140926

	Average resting level	Peak	Δ Level	Time to Peak	Area Under the Curve Low X: 201.278 High X: 598.467	Peak Area
435, P9	0.663824	0.77392	0.110095	16.10221	273.96848	6.73963

HSMM, P2, DAY 8, 439, 20 mM Caffeine, 20140927
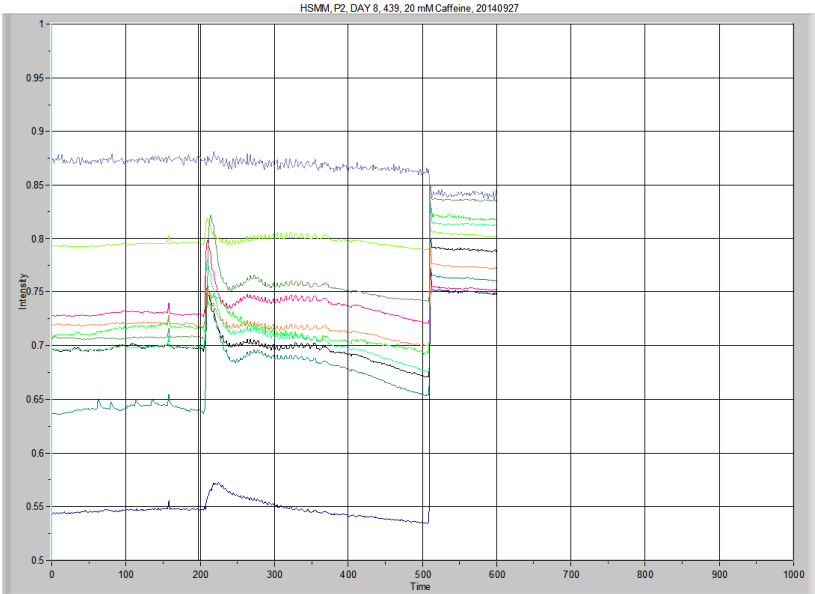
Overview

Note: the dish moved shortly after 500 seconds – so the Area Under the Curve data is taken from
Low X: 201.28 to High X: 499.176, which is different from other tracings.
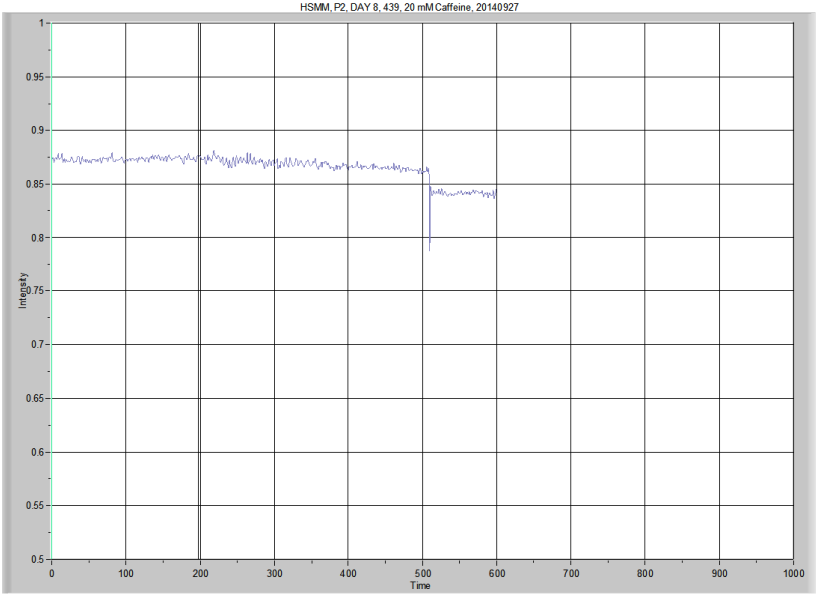
HSMM, P2, DAY 8, 439, 20 mM Caffeine, 20140927

	Average resting level	Peak	Δ Level	Time to Peak	Area Under the Curve Low X: 201.28 High X: 499.176	Peak Area
439, BG	0.872282	0.881344	0.009062	NA	258.52980	0.22693
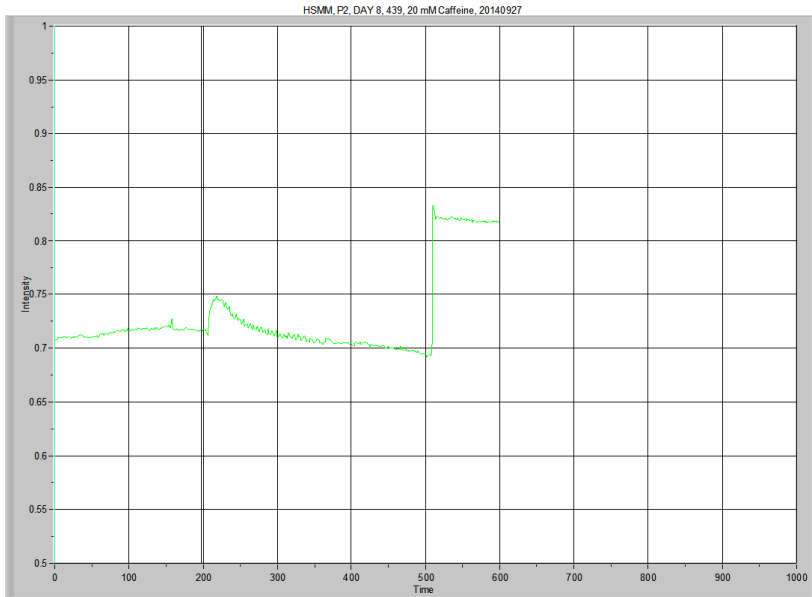
HSMM, P2, DAY 8, 439, 20 mM Caffeine, 20140927

	Average resting level	Peak	Δ Level	Time to Peak	Area Under the Curve Low X: 201.28 High X: 499.176	Peak Area
439, P1	0.713021	0.748742	0.035721	9.393134	211.92058	1.60567
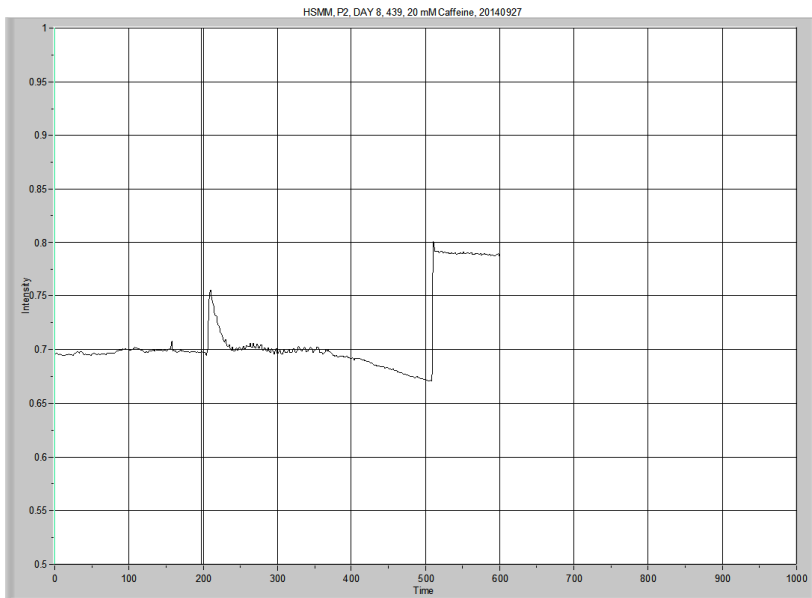
HSMM, P2, DAY 8, 439, 20 mM Caffeine, 20140927

	Average resting level	Peak	Δ Level	Time to Peak	Area Under the Curve Low X: 201.28 High X: 499.176	Peak Area
439, P2	0.697043	0.755549	0.058505	4.025548	207.25405	3.25597
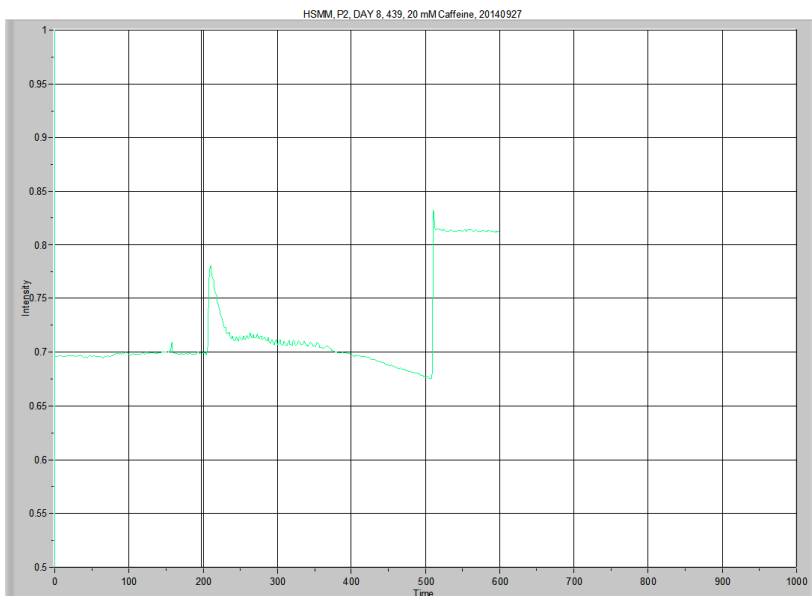
228

HSMM, P2, DAY 8, 439, 20 mM Caffeine, 20140927

	Average resting level	Peak	Δ Level	Time to Peak	Area Under the Curve Low X: 201.28 High X: 499.176	Peak Area
439, P3	0.696838	0.780337	0.083499	4.025548	209.91927	4.98727
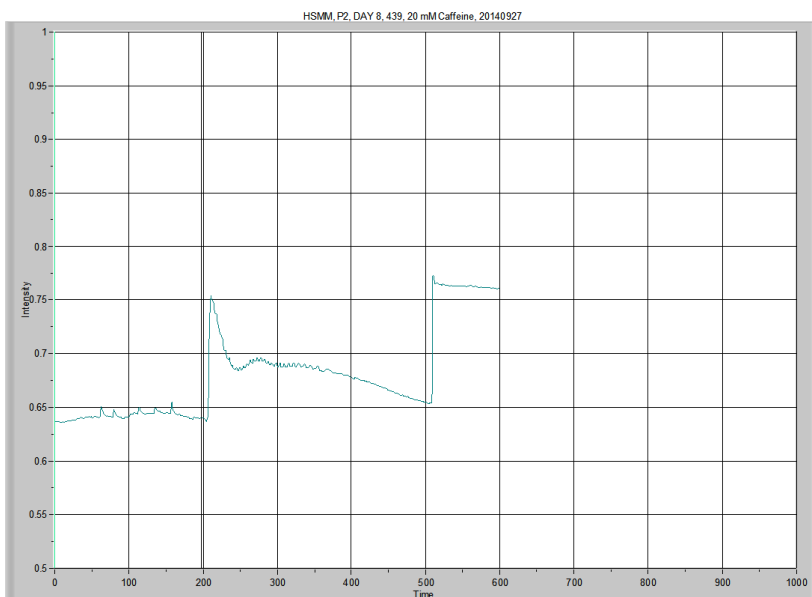
HSMM, P2, DAY 8, 439, 20 mM Caffeine, 20140927

	Average resting level	Peak	Δ Level	Time to Peak	Area Under the Curve Low X: 201.28 High X: 499.176	Peak Area
439, P4	0.640815	0.754292	0.113478	4.025548	203.30823	10.50028
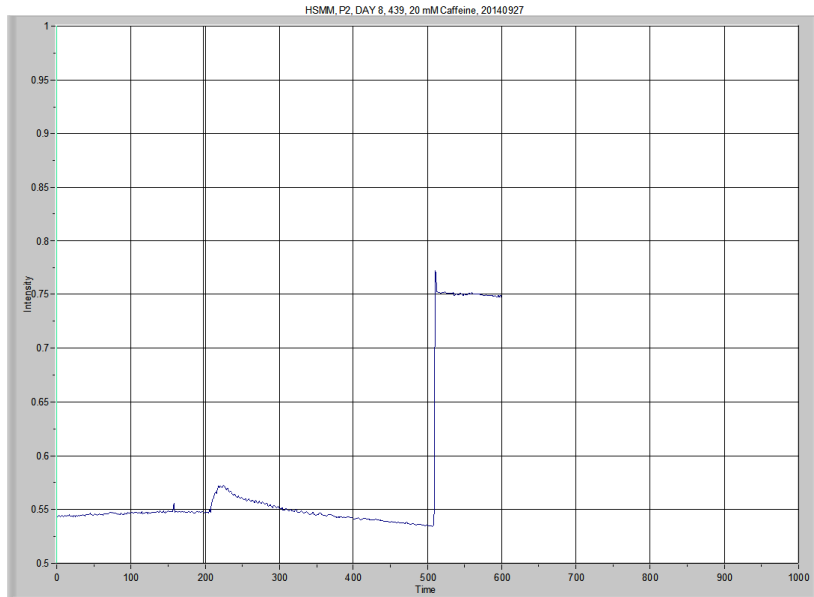
229

HSMM, P2, DAY 8, 439, 20 mM Caffeine, 20140927

	Average resting level	Peak	Δ Level	Time to Peak	Area Under the Curve Low X: 201.28 High X: 499.176	Peak Area
439, P5	0.545257	0.572074	0.026817	12.07678	163.20380	1.91049
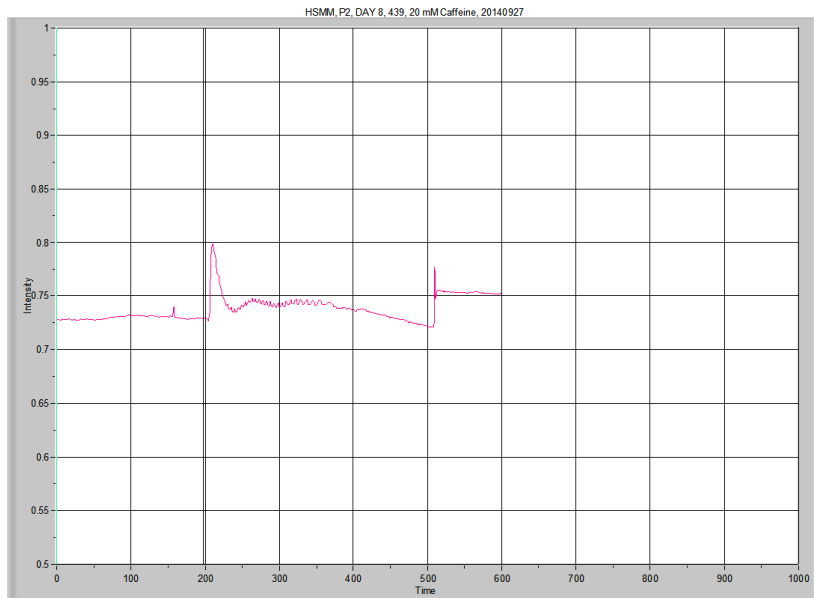
HSMM, P2, DAY 8, 439, 20 mM Caffeine, 20140927

	Average resting level	Peak	Δ Level	Time to Peak	Area Under the Curve Low X: 201.28 High X: 499.176	Peak Area
439, P6	0.729192	0.79896	0.069767	4.025548	220.34068	4.23476
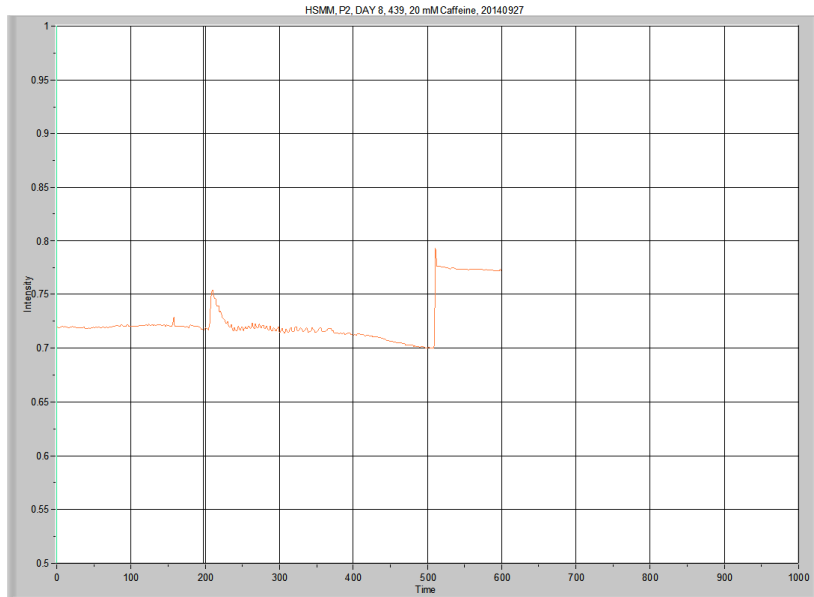
230

HSMM, P2, DAY 8, 439, 20 mM Caffeine, 20140927

	Average resting level	Peak	Δ Level	Time to Peak	Area Under the Curve Low X: 201.28 High X: 499.176	Peak Area
439, P7	0.719786	0.754261	0.034475	4.025548	213.05644	1.74251
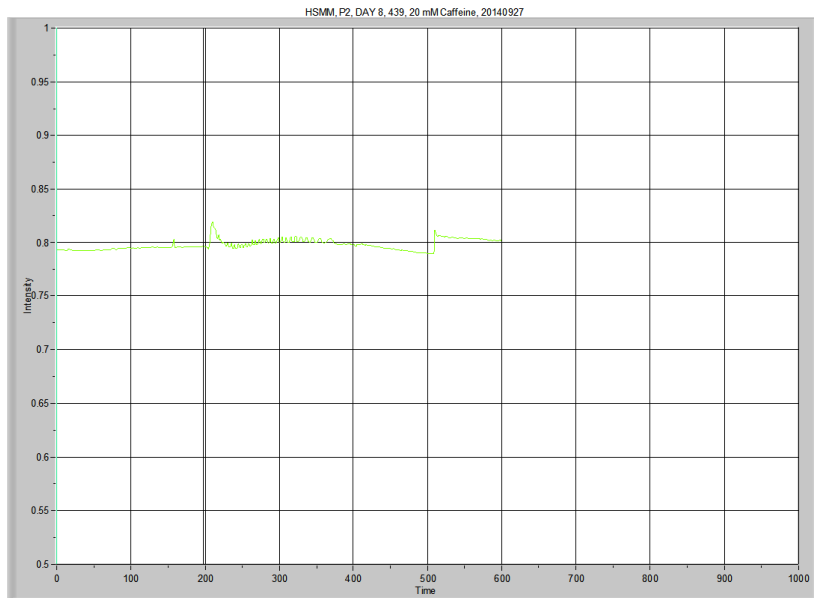
HSMM, P2, DAY 8, 439, 20 mM Caffeine, 20140927

	Average resting level	Peak	Δ Level	Time to Peak	Area Under the Curve Low X: 201.28 High X: 499.176	Peak Area
439, P8	0.793336	0.819345	0.02601	4.025548	237.81068	1.57789
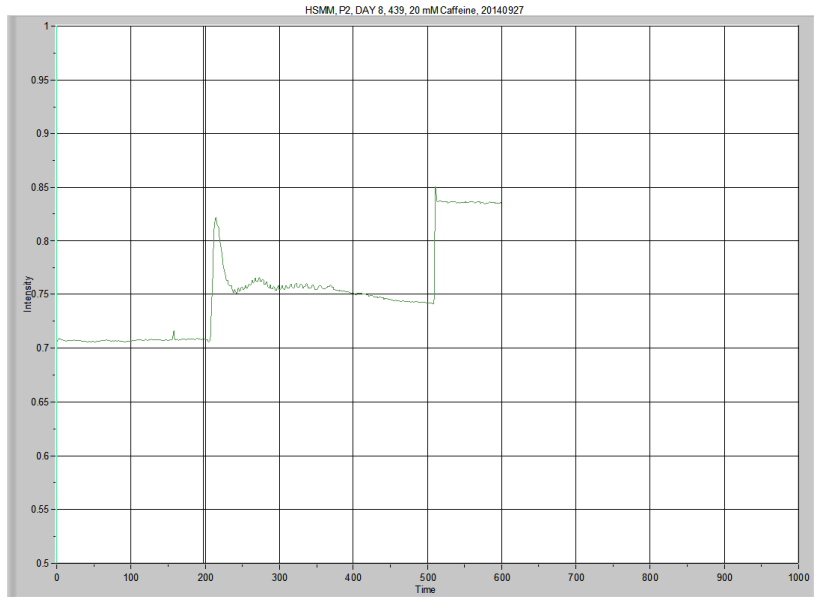
231

HSMM, P2, DAY 8, 439, 20 mM Caffeine, 20140927

	Average resting level	Peak	Δ Level	Time to Peak	Area Under the Curve Low X: 201.28 High X: 499.176	Peak Area
439, P9	0.706709	0.82177	0.115061	8.051186	224.67299	8.76381
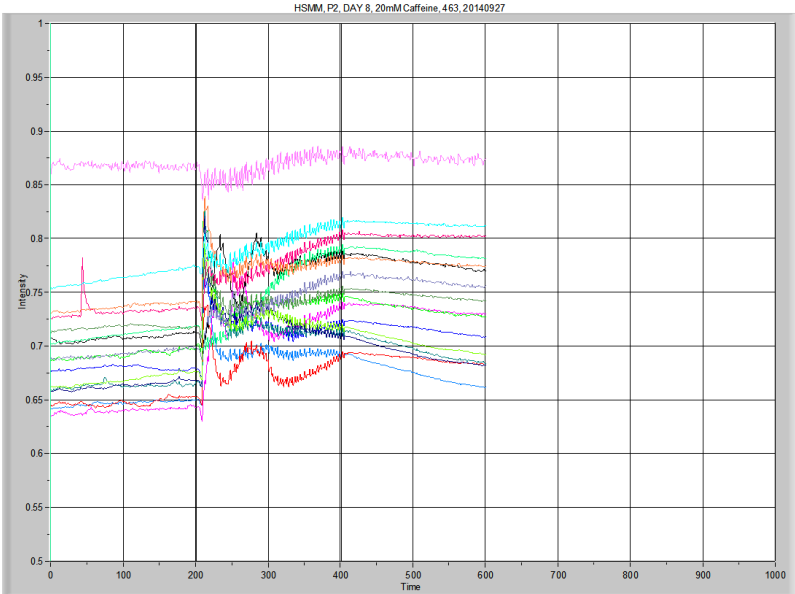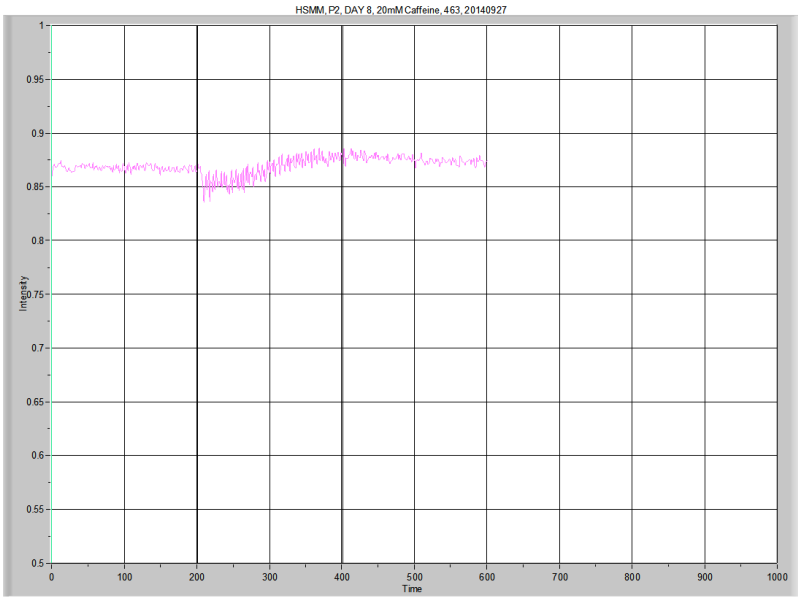
Overview

	Average resting level	Peak	Δ Level	Time to Peak	Area Under the Curve Low X: 201.28 High X: 599.817	Peak Area
463, BG	0.867208	0.885568	0.01836	NA	346.87033	0.66607
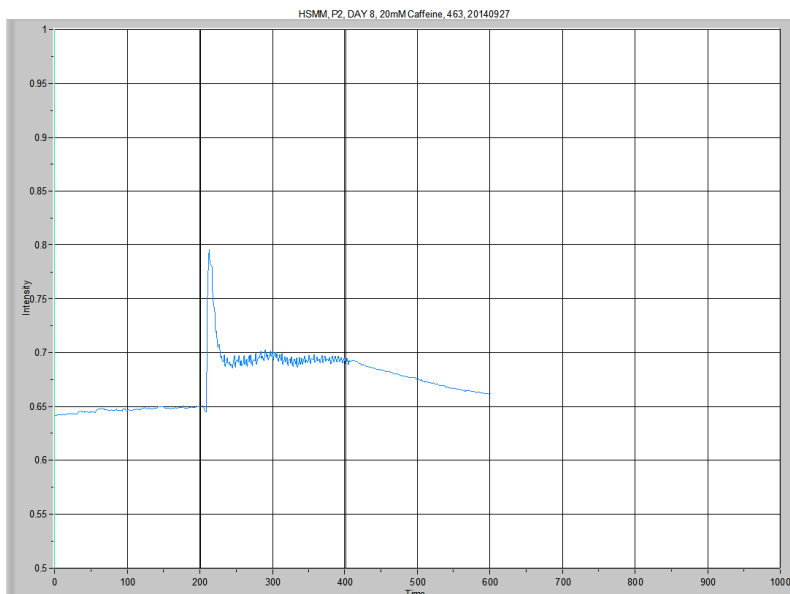
HSMM, P2, DAY 8, 20mM Caffeine, 463, 20140927

	Average resting level	Peak	Δ Level	Time to Peak	Area Under the Curve Low X: 201.28 High X: 599.817	Peak Area
463, P1	0.646351	0.795849	0.149497	2.683529	273.29485	12.11970
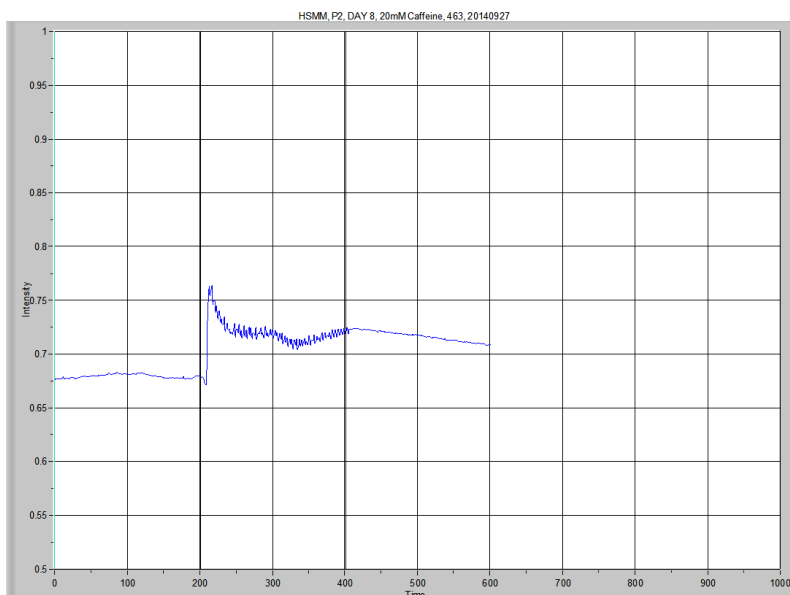
HSMM, P2, DAY 8, 20mM Caffeine, 463, 20140927

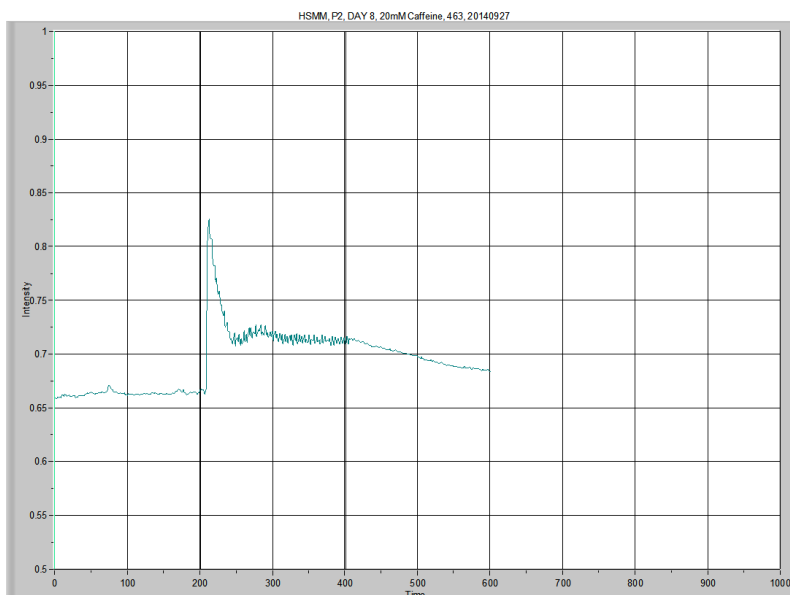|	Average resting level	Peak	Δ Level	Time to Peak	Area Under the Curve Low X: 201.28 High X: 599.817	Peak Area
463, P2	0.679026	0.763642	0.084616	6.709131	285.81634	9.46679
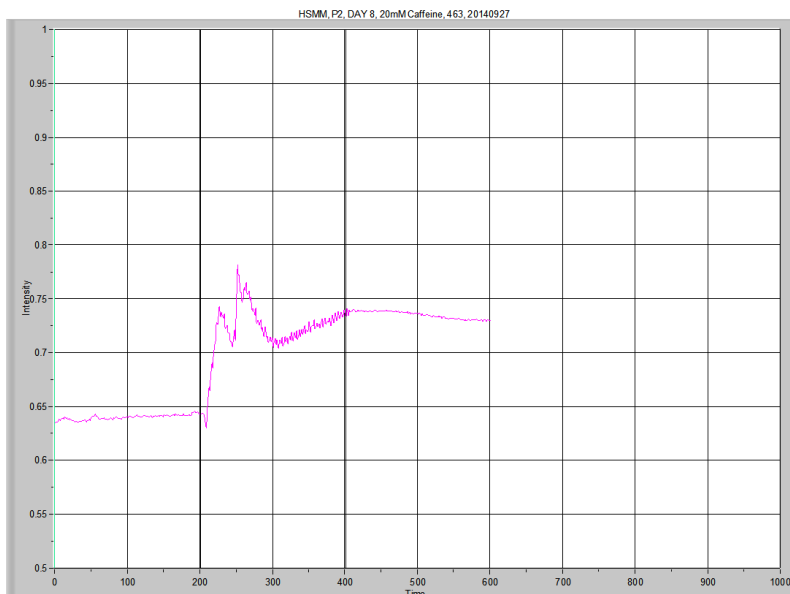
234

HSMM, P2, DAY 8, 20mM Caffeine, 463, 20140927

Did not use this for the AUC data analysis, due to double peaks

	Average resting level	Peak	Δ Level	Time to Peak	Area Under the Curve Low X: 201.28 High X: 599.817	Peak Area
463, P3	*0.639515*	*0.781492* *0.737493*	*0.141977* *0.097978*	21.46982 42.93976	289.80589	16.21174
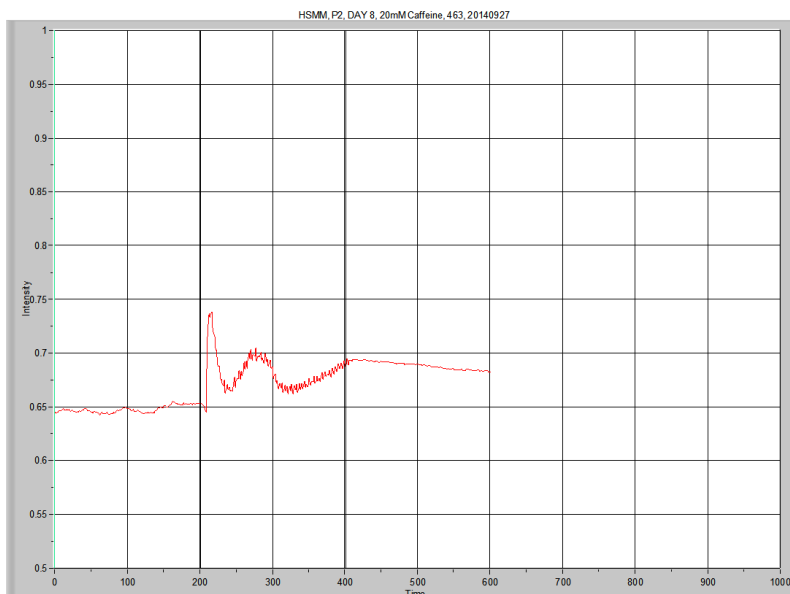
HSMM, P2, DAY 8, 20mM Caffeine, 463, 20140927

	Average resting level	Peak	Δ Level	Time to Peak	Area Under the Curve Low X: 201.28 High X: 599.817	Peak Area
463, P4	0.647124	0.73818	0.091056	6.709131	272.82097	6.72014
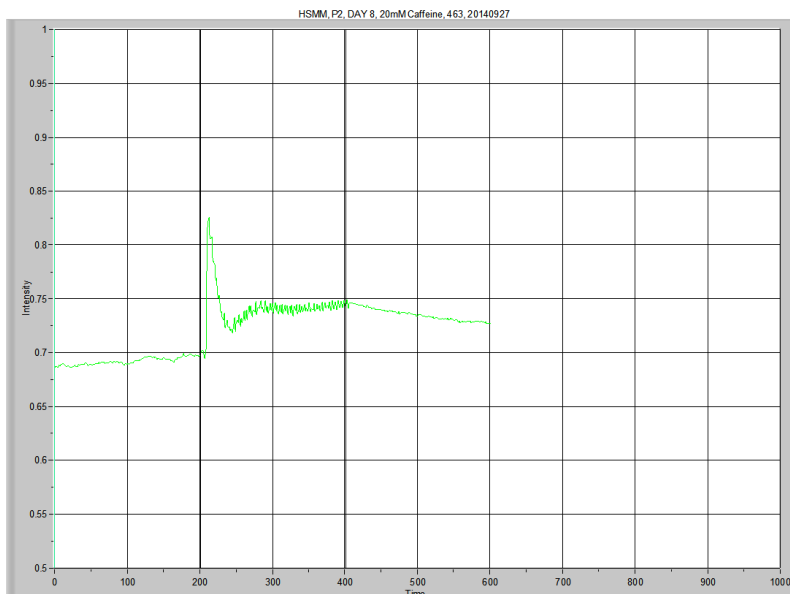
235

	Average resting level	Peak	Δ Level	Time to Peak	Area Under the Curve Low X: 201.28 High X: 599.817	Peak Area
463, P5	0.691482	0.825458	0.133976	4.025529	294.21447	10.34739
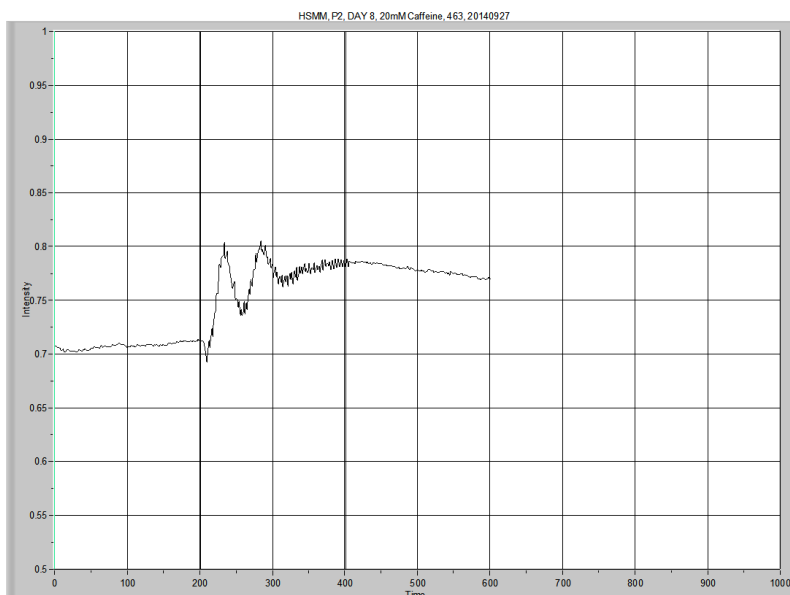
Did not use this for the AUC data analysis, due to double peaks

	Average resting level	Peak	Δ Level	Time to Peak	Area Under the Curve Low X: 201.28 High X: 599.817	Peak Area
463, P6	*0.707102*	*0.805091* *0.803821*	*0.097989* *0.096719*	22.81183 72.46102	308.29155	12.85289

236

HSMM, P2, DAY 8, 20mM Caffeine, 463, 20140927
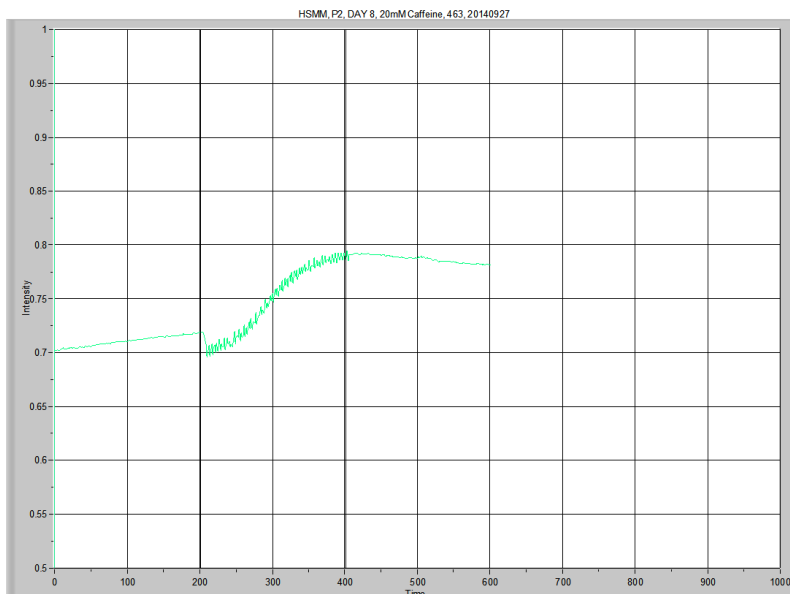
I did not use data from this tracing, as it appears the myotube moved with contraction….

	Average resting level	Peak	Δ Level	Time to Peak	Area Under the Curve Low X: 201.28 High X: 599.817	Peak Area
463, P7					305.79331	7.02105

HSMM, P2, DAY 8, 20mM Caffeine, 463, 20140927

	Average resting level	Peak	Δ Level	Time to Peak	Area Under the Curve Low X: 201.28 High X: 599.817	Peak Area
463, P8	0.662845	0.825826	0.162981	4.025529	282.57898	13.36376
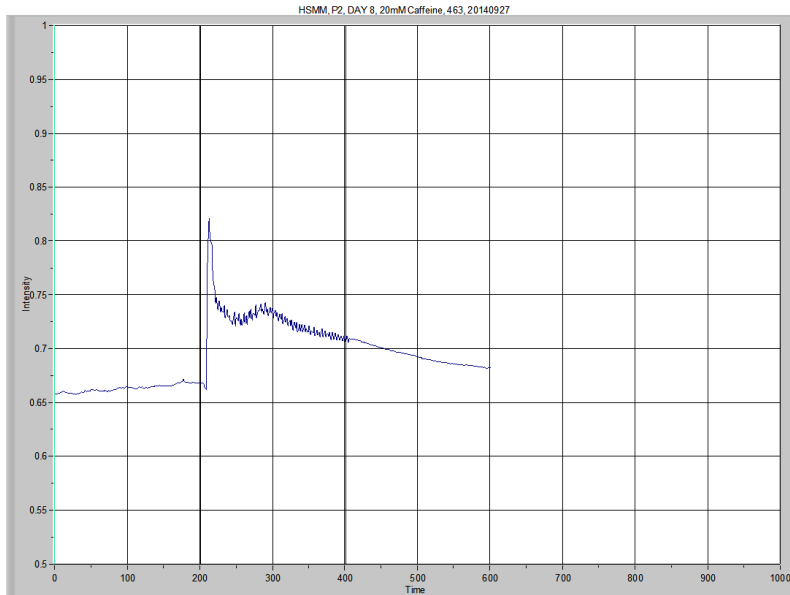
237

HSMM, P2, DAY 8, 20mM Caffeine, 463, 20140927

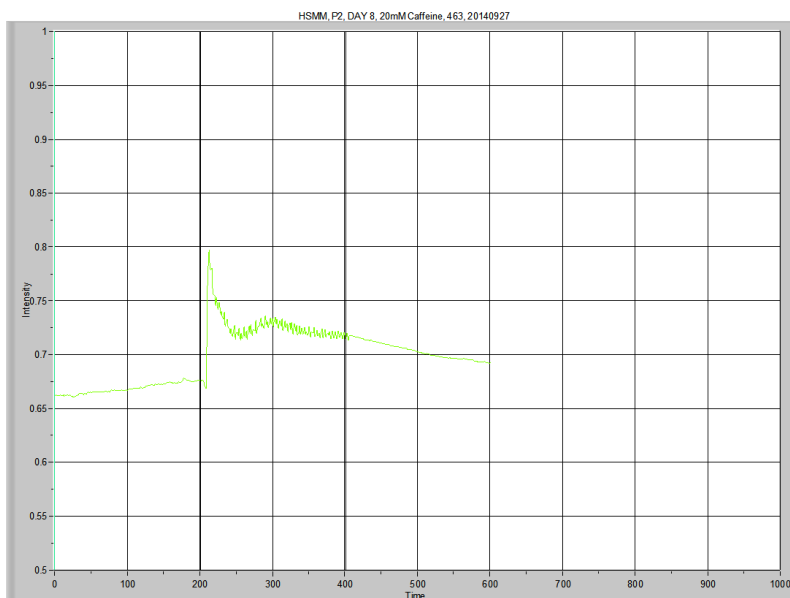|	Average resting level	Peak	Δ Level	Time to Peak	Area Under the Curve Low X: 201.28 High X: 599.817	Peak Area
463, P9	0.66274	0.821051	0.158311	4.025529	282.70240	13.69418
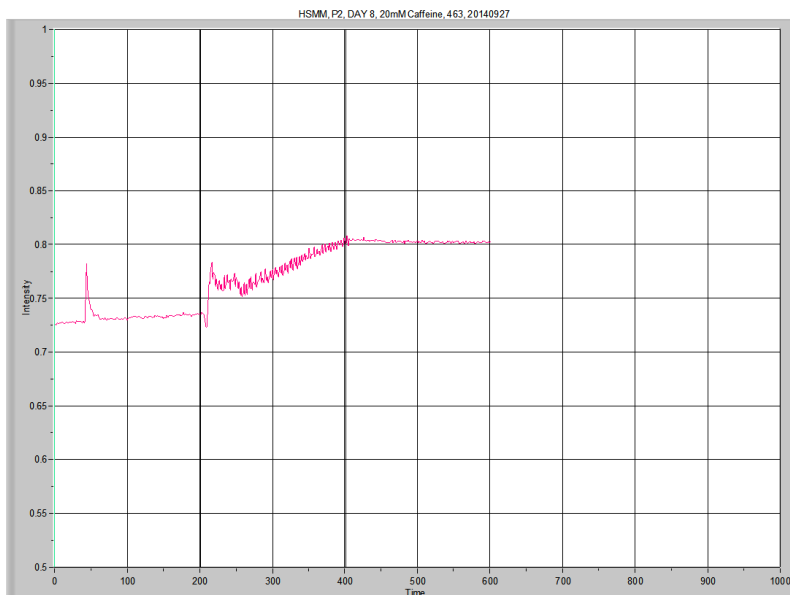
I did not use this tracing, as the myotube moved with stimulation. I am also curious what caused the spike prior to the caffeine infusion was begun.
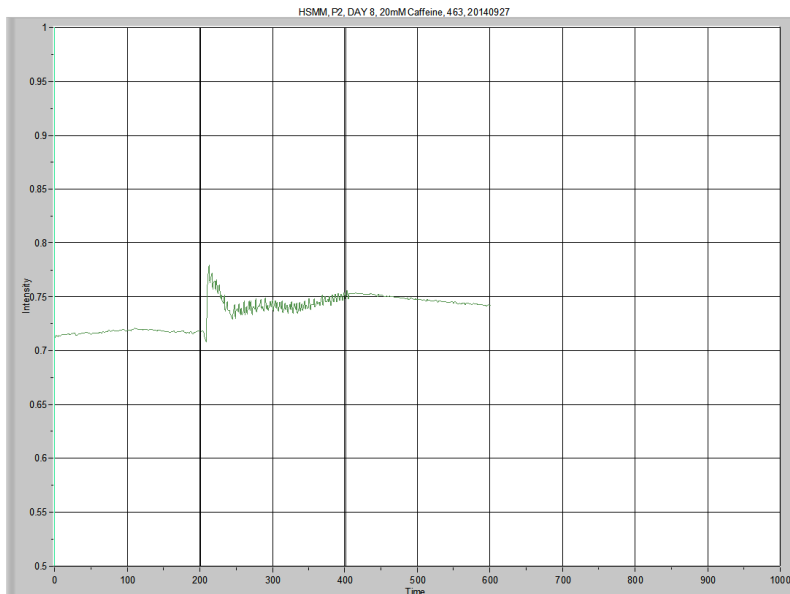
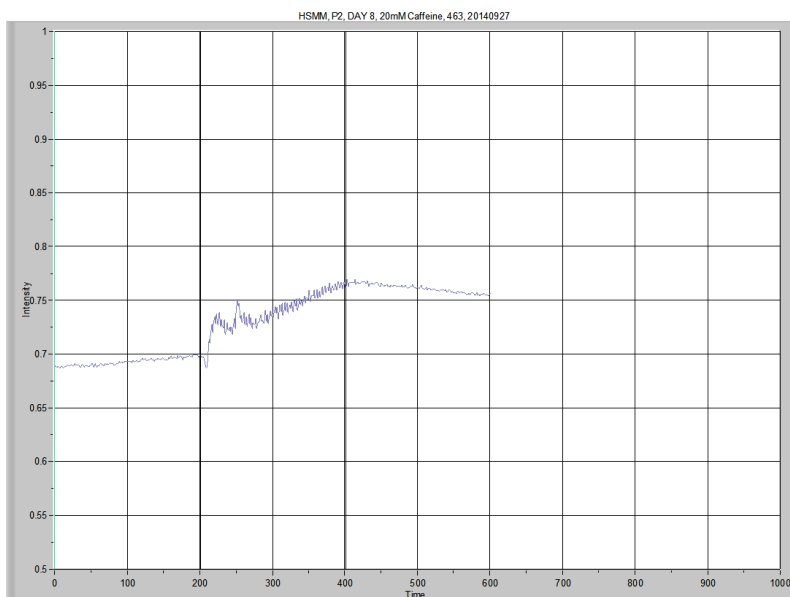|	Average resting level	Peak	Δ Level	Time to Peak	Area Under the Curve Low X: 201.28 High X: 599.817	Peak Area
463, P10					314.27458	8.00434
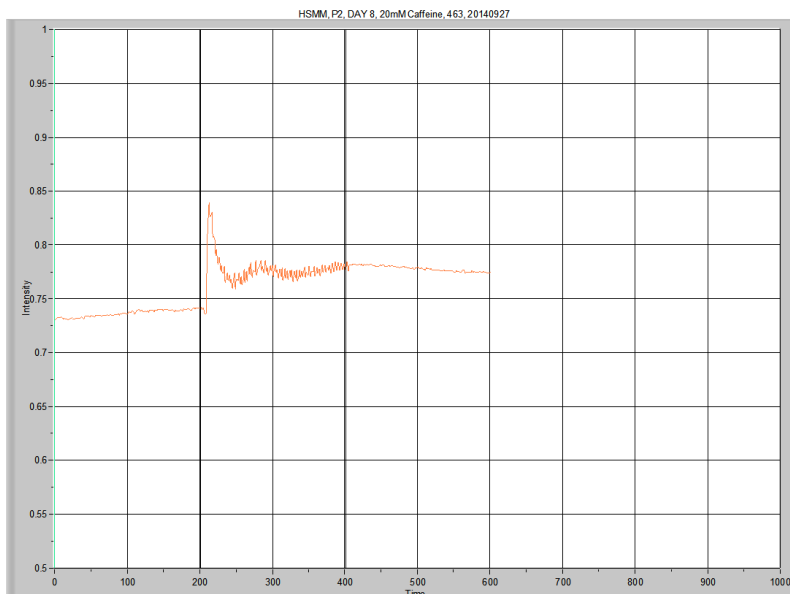
HSMM, P2, DAY 8, 20mM Caffeine, 463, 20140927

	Average resting level	Peak	Δ Level	Time to Peak	Area Under the Curve Low X: 201.28 High X: 599.817	Peak Area
463, P11	0.73589	0.839392	0.103502	4.025529	309.57836	7.92508

HSMM, P2, DAY 8, 20mM Caffeine, 463, 20140927

	Average resting level	Peak	Δ Level	Time to Peak	Area Under the Curve Low X: 201.28 High X: 599.817	Peak Area
463, P12	0.667905	0.796903	0.128998	4.025529	284.56124	11.99755

239

HSMM, P2, DAY 8, 20mM Caffeine, 463, 20140927

	Average resting level	Peak	Δ Level	Time to Peak	Area Under the Curve Low X: 201.28 High X: 599.817	Peak Area
463, P13	0.717044	0.779566	0.062522	2.683529	296.91013	6.15914

HSMM, P2, DAY 8, 20mM Caffeine, 463, 20140927

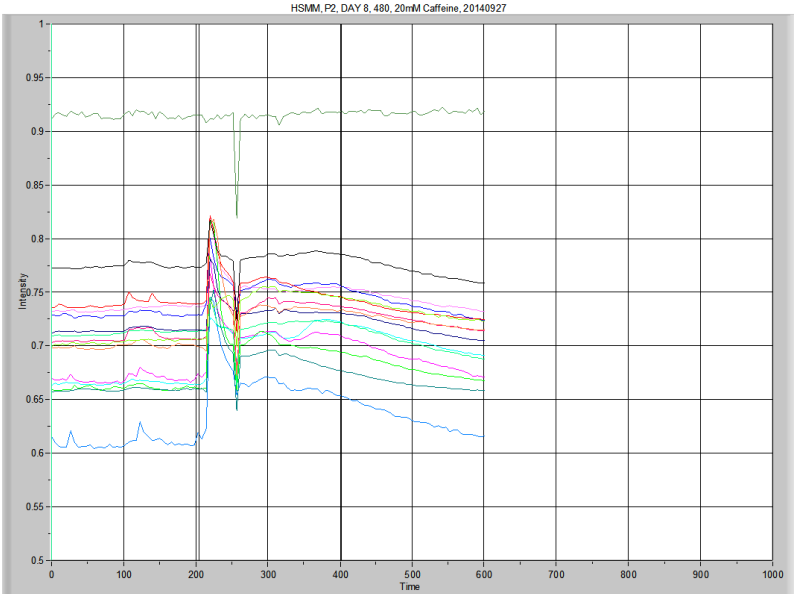*I did not use the data from this tracing, because the myotube was displaced upon stimulation with the 20mM caffeine.*

	Average resting level	Peak	Δ Level	Time to Peak	Area Under the Curve Low X: 201.28 High X: 599.817	Peak Area
463, P14					298.84627	9.04983

240

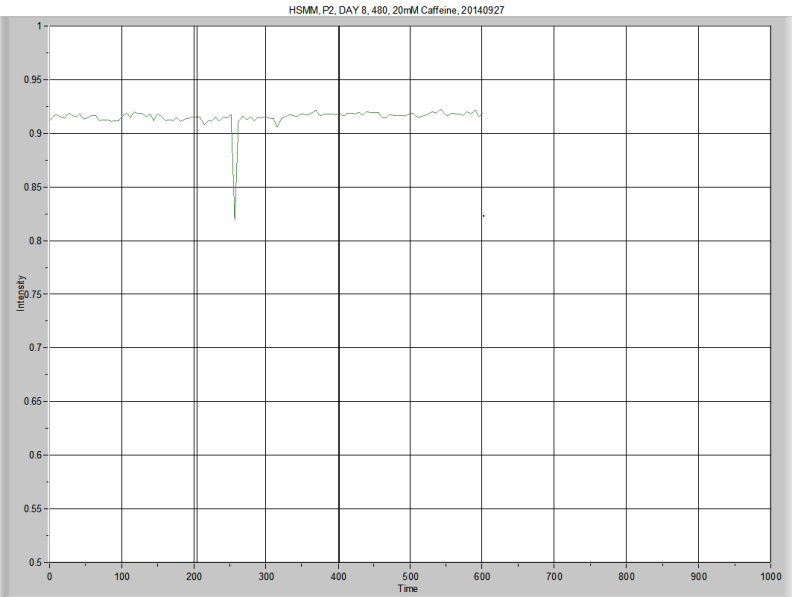HSMM, P2, DAY 8, 20mM Caffeine, 463, 20140927
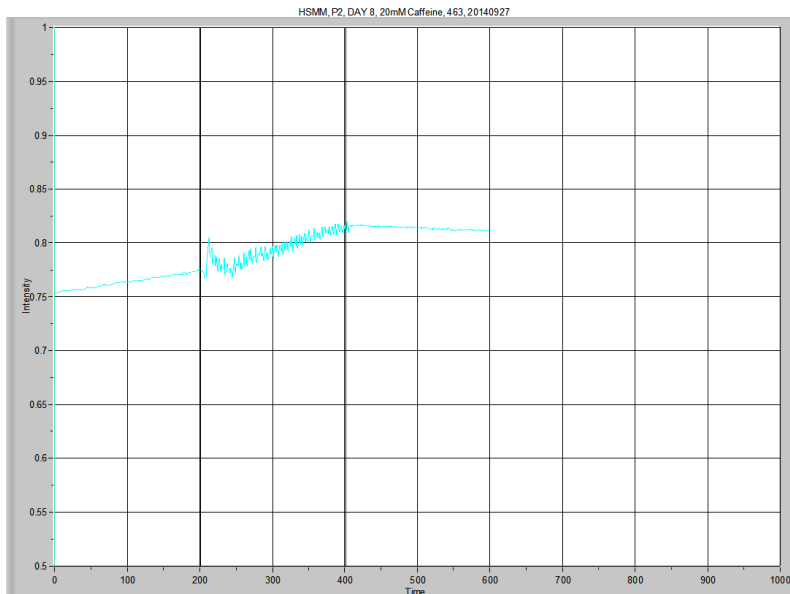
I do not plan to use this tracing, as the myotube floated away with stimulation…..

	Average resting level	Peak	Δ Level	Time to Peak	Area Under the Curve Low X: 201.28 High X: 599.817	Peak Area
463, P15					320.20367	4.41991

HSMM, P2, DAY 8, 480, 20mM Caffeine, 20140927

Overview

HSMM, P2, DAY 8, 480, 20mM Caffeine, 20140927

	Average resting level	Peak	Δ Level	Time to Peak	Area Under the Curve Low X: 203.964 High X: 601.158	Peak Area
480, BG	0.914537	0.921885	0.007347	NA	363.28003	-0.84496
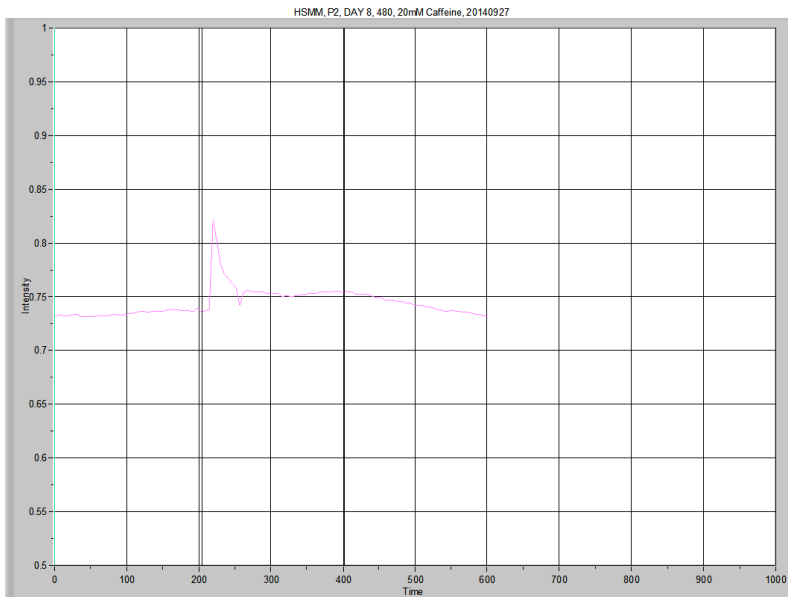
HSMM, P2, DAY 8, 480, 20mM Caffeine, 20140927

	Average resting level	Peak	Δ Level	Time to Peak	Area Under the Curve Low X: 203.964 High X: 601.158	Peak Area
480, P2	0.734021	0.821147	0.087126	10.73492	297.65079	6.22437
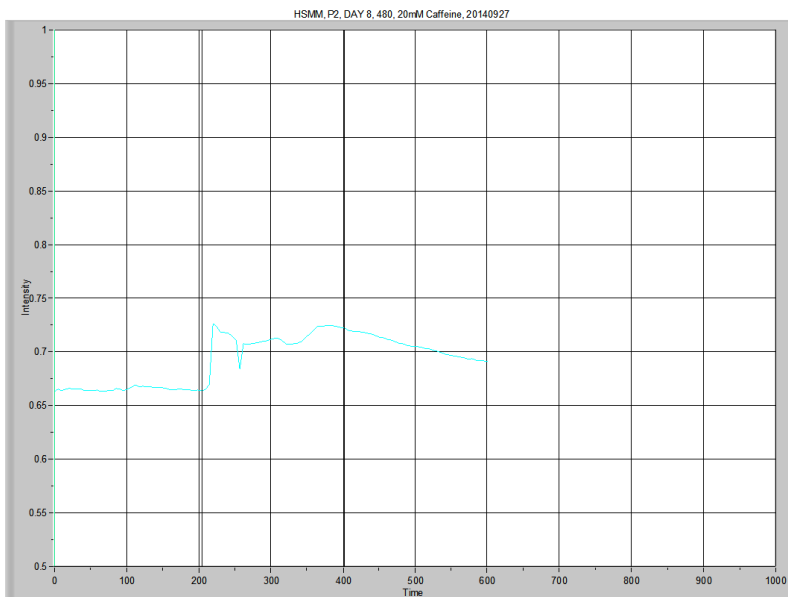
HSMM, P2, DAY 8, 480, 20mM Caffeine, 20140927

	Average resting level	Peak	Δ Level	Time to Peak	Area Under the Curve Low X: 203.964 High X: 601.158	Peak Area
480, P3	0.664977	0.72587	0.060892	10.73492	281.07861	12.06196
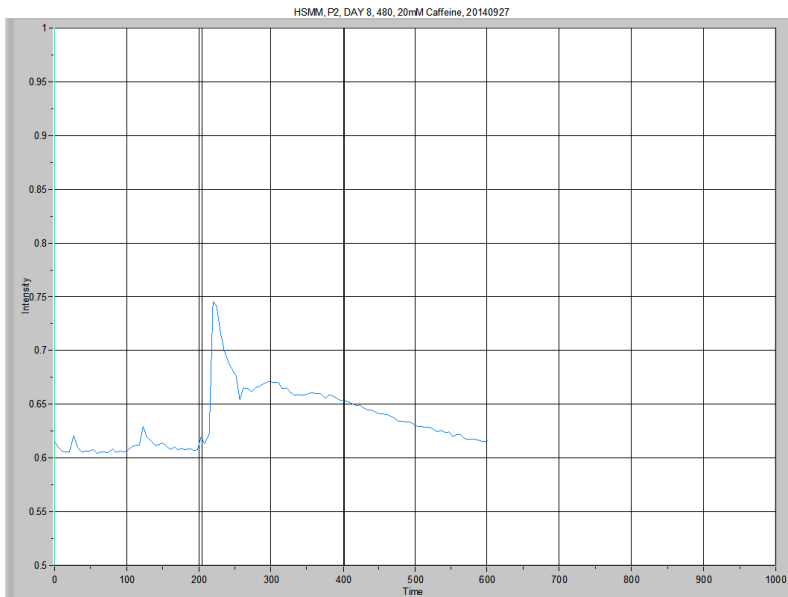
243

HSMM, P2, DAY 8, 480, 20mM Caffeine, 20140927

	Average resting level	Peak	Δ Level	Time to Peak	Area Under the Curve Low X: 203.964 High X: 601.158	Peak Area
480, P4	0.609391	0.745605	0.136214	5.36745	257.84482	12.65283
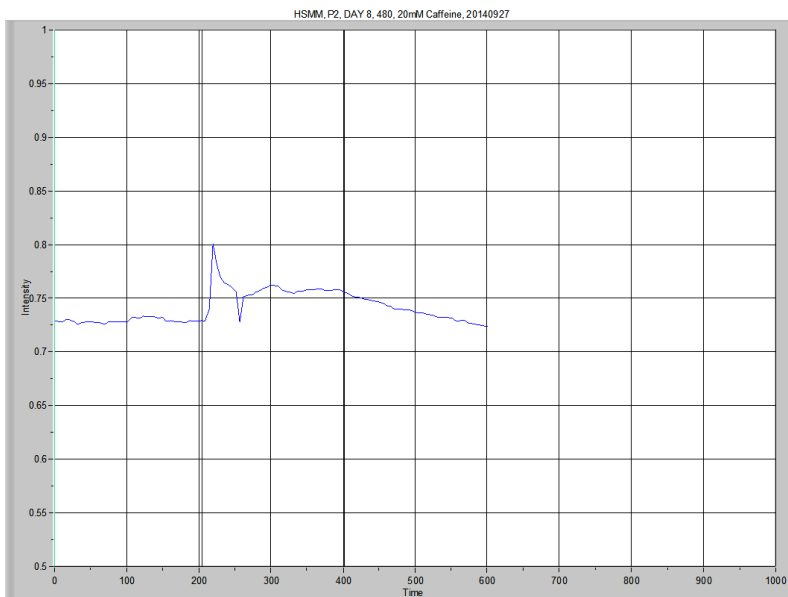
HSMM, P2, DAY 8, 480, 20mM Caffeine, 20140927

	Average resting level	Peak	Δ Level	Time to Peak	Area Under the Curve Low X: 203.964 High X: 601.158	Peak Area
480, P5	0.728701	0.800558	0.071858	5.36745	296.75194	8.26828
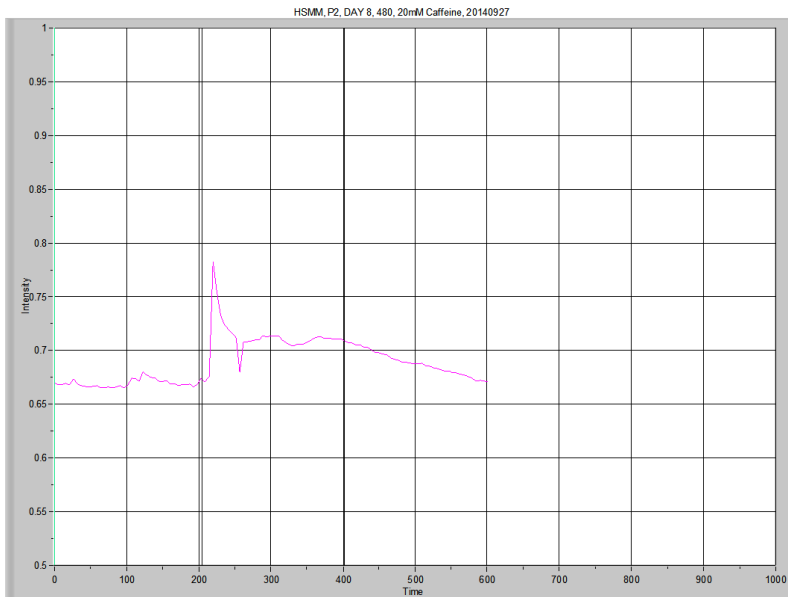
HSMM, P2, DAY 8, 480, 20mM Caffeine, 20140927

	Average resting level	Peak	Δ Level	Time to Peak	Area Under the Curve Low X: 203.964 High X: 601.158	Peak Area
480, P6	0.669124	0.78251	0.113386	5.36745	277.73645	10.61732
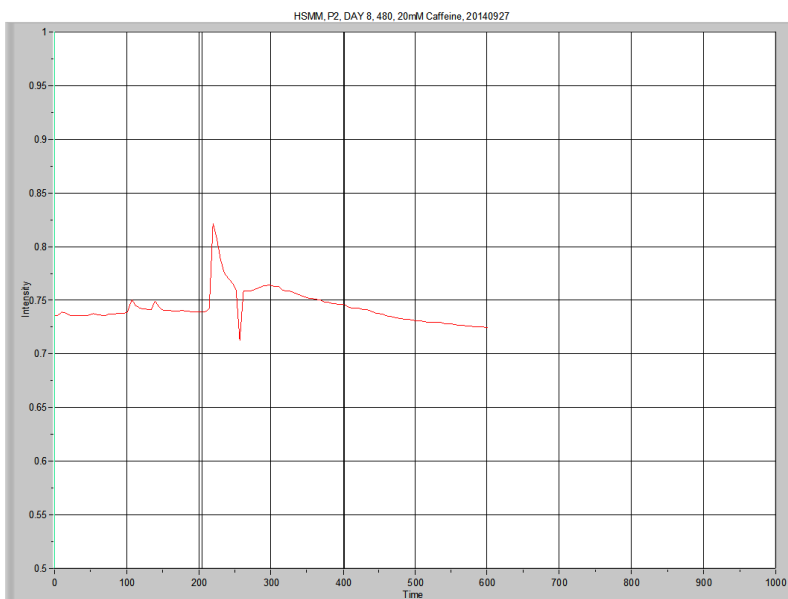
HSMM, P2, DAY 8, 480, 20mM Caffeine, 20140927

	Average resting level	Peak	Δ Level	Time to Peak	Area Under the Curve Low X: 203.964 High X: 601.158	Peak Area
480, P7	0.738821	0.821046	0.082225	10.73492	295.95079	5.40545
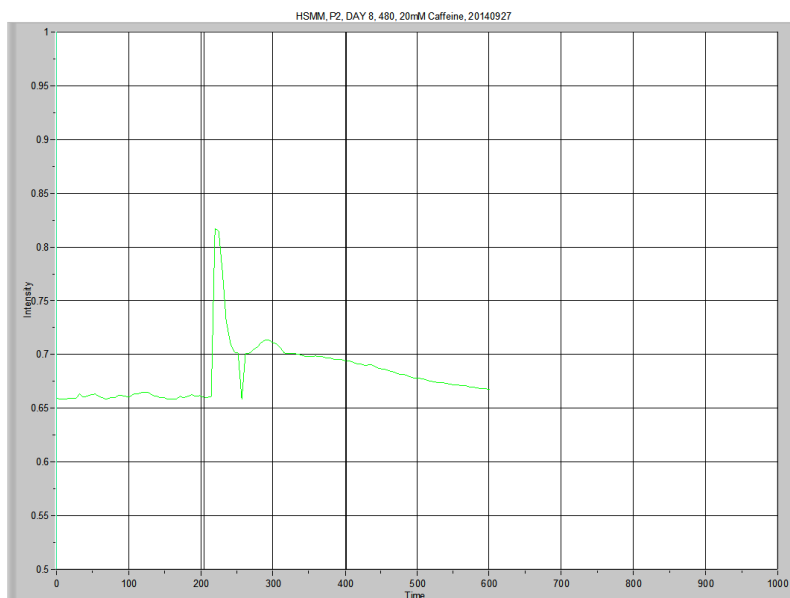
HSMM, P2, DAY 8, 480, 20mM Caffeine, 20140927

	Average resting level	Peak	Δ Level	Time to Peak	Area Under the Curve Low X: 203.964 High X: 601.158	Peak Area
480, P8	0.660438	0.816701	0.156262	5.36745	275.04256	11.55687
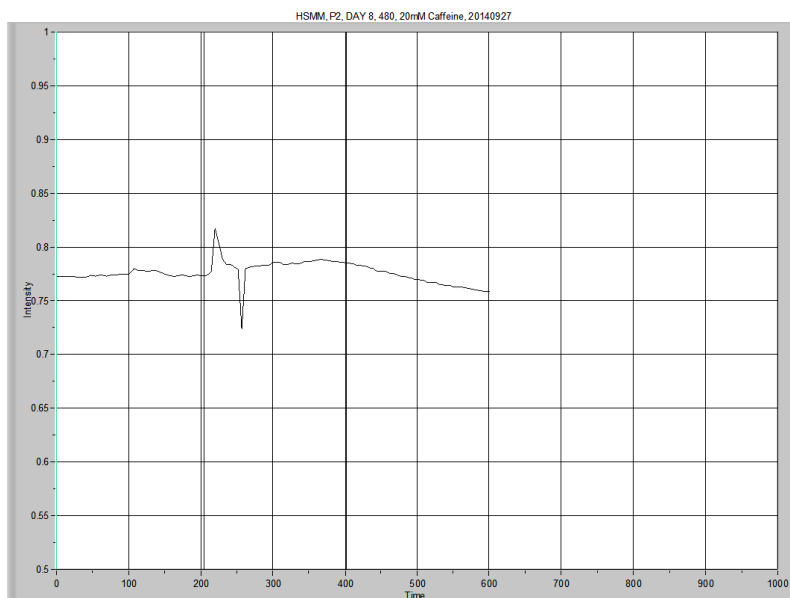
HSMM, P2, DAY 8, 480, 20mM Caffeine, 20140927

	Average resting level	Peak	Δ Level	Time to Peak	Area Under the Curve Low X: 203.964 High X: 601.158	Peak Area
480, P9	0.773932	0.816886	0.042953	10.73492	308.50199	4.33436
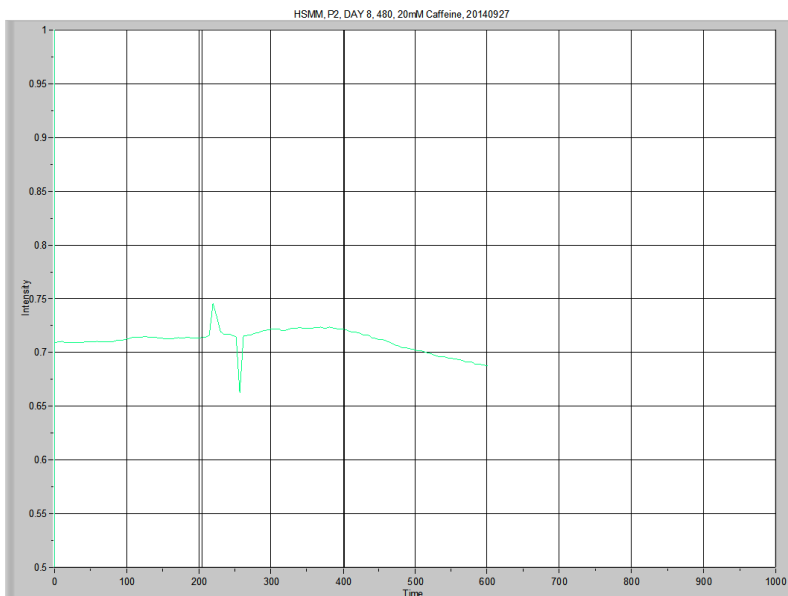
246

HSMM, P2, DAY 8, 480, 20mM Caffeine, 20140927

	Average resting level	Peak	Δ Level	Time to Peak	Area Under the Curve Low X: 203.964 High X: 601.158	Peak Area
480, P10	0.711182	0.745225	0.034043	5.36745	282.32935	4.15956
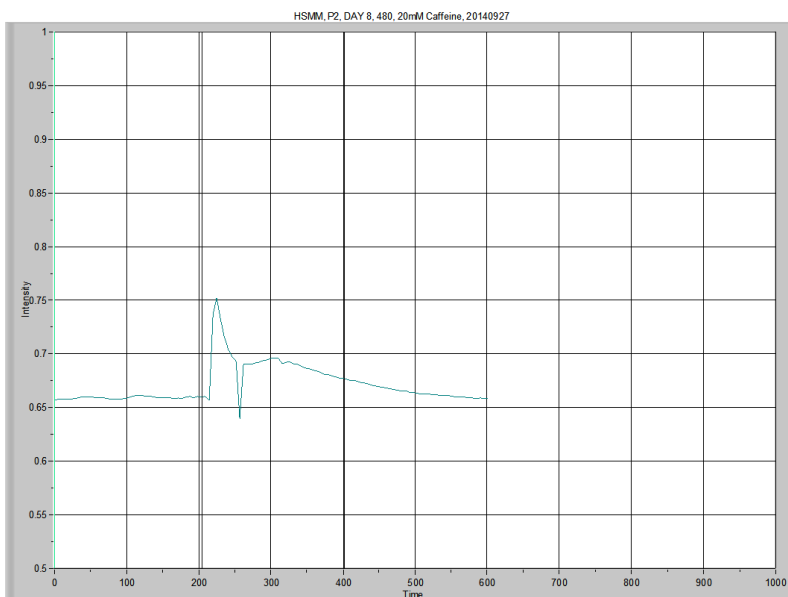
HSMM, P2, DAY 8, 480, 20mM Caffeine, 20140927

	Average resting level	Peak	Δ Level	Time to Peak	Area Under the Curve Low X: 203.964 High X: 601.158	Peak Area
480, P11	0.65871	0.751579	0.092869	21.46995	269.03958	7.33642
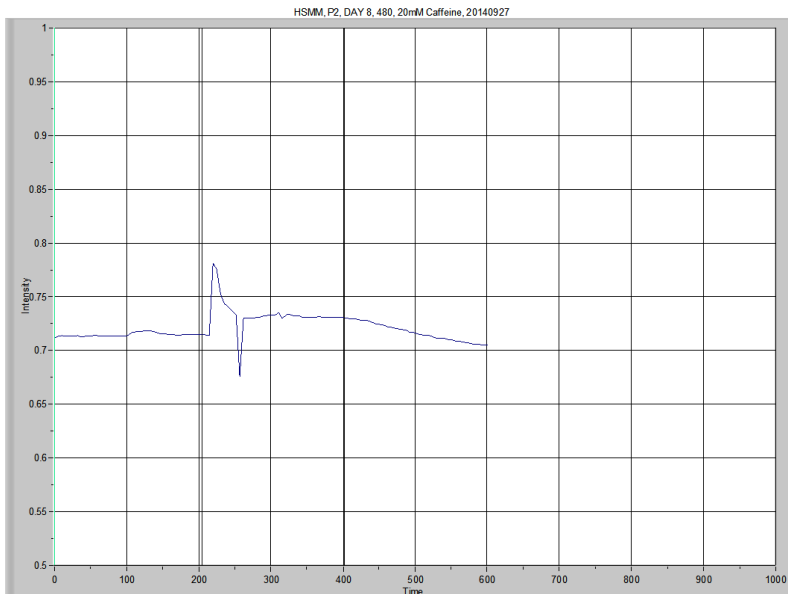
247

HSMM, P2, DAY 8, 480, 20mM Caffeine, 20140927

	Average resting level	Peak	Δ Level	Time to Peak	Area Under the Curve Low X: 203.964 High X: 601.158	Peak Area
480, P12	0.714152	0.780583	0.066431	5.36745	287.64080	5.91531
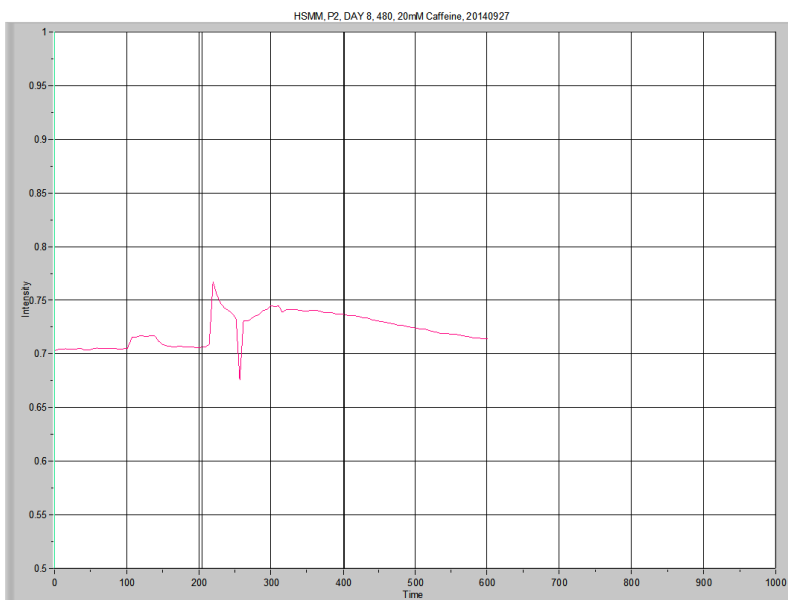
HSMM, P2, DAY 8, 480, 20mM Caffeine, 20140927

	Average resting level	Peak	Δ Level	Time to Peak	Area Under the Curve Low X: 203.964 High X: 601.158	Peak Area
480, P13	0.707212	0.766987	0.059775	5.36745	289.92484	7.97509
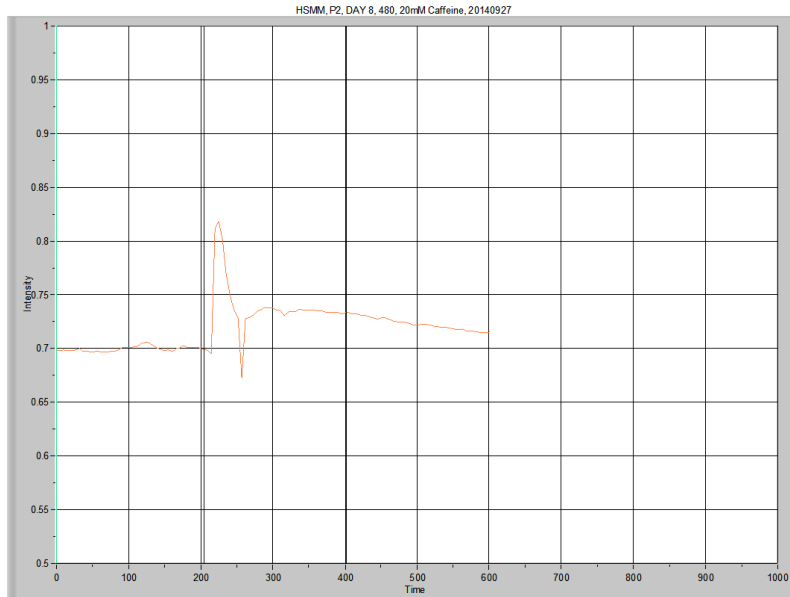
248

HSMM, P2, DAY 8, 480, 20mM Caffeine, 20140927

	Average resting level	Peak	Δ Level	Time to Peak	Area Under the Curve Low X: 203.964 High X: 601.158	Peak Area
480, P14	0.699199	0.817549	0.118351	5.367502	289.78603	9.00156

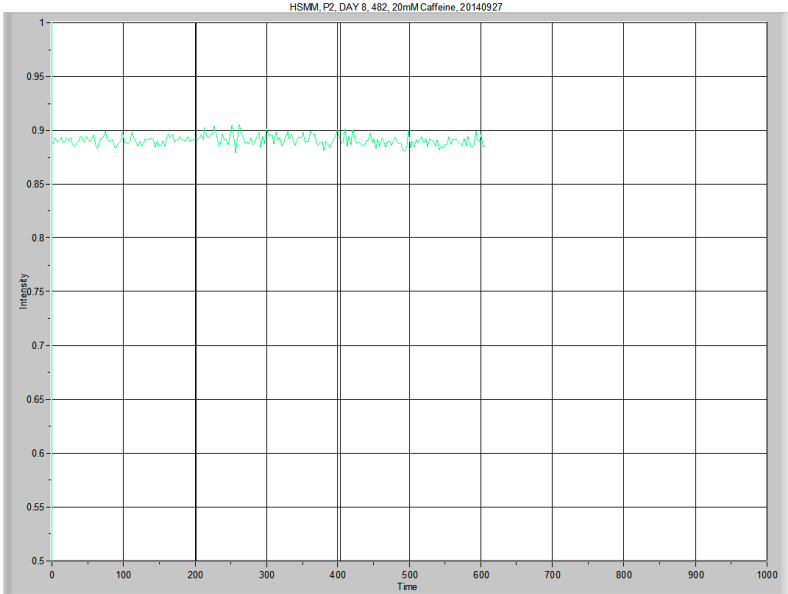HSMM, P2, DAY 8, 480, 20mM Caffeine, 20140927
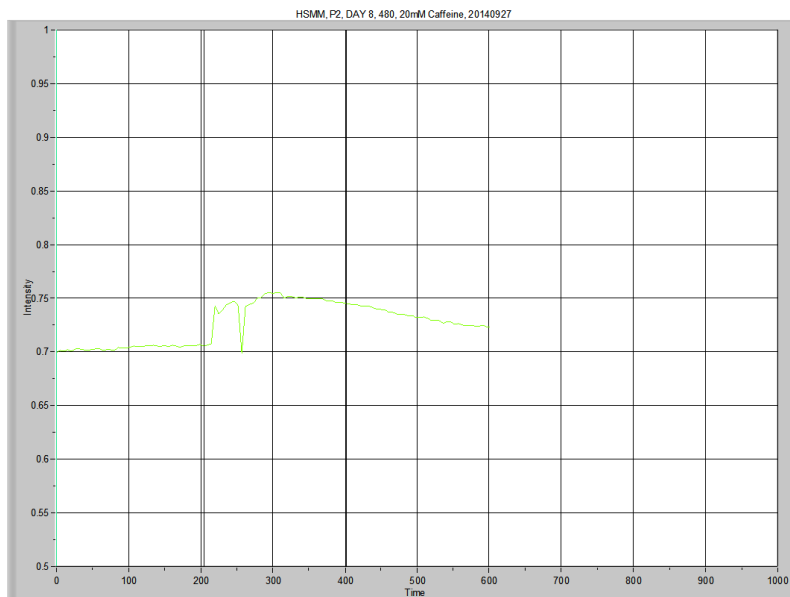
I did not use the data from this tracing, as the myotube apparently moved with stimulation.

	Average resting level	Peak	Δ Level	Time to Peak	Area Under the Curve	Peak Area
					Low X: 203.964 High X: 601.158	
480, P15	0.70206	0.755093	0.053032	Unable to determine	293.13022	9.56464
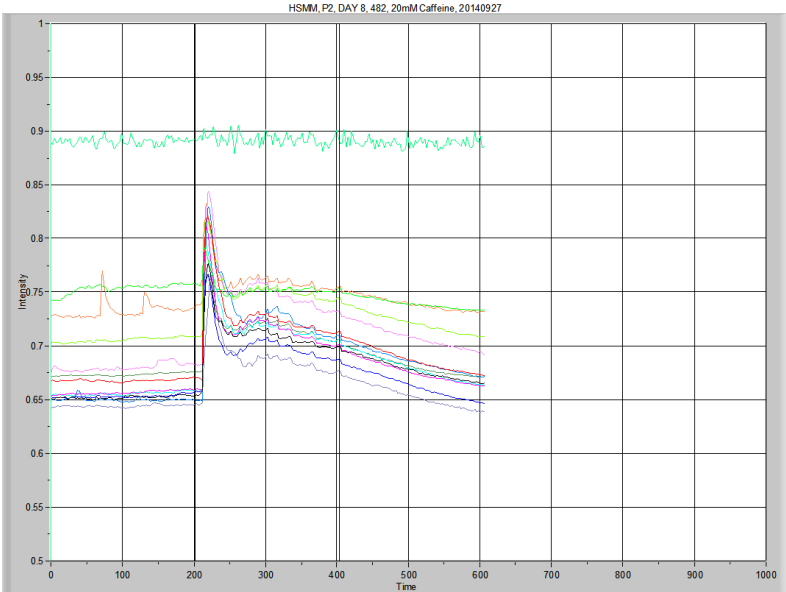
249

Overview

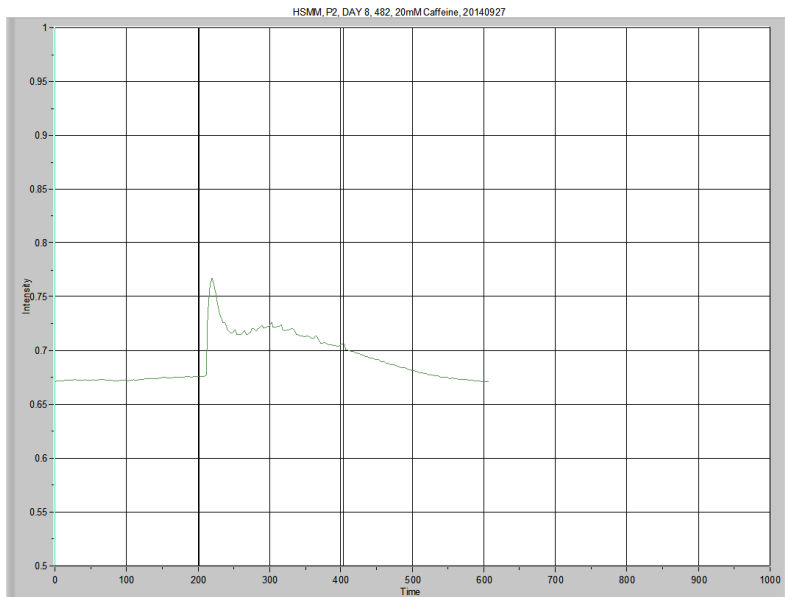|	Average resting level	Peak	Δ Level	Time to Peak	Area Under the Curve Low X: 201.28 High X: 598.475	Peak Area
482, BG	0.89016	0.90537	0.01521	NA	353.68479	-0.19022

HSMM, P2, DAY 8, 482, 20mM Caffeine, 20140927
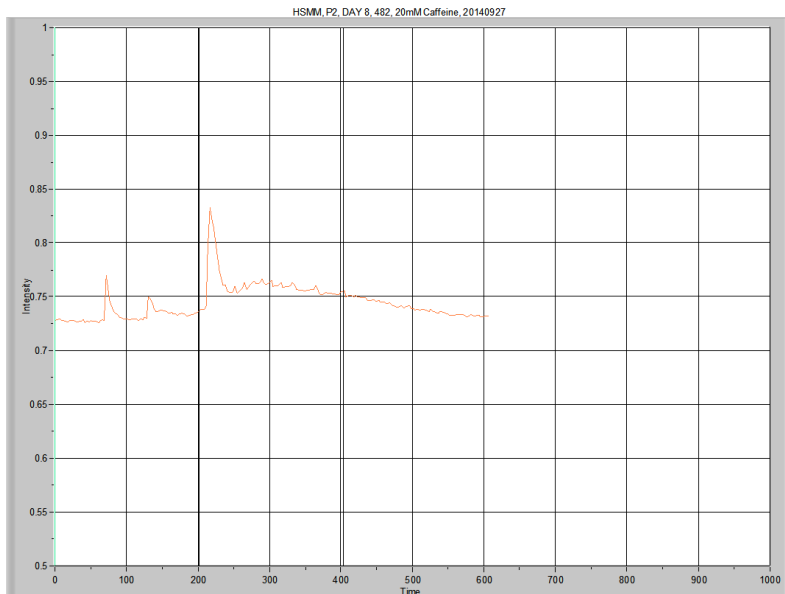
I did not use the data from this tracing due to the unexplained peaks prior to20mM caffeine.
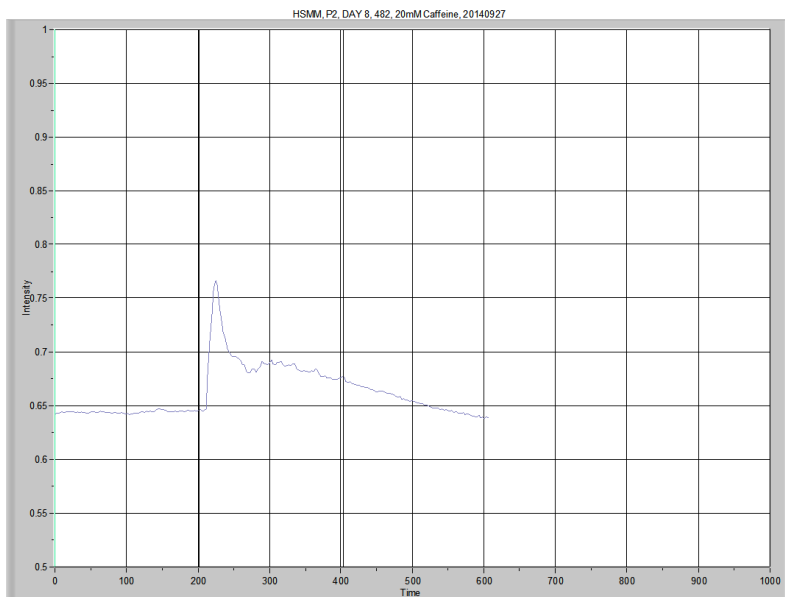
	Average resting level (prior to first premature spike)	Peak	Δ Level	Time to Peak	Area Under the Curve Low X: 201.28 High X: 598.475	Peak Area
482, P1	*0.7272*	*0.83279*	*0.105589*	5.36748	298.10550	6.83122
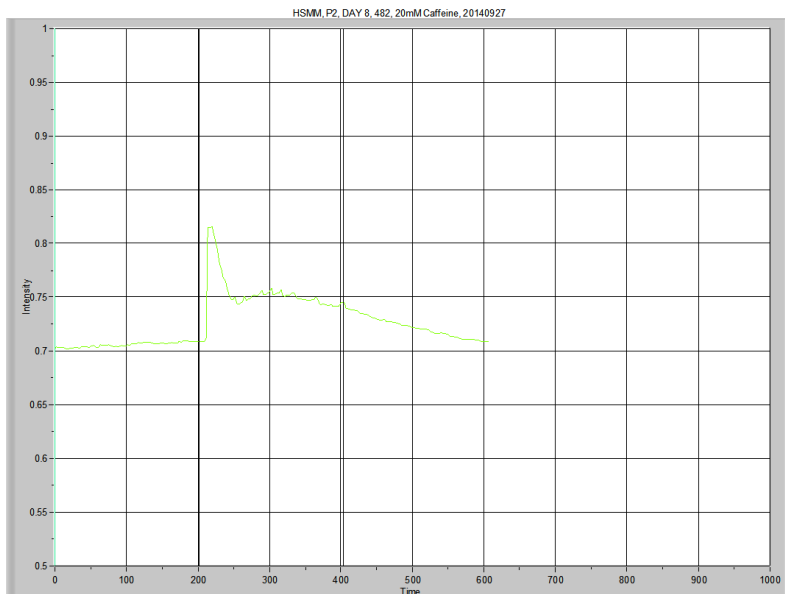
HSMM, P2, DAY 8, 482, 20mM Caffeine, 20140927

	Average resting level	Peak	Δ Level	Time to Peak	Area Under the Curve Low X: 201.28 High X: 598.475	Peak Area
482, P2	0.705393	0.815412	0.110019	5.367479	293.03694	11.58244

251

	Average resting level	Peak	Δ Level	Time to Peak	Area Under the Curve Low X: 201.28 High X: 598.475	Peak Area
482, P3	0.672968	0.76739	0.094421	8.051202	278.07143	10.73985

	Average resting level	Peak	Δ Level	Time to Peak	Area Under the Curve Low X: 201.28 High X: 598.475	Peak Area
482, P4	0.643841	0.766411	0.12257	13.4187	266.92493	11.86573
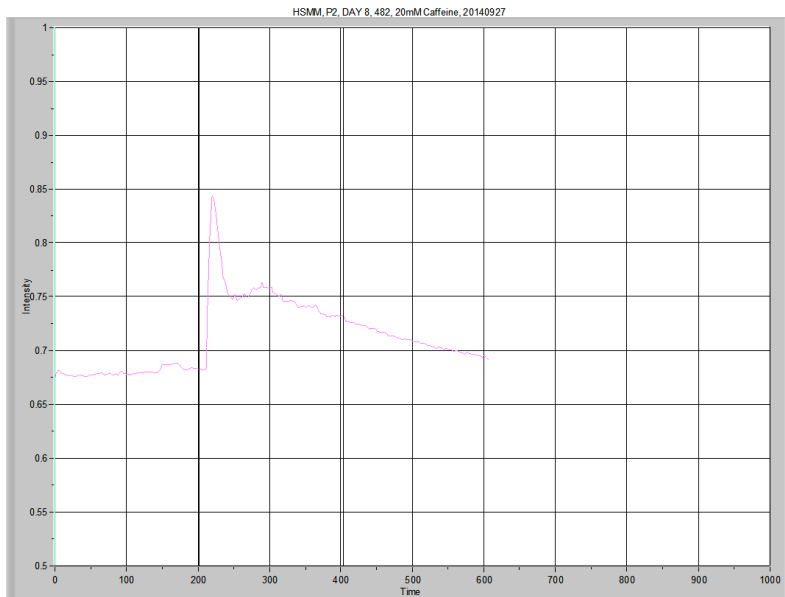
252

HSMM, P2, DAY 8, 482, 20mM Caffeine, 20140927

	Average resting level	Peak	Δ Level	Time to Peak	Area Under the Curve Low X: 201.28 High X: 598.475	Peak Area
482, P5	0.679852	0.843902	0.16405	10.73491	289.78241	16.62226
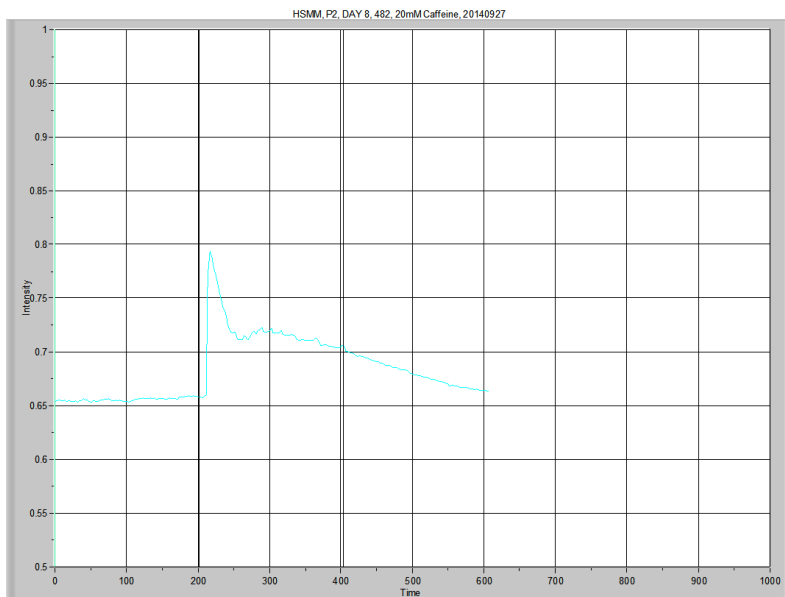
HSMM, P2, DAY 8, 482, 20mM Caffeine, 20140927

	Average resting level	Peak	Δ Level	Time to Peak	Area Under the Curve Low X: 201.28 High X: 598.475	Peak Area
482, P6	0.655444	0.7935	0.138056	8.051185	277.64755	15.18204
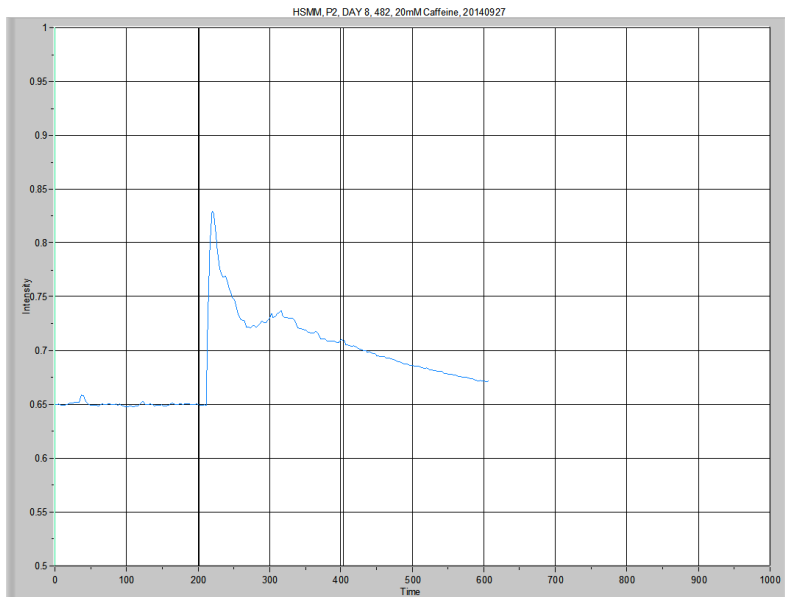
253

HSMM, P2, DAY 8, 482, 20mM Caffeine, 20140927

	Average resting level	Peak	Δ Level	Time to Peak	Area Under the Curve Low X: 201.28 High X: 598.475	Peak Area
482, P7	0.649809	0.829643	0.179835	8.051202	281.21981	18.84237
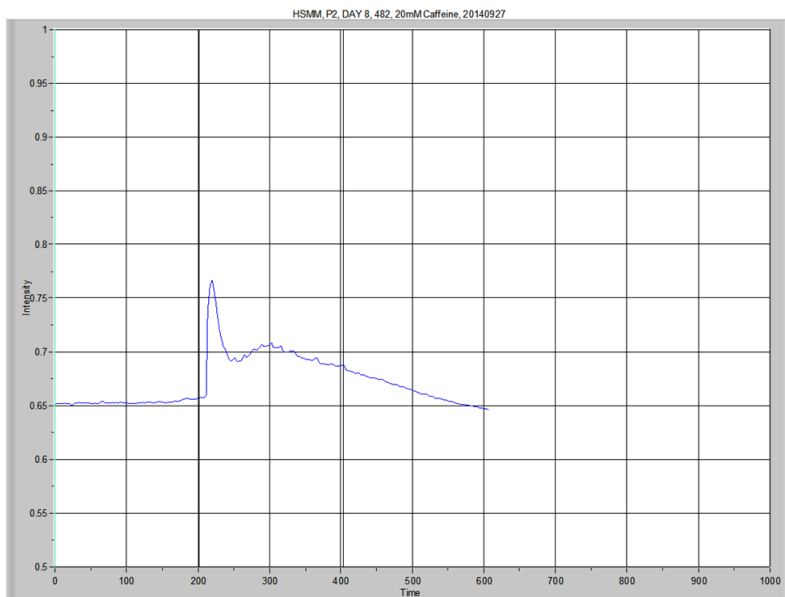
HSMM, P2, DAY 8, 482, 20mM Caffeine, 20140927

	Average resting level	Peak	Δ Level	Time to Peak	Area Under the Curve Low X: 201.28 High X: 598.475	Peak Area
482, P8	0.652778	0.766267	0.113489	10.73491	270.88564	11.92615
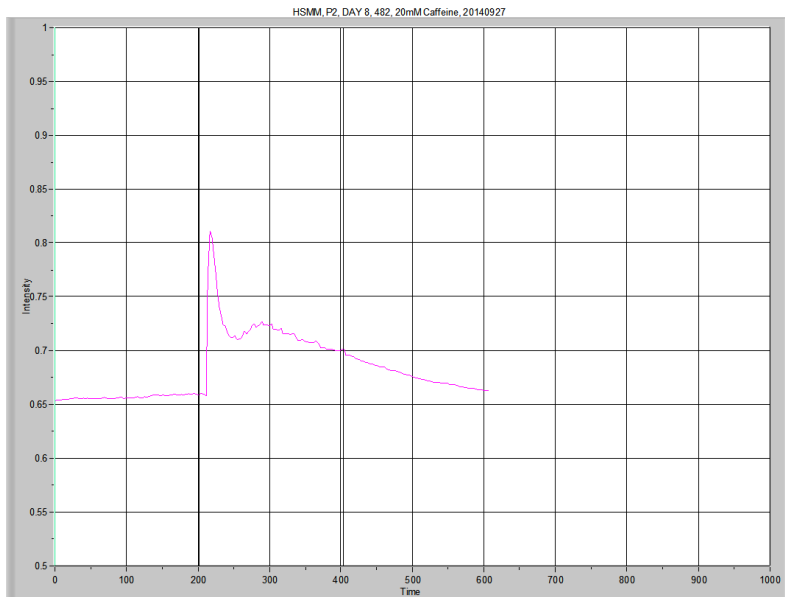
254

HSMM, P2, DAY 8, 482, 20mM Caffeine, 20140927

	Average resting level	Peak	Δ Level	Time to Peak	Area Under the Curve Low X: 201.28 High X: 598.475	Peak Area
482, P9	0.656377	0.810791	0.154414	2.683706	276.77660	14.33207
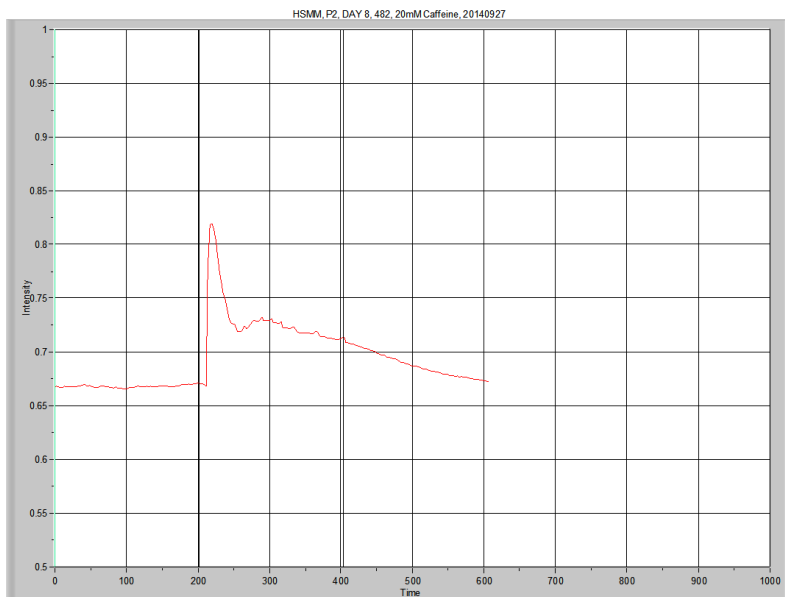
HSMM, P2, DAY 8, 482, 20mM Caffeine, 20140927

	Average resting level	Peak	Δ Level	Time to Peak	Area Under the Curve Low X: 201.28 High X: 598.475	Peak Area
482, P10	0.667594	0.818949	0.151354	5.367428	281.31901	14.44325
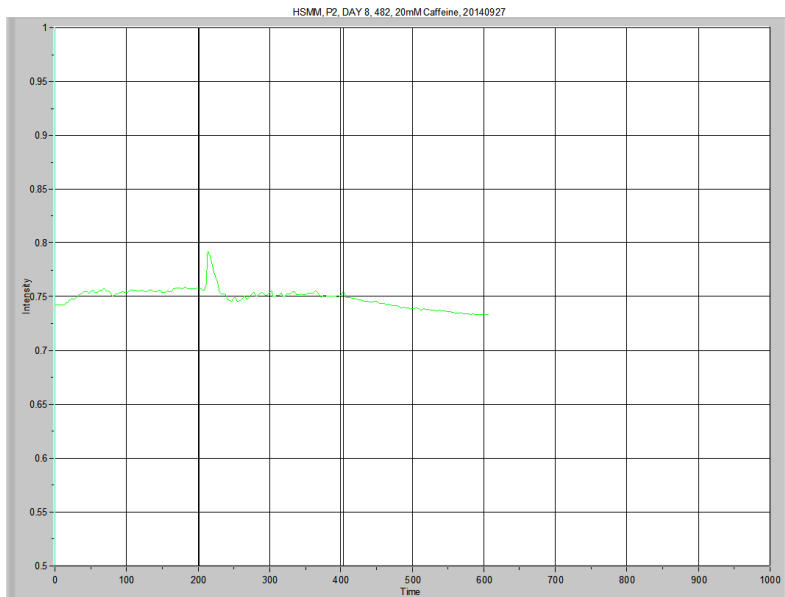
	Average resting level	Peak	Δ Level	Time to Peak	Area Under the Curve Low X: 201.28 High X: 598.475	Peak Area
482, P11	0.753203	0.792483	0.03928	2.683774	296.65582	0.68882
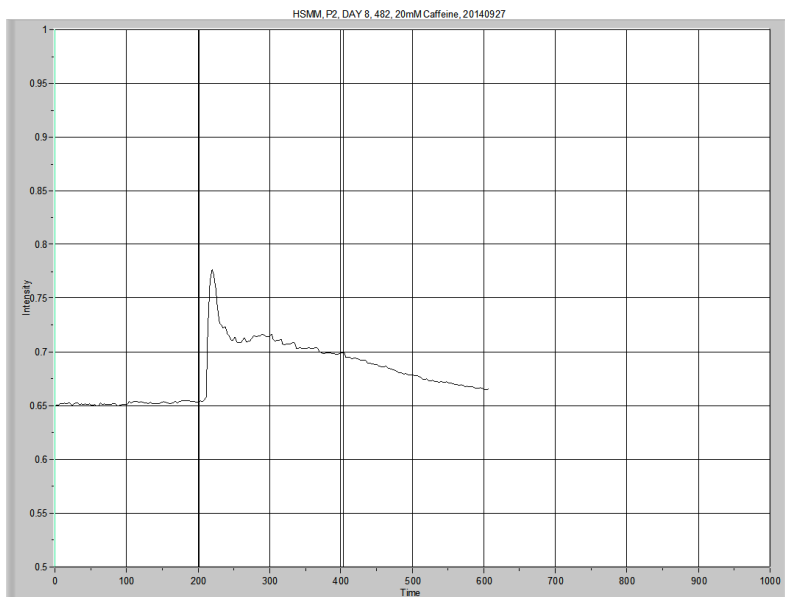
	Average resting level	Peak	Δ Level	Time to Peak	Area Under the Curve Low X: 201.28 High X: 598.475	Peak Area
482, P12	0.651929	0.776972	0.125043	10.73491	275.72802	13.82621
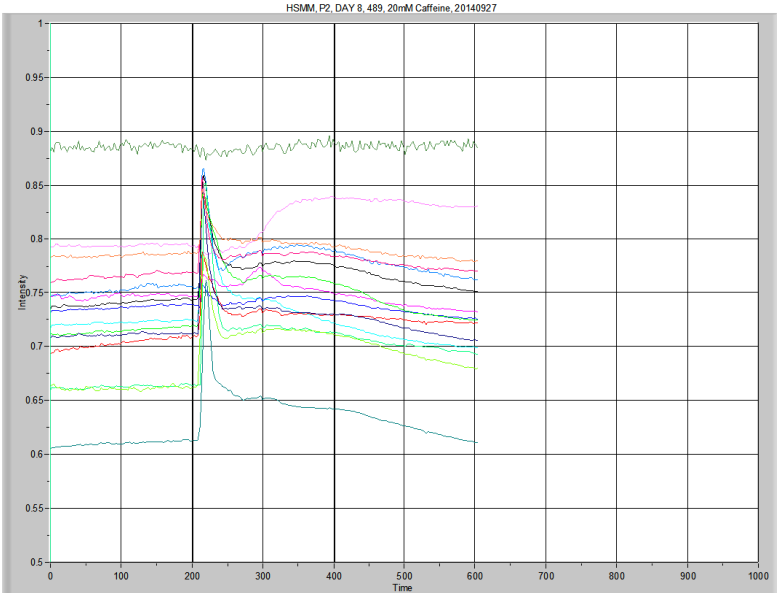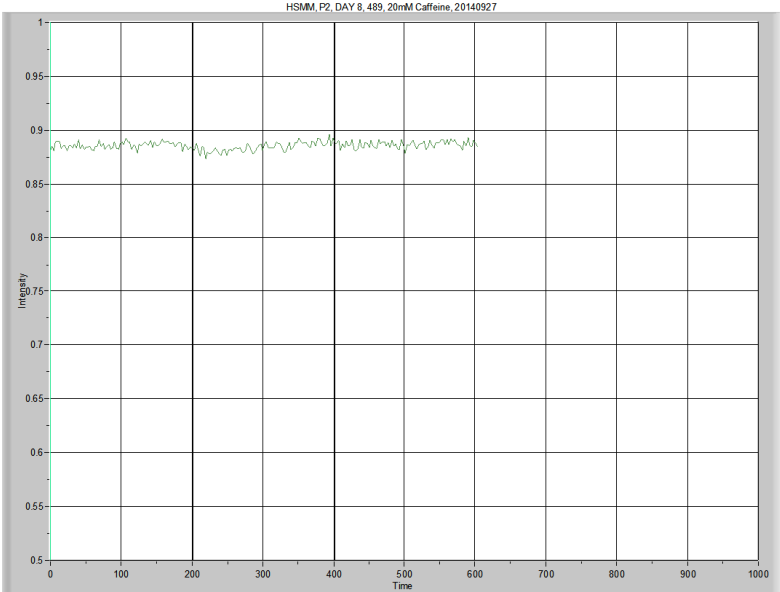
256

Overview

	Average resting level	Peak	Δ Level	Time to Peak	Area Under the Curve Low X: 201.28 High X: 598.475	Peak Area
489, BG	0.885414	0.895248	0.009834	NA	351.50493	-0.63925

HSMM, P2, DAY 8, 489, 20mM Caffeine, 20140927
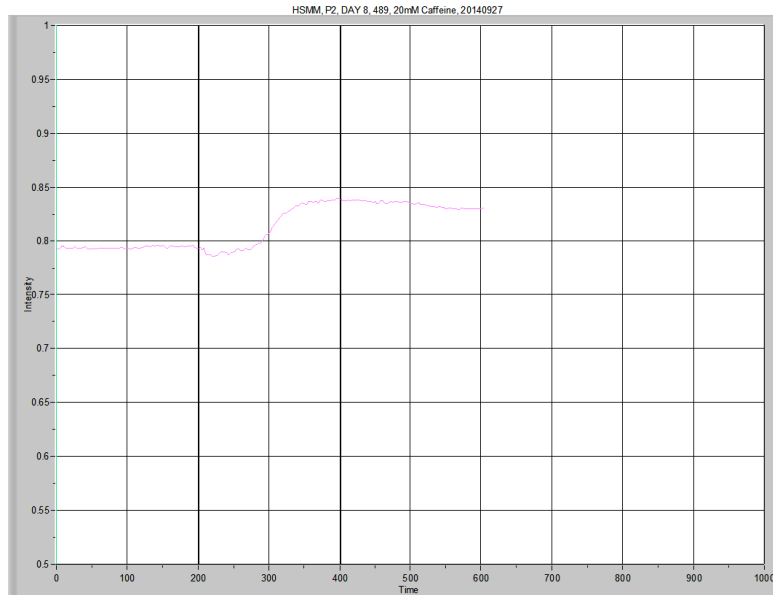
It looks as though this myotube floated out of ROI range with stimulation, so did not use this data.

	Average resting level	Peak	Δ Level	Time to Peak	Area Under the Curve Low X: 201.28 High X: 598.475	Peak Area
489, P1					326.68863	4.53732
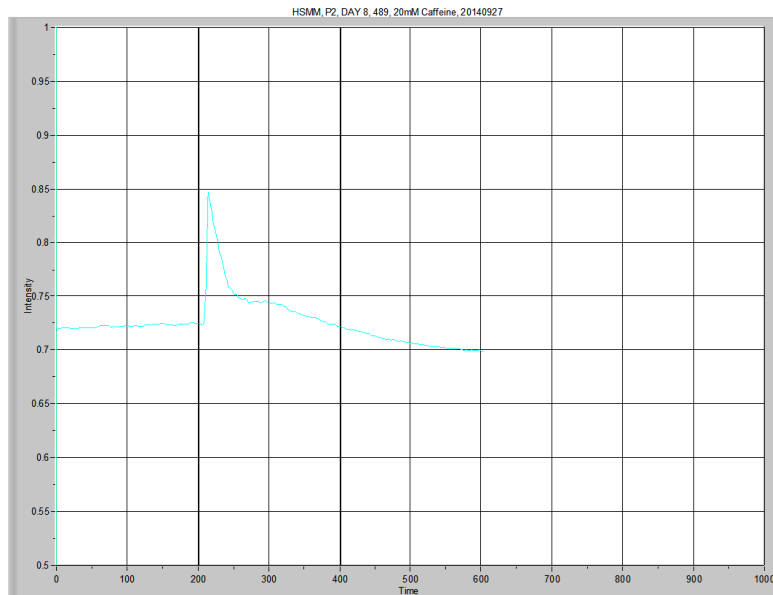
HSMM, P2, DAY 8, 489, 20mM Caffeine, 20140927

	Average resting level	Peak	Δ Level	Time to Peak	Area Under the Curve Low X: 201.28 High X: 598.475	Peak Area
489, P2	0.722022	0.846459	0.124437	5.367519	289.02905	6.20696
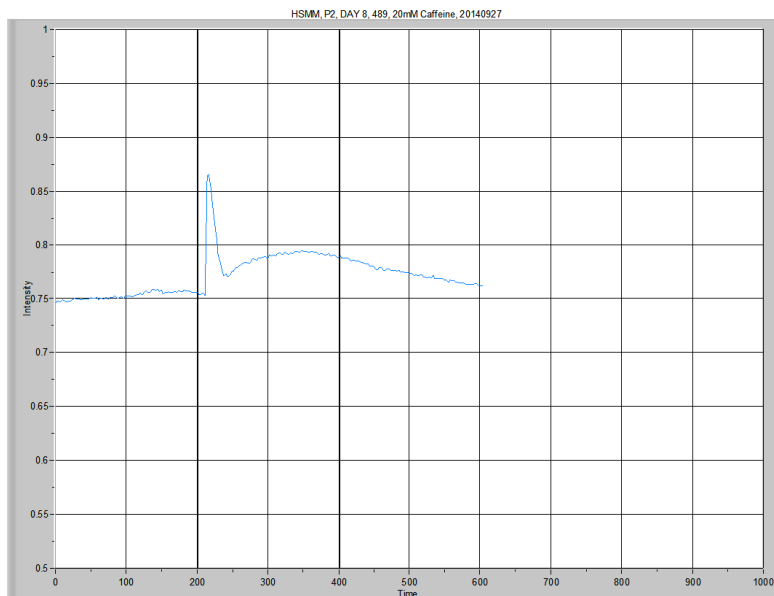
258

HSMM, P2, DAY 8, 489, 20mM Caffeine, 20140927

	Average resting level	Peak	Δ Level	Time to Peak	Area Under the Curve Low X: 201.28 High X: 598.475	Peak Area
489, P3	0.752488	0.865183	0.112695	5.367497	310.54630	9.23436
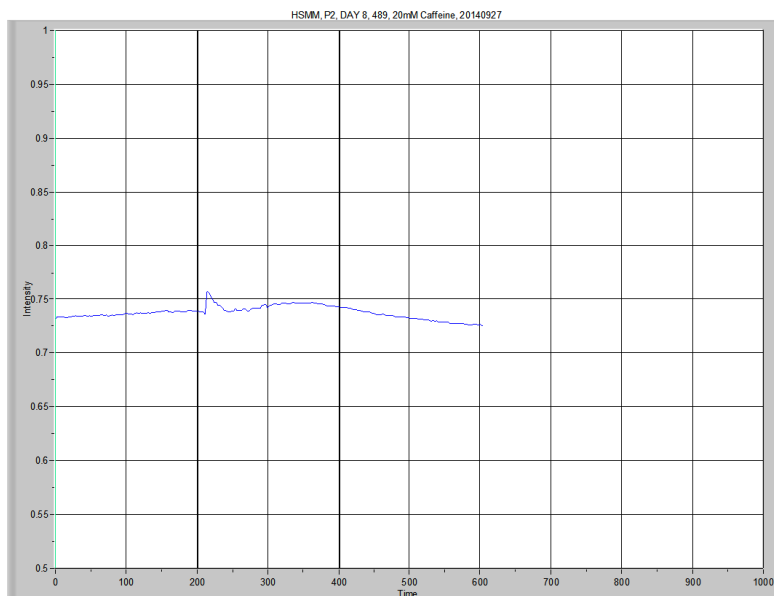
HSMM, P2, DAY 8, 489, 20mM Caffeine, 20140927

	Average resting level	Peak	Δ Level	Time to Peak	Area Under the Curve Low X: 201.28 High X: 598.475	Peak Area
489, P4	0.735965	0.757536	0.021571	2.683806	293.25098	2.44157
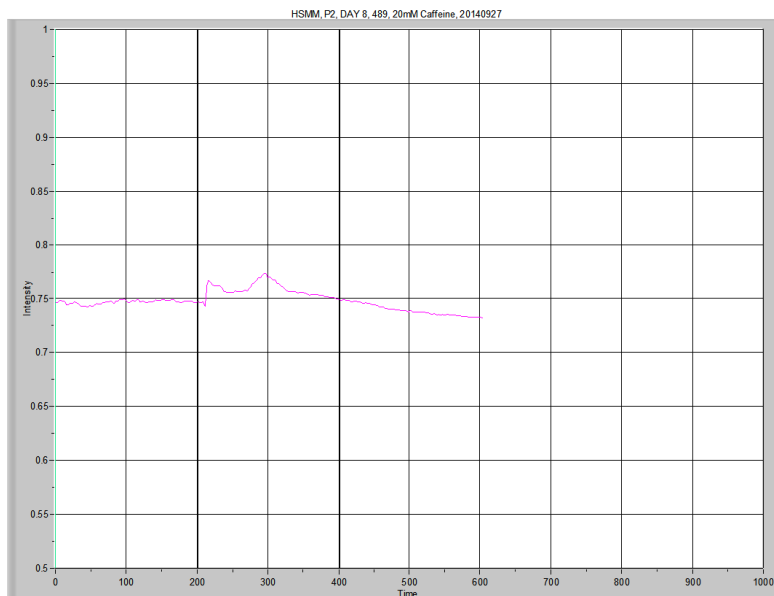
259

HSMM, P2, DAY 8, 489, 20mM Caffeine, 20140927

	Average resting level	Peak	Δ Level	Time to Peak	Area Under the Curve Low X: 201.28 High X: 598.475	Peak Area
489, P5	0.746617	0.773257 0.766897	0.02664 0.02028	2.683691 80.51224	297.40509	3.57629
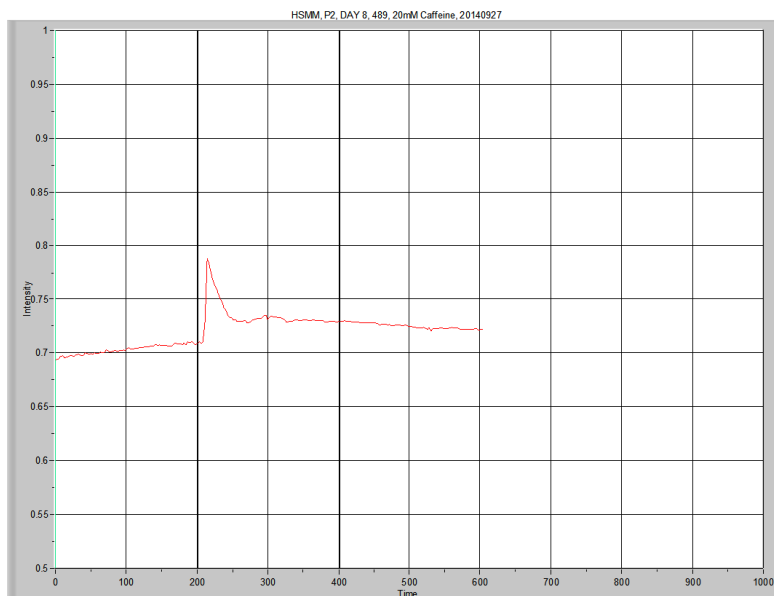
HSMM, P2, DAY 8, 489, 20mM Caffeine, 20140927

	Average resting level	Peak	Δ Level	Time to Peak	Area Under the Curve Low X: 201.28 High X: 598.475	Peak Area
489, P6	0.702732	0.787571	0.08484	2.683806	289.76956	5.75315
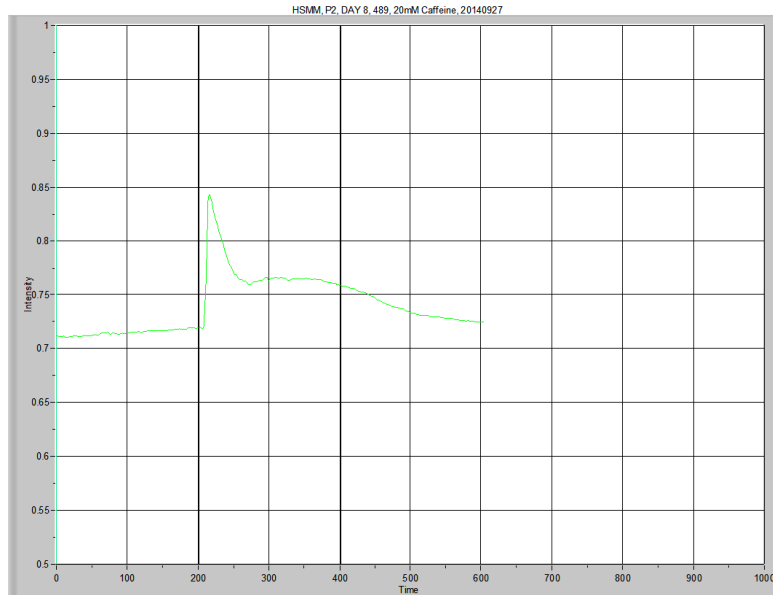
260

HSMM, P2, DAY 8, 489, 20mM Caffeine, 20140927

	Average resting level	Peak	Δ Level	Time to Peak	Area Under the Curve Low X: 201.28 High X: 598.475	Peak Area
489, P7	0.714466	0.842757	0.128291	13.41871	299.30246	12.48830
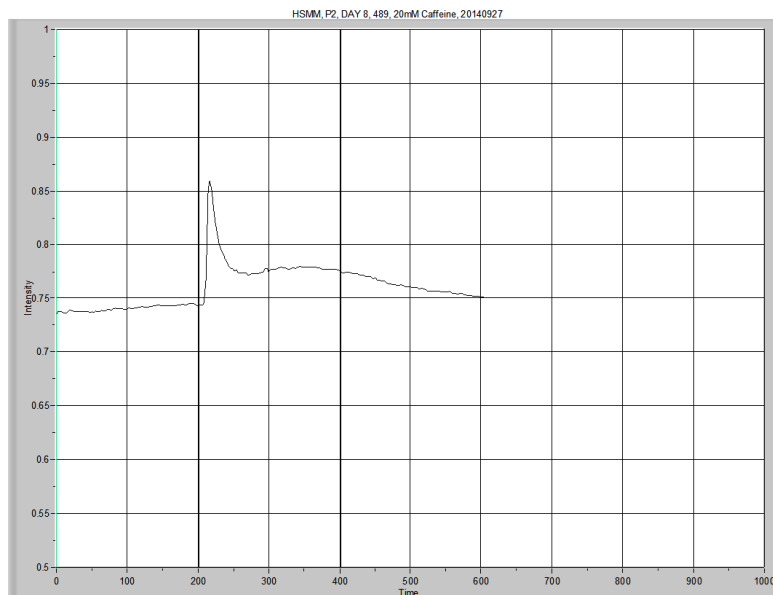
HSMM, P2, DAY 8, 489, 20mM Caffeine, 20140927

	Average resting level	Peak	Δ Level	Time to Peak	Area Under the Curve Low X: 201.28 High X: 598.475	Peak Area
489, P8	0.740209	0.858683	0.118474	8.05121	306.26785	9.54928
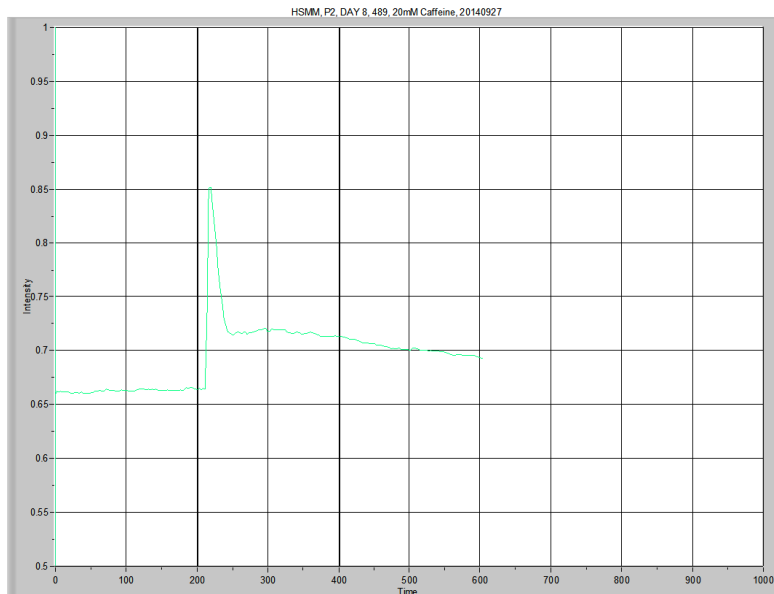
261

HSMM, P2, DAY 8, 489, 20mM Caffeine, 20140927

	Average resting level	Peak	Δ Level	Time to Peak	Area Under the Curve Low X: 201.28 High X: 598.475	Peak Area
489, P9	0.66254	0.85132	0.18878	5.367449	282.99484	13.38245
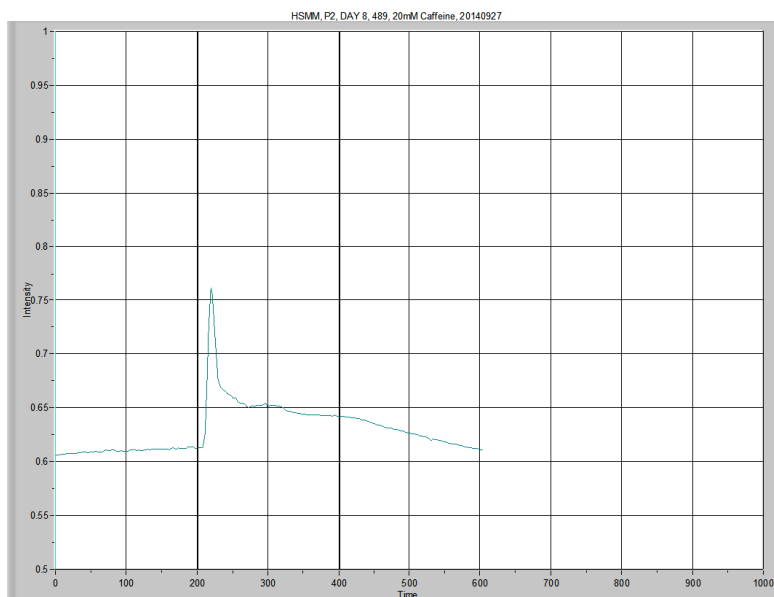
HSMM, P2, DAY 8, 489, 20mM Caffeine, 20140927

	Average resting level	Peak	Δ Level	Time to Peak	Area Under the Curve Low X: 201.28 High X: 598.475	Peak Area
489, P10	0.608372967	0.761803	0.151919	10.73497	254.39080	11.34047
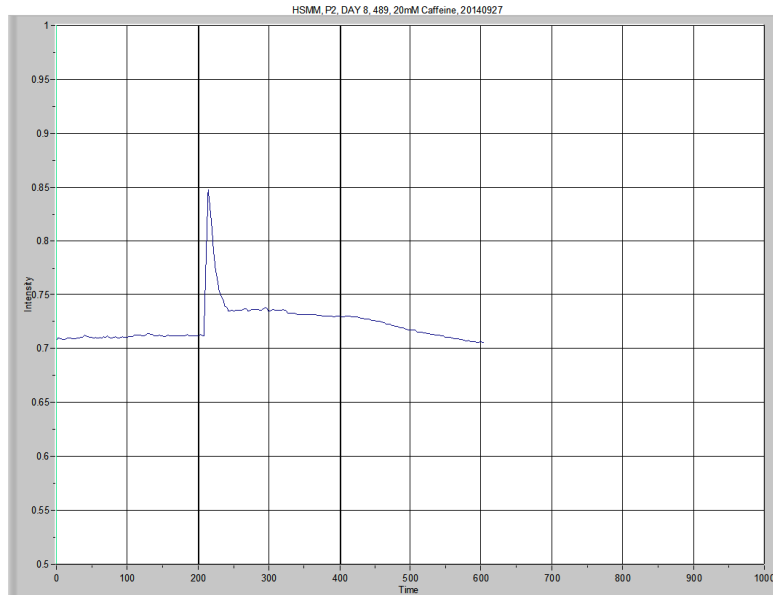
262

HSMM, P2, DAY 8, 489, 20mM Caffeine, 20140927

	Average resting level	Peak	Δ Level	Time to Peak	Area Under the Curve Low X: 201.28 High X: 598.475	Peak Area
489, P11	0.71078	0.847666	0.136886	2.683806	289.46645	7.83076
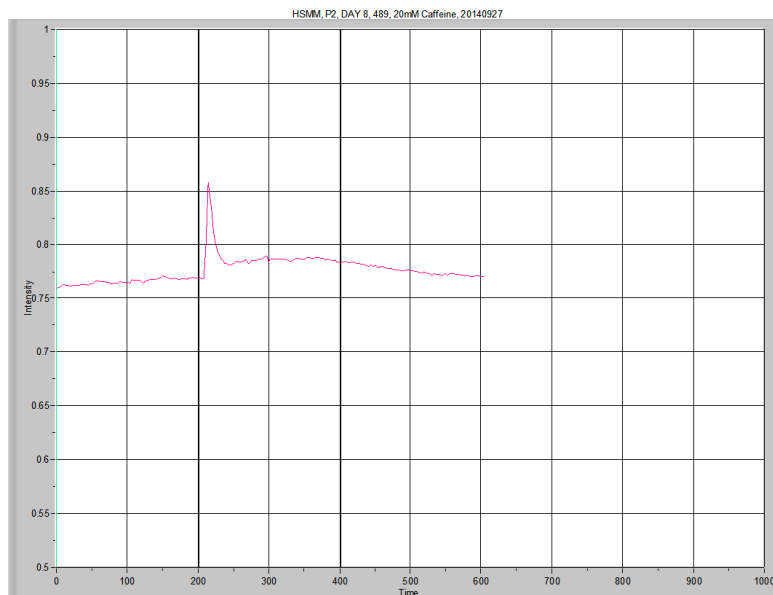
HSMM, P2, DAY 8, 489, 20mM Caffeine, 20140927

	Average resting level	Peak	Δ Level	Time to Peak	Area Under the Curve Low X: 201.28 High X: 598.475	Peak Area
489, P12	0.765135	0.857447	0.092312	8.051264	310.55998	4.95591
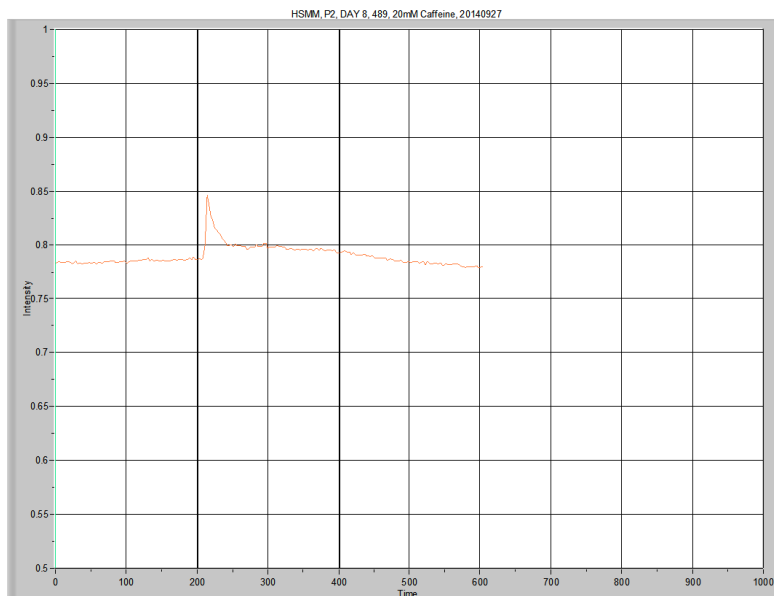
263

HSMM, P2, DAY 8, 489, 20mM Caffeine, 20140927

	Average resting level	Peak	Δ Level	Time to Peak	Area Under the Curve Low X: 201.28 High X: 598.475	Peak Area
489, P13	0.784501	0.845871	0.06137	2.683806	314.75113	4.05643
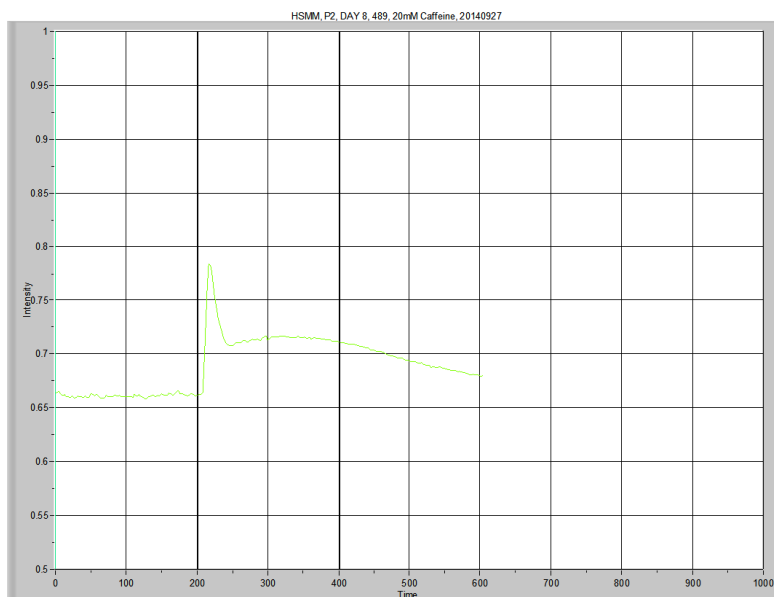
HSMM, P2, DAY 8, 489, 20mM Caffeine, 20140927

	Average resting level	Peak	Δ Level	Time to Peak	Area Under the Curve Low X: 201.28 High X: 598.475	Peak Area
489, P14	0.66108	0.783728	0.122647	16.1024	280.13071	13.67516
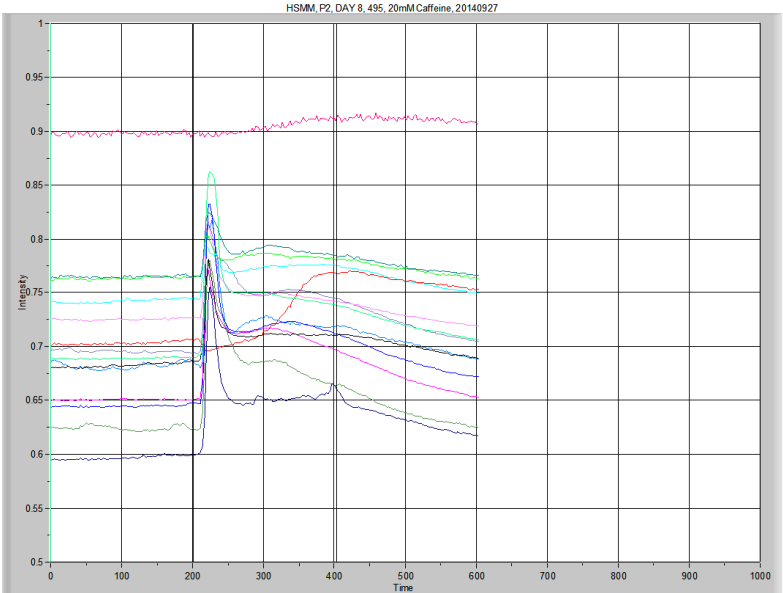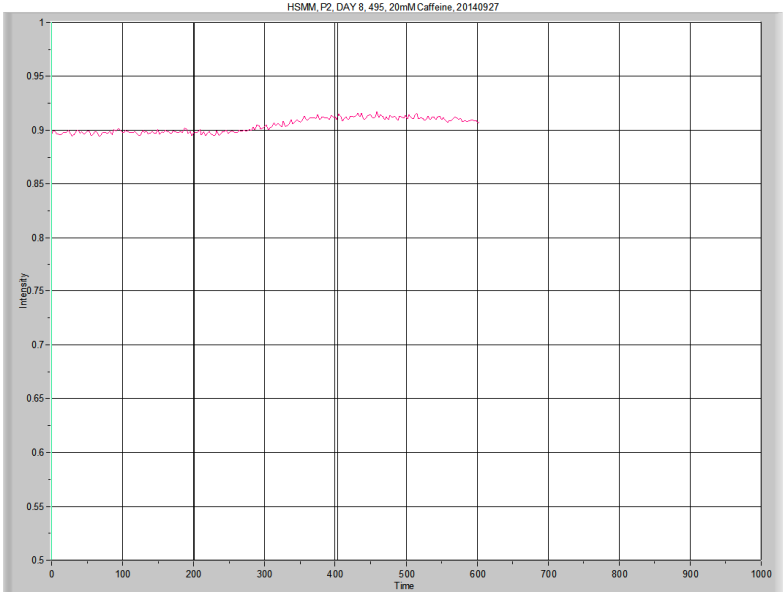
264

Overview

	Average resting level	Peak	Δ Level	Time to Peak	Area Under the Curve Low X: 201.279 High X: 598.471	Peak Area
495, BG	0.897465	0.91656	0.019095	NA	360.28068	1.50335
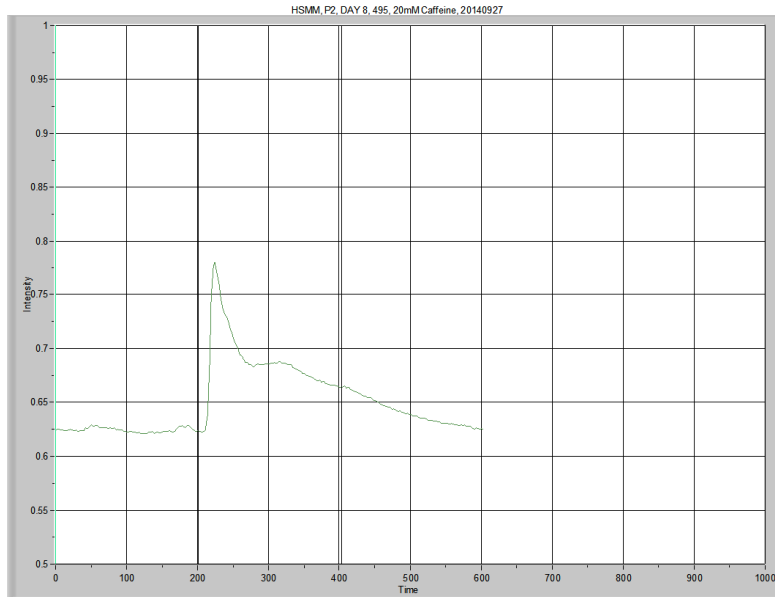
	Average resting level	Peak	Δ Level	Time to Peak	Area Under the Curve Low X: 201.279 High X: 598.471	Peak Area
495, P1	0.624195	0.780105	0.155909	16.10236	263.87300	15.88514
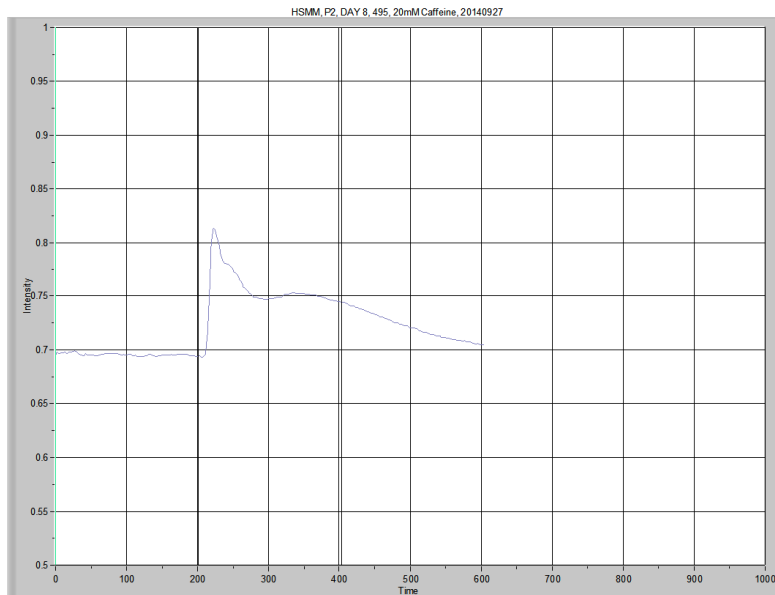
	Average resting level	Peak	Δ Level	Time to Peak	Area Under the Curve Low X: 201.279 High X: 598.471	Peak Area
495, P2	0.695467	0.813328	0.117862	16.10236	293.23368	15.49706
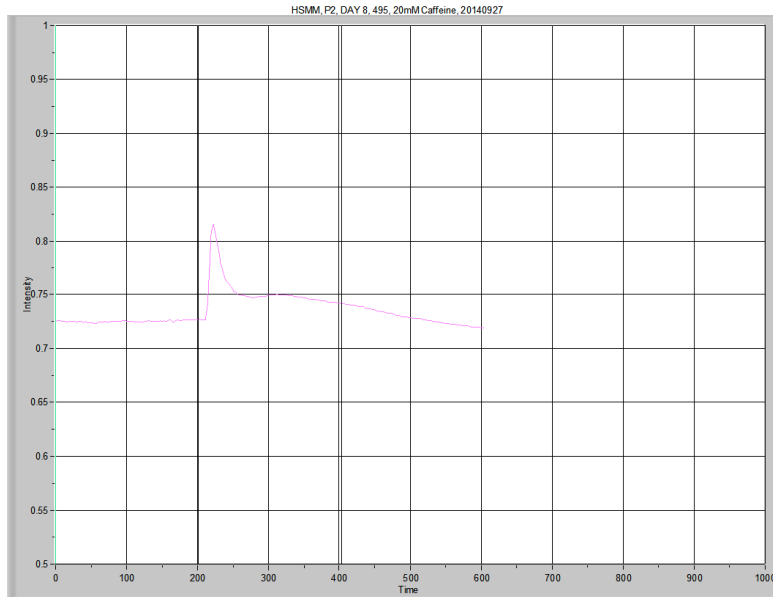
266

HSMM, P2, DAY 8, 495, 20mM Caffeine, 20140927

	Average resting level	Peak	Δ Level	Time to Peak	Area Under the Curve Low X: 201.279 High X: 598.471	Peak Area
495, P3	0.724921	0.814979	0.090058	13.41859	294.18005	6.93120
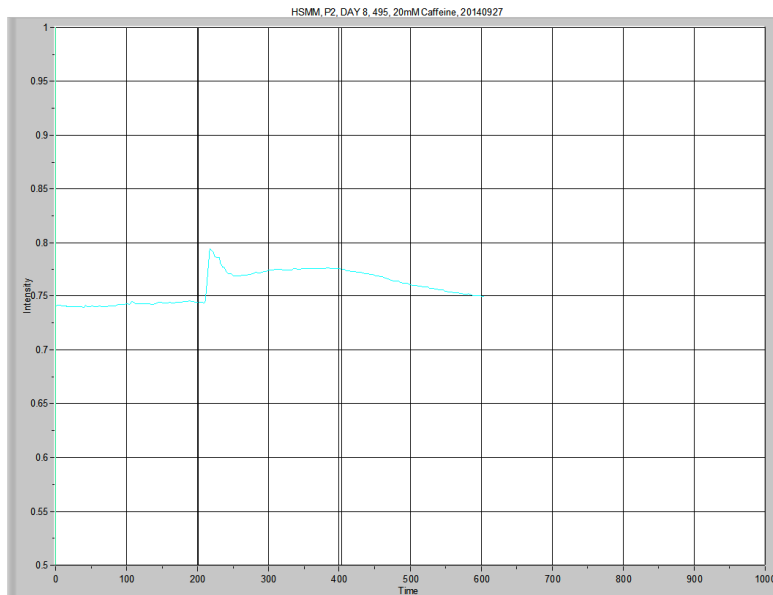
HSMM, P2, DAY 8, 495, 20mM Caffeine, 20140927

	Average resting level	Peak	Δ Level	Time to Peak	Area Under the Curve Low X: 201.279 High X: 598.471	Peak Area
495, P4	0.742057	0.794196	0.052139	5.367431	304.80446	7.89923
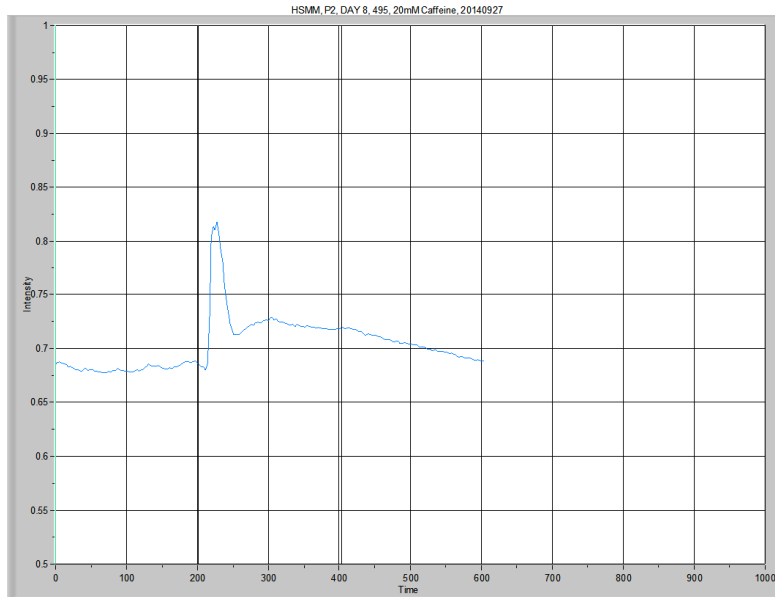
267

HSMM, P2, DAY 8, 495, 20mM Caffeine, 20140927

	Average resting level	Peak	Δ Level	Time to Peak	Area Under the Curve Low X: 201.279 High X: 598.471	Peak Area
495, P5	0.681793	0.817407	0.135614	13.4186	284.17426	11.19224
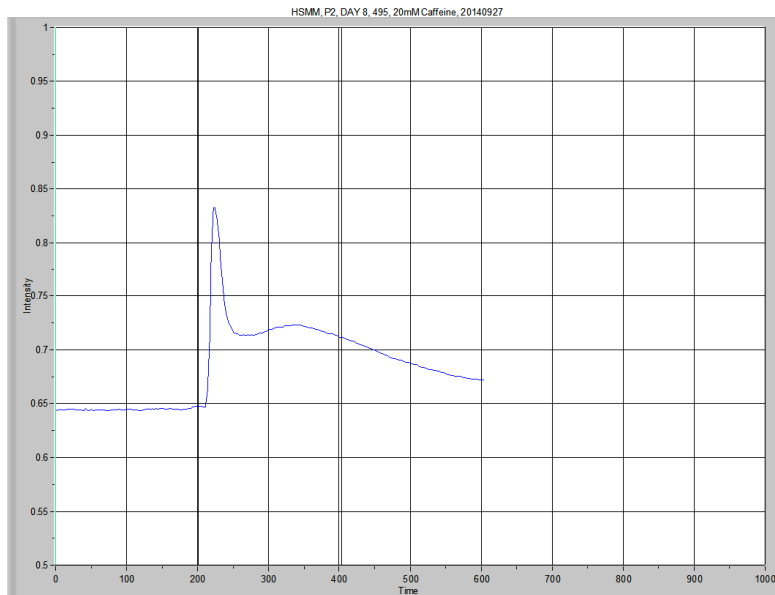
HSMM, P2, DAY 8, 495, 20mM Caffeine, 20140927

	Average resting level	Peak	Δ Level	Time to Peak	Area Under the Curve Low X: 201.279 High X: 598.471	Peak Area
495, P6	0.644412	0.832251	0.187839	13.41863	280.12483	18.11291
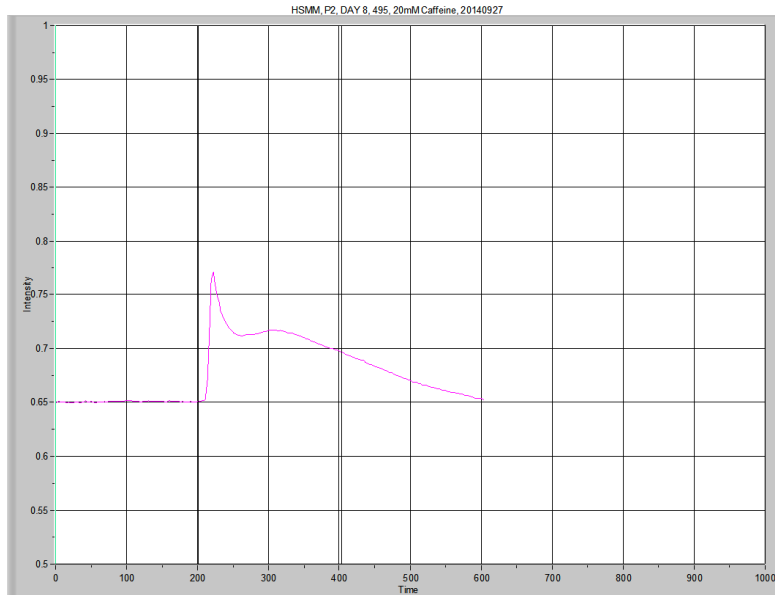
268

HSMM, P2, DAY 8, 495, 20mM Caffeine, 20140927

	Average resting level	Peak	Δ Level	Time to Peak	Area Under the Curve Low X: 201.279 High X: 598.471	Peak Area
495, P7	0.650416	0.77089	0.120475	16.10232	274.73259	15.71292

HSMM, P2, DAY 8, 495, 20mM Caffeine, 20140927
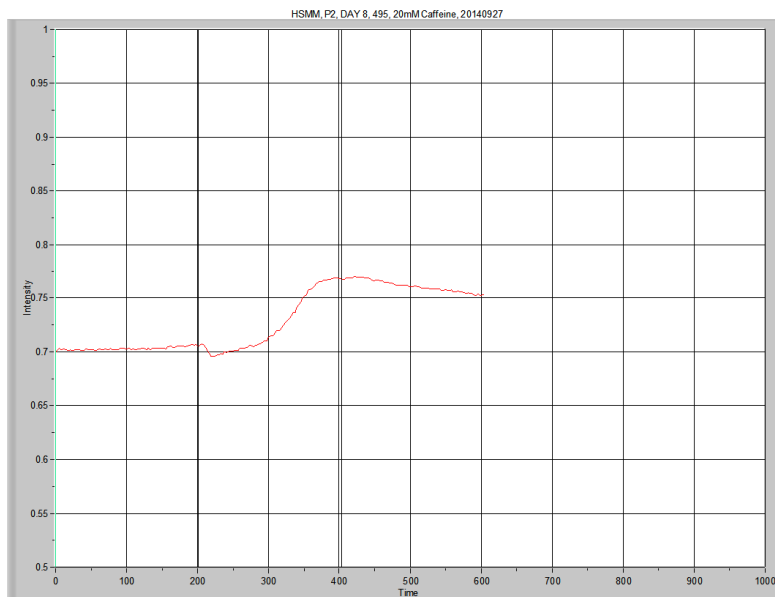
I will not be using data from this tracing, as it appears the myotube moved once stimulated with 20mM caffeine.

	Average resting level	Peak	Time to Peak	Area Under the Curve Low X: 201.279 High X: 598.471	Peak ARea
495, P8				295.11911	5.63479
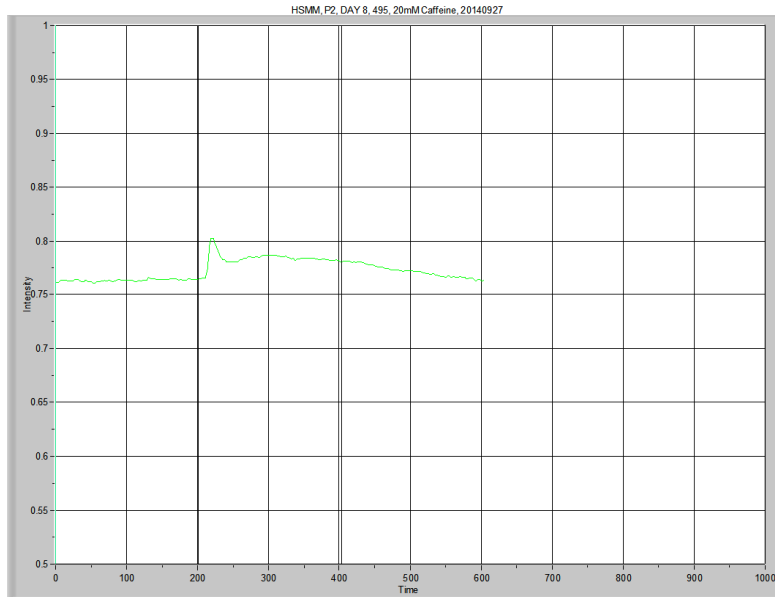
269

HSMM, P2, DAY 8, 495, 20mM Caffeine, 20140927

	Average resting level	Peak	Δ Level	Time to Peak	Area Under the Curve Low X: 201.279 High X: 598.471	Peak Area
495, P9	0.763026	0.802589	0.039563	5.367407	308.87264	5.50282
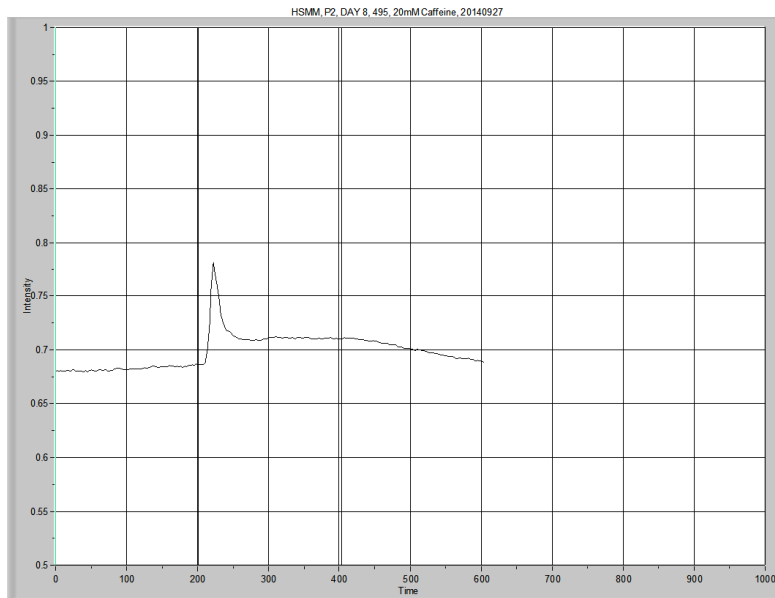
HSMM, P2, DAY 8, 495, 20mM Caffeine, 20140927

	Average resting level	Peak	Δ Level	Time to Peak	Area Under the Curve Low X: 201.279 High X: 598.471	Peak Area
495, P10	0.682257	0.780962	0.098705	16.10232	280.96170	7.76893
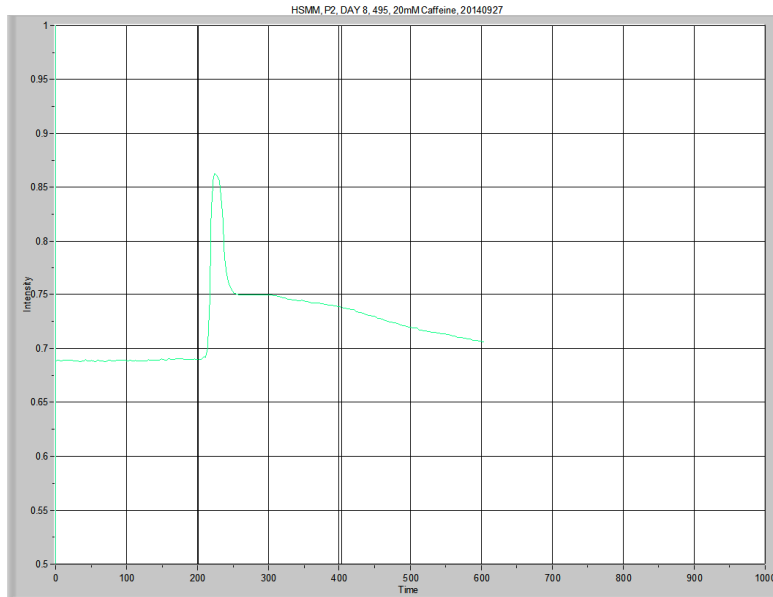
270

HSMM, P2, DAY 8, 495, 20mM Caffeine, 20140927

	Average resting level	Peak	Δ Level	Time to Peak	Area Under the Curve Low X: 201.279 High X: 598.471	Peak Area
495, P11	0.688793	0.862224	0.173431	10.73488	292.69607	15.35942
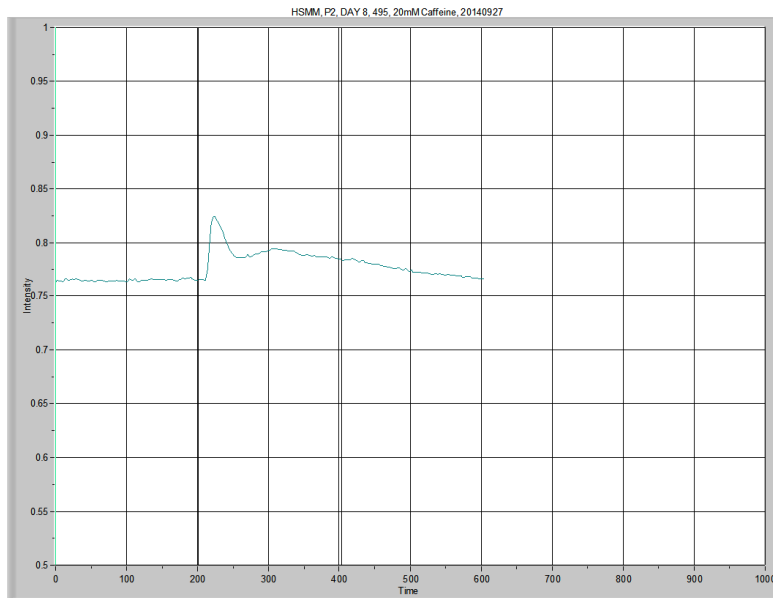
HSMM, P2, DAY 8, 495, 20mM Caffeine, 20140927

	Average resting level	Peak	Δ Level	Time to Peak	Area Under the Curve Low X: 201.279 High X: 598.471	Peak Area
495, P12	0.764523	0.824151	0.059628	8.051109	310.81125	6.77337
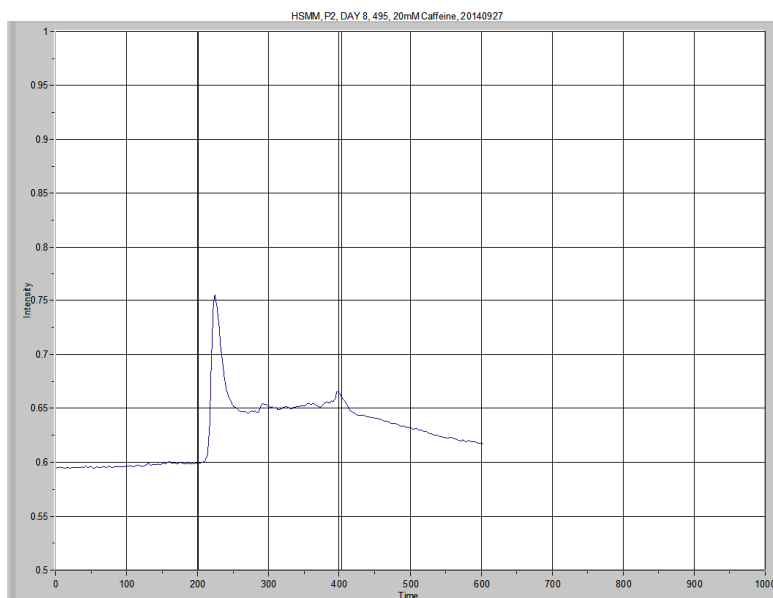
271

HSMM, P2, DAY 8, 495, 20mM Caffeine, 20140927

	Average resting level	Peak	Δ Level	Time to Peak	Area Under the Curve Low X: 201.279 High X: 598.471	Peak Area
495, P13	0.596495	0.755567	0.159072	18.78609	255.78235	14.14028
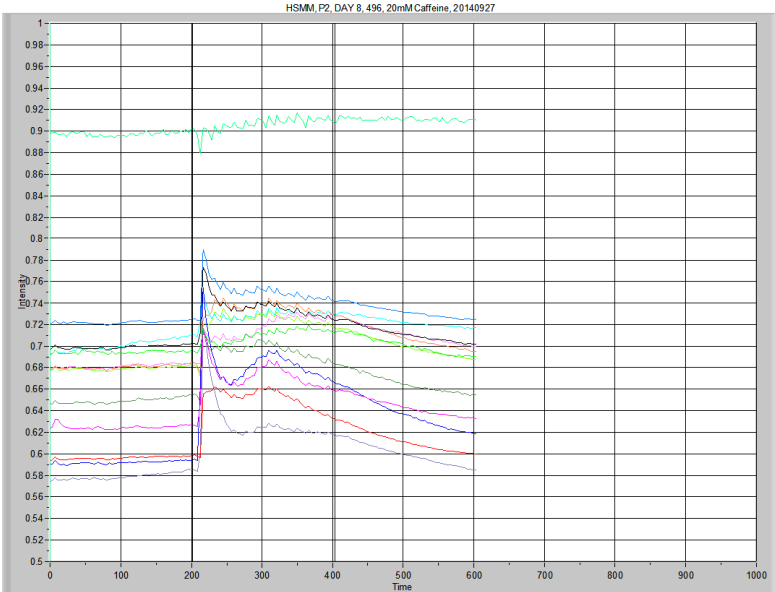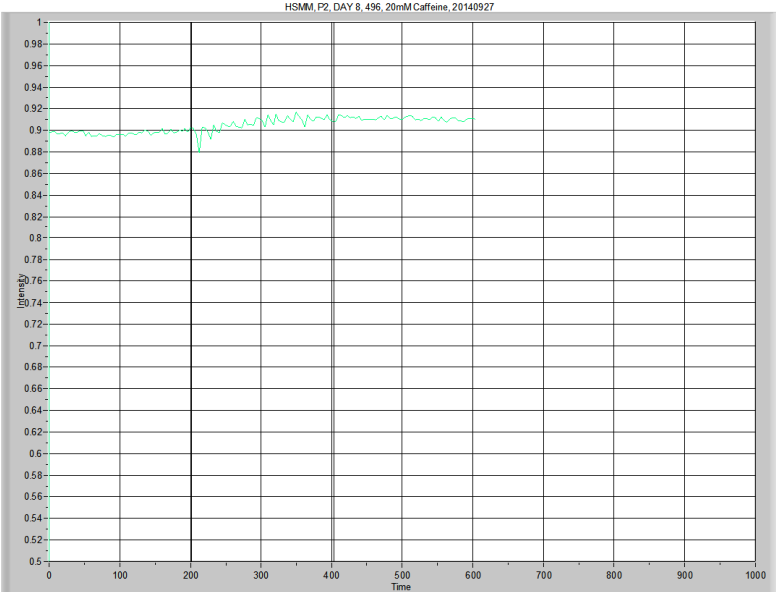
Overview

	Average resting level	Peak	Δ Level	Time to Peak	Area Under the Curve Low X: 201.279 High X: 599.813	Peak Area
496, BG	0.896639	0.916308	0.019669	NA	361.95929	0.83373
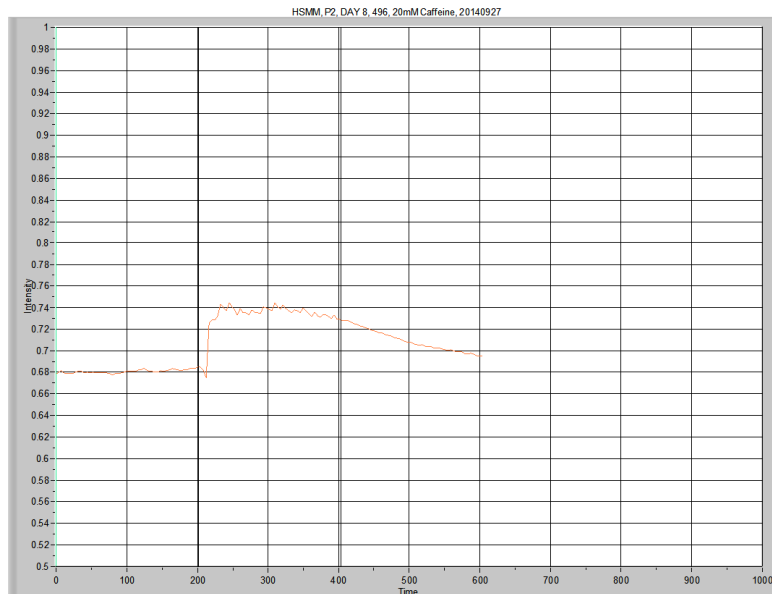
HSMM, P2, DAY 8, 496, 20mM Caffeine, 20140927

	Average resting level	Peak	Δ Level	Time to Peak	Area Under the Curve Low X: 201.279 High X: 599.813	Peak Area
496, P1	0.680238	0.744598	0.06436	32.20464	287.31129	12.47064
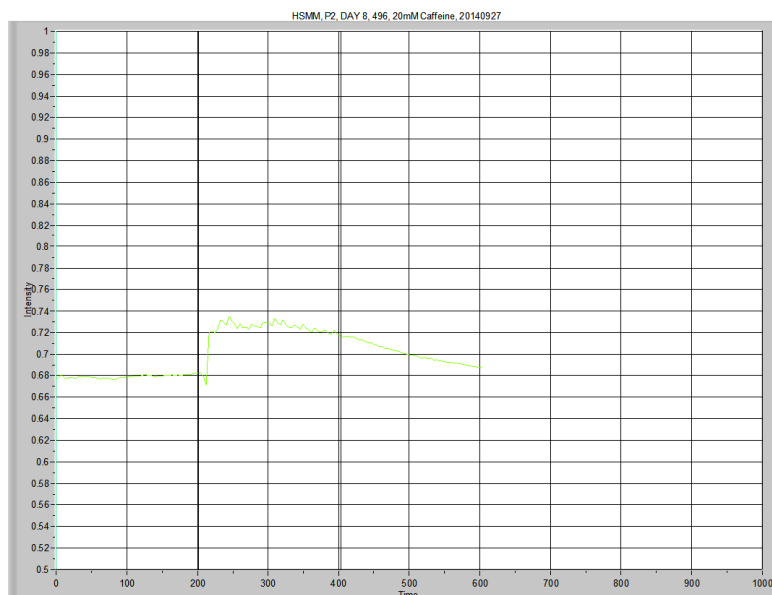
HSMM, P2, DAY 8, 496, 20mM Caffeine, 20140927

	Average resting level	Peak	Δ Level	Time to Peak	Area Under the Curve Low X: 201.279 High X: 599.813	Peak Area
496, P2	0.678724	0.734649	0.055925	28.17917	283.56228	10.65482
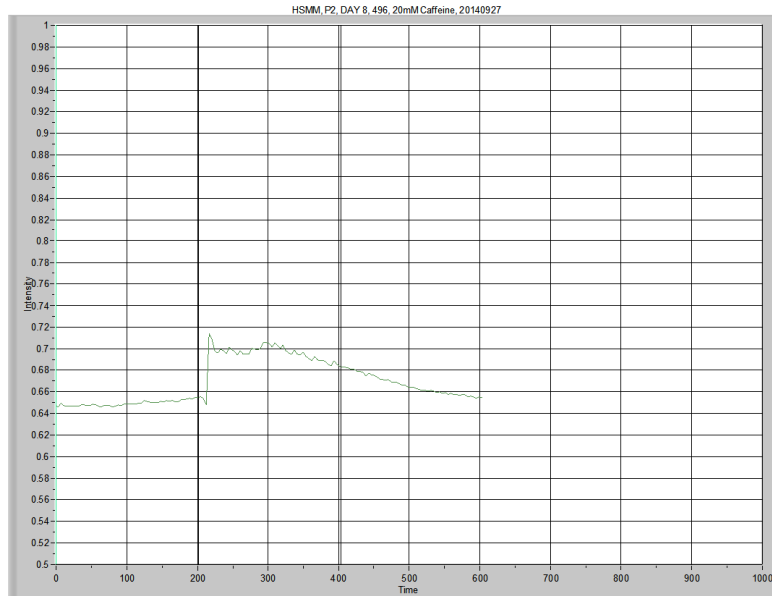
274

HSMM, P2, DAY 8, 496, 20mM Caffeine, 20140927

	Average resting level	Peak	Δ Level	Time to Peak	Area Under the Curve Low X: 201.279 High X: 599.813	Peak Area
496, P3	0.648485	0.714055	0.06557	4.025468	271.05829	10.13188
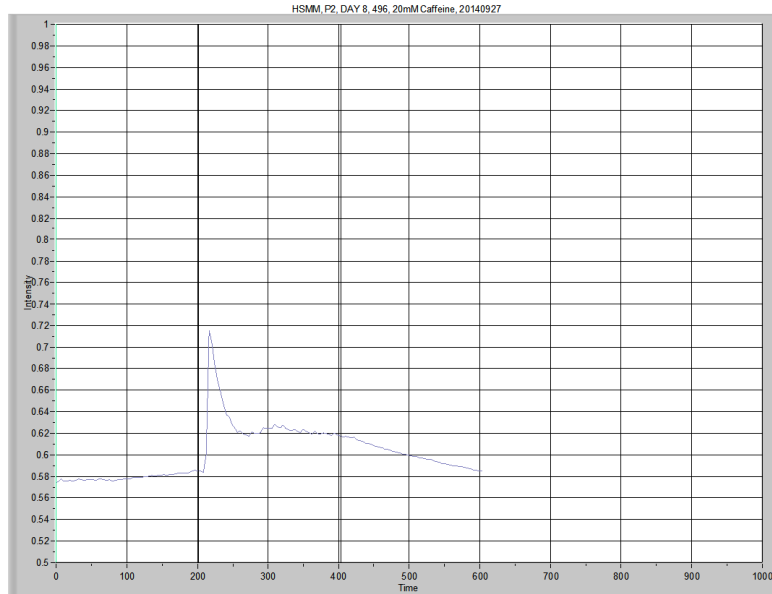
HSMM, P2, DAY 8, 496, 20mM Caffeine, 20140927

	Average resting level	Peak	Δ Level	Time to Peak	Area Under the Curve Low X: 201.279 High X: 599.813	Peak Area
496, P4	0.578061	0.715258	0.137197	12.07673	244.62857	11.56956
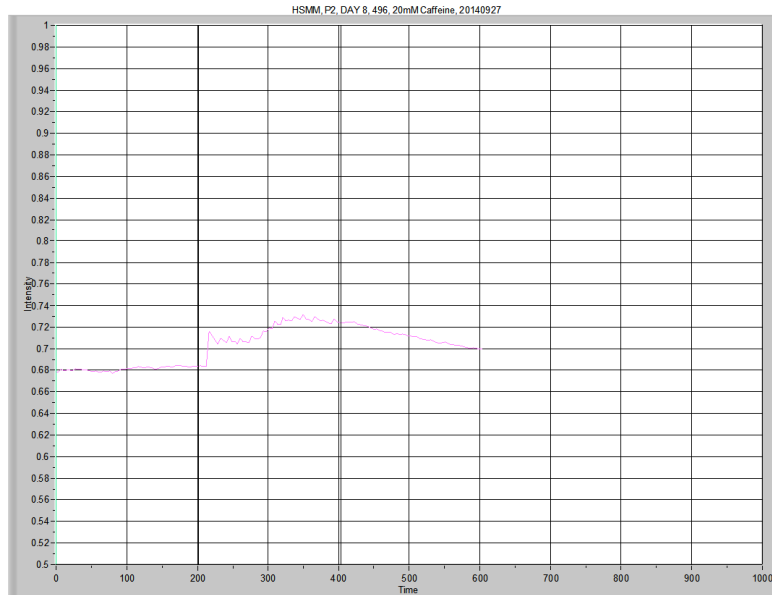
HSMM, P2, DAY 8, 496, 20mM Caffeine, 20140927

	Average resting level	Peak	Δ Level	Time to Peak	Area Under the Curve Low X: 201.279 High X: 599.813	Peak Area
496, P5	0.680736	0.731618	0.050882	Unable to measure	284.47128	8.93895
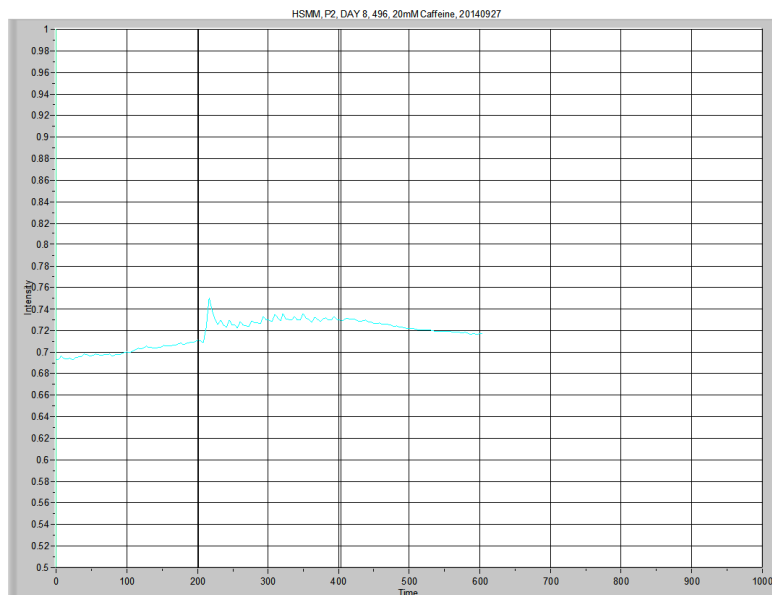
HSMM, P2, DAY 8, 496, 20mM Caffeine, 20140927

	Average resting level	Peak	Δ Level	Time to Peak	Area Under the Curve Low X: 201.279 High X: 599.813	Peak Area
496, P6	0.699627	0.750508	0.050881	8.051152	289.23055	4.86998
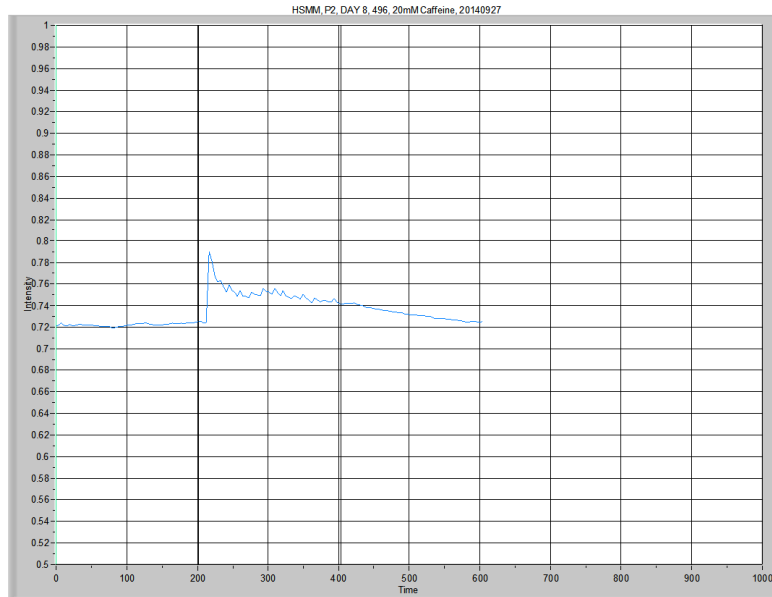
276

HSMM, P2, DAY 8, 496, 20mM Caffeine, 20140927

	Average resting level	Peak	Δ Level	Time to Peak	Area Under the Curve Low X: 201.279 High X: 599.813	Peak Area
496, P7	0.721657	0.789803	0.068146	4.025468	295.35119	6.56223
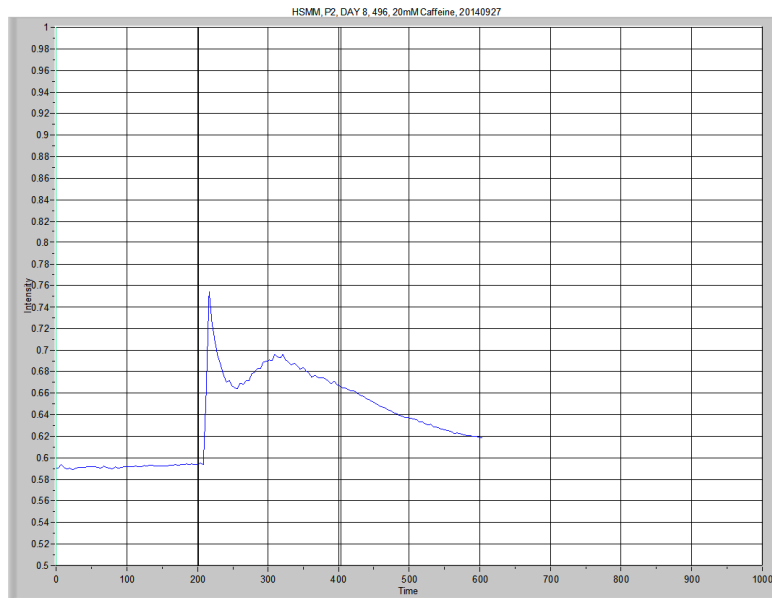
HSMM, P2, DAY 8, 496, 20mM Caffeine, 20140927

	Average resting level	Peak	Δ Level	Time to Peak	Area Under the Curve Low X: 201.279 High X: 599.813	Peak Area
496, P8	0.591491	0.754389	0.162898	4.025468	262.43530	20.78314
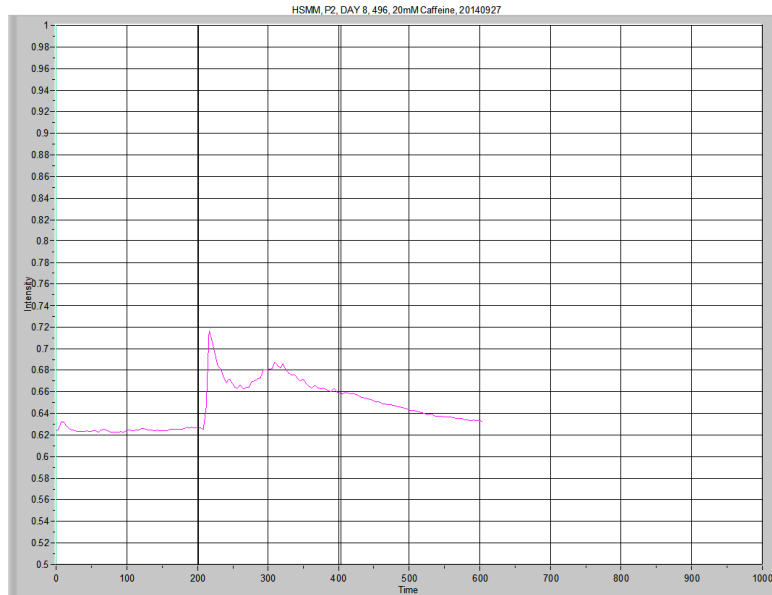
277

HSMM, P2, DAY 8, 496, 20mM Caffeine, 20140927

	Average resting level	Peak	Δ Level	Time to Peak	Area Under the Curve Low X: 201.279 High X: 599.813	Peak Area
496, P9	0.624324	0.716835	0.092511	4.025468	262.04399	10.89036
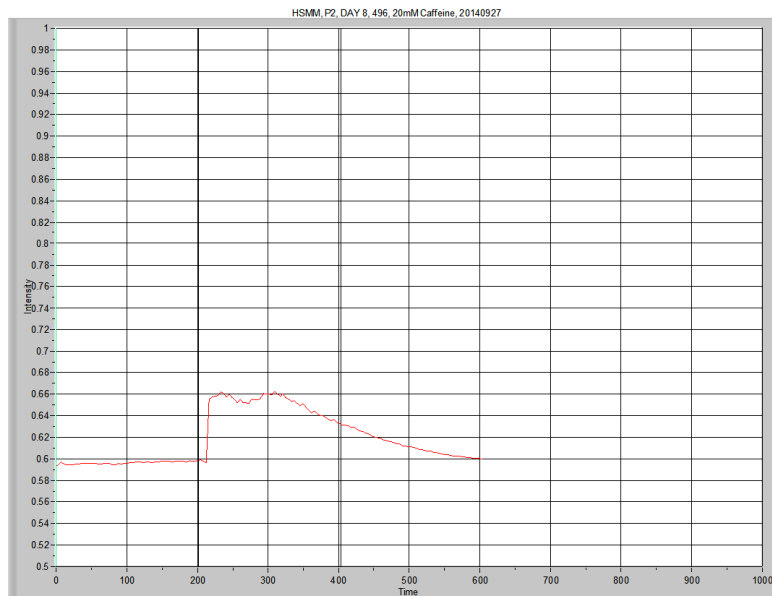
HSMM, P2, DAY 8, 496, 20mM Caffeine, 20140927

	Average resting level	Peak	Δ Level	Time to Peak	Area Under the Curve Low X: 201.279 High X: 599.813	Peak Area
496, P10	0.59578	0.662596	0.066816	16.10239	251.31642	12.41877
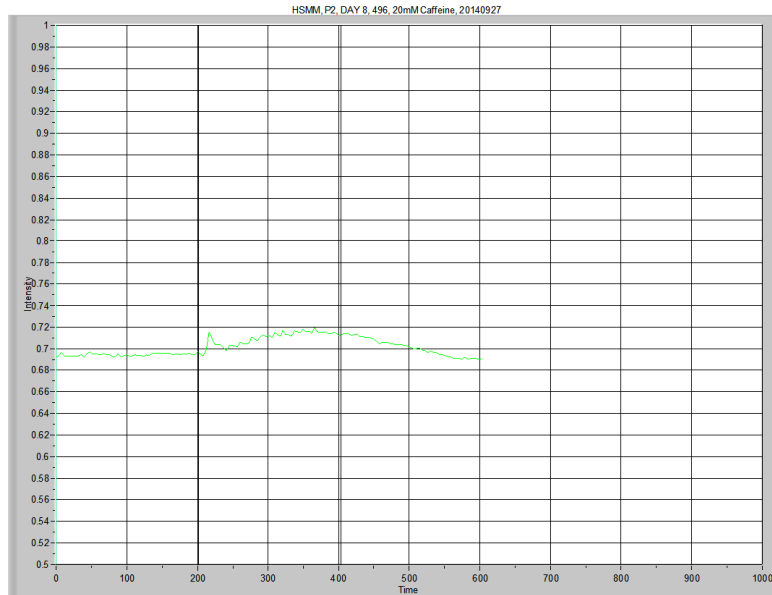
278

HSMM, P2, DAY 8, 496, 20mM Caffeine, 20140927

	Average resting level	Peak	Δ Level	Time to Peak	Area Under the Curve Low X: 201.279 High X: 599.813	Peak Area
496, P11	0.694015	0.719354	0.025339	Unable to measure	281.14398	4.81783
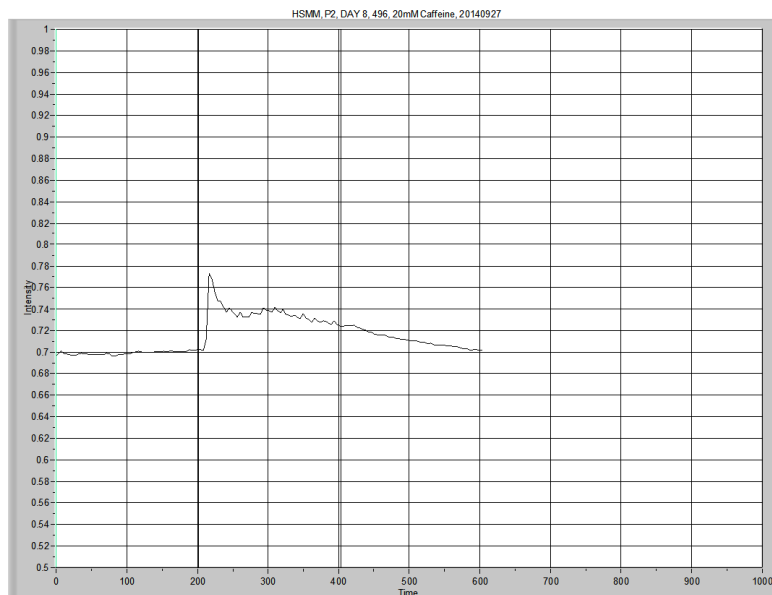
HSMM, P2, DAY 8, 496, 20mM Caffeine, 20140927

	Average resting level	Peak	Δ Level	Time to Peak	Area Under the Curve Low X: 201.279 High X: 599.813	Peak Area
496, P12	0.698606	0.773414	0.074808	8.051152	288.21593	8.56422

279

Data Collected: HSMM, Flow Cytometry for MUSE ™ Cell Cycle Assay

CNTRL A	G0/ G1	S	G2/M	Debris
% Gated	84.6	11.5	1.9	77.4
Mean	3214.6	5506.5	9005.5	24.9
%CV	6.0	15.4	10.7	400.2
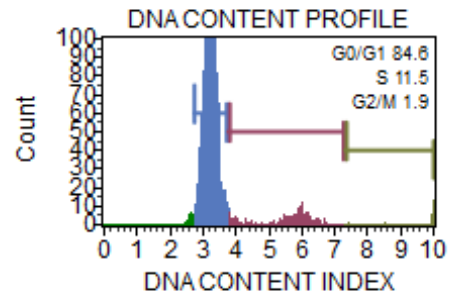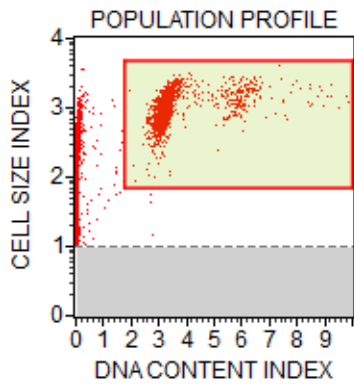
CNTRL C	G0/ G1	S	G2/M	Debris
% Gated	83.2	12.8	2.7	82.1
Mean	3033.6	5184.7	8803.6	26.4
%CV	6.2	15.3	12.5	672.0
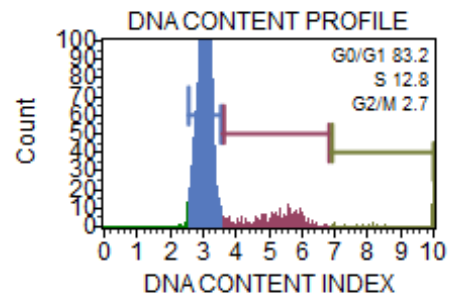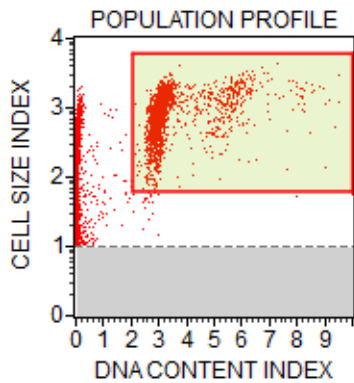
Serum Sample 228	G0/ G1	S	G2/M	Debris
% Gated	84.3	11.6	2.4	81.3
Mean	3215.9	5314.5	8757.4	23.4
%CV	5.5	17.8	11.8	443.4
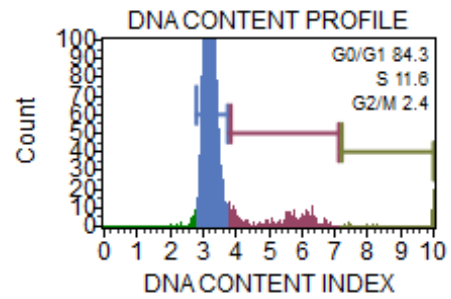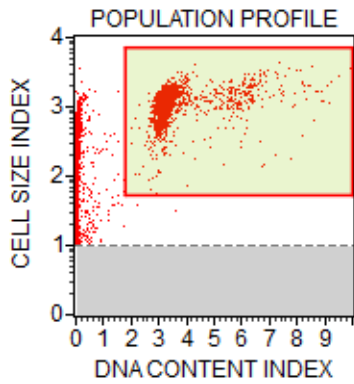
Serum Sample 368	G0/ G1	S	G2/M	Debris
% Gated	83.2	13.8	1.8	69.1
Mean	3162.3	5434.4	9133.4	25.4
%CV	5.8	15.6	9.8	603.5
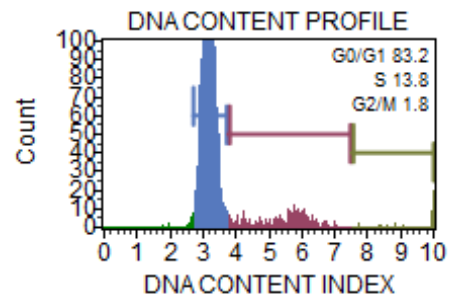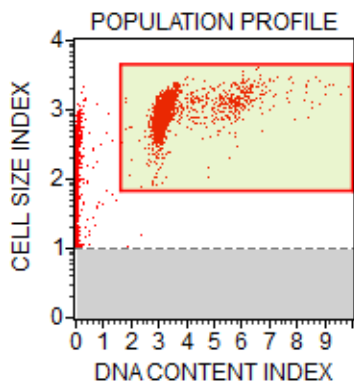
Serum Sample 380	G0/ G1	S	G2/M	Debris
% Gated	79.8	15.4	2.8	77.9
Mean	3097.4	5186.5	8926.8	46.3
%CV	5.8	16.7	11.6	415.0
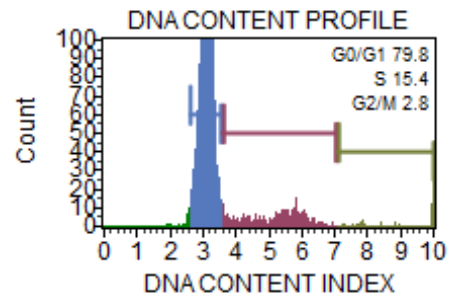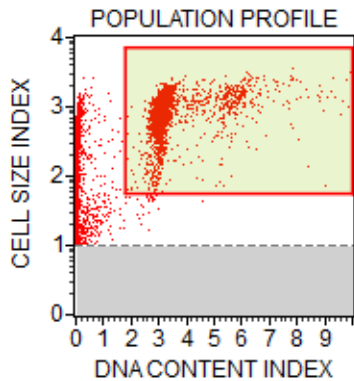
Serum Sample 390	G0/ G1	S	G2/M	Debris
% Gated	85.3	12.5	1.2	78.1
Mean	3108.5	5202.2	9172.9	31.0
%CV	5.5	18.3	10.2	563.9
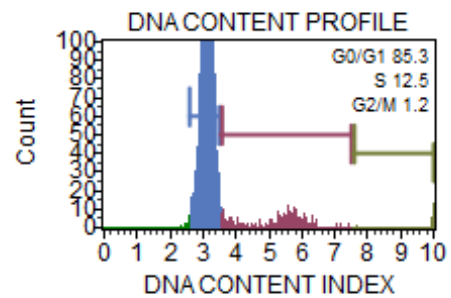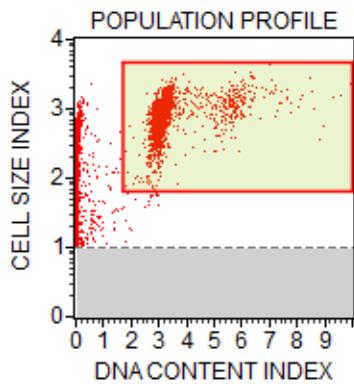
Serum Sample 391	G0/ G1	S	G2/M	Debris
% Gated	85.5	11.7	1.0	79.3
Mean	3084.5	5124.2	9233.0	27.7
%CV	5.6	20.2	8.5	500.8
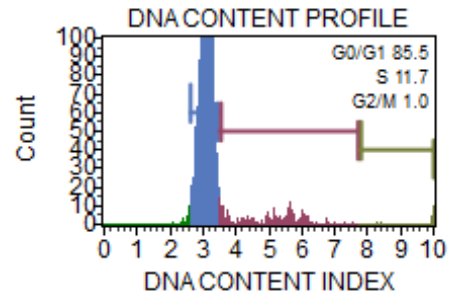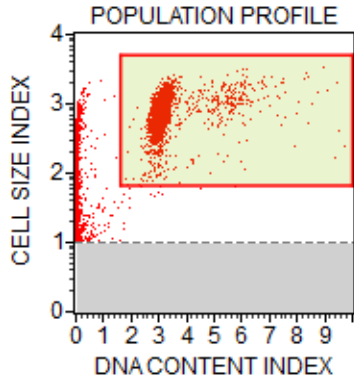
Serum Sample 397	G0/ G1	S	G2/M	Debris
% Gated	75.9	17.8	4.9	87.7
Mean	3004.0	4746.7	8310.9	20.0
%CV	6.0	18.4	15.5	420.1
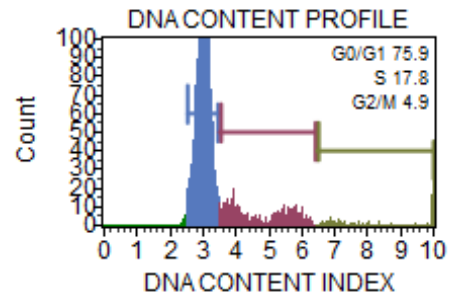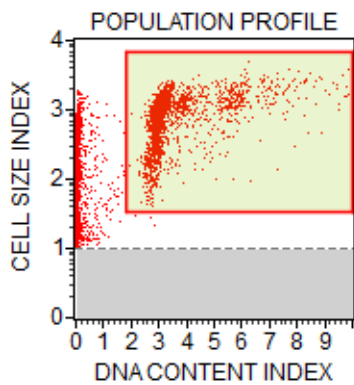
Serum Sample 403	G0/ G1	S	G2/M	Debris
% Gated	79.6	15.3	3.0	83.3
Mean	3041.1	5171.0	8784.1	30.3
%CV	5.9	17.7	11.8	491.1
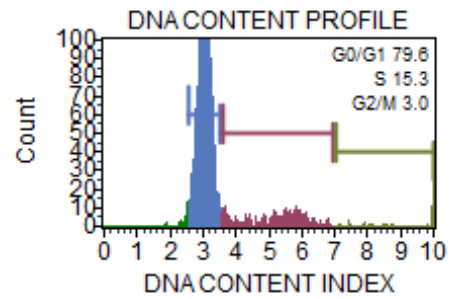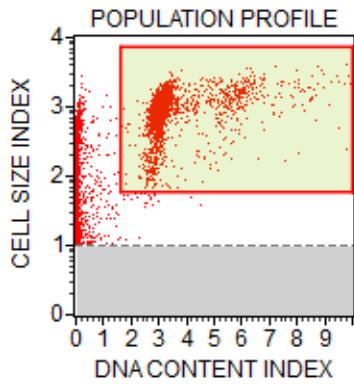
Serum Sample 428	G0/ G1	S	G2/M	Debris
% Gated	79.5	16.0	2.8	85.4
Mean	2912.1	4968.0	8946.7	28.0
%CV	6.1	18.2	11.7	531.0
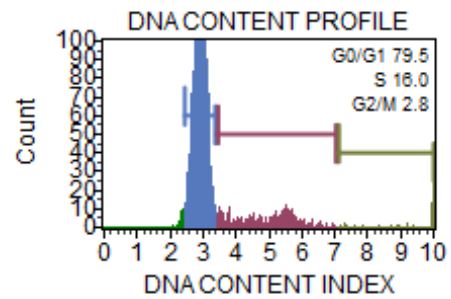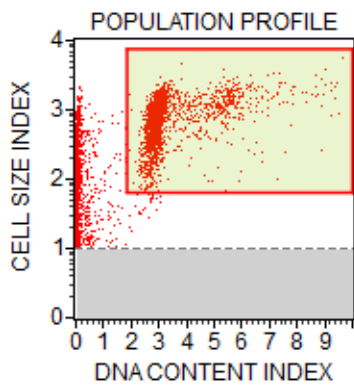
Serum Sample 435	G0/ G1	S	G2/M	Debris
% Gated	79.4	15.9	3.1	71.2
Mean	3154.4	5152.2	8753.7	27.9
%CV	5.4	18.5	12.4	632.3
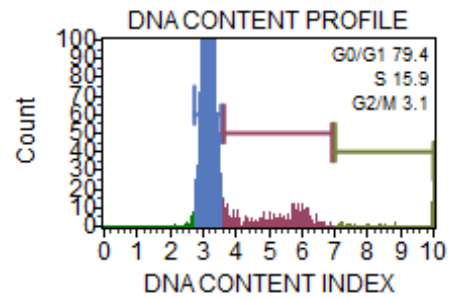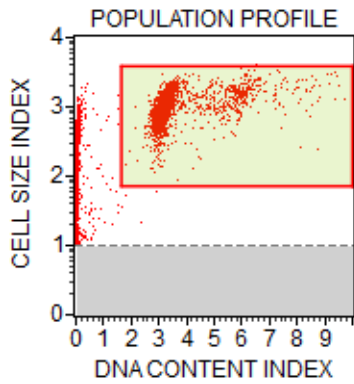
Serum Sample 439	G0/ G1	S	G2/M	Debris
% Gated	80.5	14.5	3.0	72.8
Mean	3117.1	5209.1	8919.5	26.7
%CV	5.3	18.7	10.9	456.4
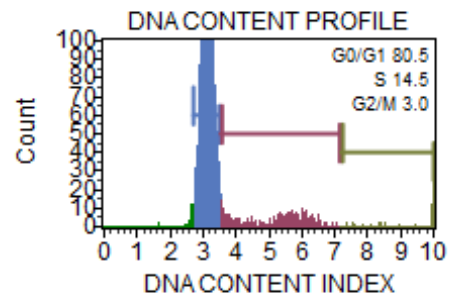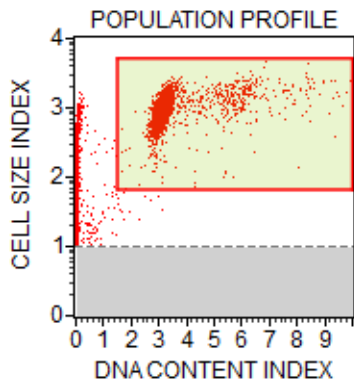
Serum Sample 463	G0/ G1	S	G2/M	Debris
% Gated	85.9	10.6	1.9	80.5
Mean	3123.1	5095.1	8386.7	28.9
%CV	5.3	17.4	14.8	543.3
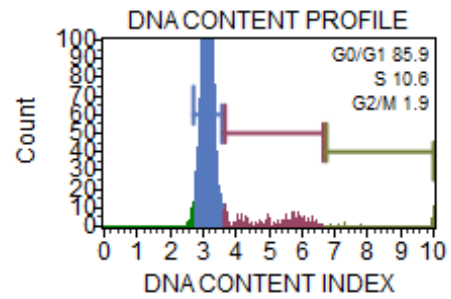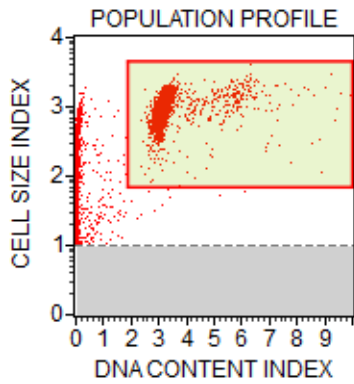
Serum Sample 480	G0/ G1	S	G2/M	Debris
% Gated	83.8	12.5	2.0	85.1
Mean	3104.1	5062.3	9142.4	26.6
%CV	5.7	17.7	10.7	463.3
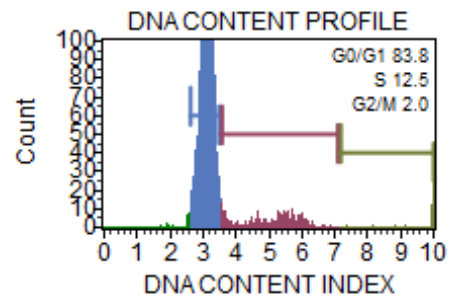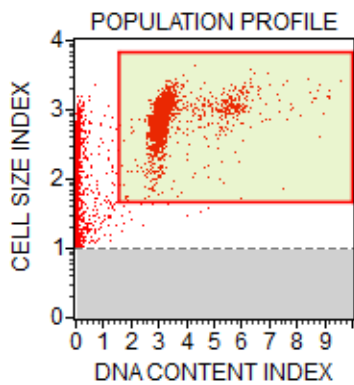
Serum Sample 482	G0/ G1	S	G2/M	Debris
% Gated	79.8	15.6	2.3	80.2
Mean	3142.4	5138.2	8977.2	34.1
%CV	5.7	19.3	9.6	409.4
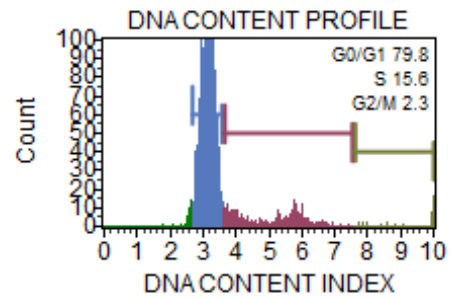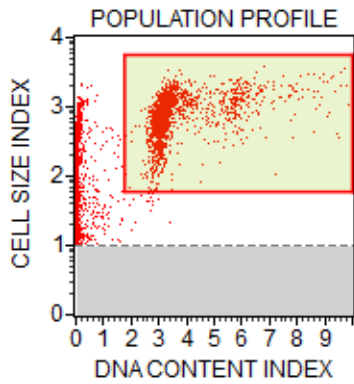
Serum Sample 489	G0/ G1	S	G2/M	Debris
% Gated	84.4	13.4	1.2	82.9
Mean	3117.7	5310.2	8642.0	54.5
%CV	5.9	17.1	7.8	929.2
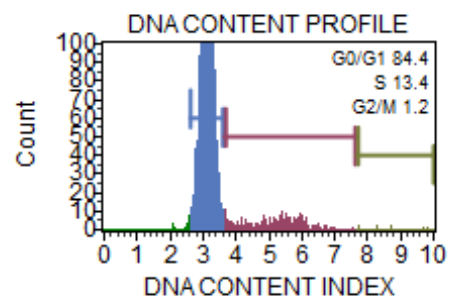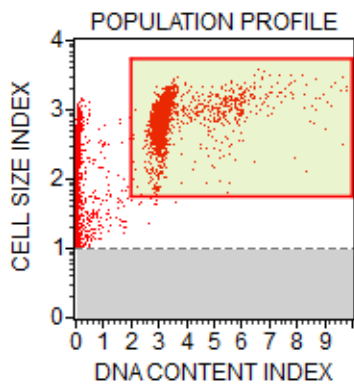
Serum Sample 495	G0/ G1	S	G2/M	Debris
% Gated	80.9	13.3	3.8	82.9
Mean	3008.4	4955.2	8530.3	20.4
%CV	5.9	16.0	15.7	417.9
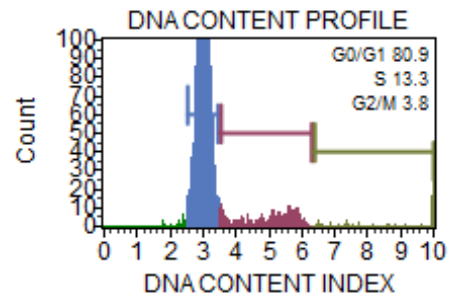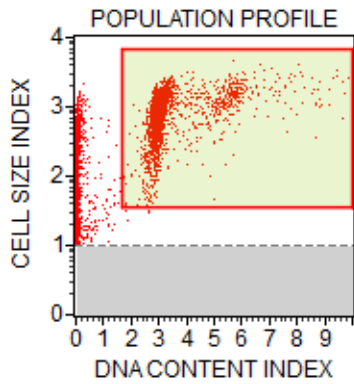
Serum Sample 496	G0/ G1	S	G2/M	Debris
% Gated	75.9	17.5	4.2	81.9
Mean	3024.8	5133.9	8781.3	32.3
%CV	5.4	17.4	12.8	483.8

Cell Cycle Analysis CNTRL A

Legend: G0/ G1, S, G2/M, Debris

Cell Cycle Analysis CNTRL C

Legend: G0/ G1, S, G2/M, Debris

**Cell Cycle Analysis
Serum Sample 228**

- G0/ G1
- S
- G2/M
- Debris
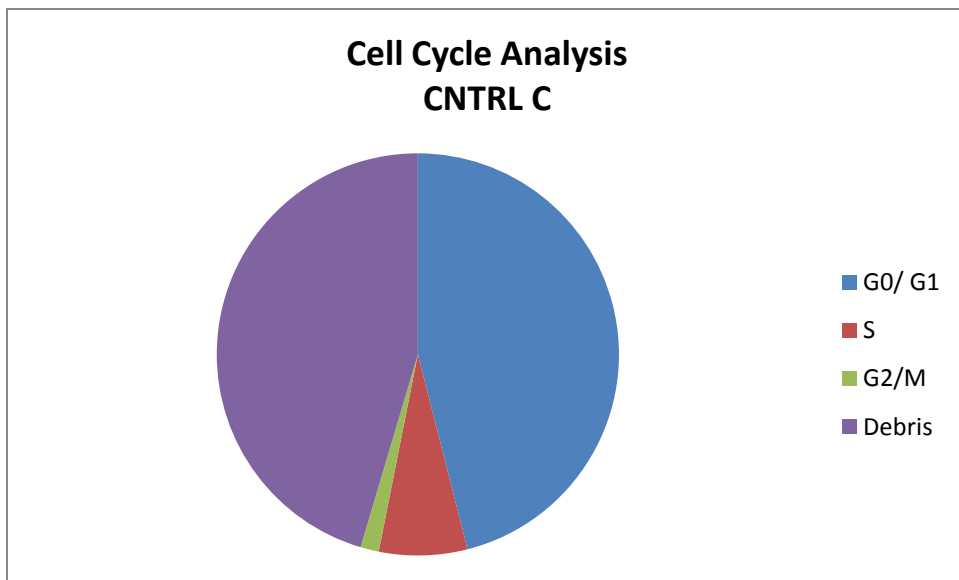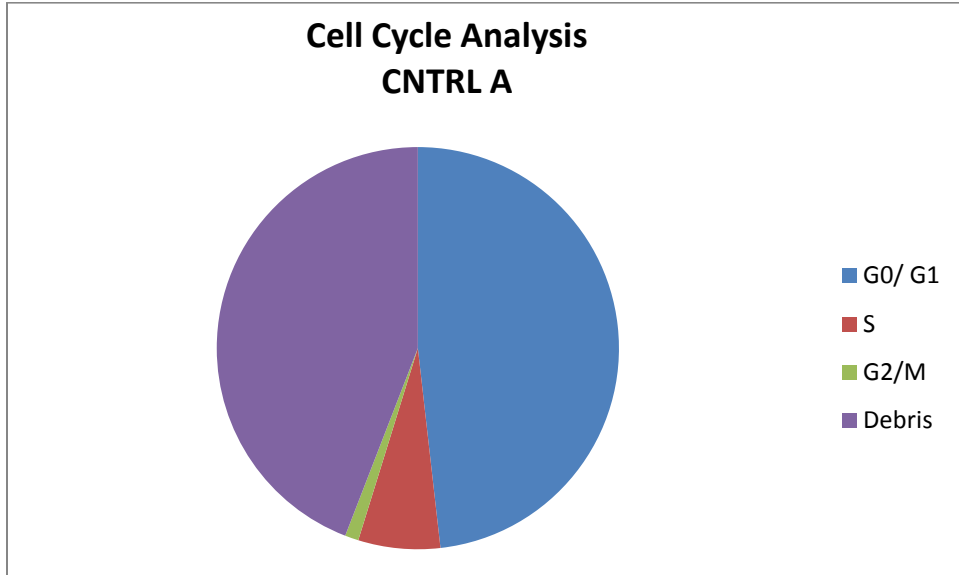
**Cell Cycle Analysis
Serum Sample 368**
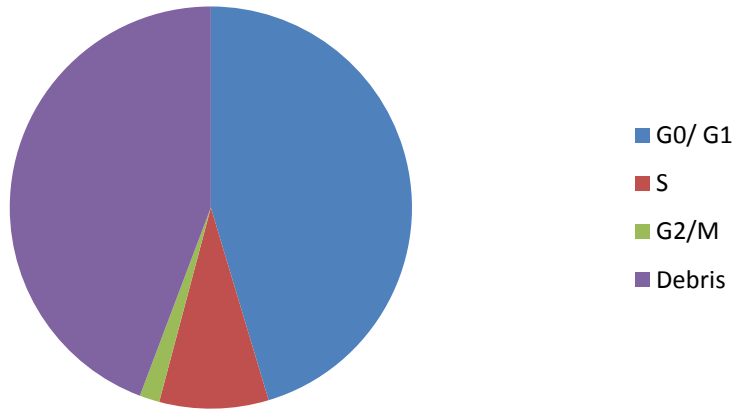
- G0/ G1
- S
- G2/M
- Debris

**Cell Cycle Analysis
Serum Sample 380**

G0/ G1
S
G2/M
Debris

**Cell Cycle Analysis
Serum Sample 390**

G0/ G1
S
G2/M
Debris

**Cell Cycle Analysis
Serum Sample 391**

- G0/ G1
- S
- G2/M
- Debris

**Cell Cycle Analysis
Serum Sample 397**

- G0/ G1
- S
- G2/M
- Debris

Cell Cycle Analysis
Serum Sample 403

G0/ G1
S
G2/M
Debris

Cell Cycle Analysis
Serum Sample 428

G0/ G1
S
G2/M
Debris

**Cell Cycle Analysis
Serum Sample 435**

G0/ G1
S
G2/M
Debris

**Cell Cycle Analysis
Serum Sample 439**

G0/ G1
S
G2/M
Debris

Cell Cycle Analysis
Serum Sample 463

G0/ G1
S
G2/M
Debris

Cell Cycle Analysis
Serum Sample 480

G0/ G1
S
G2/M
Debris

Cell Cycle Analysis
Serum Sample 482

Legend: G0/ G1, S, G2/M, Debris

Cell Cycle Analysis
Serum Sample 489

Legend: G0/ G1, S, G2/M, Debris

**Cell Cycle Analysis
Serum Sample 495**

- G0/ G1
- S
- G2/M
- Debris
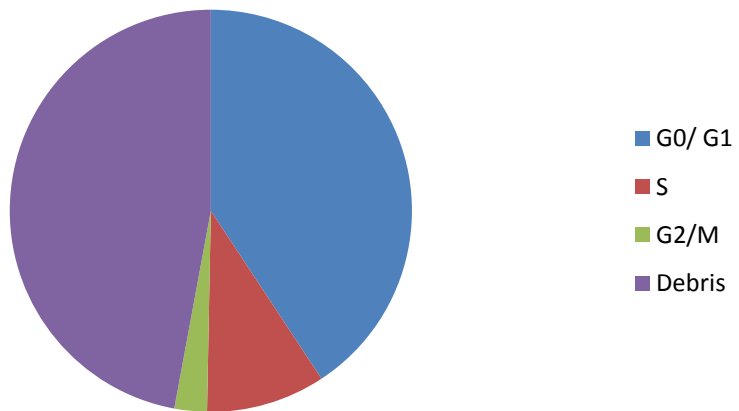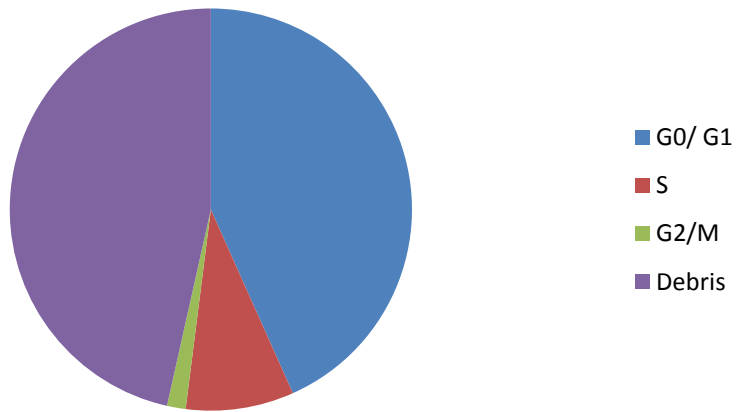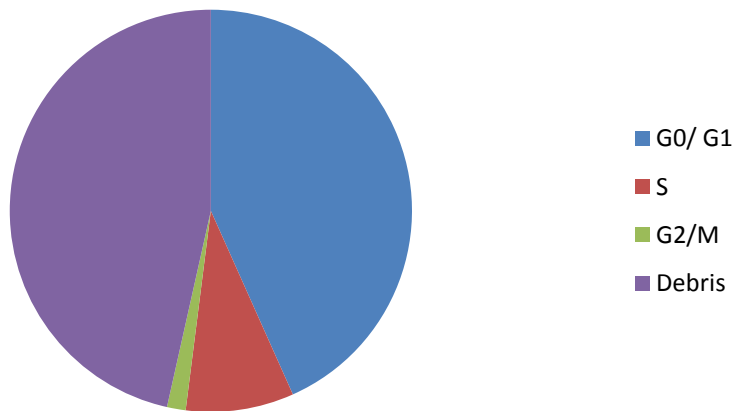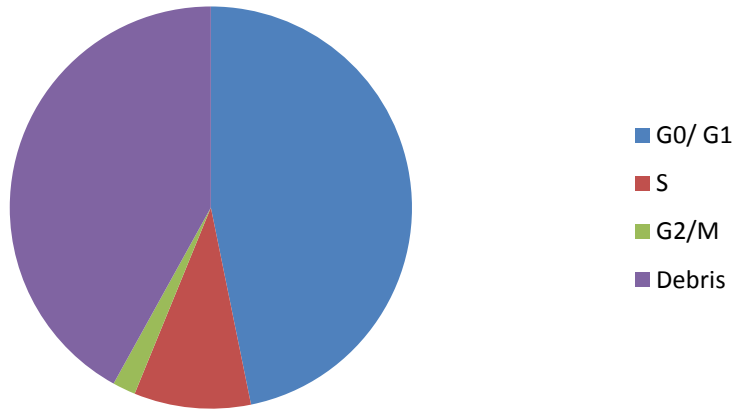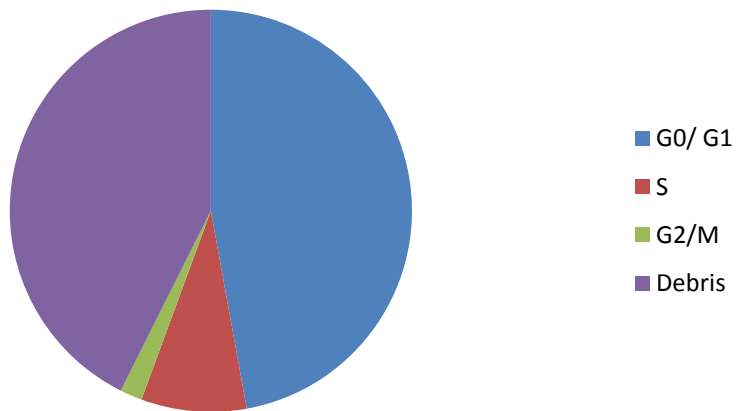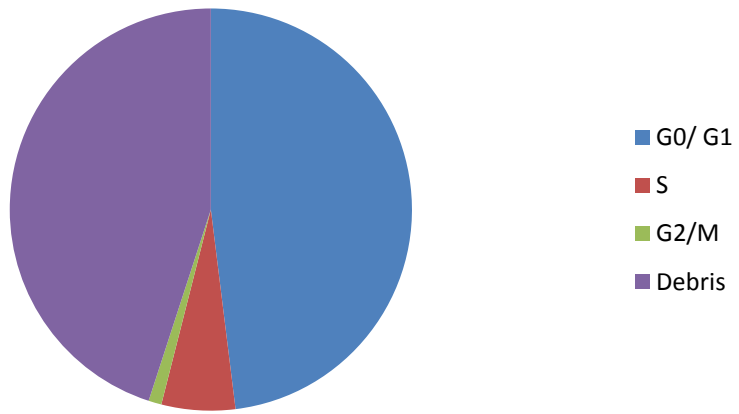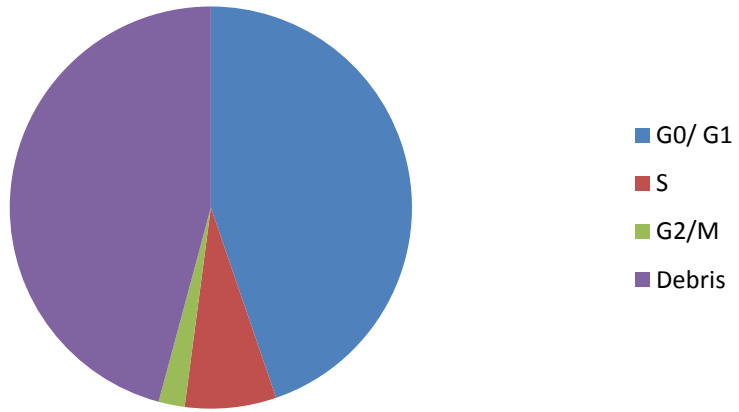
**Cell Cycle Analysis
Serum Sample 496**

- G0/ G1
- S
- G2/M
- Debris

Appendix J

Comprehensive Tables, Data Collected

Table 10. Comprehensive Table, Fracture Status Groups

	CNTRL Group, No Non-Traumatic Fracture									CASE Group, Non-Traumatic Fracture Present								
ID #	228	428	435	439	482	489	495	496	CNTRL Group, AVG	368	380	390	391	397	403	463	480	CASE Group, AVG
Patient Information																		
Age	73.6	65	57.7	62.2	52.3	60.6	70.1	63.8	**63.2**	70.8	67.7	59.6	62.2	68.2	66.4	50.7	67.8	**64.2**
T-Spine	0.76	-1.32	0.35	-2.09	-1.46	-0.08	0.38	-1.95	**-0.68**	-1.05	-0.65	-1.91	-2.39	0.83	-0.48	-1.08	-0.70	**-0.93**
T-Hip	-0.84	-0.08	-0.43	-0.65	-1.78	-0.95	-0.97	-0.34	**-0.75**	-1.43	-0.97	-0.57	-1.51	-0.68	-0.92	-1.46	-1.36	**-1.11**
Fracture (Y/N)	N	N	N	N	N	N	N	N		Y	Y	Y	Y	Y	Y	Y	Y	
Myogenic Differentiation																		
Myotube Nuclei	856.2	1102.6	1134	1121.4	1220.8	1219.4	1289	1111.8	**1131.9***	970.6	938.2	1002.8	901.8	980.2	1036.6	1139.8	1404.2	**1046.8***
Total Nuclei	1233.4	1440.4	1348.4	1343.4	1467.8	1467.2	1592	1413.8	**1413.3***	1299.4	1259.2	1364.8	1337.2	1291.2	1336.2	1365.6	1649.4	**1362.9***
Fusion Index	69.4	76.4	84.2	83.6	83.2	83.2	81.2	78.6	**79.98***	74.8	74.4	73.8	67.6	75.8	76.4	83.2	85.0	**76.4***
Intracellular Calcium Homeostasis																		
Resting Level	0.71	0.64	0.67	0.69	0.67	0.72	0.69	0.66	**0.68**	0.68	0.71	0.68	0.67	0.66	0.69	0.68	0.70	**0.68**
Peak Level	0.80	0.76	0.76	0.76	0.80	0.82	0.80	0.74	**0.78**	0.77	0.79	0.78	0.77	0.76	0.80	0.80	0.78	**0.78**
Δ Level	0.08	0.12	0.08	0.07	0.14	0.11	0.12	0.07	**0.10**	0.10	0.10	0.10	0.10	0.09	0.10	0.10	0.10	**0.10**
Time to Peak	9.39	7.74	12.08	4.60	7.81	6.10	12.75	12.08	**9.07**	8.32	7.95	8.07	17.44	8.42	9.07	9.10	8.90	**9.66**
Area Under the Curve	289.79	264.75	278.10	--	282.18	296.96	287.02	275.06	**281.98**	279.40	289.54	280.85	278.29	268.92	284.01	286.94	287.62	**281.95**
Cell Cycle Analysis																		
G0/G1	84.35	79.55	79.4	80.53	79.82	84.38	80.95	75.88	**80.61**	83.24	79.83	85.32	85.52	75.85	79.59	85.95	83.76	**82.38**
S	11.55	15.96	15.93	14.47	15.58	13.37	13.29	17.54	**14.71**	13.79	15.45	12.5	11.7	17.84	15.34	10.6	12.51	**13.72**
G2/M	2.36	2.76	3.14	3.04	2.34	1.2	3.8	4.18	**2.85**	1.75	2.82	1.17	0.98	4.86	3.04	1.87	1.96	**2.31**

Table 11. Comprehensive Table, T-Score Status Groups

ID #	CNTRL Group, T-Score > -1.0								CASE Group, T-Score < -1.0									
	228	380	397	403	435	489	495	CNTRL Group, AVG	368	390	391	428	439	463	480	482	496	CASE Group, AVG
Patient Information																		
Age	73.6	67.7	68.2	66.4	57.7	60.6	70.1	66.3	70.8	59.6	62.2	65	62.2	50.7	67.8	52.3	63.8	61.6
T-Spine	0.755	-0.654	0.831	-0.484	0.353	-0.084	0.379	0.157	-1.050	-1.909	-2.390	-1.316	-2.086	-1.081	-0.703	-1.455	-1.948	-1.549
T-Hip	-0.844	-0.969	-0.682	-0.919	-0.426	-0.954	-0.966	-0.823	-1.432	-0.572	-1.506	-0.077	-0.651	-1.460	-1.362	-1.781	-0.335	-1.020
Fracture (Y/N)	N	Y	Y	Y	N	N	N		Y	Y	Y	N	N	Y	Y	N	N	
Myogenic Differentiation																		
Myotube Nuclei	856.2	938.2	980.2	1036.6	1134	1219.4	1289	1064.8	970.6	1002.8	901.8	1102.6	1121.4	1139.8	1404.2	1220.8	1111.8	1108.4
Total Nuclei	1233.4	1259.2	1291.2	1336.2	1348.4	1467.2	1592	1361.1	1299.4	1364.8	1337.2	1440.4	1343.4	1365.6	1649.4	1467.8	1413.8	1409.1
Fusion Index	69.4	74.4	75.8	76.4	84.2	83.2	81.2	77.8	74.8	73.8	67.6	76.4	83.6	83.2	85.0	83.2	78.6	78.5
Intracellular Calcium Homeostasis																		
Resting Level	0.71	0.71	0.66	0.69	0.67	0.72	0.69	**0.69***	0.68	0.68	0.67	0.64	0.69	0.68	0.70	0.67	0.66	**0.67***
Peak Level	0.80	0.79	0.76	0.80	0.76	0.82	0.80	**0.79***	0.77	0.78	0.77	0.76	0.76	0.80	0.78	0.80	0.74	**0.77***
Δ Level	0.079	0.098	0.086	0.095	0.084	0.105	0.116	0.949	0.096	0.101	0.103	0.117	0.066	0.096	0.097	0.135	0.068	0.977
Time to Peak	9.393	7.953	8.417	9.068	12.077	6.099	12.748	9.394	8.324	8.065	17.444	7.742	4.601	9.100	8.899	7.807	12.077	9.340
Area Under the Curve	289.792	289.540	268.924	284.013	278.095	296.956	287.021	284.906	279.397	280.846	278.287	264.753	---	286.942	287.620	282.180	275.064	279.386
Cell Cycle Analysis																		
G0/G1	84.35	79.83	75.85	79.59	79.4	84.38	80.95	80.62	83.24	85.32	85.52	79.55	80.53	85.95	83.76	79.82	75.88	82.17
S	11.55	15.45	17.84	15.34	15.93	13.37	13.29	14.68	13.79	12.5	11.7	15.96	14.47	10.6	12.51	15.58	17.54	13.85
G2/M	2.36	2.82	4.86	3.04	3.14	1.2	3.80	3.03	1.75	1.17	0.98	2.76	3.04	1.87	1.96	2.34	4.18	2.23

REFERENCES

Abreu, E. L., Stern, M., & Brotto, M. (2012). Bone–muscle interactions: ASBMR Topical

    Meeting, July 2012. *IBMS BoneKEy*, *9*. doi:10.1038/bonekey.2012.239

Acharyya, S., Oskarsson, T., Vanharanta, S., Malladi, S., Kim, J., Morris, P. G.,…Massague,

    J. (2012). A CXCL1 paracrine network links cancer chemoresistance and metastasis.

    Cell, 150, 165-178. doi: 10.1016/j.cell.2012.04.042

Ackoff, R. L. (1981). *Creating the corporate future.* New York, NY: Wiley.

Addison, C., Daniel, T. O., Burdick, M. D., Liu, H., Ehlert, J. E., Xue, Y. Y.,…Strieter, R.

    M. (2000). The CXC chemokine receptor 2, CXCR2, is the putative receptor of ELR$^+$

    CXC chemokine-induced angiogenic activity. *The Journal of Immunology,*

    165(9),5269-5277. doi: 10.4049/jimmunol.165.9.5269

Agas, D., Marchetti, L., Hurley, M. M., & Sabbieti, M. G. (2013). Prostaglandin F2α: A bone

    remodeling mediator. *Journal of Cellular Physiology*, *228*(1), 25–29.

    doi:10.1002/jcp.24117

Albright, F., Smith, P.H., & Richardson, A.M. (1941). Postmenopausal osteoporosis.

    Journal of the American Medical Association, 116, 2465-2474.

Andersen, J. (2003). Muscle fibre type adaptation in the elderly human muscle.

    Scandinavian Journal of Medicine & Science in Sports, 13(1), 40-47. doi:

    10.1034/j.1600-0838.2003.00299.x

Andersen, K., & Pedersen, B. (2008). The role of inflammation in vascular insulin

    resistance with focus on IL-6. *Hormone and Metabolic Research*, *40*(09), 635–639.

    doi:10.1055/s-0028-1083810

Andersson, D. C., Betzenhauser, M. J., Reiken, S., Meli, A. C., Umanskaya, A., Xie,

W.,…Marks, A. R. (2011). Ryanodine receptor oxidation causes intracellular

calcium leak and muscle weakness in aging. *Cell Metabolism, 14*(2), 196-201. doi:

10.1016/j.cmet.2011.05.014

Arnold, A.-S., Egger, A., & Handschin, C. (2011). PGC-1α and myokines in the aging

muscle – A Mini-Review. *Gerontology*, *57*(1), 37–43. doi:10.1159/000281883

Arthur S. T., & Cooley, I.D. (2012). The effect of physiological stimuli on sarcopenia;

Impact of Notch and Wnt signaling on impaired aged skeletal muscle repair.

International Journal of Biological Sciences, 8(5):731-760. doi:10.7150/ijbs.4262

Auron-Gomez, M., & Michota, F. (2008). Medical management of hip fracture. *Clinics in

Geriatric Medicine, 24*, 701-719. doi: 10.1016/j.cger.2008.07.002

Baim, S. (2011). Assessment of fracture risk. *Rheumatic Diseases Dlinics of North

America, 31*(3):453-470. doi: 10.1016/j.rdc.2011.07.001

Barton, E.R. (2006). The ABCs of IGF-I isoforms: Impact on muscle hypertrophy and

implications for repair. *Applied Physiology, Nutrition, and Metabolism, 31*(6), 791-

797. doi: 10.1139/h06-054

Baumgartner, R. N. (2000). Body composition in healthy aging. *Annals: The New York

Academy of Sciences, 904*, 437-448.

Baumgartner, R. N., Koehler, K. M., Gallagher, D., Romero, L., Heymsfield, S. B., Ross, R.

R.,…Lindeman, R. D. (1998). Epidemiology of sarcopenia among the edlerly in New

Mexico. *American Journal of Epidemiology, 147* (8), 755-763.

Baumgartner, R. N., Wayne, S. J., Waters, D. L., Janssen, I., Gallagher, D., & Morley, J.

(2004). Sarcopenic obesity predicts instrumental activities of daily living disability in

the elderly. *Obesity Research, 12*(12), 1995-2004. doi: 10.1038.oby.2004.250

Baylor, S. M. & Hollingworth, S. (2012). Intracellular calcium movements during

    excitation-contraction coupling in mammalian slow-twitch and fast-twitch muscle

    fibers. *The Journal of Cell Biology, 139*(4), 261-272. doi: 10.1085/jgp.201210773

Becker, D. J., Kilgore, M. L., & Morrisey, M. A. (2010). The societal burden of

    osteoporosis. *Current Rheumatology Reports, 12*(3), 186-191. doi: 10.1007/s11926-

    010-0097-y

Berchtold, M. W., Brinkmeier, H., & Müntener, M. (2000). Calcium ion in skeletal muscle:

    Its crucial role for muscle function, plasticity, and disease. *Physiological Reviews*,

    80(3), 1215–1265. Retrieved from http://physrev.physiology.org/content/80/3/1215

Bertalanffy, L. von. (1969). *General Systems Theory.* New York, NY: Braziller.

Bloom, D.E., & Canning, D. (2006). Booms, busts and echoes: How the biggest

    demographic upheaval in history is affecting global development. *Finance and*

    Development, 43(3). Retrieved from:

    http://www.imf.org/external/pubs/ft/fandd/2006/09/bloom.htm

Blume, S. W., & Curtis, J. R. (2011). Medical costs of osteoporosis in the elderly Medicare

    population. *Osteoporosis International, 22*(6), 1835-1844. doi: 10.1007/s00198-010-

    1419-7

Body, J., Bergmann, P., Boonen, S., Boutsen, Y., Bruyere, O., Devogelaer, J.P., …

    Reginster, J. Y. (2011). Non-pharmacological management of osteoporosis: A

    consensus of the Belgian Bone Club. *Osteoporosis International, 22*, 2769-2788. doi:

    10.1007/s00198-011-1545-x

Bonewald, L. F. (2011). The amazing osteocyte. *Journal of Bone and Mineral Research*,

    26(2), 229–238. doi:10.1002/jbmr.320

Bonewald, L. F., & Wacker, M. J. (2012). FGF23 production by osteocytes. *Pediatric Nephrology*, *28*(4), 563–568. doi:10.1007/s00467-012-2309-3

Bouchard, D. R., & Janssen, I. (2009). Dynapenic-obesity and physical function in older adults. *Journal of Gerontology: Medical Sciences,65A*(1), *1-7. doi: 10.1093/gerona/glp159*

Bouchard, D. R., Dionne, I. J., & Brochu, M. (2009). Sarcopenic/obesity and physical capacity in older men and women: data from the nutrition as a determinant of successful aging (NuAge)- the Quebec longitudinal sudy. *Obesity (Silver Spring), 11*, 2082-2088. doi: 10.1038/oby.2009.109

Bradley, S.M. (2011). Falls in older adults. *Mount Sinai Journal of Medicine, 78*, 590-595. doi: 10.1002.msj.20280

Brotto, M., & Abreu, E. L. (2012). Sarcopenia: Pharmacology of today and tomorrow. *The Journal of Pharmacology and Experimental Therapeutics, 343*(3), 540-546. doi: 10.1124/jpet.112.191759

Buford, T. W., Anton, S. D., Judge, A. R., Marzetti, E., Wohlgemuth, S. E., Carter, C. S., … Manini, T. M. (2010). Models of accelerated sarcopenia: Critical pieces for solving the puzzle of age-related muscle atrophy. *Ageing Research Reviews*, *9*(4), 369–383. doi:10.1016/j.arr.2010.04.004

Burattini, S., Ferri, P., Battistelli, M., Curci, R., Luchetti, F., & Falcieri, E. (2004). C2C12 murine myoblasts as a model of skeletal muscle development: Morpho-functional characterization. *European Journal of Histochemistry, 48*(3), 223-234.

Burger, E. H., & Klein-Nulend, J. (1999). Mechanotransduction in bone—role of the lacuno-

304

canalicular network. *The FASEB Journal*, *13*(9001), 101–112. Retrieved from

http://www.fasebj.org/content/13/9001/101

Campana, D. (2003). Determination of minimal residual disease in leukaemia patients.

British Journal of Haematology, *121*(6), 823–838. doi:10.1046/j.1365-

2141.2003.04393.x

Campbell, N. & Reece, J. (2004). *Biology* (7th ed.). San Francisco, CA: Pearson Benjamin

Cummings.

Capes, E. M., Loaiza, R., & Valdivia, H. H. (2011). Ryanodine receptors. *Skeletal Muscle,*

1(18). doi: 10.1186/2044-5040-1-18

Cefalu, C. A. (2011). Theories and mechanisms of aging. *Clinics in Geriatric Medicine,*

*27,*491-506. doi: 10.1016/j.cger.2011.07.001

Chan, J. K.-K., Harry, L., Williams, G., & Nanchahal, J. (2012). Soft-tissue reconstruction

of open fractures of the lower limb: Muscle versus fasciocutaneous flaps. *Plastic and*

Reconstructive Surgery, *130*(2), 284e–295e. doi:10.1097/PRS.0b013e3182589e63

Chan M. (2012). The new normal: Life after sixty. Lecture delivered at the Congress on

Gerontology and Geriatrics and the 20th International Seminar on Care for the

Elderly, Havana, Cuba, 30 March 2012. Retrieved from:

http://www.who.int/dg/speeches/2012/ageing_20120330/en/index.html

Chan, C.Y., Masui, O., Krakovska, O., Belozerov, V. E., Voisin, S., Ghanny, S., … Sui,

K.W. (2007). Identification of differentially regulated secretome components during

skeletal myogenesis. *Molecular and Cellular Proteomics, 10*, 1-20. doi:

10.10.1074/mcp.M110.004804

Chen, P., Lin, M., Peng, L., Liu, C., Chang, C., Lin, Y., & Chen, L. (2012). Predicting cause-

specific mortality of older men living in the veterans home by handgrip strength and

walking speed: A 3-year, prospective cohort study in Taiwan. *Journal of the*

American Medical Directors Association, 13, 517-521. doi:

10.1016/j.jamda.2012.02.002

Choquette, S., Bouchard, D. R., Doyon, C. Y., Senechal, M., Brochu, M., & Dionne, I. J.

(2010). Relative strength as a determinant of mobility in elders 67-84 years of age.

Journal of Nutritional Health and Aging, 14(3), 190-195. doi: 10.1007/s12603-010-

0047-4

Christiansen, C., Tanko, L. B., Warming, L., Moelgaard, A., Christgau, S., Qvist, P.,…

Hoyle, N. (2003). Dose dependent effects on bone resorption and formation of

intermittently administered intravenous ibandronate. *Osteoporosis International,*

*14,*609-613. doi: 10.1007/s00198-0031409-0

Clark, B. C., Fernhall, B., & Ploutz-Snyder, L.L. (2006). Adaptations in human

neuromuscular function following prolonged unweighting: I. Skeletal muscle

contractile properties and applied ischemia efficacy. *Journal of Applied Physiology,*

*101,*256-263. doi: 10.1152/japplphysiol.01402.2005

Clark, B. C., & Manini, T. M. (2008). Sarcopenia ≠ dynapneia. *Journal of Gerontology,*

63A(8), 829-834.

Clark, N.M. (2011). From our founding director. *The Center for Managing Chronic*

Disease. Retrieved from http://cmcd.sph.umich.edu/what-is-chronic-disease.html

Coiro, V., Volpi, R., Cataldo, S., Magotti, M. G., Maffei, M. L., Giumelli, C., … Chiodera,

P. (2012). Effect of physiological exercise on osteocalcin levels in subjects with

adrenal incidentaloma. *Journal of endocrinological investigation*, *35*(4), 357–358.

Cooper, A. (1844). *A treatise on dislocations, and on fractures of the joints.* Philadelphia: Lea and Blanchard

Cosqueric, G., Sebag, A., Ducolombier, C., Thomas, C., Piette, F., & Weill-Engerer, S. (2006). Sarcopenia is predictive of nosocomial infection in care of the elderly. *British Journal of Nutrition, 96*(5), 895-901. doi: 10.1017/BJM20061943

Crepaldi, G., & Maggi, S. (2005). Sarcopenia and osteoporosis: A hazardous duet. *Journal of endocrinological investigation*, *28*(10 Suppl), 66–68.

Cruz-Jentoft, A. (2013). Sarcopenia: A clinical review. *Reviews in Clinical Gerontology, 23*, 267-274. doi: 10.1017/S095925981.3000154

Cummings, S. R., Black, D. M., Nevitt, M. C., Browner, W., Cauley, J., Ensrud, K. … Vogt, T. M. (1993). Bone density at various sites for prediction of hip fractures. The Study of Osteoporotic Fractures Research Group. *Lancet, 341*(8837), 72-75.

Dallas, S. L., Prideaux, M., & Bonewald, L. F. (2013). The osteocyte: An endocrine cell ... and more. *Endocrine Reviews*, *34*(5), 658–690. doi:10.1210/er.2012-1026

Davison, K.K., Ford, E. S., Cogswell, M. E., & Dietz, W. H. (2002). Percentage of body fat and body mass index are associated with mobility limitations in peole aged 70 and older from NHANES III. *Journal of the American Geriatrics Society, 50*(11), 1802-1809.

Depp, C.A., & Jeste, D.V. (2009). Definitions and predictors of successful aging: A comprehensive review of larger quantitative studies. *The Journal of Lifelong Learning in Psychiatry, 7*(1), 137-150.

Deschenes, M. R., (2004). Effects of aging on muscle fibre type and size. *Sports Medicine, 34*(12), 809-824. doi: 10.2165/00007256-200434120-00002

Di Monaco, M. Vallero, F., Di Monaco, R., & Tappero, R. (2011). Prevalence of sarcopenia

    and its association with osteoporosis in 313 older women following hip fracture.

    Archives of Gerontology and Geriatrics, 52, 71-74. doi:

    10.1016.j.archger.2010.02.002

Drew, B., Phaneuf, S., Dirks, A., Selman, C., Gredilla, R., Lezza, A., Barja, G., &

    Leeuwenburgh, C. (2003). Effects of aging and caloric restriction on mitochondrial

    energy production in gastrocnemius muscle and heart. *American Journal of*

    *Physiology - Regulatory, Integrative and Comparative Physiology, 284,*R474-R480.

    doi: 10.1152/ajpregu.00455.2002

Ducy, P., Desbois, C., Boyce, B., Pinero, G., Story, B., Dunstan, C., … Karsenty, G. (1996).

    Increased bone formation in osteocalcin-deficient mice. *Nature*, *382*(6590), 448–52.

    doi:http://dx.doi.org.proxy.library.umkc.edu/10.1038/382448a0

Ducy, P., Zhang, R., Geoffroy, V., Ridall, A. L., & Karsenty, G. (1997). Osf2/Cbfa1: A

    Transcriptional activator of osteoblast differentiation. *Cell*, *89*(5), 747–754.

    doi:10.1016/S0092-8674(00)80257-3

Dutta, C. (1997). Significance of sarcopenia in the elderly. *The Journal of Nutrition*, *127*(5S),

    992S–993S. Retrieved from

    http://search.proquest.com.proxy.library.umkc.edu/docview/197430384

Evans, W. J., & Campbell, W. W. (1993). Sarcopenia and age-related changes in body

    composition and functional capacity. *The Journal of Nutrition*, *123*(2 Suppl), 465–

    468.

Fielding, R. A., Vellas, B., Evans, W. J., Bhasin, S., Morley, J. E., Newman, A. B., …

Zamboni, M. (2011). Sarcopenia: An undiagnosed condition in older adults. Current

consensus definition: prevalence, etiology, and consequences. International working

group on sarcopenia. *Journal of the American Medical Directors Association*, *12*(4),

249–256. doi:10.1016/j.jamda.2011.01.003

Fleisch, H., Graham, R., Russell, G. & Francis, M. D. (1969). Diphosphonates inhibit

hydroxyapatite dissolution in vitro and bone resorption in tissue culture in vivo.

Science, 165(3899), 1262-1264.

Florini, J. R., Ewton, D. Z., Magri, K. A., & Mangiacapra, F. J. (1993) IGFs and muscle

differentiation. *Advanced Experimental Medical Biology, 343,* 319–326.

Frost, H. M. (1996). Perspectives: A proposed general model of the "mechanostat"

(suggestions from a new skeletal-biologic paradigm). *The Anatomical record*, *244*(2),

139–147. doi:10.1002/(SICI)1097-0185(199602)244:2<139::AID-AR1>3.0.CO;2-X

Glund, S., Deshmukh, A., Long, Y. C., Moller, T., Koistinen, H. A., Caidahl, K.,…Krook, A.

(2007). Interleukin-6 directly increases glucose metabolism in resting human skeletal

muscle. *Diabetes, 56*(6), 1630-1637. doi: 10.2337/db06-1733

Goldspink, D. F., & Goldspink, G. (1986). The role of passive stretch in retarding muscle

atrophy. In W. A. Nix & G. Vrbová (Eds.), *Electrical stimulation and neuromuscular

disorders* (pp. 91–100). Berlin, Heidelberg: Springer Berlin Heidelberg. Retrieved

from http://www.springerlink.com/index/10.1007/978-3-642-71337-8_10

Gomez-Pinilla, F. (2002). Voluntary exercise induces a BDNF-mediated mechanism that

promotes neuroplasticity. *Journal of Neurophysiology*, *88*(5), 2187–2195.

doi:10.1152/jn.00152.2002

Goodpaster, B. H., Park, S. W., Harris, T. B., Kritchevsky, S. B., Nevitt, M., Schwartz, … &

Newman, A. B., for the Health ABC Study. (2006). The loss of skeletal muscle

strength, mass, and quality in older adults: The health, aging and body composition

study. *The Journals of Gerontology Series A: Biological Sciences and Medical

Sciences, 61*(10), 1059-1064. doi: 10.1093/gerona/61.10.1059

Gruning, N., Lehrach, H., & Ralser, M. (2010). Regulatory crosstalk in metabolic network.

Cell Press, 35(4), 220-227. doi:10.1016/j.tibs.2009.12.001

Haber, D. (2010). *Health promotion and aging (5th ed.).* New York: Springer Publishing

Company

Habib, F., Eshra, D. M. K., & Dawood, H. (2012). Assessment and modification of risk

behavior of osteoporosis among childbearing working women. *Journal of American

Science, 8*(9), 111-119.

Hamrick, M.W., McPherron, A. C., & Lovejoy, C. O. (2002). Bone mineral content and

density in the humerus of adult myostatin-deficient mice. *Calcified Tissue

International*, *71*(1), 63–68. doi:10.1007/s00223-001-1109-8

Hamrick, M. W. (2003). Increased bone mineral density in the femora of GDF8 knockout

mice. *The Anatomical Record*, *272A*(1), 388–391. doi:10.1002/ar.a.10044

Hamrick, M. W., Samaddar, T., Pennington, C., & McCormick, J. (2005). Increased

muscle mass with myostatin deficiency improves gains in bone strength with

exercise. *Journal of Bone and Mineral Research*, *21*(3), 477–483.

doi:10.1359/JBMR.051203

Hamrick, M. W., Ding, K. H., Pennington, C., Chao, Y. J., Wu, Y.-D., Howard, B., … Isales,

C. M. (2006). Age-related loss of muscle mass and bone strength in mice is

associated with a decline in physical activity and serum leptin. *Bone*, *39*(4), 845–853.

doi:10.1016/j.bone.2006.04.011

Harman, D. (1956). Aging: A theory based on free radical and radiation chemistry.

Journal of Gerontology, 11(3), 298-300.

Harman, D. (1972). Free radical theory of aging: Dietary implications. *The American*

Journal of Clinical Nutrition, 25, 839-843.

Hayutin, A., Beals, M., & Borges, E. (2013). The aging US workforce: A chartbook of

demographic shifts. Standford Center on Longevity. Retrieved from:

http://longevity.stanford.edu

Heiden, T., Auer, G., & Tribukait, B. (2000). Reliability of DNA cytometric S-phase analysis

in surgical biopsies: Assessment of systematic and sampling errors and comparison

between results obtained by image and flow cytometry. *Cytometry*, *42*(3), 196–208.

doi:10.1002/1097-0320(20000615)42:3<196::AID-CYTO6>3.0.CO;2-M

Hekimi, S., Lapoint, J., & Wen, Y. (2011). Taking a "good" look at free radicals in the

aging process. *Trends in Cell Biology, 21*(10), 569-576. doi:

10.1016/j.tcb.2011.06.008

Hirokawa, N., Niwa, S., & Tanaka, Y. (2010). Molecular motors in neurons: Transport

mechanisms and roles in brain function, development, and disease. *Neuron*, *68*(4),

610–638. doi:10.1016/j.neuron.2010.09.039

Hofbauer, L. G., Brueck, C., Singh, S. K., & Dobnig, H. (2007). Osteoporosis in patients

with diabetes mellitus. *Journal of Bone and Mineral Research, 22*(9), 1317-1328.

doi: 10.1359/JBMR.070510

Hol, J., Wilhelmsen, L., & Haraldsen, G. (2010). The murine IL-8 homologues KC, MIP-2,

and LIX are found in endothelial cytoplasmic granules but not in the Weibel-Palade

bodies. *Jounral of Leukocyte Biology, 87,*501-508. doi: 10.1189/jlb.0809532

Holz, G. G., & Habener, J. F. (1992). Signal transduction crosstalk in the endocrine system:

pancreatic beta-cells and the glucose competence concept. *Trends in Biochemical*

Sciences, *17*(10), 388–393.

Hopkins, P. M. (2006). Skeletal muscle physiology. *British Journal of Anaesthesia CEPD*

Reviews, 6(1), 1-6. doi: 10.1093/bjaceaccp/mki062

Hughes, V. A., Frontera, W. R., Wood, M., Evans, W. J., Dallal, G. E., Roubenoff, R., &

Singh, M. A. (2001). Longitudinal muscle strength changes in older adults:

Influence of muscle mass, physical activity, and health. *Journal of Gerontology*

Series A: Biological Sciences and Medical Sciences, 56(5), B209-B217.

Jackson, M. J. (2009). Skeletal muscle aging: Role of reactive oxygen species. *Critical*

Care Medicine, 37(10 Suppl), S368-S371. doi: 10.1097/CCM.0b013e3181b6f97f

Jackson, M. J., & McArdle, A. (2011). Age-related changes in skeletal muscle reactive

oxygen species generation and adaptive responses to reactive oxygen species.

Journal of Physiology, 589, 2139-2145. doi: 10.1113/jphysiol.2011.206623

Jähn, K., Lara-Castillo, N., Brotto, L., Mo, C. L., Johnson, M. L., Brotto, M., & Bonewald,

L. F. (2012). Skeletal muscle secreted factors prevent glucocorticoid-induced

osteocyte apoptosis through activation of β-catenin. *European cells & materials*, *24*,

197–209; discussion 209–10.

Janssen, I. (2006). Influence of sarcopenia on the development of physical disability: The

Cardiovascular Health Study. *Journal of the American Geriatrics Society*, *54*(1), 56–62. doi:10.1111/j.1532-5415.2005.00540.x

Janssen, I. (2007). Morbidity and mortality risk associated with an overweight BMI in older men and women. *Obesity*, 1*5*(7): 1827–1840. doi:10.1038/oby.2007.217.

Janssen, I., Heymsfeld, S. B., & Ross, R. R. (2002). Low relative skeletal muscle mass (sarcopenia) in older persons is associated with functional impairment and physical disability. *Journal of the American Geriatrics Society, 50*, 889-896. doi: 10.1046/j.1532-5415.2002.50213.x

Janssen, I., & Ross, R. (2005). Linking age-related changes in skeletal muscle mass and composition with metabolism and disease. *Journal of Nutritional Health and Aging, 9*(6), 408-419.

Janssen, I., Shepard, D.S., Katzmarzyk, P.T., & Roubenoff, R. (2004). The healthcare costs of sarcopenia in the United States. *Journal of the American Geriatric Society, 52*, 80-85. doi: 10.1111/j.1532-5415.2004.52014.x

Jensen, G. L., & Friedmann, J. M. (2002). Obesity is associated with functional decline in community-dwelling rural older persons. *Journal of the American Geriatrics Society, 50*(5), 918-923. doi: 10.1046/j.1532-5415.2002.50220.x

Jouliaekaza, D., & Cabello, G. (2007). The myostatin gene: Physiology and pharmacological relevance. *Current Opinion in Pharmacology*, *7*(3), 310–315. doi:10.1016/j.coph.2006.11.011

Kamel, H. K. (2003). Sarcopenia and aging. *Nutrition Reviews, 61*(5), 157-167. doi: 10.1301/nr.2003.may.157-167

Karakelides, H., & Nair, K. S. (2005). Sarcopenia of aging and its metabolic impact.

Current Topics in Developmental Biology, 68, 123-148. doi: 10.1016/S0070-2153(05)68005-2

Karasik, D., & Kiel, D. P. (2010). Evidence for pleiotropic factors in genetics of the musculoskeletal system. *Bone*, *46*(5), 1226–1237. doi:10.1016/j.bone.2010.01.382

Karsenty, G., & Ferron, M. (2012). The contribution of bone to whole-organism physiology. *Nature*, *481*(7381), 314–320. doi:10.1038/nature10763

Karsenty, G., & Wagner, E. F. (2002). Reaching a genetic and molecular understanding of skeletal development. *Developmental cell*, *2*(4), 389–406.

Keller, C. (2001). Transcriptional activation of the IL-6 gene in human contracting skeletal muscle: Influence of muscle glycogen content. *The FASEB Journal*. doi:10.1096/fj.01-0507fje

Kim, H. J., Higashimori, T., Park, S. Y., Choi, H., Dong, J., Kim, Y. J.,…Kim, J. K. (2004). Differential effects of interleukin-6 and -10 on skeletal muscle and liver insulin action in vivo. *Diabetes, 53*(4), 1060-1067. doi: 10.2337/diabetes.53.4.1060

Kim, T. N., Park, M. S., Yang, S. J., Yoo, H. J., Kang, H. J., Song, W.,…Choi, K. M. (2010). Prevalence and determinant factors of sarcopenia in patients with type 2 diabetes. *Diabetes Care, 33*(7), 1497-1499. doi: 10.2337/dc09-2310

Klein-Nulend, J., Plas, A. van der, Semeins, C. M., Ajubi, N. E., Frangos, J. A., Nijweide, P. J., & Burger, E. H. (1995). Sensitivity of osteocytes to biomechanical stress in vitro. *The FASEB Journal*, *9*(5), 441–445. Retrieved from http://www.fasebj.org/content/9/5/441

Knight, J. A. (1998). Free radicals: Their history and current status. *Annals of Laboratory and Clinical Science, 28*(6), 331-346.

Kurek, J. B., Bower, J. J., Romanella, M., Koentgen, F., Murphy, M., & Austin, L. (1997). The role of leukemia inhibitory factor in skeletal muscle regeneration. *Muscle & Nerve*, *20*(7), 815–822.

Lajeunesse, D., Kiebzak, G. M., Frondoza, C., & Sacktor, B. (1991). Regulation of osteocalcin secretion by human primary bone cells and by the human osteosarcoma cell line MG-63. *Bone and mineral*, *14*(3), 237–250.

Lammes, E., & Akner, G. (2006). Resting metabolic rate in elderly nursing home patients with multiple diagnoses. *Journal of Nutritional Health and Aging, 10*(4), 263-270.

Lang, T. F. (2011). The bone-muscle relationship in men and women. *Journal of Osteoporosis*, *2011*, 1–4. doi:10.4061/2011/702735

Leboime, A., Confavreux, C. B., Mehsen, N., Paccou, J., David, C., & Roux, C. (2010). Osteoporosis and mortality. *Joint Bone Spine 77,* S107-S112.

Lee, C. G., Boyko, E. J., Strotmeyer, E. S., Lewis, C. E., Cawthon, P. M., Hoffman, A. R., …Orwoll, E. S. (2011). Association between insulin resistance and lean mass loss and fat mass gain in older men without diabetes mellitus. *Journal of the American Geriatric Society, 59*(7), 1217-1224. doi: 10.1111/j.1532-5415.2011.03472.x

Lee, N. K., Sowa, H., Hinoi, E., Ferron, M., Ahn, J. D., Confavreux, C., … Karsenty, G. (2007). Endocrine regulation of energy metabolism by the skeleton. *Cell*, *130*(3), 456–469. doi:10.1016/j.cell.2007.05.047

Le Grand, F., & Rudnicki, M.A. (2007). Skeletal muscle satellite cells and adult myogenesis. *Current Opinion in Cell Biology, 19,*628-633. doi: 10.1016/j.ceb.2007.09.012

Levine, R. L. (2002). Carbonyl modified proteins in cellular regulation, aging, and disease.

Free Radical Biology and Medicine, 32(9), 790-796. doi: 10.1016/S0891-5849(02)00765-7

Li, Y., & Huard, J. (2002). Differentiation of muscle-derived cells into myofibroblasts in injured skeletal muscle. *The American Journal of Pathology*, *161*(3), 895–907. doi:10.1016/S0002-9440(10)64250-2

Liochev, S. I. (2013). Reactive oxygen species and the free radical theory of aging. *Free Radical Biology and Medicine, 60*, 1-4. doi: 10.1016/j.freeradiomed.2013.02.011

Lonza. (2012). Clonetics™ skeletal muscle myoblast cell systems. Retrieved from http://www.lonza.com.

MacIntosh, B. R., Gardiner, P. F., & McComas, A. J. (2006). *Skeletal muscle: Form and function*. Champaign, Illinois: Human Kinetics.

Magkos, F., Wang, X., & Mittendorfer, B. (2010). Metabolic actions of insulin in men and women. *Nutrition, 26*, 686-693. doi: 10.1016/j.nut.2009.10.013

Manring, H., Abreu, E., Brotto, L., Weisleder, N., & Brotto, M. (2014). Novel excitation-contraction coupling related genes reveal aspects of muscle weakness beyond atrophy -- new hopes for treatment of musculoskeletal diseases. *Frontiers in Physiology, 5*(37). 1-12. doi: 103389/fphys.2014.00037

Marotti, G., Ferretti, M., Muglia, M. A., Palumbo, C., & Palazzini, S. (1992). A quantitative evaluation of osterblast-osteocyte relationships on growing endosteal surface of rabbitt tibiae. *Bone, 13*, 363-368.

Martin, A., Liu, S., David, V., Li, H., Karydis, A., Feng, J. Q., & Quarles, L. D. (2011). Bone

proteins PHEX and DMP1 regulate fibroblastic growth factor Fgf23 expression in

osteocytes through a common pathway involving FGF receptor (FGFR) signaling.

The FASEB Journal, *25*(8), 2551–2562. doi:10.1096/fj.10-177816

Matthews, V. B., Åström, M.-B., Chan, M. H. S., Bruce, C. R., Krabbe, K. S., Prelovsek, O.,

… Febbraio, M. A. (2009). Brain-derived neurotrophic factor is produced by skeletal

muscle cells in response to contraction and enhances fat oxidation via activation of

AMP-activated protein kinase. *Diabetologia*, *52*(7), 1409–1418. doi:10.1007/s00125-

009-1364-1

McCloskey, E. (2009). FRAX: Identifying people at high risk of fracture. *International*

Osteoporosis Foundation. Retrieved from

http://osteoporosis.org.za/general/downloads/FRAX-report-09.pdf.

McDonagh, M. J., Hayward, C. M., & Davies, C. T. (1983). Isometric training in human

elbow flexor muscles: The effects on voluntary and electrically evoked forces. *The*

Journal of Bone and Joint Surgery, 65B(3), 355-358.

McLaughlin, S.J., Connell, C. M., Heeringa, S. G., Li, L. W., & Roberts, J.S. (2009).

Successful aging in the United States: Prevalence estimates from a national sample of

older adults. *Journal of Gerontology: Social Sciences, 65B*(2), 216-226.

doi:10.1093/geronb/gbp101.

McPherron, A. C., Lawler, A. M., & Lee, S.-J. (1997). Regulation of skeletal muscle mass in

mice by a new TGF-p superfamily member. *nature*, *387*(6628), 83–90.

doi:10.1038/387083a0

Medvedev, Z. A. (2008). An attempt at a rational classification of theories of aging.

Biological Reviews, 65(3), 375-398. doi: 10.11111/j.1469-185X.1990.tb01428.x

Miquel, J., Economos, A. C., Fleming, J., & Johnson, J. E. (1980). Mitochondrial role in

    cell aging. *Experimental Gerontology, 15*(6), 575-591. doi: 10.1016/0531-

    5565(80)90010-8

Mitchell, W. K., Williams, J., Atherton, P., Larvin, M., Lund, J., & Narici, M. (2012).

    Sarcopenia, dynapenia, and the impact of advancing age on human skeletal muscle

    size and strength: A quantitative review. *Frontiers in Physiology, 3*, 1-18. doi:

    10.3389/fphys.2012.00260

Mo, C., Romero-Suarez, S., Bonewald, L., Johnson, M., & Brotto, M. A. (2012).

    Prostaglandin E2: From clinical applications to its potential role in bone-muscle

    crosstalk and myogenic differentiation. *Recent Patents in Biotechnology, 6*(3), 223-

    229. doi: 10.2174/1872208311206030223

Morissette, M. R., Stricker, J. C., Rosenberg, M. A., Buranasombati, C., Levitan, E. B.,

    Mittleman, M. A., & Rosenzweig, A. (2009). Effects of myostatin deletion in aging

    mice. *Aging Cell*, *8*(5), 573–583. doi:10.1111/j.1474-9726.2009.00508.x

Morley, J. E., Baumgartner, R. N., Roubenoff, R., Mayer, J., & Nair, K. S. (2001).

    Sarcopenia. *Journal of Laboratory and Clinical Medicine, 137*(4), 231-243. doi:

    10.1067/mlc.2001.113504

Muhlethaler, R., Stuck, A. E., Minder, C. E., & Frey, B. M. (1995). The prognostic

    significance of protein-energy malnutrition in geriatric patients. *Age and Ageing,*

    24(3), 193-197. doi: 10.1093/ageing/24.3.193

Mundy, G. R. (1993). Role of cytokines in bone resorption. *Journal of Cellular*

    Biochemistry, *53*(4), 296–300. doi:10.1002/jcb.240530405

Muravchick, S. (2000). Preoperative assessment of the elderly patient. *Geriatric*

Anesthesia, 18(1), 71-89.

Nag, A. C., & Foster, J. D. (1981). Myogenesis in adult mammalian skeletal muscle *in vitro*. *Journal of Anatomy, 132*, 1-18.

National Osteoporosis Foundation. (2010). Clinician's guide to prevention and treatment of Osteoporosis (NOF Publication No. B120-0110). Washington, DC: US Government Printing Office. Retrieved from:

http://nof.org/files/nof/public/content/file/344/upload/159.pdf

Newman, A. B., Kupelian, V., Visser, M., Simonsick, E., Goodpaster, B., Nevitt, M.,…Harris, T.B. (2003). Sarcopenia: Alternative definitions and associations with lower extremity function. *Journal of American Geriatric Society, 51*(11), 1602-1609. doi: 10.1046/j.1532-5415.2003.51534.x

Niccoli, T., & Patridge, L. (2012). Aeging as a risk factor for disease. *Current Biology, 22*, R741-R752. doi: 10.1016/j.cub.2012.07.024

Nielsen, A. R., & Pedersen, B. K. (2007). The biological roles of exercise-induced cytokines: IL-6, IL-8, and IL-15. *Applied Physiology, Nutrition, and Metabolism*, *32*(5), 833–839. doi:10.1139/H07-054

Olson, S. (2013). Public health for an aging society. *Health Promotion Practice, 14*(1). 7-9. doi: 10.1177/1524839912469206

Orestes-Cardoso, S. M., Nefussi, J. R., Hotton, D., Mesbah, M., Orestes-Cardoso, M. D. S., Robert, B., & Berdal, A. (2001). Postnatal Msx1 expression pattern in craniofacial, axial, and appendicular skeleton of transgenic mice from the first week until the second year. *Developmental Dynamics*, *221*(1), 1–13. doi:10.1002/dvdy.1120

Papapoulos, S. E., & Schimmer, R. C. (2007). Changes in bone remodeling and antifracture

efficacy of intermittent bisphosphonate therapy: Implications from clinical studies with ibandronate. *Annals of the Rheumatic Diseases, 66*, 853-858. doi: 10.1136/ard.2006.064931

Park, K. H., Zaichenko, L., Brinkoetter, M., Thakkar, B., Sahin-Efe, A., Joung, K. E., … Mantzoros, C. S. (2013). Circulating irisin in relation to insulin resistance and the metabolic syndrome. *The Journal of clinical endocrinology and metabolism*. doi:10.1210/jc.2013-2373

Pasco, J. A., Seeman, E., Henry, J., Merriman, E. N., Nicholson, G. C., & Kotowicz, M. A. (2006). The population burden of fractures originates in women with osteopenia, not osteoporosis. *Osteoporosis International, 17*(9), 1404-1409. doi: 10.1007/s00198-006-0135-9

Pearson, O. M., & Lieberman, D. E. (2004). The aging of Wolff's ?law?: Ontogeny and responses to mechanical loading in cortical bone. *American Journal of Physical Anthropology*, *125*(S39), 63–99. doi:10.1002/ajpa.20155

Pedersen, B. K., Akerstrom, T. C. A., Nielsen, A. R., & Fischer, C. P. (2007). Role of myokines in exercise and metabolism. *Journal of Applied Physiology*, *103*(3), 1093–1098. doi:10.1152/japplphysiol.00080.2007

Pedersen, B. K., Steensberg, A., Fischer, C., Keller, C., Keller, P., Plomgaard, P., … Saltin, B. (2003). Searching for the exercise factor: is IL-6 a candidate? *Journal of Muscle Research and Cell Motility*, *24*(2-3), 113–119.

Pedersen, L., Olsen, C. H., Pedersen, B. K., & Hojman, P. (2012). Muscle-derived expression

of the chemokine CXCL1 attenuates diet-induced obesity and improves fatty acid

oxidation in the muscle. *AJP: Endocrinology and Metabolism*, *302*(7), E831–E840.

doi:10.1152/ajpendo.00339.2011

Poljsak, B. (2011). Strategies for reducing or preventing the generation of oxidative stress.

Oxidative Medicine and Cellular Longevity, 14(4), 1-15. doi: 10.1155/2011/194586

Polli, J. E. (2008). In vitro studies are sometimes better than conventional human

pharmacokinetic in vivo studies in assessing bioequivalence of immediate-release

solid oral dosage forms. *The AAPS Journal*, *10*(2), 289–299. doi:10.1208/s12248-

008-9027-6

Porter, G. A., Makuck, R. F., & Rivkees, S.A. (2002). Recudtion in intracellular calcium

levels inhibits myoblast differentiation. *The Journal of Biological Chemistry,

277*(32), 28942-28947. doi: 10.1074/jbc.M203961200

Protho, J. W., & Rosenbloom, C. A. (1995). Body measurements of black and whit elderly

persons with emphasis on body composition. *Gerontology, 41*(1), 22-38. doi:

10.1159/000213659

Pucca, A. A., Daly, M. J., Brewster, S. J., Matise, T. C., Barrett, J., Shea-Drinkwater,

M.,…Perls, T. (2001). A genome-wide scan for linkage to human exceptional

longevity identifies a locus on chromosome 4. *Proceedings of the National Academy

of Sciences, 98*(18), 10505-10508. doi: 10.1073/pnas.181337598

Rappolee, D. A., & Armant, D. R. (2009). Cell signaling. In S. Krawetz (Ed.),

Bioinformatics for Systems Biology (pp. 89-104). New York, NY: Humana Press.

Ray, N.F., Chan, J. K., Thamer, M., & Melson, L. J. (1997). Medical expenditures for the

treatment of osteoporotic fractures in the United States in 1995: Report from the National Osteoporosis Foundation. *Journal of Bone and Mineral Research, 12*(1), 24-35. doi: 10.1359/jbmr.1997.12.1.24

Recker, R. R., & Barger-Lux, M. J. (2004). The elusive concept of bone quality. *Current Osteoporosis Reports, 2*, 97-100. doi: 10.1007/s11914-004-0017-z

Rizzoli, R., Boonen, S., Brandi, M.L., Burlet, N., Delmas, P., & Reginster, J. Y. (2008). The role of calcium and vitamin D in the management of osteoporosis. *Bone, 42*, 246-249. doi: 10.1016/j.bone.2007.10.005

Rolland Y., Lauwers-Cances V., Cristini C., Abellan van Kan, G., Janssen, I., Morley, J.E., & Vellas, B. (2009). Difficulties with physical function associated with obesity, sarcopenia, and sarcopenic-obesity in communitydwelling elderly women: The EPIDOS (EPIDemiologie de l'OSteoporose) Study. *American Journal of Clinical Nutrition, 89*(6),1895–900. doi: 10.3945/ajcn.2008.26950

Romano, A. D., Serviddio, G., de Matthaeis, A., Bellanti, F., & Vendemiale, G. (2010). Oxidative stress and aging. *Journal of Nephrology*, *23 Suppl 15*, S29–36.

Rosenberg, I. (1989). Summary comments: Epidemiological and methodological problems in determining nutritional status of older persons. *American Journal of Clinical Nutrition, 50*, 1231-1233.

Roubenoff, R. (2007). Physical activity, inflammation, and muscle loss. *Nutrition Reviews, 65*(12), S208-S212. doi: 10.1301/nr.2007.dec.S208-S212

Roubenoff, R., (2008). Excess baggage: Sarcopenia, obesity and cancer outcomes. *The Lancet Oncology, 9*(7), 605-607. doi: 10.1016/S1470-2045(08)70160-8

Roubenoff, R., & Castenada, C. (2001). Sarcopenia -- Understanding the dynamics of aging

muscle. *American Journal of the American Medical Association, 286*(10), 1230-1231. doi: 10.1001/jama.286.10.1230

Roubenoff, R., & Hughes, V. (2000). Sarcopenia: Current concepts. *Journal of Gerontology Series A: Biological Sciences and Medical Sciences, 9,* 605-607.

Rubenstein, L. Z., & Josephson, K. R. (2006). Falls and their prevention in elderly people: What does the evidence show? *Medical Clinics of North America, 90,*807-824. doi: 10.1016/j.mcna.2006.05.013

Rubio, N., & Sanz-Rodriguez, F. (2006). Induction of the CXCL1 (KC) chemokine in mouse astrocytes by infection with the murine encephalomyelitis virus of Theiler. *Virology, 358*, 98-108. doi: 10.1016/j.virol.2006.08.003

Salucci, S., Battistelli, M., Burattini, S., Squillace, C., Canonico, B., Gobbi, P., … Falcieri, E. (2010). C2C12 myoblast sensitivity to different apoptotic chemical triggers. *Micron*, *41*(8), 966–973. doi:10.1016/j.micron.2010.07.002

Satariano, W. A., Guralnik, J.M., Jackson, R.J., Marottoli, R.A., Phelan, E. A., & Prohaska, T. R. (2012). Mobility and aging: New directions for public health action. *American Journal of Public Health, 102*(8), 1508-1515. doi: 10.2105/AJPH.2011.300631

Schapira, D., & Schapira, C. (1992). Osteoporosis: The evolution of a scientific term. *Osteoporosis International*, *2*(4), 164–167. doi:10.1007/BF01623921

Schrager, M. A., Metter, E. J., Simonsick, E., Ble, A., Bandinelli, S., Lauretani, F., & Ferrucci, L. (2007). Sarcopenic obesity and inflammation in the InCHIANTI study. *Journal of Applied Physiology, 102*(3), 919-925. doi: 10.1152/japplphysiol.00627.2006

Schwartz, A. V., Nevitt, M. C., Brown, B. W., & Kelsey, J. L. (2005). Increased falling as a

risk factor for fracture among older women. *American Journal of Epidemiology, 161*, 180-185. doi: 10.1093/aje/kwi023

Scott, D., Blizzard, L., Fell, J., & Jones. G. (2011). The epidemiology of sarcopenia in community living older adults: What role does lifestyle play? *Journal of Cachexia Sarcopenia and Muscle, 2*, 125-134. doi: 10.1007/s13539-011-0036-4

Seale, P., Bjork, B., Yang, W., Kajimura, S., Chin, S., Kuang, S., … Spiegelman, B. M. (2008). PRDM16 controls a brown fat/skeletal muscle switch. *Nature*, *454*(7207), 961–967. doi:10.1038/nature07182

Sena, L. A., & Chandel, N. S. (2012). Physiological roles of mitochondrial reactive oxygen species. *Molecular Cell, 48*(2), 158-167. doi: 10.1016/j.molcel.2012.09.025

Sener, A. G., & Afsar, I. (2012). Infection and autoimmune disease. *Rheumatology International, 32, 3331-3338. doi: 10.1007/s00296-012-2451-z*

Shefer, G., Van de Mark, D. P., Richardson, J. B., & Yablonka-Reuveni, Z. (2006). Satellite-cell pool size does matter: Defining the myogenic potency of aging skeletal muscle. *Developmental Biology, 294*(1), 50-66. doi: 10.1016/j.ydbio.2006.02.022

Shimada, T., Kakitani, M., Yamazaki, Y., Hasegawa, H., Takeuchi, Y., Fujita, T., … Yamashita, T. (2004). Targeted ablation of Fgf23 demonstrates an essential physiological role of FGF23 in phosphate and vitamin D metabolism. *The Journal of Clinical Investigation*, *113*(4), 561–568. doi:10.1172/JCI19081

Sirola, J., & Kröger, H. (2011). Similarities in acquired factors related to postmenopausal osteoporosis and sarcopenia. *Journal of Osteoporosis*, *2011*, 1–14. doi:10.4061/2011/536735

Sornay-Rendu, E., Munoz, F., Garnero, P., Duboeuf, F., & Delmas, P.D. (2005).

Identification of osteopenic women at high risk of fracture: The OFELY study. *Journal of Bone and Mineral Research, 20*(1), 1813-1819. doi: 10.1359/JBMR.050609

Srikanthan, P., & Karlamangla, A. S. (2014). Muscle mass index as a predictor of longevity in older adults. *The American Journal of Medicine, 127*(6), 547-553. doi: 10.1016/j.amjmed.2014.02.007

Srikanthan, P., Hevener, A. L., & Karlamangla, A. S. (2010). Sarcopenia exacerbates obesity-associated insulin resistance and dysglycemia: Findings from the National Health and Nutrition Examination Survey III. *PLOS ONE, 5*(5), 1-7. doi: 10.1371/journal.pone.0010805

Stadtman, E. R. (2004). Role of oxidant species in aging. *Current Medicinal Chemistry, 11*(9), 1105-1112. doi: 10.2174/0929867043365341

Steensberg, A., Hall, G., Osada, T., Sacchetti, M., Saltin, B., & Pedersen, B. K. (2000). Production of interleukin-6 in contracting human skeletal muscles can account for the exercise-induced increase in plasma interleukin-6. *The Journal of Physiology*, *529*(1), 237–242. doi:10.1111/j.1469-7793.2000.00237.x

Tanaka, K., Matsuo, T., Ohta, M., Sato, T., Tezuka, K., Nijweide, P. J., … Kumegawa, M. (1995). Time-lapse microcinematography of osteocytes. *Mineral and Electrolyte Metabolism*, *21*(1-3), 189–192.

Taylor, B. C., Schreiner, P. J., Stone, K. L., Fink, H. A., Cummings, S. R., Nevitt, M. C., … Ensrud, K. E. (2004). Long-term prediction of incident hip fracture risk in elderly white women: Study of osteoporotic fractures. *Journal of the American Geriatrics Society, 52*, 1479-1486. doi: 10.1111/j.1532-5415.2004.52410.x

U. S. Department of Commerce, U. S. Census Bureau. (2011). *Population estimates.*

    Retrieved from www.census.gov

U.S. Department of Health and Human Services, Center for Disease Control and Prevention

    (2013). *National Vital Statistics Report.* Retrieved from

    http://www.cdc.gov/nchs/nvss.htm

Valkema, R., Vismans, F. J., Papapoulos, S. E., Pauwels, E. K., & Bijvoet, O. L. (1989).

    Maintained improvement in calcium balance and bone mineral content in pateints

    with osteoporosis treated with the bisphosphonate APD. *Bone and Mineral, 5*(2), 183-

    192.

Van Breukelen, F. J. M., Bijvoet, O. M., & Van Oosterom, A.T. (1979). Inhibition of

    osteolytic bone lesions by (3-Amino-1-Hydroxypropylidene)-1, 1-Bisphosphonate

    (APD). *The Lancet, 313*(8120), 803-805. doi: 10.1016/S0140-6736(79)91319-9

Vandervoort, A. A., & Symons, T. B. (2001). Functional and metabolic consequences of

    sarcopenia. *Canadian Journal of Applied Physiology, 26*(1), 90-101. doi:

    10.1139/h01-007

Veliça, P., & Bunce, C. M. (2011). A quick, simple and unbiased method to quantify C2C12

    myogenic differentiation. *Muscle & Nerve*, *44*(3), 366-370. doi:10.1002/mus.22056

Vermeer, C., Knapen, M. H. J., & Schurgers, L. J. (1998). Vitamin K and metabolic bone

    disease. *Journal of Clinical Pathology, 51*, 424-426. doi: 10.1136/jcp.51.6.424

Versluis, R., Papapolous, S. E., de Bock, G. H., Zwinderman, A. H., Petri, H., van de Ven,

    C. M., & Springer, M.P. (2001). Clinical risk factors as predictors of postmenopausal

    osteoporosis in general practice. *British Journal of General Practice, 51*, 806-810.

Visser, M., Harris, T. B., Fox, K. M., Hawkes, W., Hebel, J. R., YuYahiro, J.,…Magaziner,

J. (2000). Change in muscle mass and muscle strength after a hip fracture: Relationship to mobility recovery. *Journal of Gerontology, 55A*(8), M434-M440.

Vos, T., Flaxman, A. D., Naghavi, M., Lozano, R., Michaud, C., Shibuya, K.,…Murray, C. J. (2012). Years lived with disability (YLDs) for 1160 sequelae of 289 diseases and injuries 1990-2010: A systematic analysis for the Global Burden of Disease Study 2010. *Lancet, 308*, 2163-2196. doi: 10.1016/S0140-6736(12)61729-2

Wagers, A. J., & Conboy, I. M. (2005). Cellular and molecular signatures of muscle regeneration: Current concepts and controversies in adult myogenesis. *Cell*, *122*(5), 659–667. doi:10.1016/j.cell.2005.08.021

Wainwright, S. A., et al., for the Study of Osteoporotic Fractures Research Group. (2005). Hip fracture in women without osteoporosis. *The Journal of Clinical Endocrinology & Metabolism, 90*(5), 2787-2793. doi: 10.1210/jc.2004-1568

Walrand, S., Guillet, C., Salles, J., Cano, N., & Boirie, Y. (2011). Physiopathological mechanism of sarcopenia. *Clinical Geriatric Medicine, 27*, 365-385. doi: 10.1016/j.cger.2011.03.005

Walsh, M.C., Hunter, G.R., & Livingstone M.B. (2006). Sarcopenia in premenopausal and postmenopausal women with osteopenia, osteoporosis and normal bone density. *Osteoporosis International, 17,* 61-67. doi: 10.1007/s00198-005-1900-x

Wang, Q., Alén, M., Nicholson, P., Suominen, H., Koistinen, A., Kröger, H., & Cheng, S. (2007). Weight-bearing, muscle loading and bone mineral accrual in pubertal girls— A 2-year longitudinal study. *Bone*, *40*(5), 1196–1202. doi:10.1016/j.bone.2006.12.054

Wang, X. M., Hamza, M., Wu, T. X., & Dionne, R. A. (2009). Up-regulation of IL-6, IL-8,

and CCL2 gene expression after acute inflammation: Correlation to clinical pain. *Pain, 142*(3), 275-283. doi: 10.1016/j.pain.2009.02.001

Winkler, D. G., Sutherland, M. K., Geoghegan, J. C., Yu, C., Hayes, T., Skonier, J. E., … Latham, J. A. (2003). Osteocyte control of bone formation via sclerostin, a novel BMP antagonist. *The EMBO Journal*, *22*(23), 6267–6276. doi:10.1093/emboj/cdg599

Wolff, J.L., Starfield, B., & Anderson, G. (2002). Prevalence, expenditures, and complications of multiple chronic conditions in the elderly. *Archives of Internal Medicine, 162,* 2269-2276. doi: 10.1001/archinte.162.20.2269

World Health Organization (1994). *Assessment of fracture risk and its application to screening for postmenopausal Osteoporosis.* Report of a WHO Study Group. Geneva, World Health Organization, (WHO Technical Report Series, No. 843).

Wu, S.Y., & Green, A. (2000). Projection of chronic illness prevalence and cost inflation. Santa Monica, CA: RAND. Health; 2000. 6 National Centers for Health Statistics. Retrieved from http://www.nationalhealthcouncil.org.

Yach, D., Hawkes, C., Gould, C.L., & Hofman, K. J. (2004). The global burden of chronic disease: Overcoming the impediments. *Journal of the American Medical Association, 291*(21), 2616-2622.

Yamashita, T., Haesang, J. A., Bailer, J., Nelson, I. M., & Mehdizadeh, S. (2011). Fall risk factors in community-dwelling elderly who receive Medicaid-supported home-and community based care services. *Journal of Aging Health, 23*, 682-703. doi: 10.1177/0898264310390941

Zaki, M. E., Hussien, F. H., & Abd El-Shafy El Banna, R. (2009). Osteoporosis among ancient Egyptians. *International Journal of Osteoarchaeology, 19*(1), 78-89. doi:

10.1002/oa.978

Zanchetta, J. R., Plotkin, H., & Filgueira, M. L. A. (1995). Bone mass in children: Normative

values for the 2–20-year-old population. *Bone*, *16*(4), S393–S399.

doi:10.1016/S8756-3282(95)80505-2

Zimmers, T. A. (2002). Induction of cachexia in mice by systemically administered

myostatin. *Science*, *296*(5572), 1486–1488. doi:10.1126/science.1069525

Zoico, E., Di Francesco, V., Guralnik, J. M., Mazzali, G., Bortolani, A., Guariento, S., …

Zamboni, M. (2004). Physical disability and muscular strength in relation to obesity

and different body composition indexes in a sample of health elderly women.

International Journal of Obesity and Related Metabolic Disorders, 28(2), 234-241.

Zoico, E., & Roubenoff, R. (2002). The role of cytokines in regulating protein metabolism

and muscle function. *Nutrition Review, 60,* 39-51.

VITA

Janalee Isaacson was born on June 11, 1960, in Kansas City, Missouri. Most of her childhood years were spent in Manhattan, Kansas, where she was educated in local public schools and graduated from Manhattan High School in 1978. After attending Kansas State University, Janalee transferred and earned her Bachelors of Science in Nursing degree from the University of Kansas Medical Center. Her clinical practice was in adult medical surgical settings, including oncology and neurology. In 1994, she joined the faculty of the Associate Degree Nursing Program at Johnson County Community College.

Janalee was awarded her Masters of Science in Nursing from the University of Kansas Medical Center in 1998. At that time, she continued to work clinically and to teach prelicensure nursing students. In 2005, Janalee helped develop and became the facilitator for the JCCC RN Refresher Academy, a course developed for registered nurses who had been away from the clinical setting and whose goal it was to return to the patient care arena.

In 2010, Janalee began work toward her Ph.D. in Nursing at the University of Missouri-Kansas City, with an emphasis in physiology. During her time in the Ph.D. Program, Janalee worked in the Brotto Skeletal Muscle Biology Research Lab in addition to her teaching responsibilities. Upon completion of her degree requirements, Janalee plans to continue both her teaching and her research with the goal of improving patient care for older adults.